Biogenic Volatile Organic Compounds and their Role in the Formation of Ozone and Aerosols

Christoph Spirig

Diss. ETH No. 15163

DISS. ETH NO. 15163

BIOGENIC VOLATILE ORGANIC COMPOUNDS AND THEIR ROLE IN THE FORMATION OF OZONE AND AEROSOLS

A dissertation submitted to the
SWISS FEDERAL INSTITUTE OF TECHNOLOGY ZURICH

for the degree of
Doctor of Natural Sciences

presented by

CHRISTOPH SPIRIG
Dipl. Natw. ETH
born 21.06.1972

citizen of
Widnau (SG) and Diepoldsau (SG)

Accepted on the recommendation of

Prof. Thomas Peter, examiner
Dr. Albrecht Neftel, co-examiner
Dr. Alex B. Guenther, co-examiner

2003

Cover picture: Great Smoky Mountains National Park, USA, © QT Luong/terragalleria.com

Contents

Abstract

The biosphere emits large amounts of trace gases with significant impacts on atmospheric chemistry. Globally, plants release much higher amounts of volatile organic compounds (VOCs) than anthropogenic sources. VOCs are precursors for the formation of ozone and fine particulate matter. Within two major field experiments, the role of VOCs in the formation of these secondary pollutants was studied, with a particular emphasis on the impact of biogenic sources.

The effects of VOCs on ozone formation was investigated within the PIPAPO (Pianura Padana Produzione di Ozone) field experiment in the Po Valley, northern Italy. The project investigated which species or group of species limit the formation of photooxidants. PIPAPO aimed to determine the temporal behavior and spatial extent of VOC- and NO_x-sensitive areas of ozone production for the highly industrialized surroundings of Milan.
Two intensive observation periods (IOP) took place in May and early June 1998, during two episodes that were characterized by strong photochemical smog. During such conditions, air masses of Milan are advected north towards the Alps. At two surface sites 5 and 35 km north of downtown Milan, measurements of various photo-oxidants and its precursors were used to characterize the local ozone production. In particular, the sensitivity of ozone production to changes in the concentrations of NOx and VOCs were determined by steady state calculations. Ozone production at the outskirts of Milan was VOC-sensitive. The rural site at Verzago, 35 km north of Milan exhibited mainly NO_x-sensitive ozone production, but also VOC-sensitive periods. These were characterized by direct advection of air masses from downtown Milan.

A one-dimensional photochemical model was used to study the relations between these local quantities and the integrated perspective, the sensitivity of O_3 concentration to its precursor emissions. A quantitative description of the ozone concentration sensitivity from local sensitivities of ozone production is not possible because of the nonlinear relationships between emissions and concentrations. However, useful qualitative information could be derived from local observations. The Milan plume switched from a VOC- to a NO_x-sensitive ozone regime on its way north 4-5 hours downwind of the city center.
A definitive conclusion on the impact of biogenic VOCs on the ozone production in the Po Valley was not possible from the data gathered during PIPAPO, although some evidence for their significance was found. Total VOC-reactivity at Verzago was dominated by biogenic isoprene. Isoprene concentrations increased significantly right after the IOPs, indicating that seasonal variations lead to an even stronger influence of biogenic emissions later in the summer. Measurements of concentrations at surface sites allow only limited conclusions on the influence of biogenic VOCs on regional chemistry, in particular at locations with a heterogeneous distribution of vegetation, as in the case of Verzago. Isoprene emissions are often dominated by single tree species. Therefore, flux measurements of VOCs, ideally representative for a large area, are required to assess the influence of biogenic emissions on regional chemistry.
Such flux measurements were the objective in the second experiment of this work, the field campaign within the OSOA (Origin and formation of secondary organic aerosol) project in southern Finland. The focus of OSOA was the investigation of processes leading to formation of secondary organic aerosol. Some of the biogenic VOCs are known to produce low volatile compounds upon oxidation which condense onto existing particles or may even form new particles.

VOC concentrations were measured throughout the planetary boundary layer by means of tethered balloons. Monoterpenes were the most important biogenic compounds over this

Boreal forest site. Mean mixed layer concentrations of total monoterpenes varied between 10 and 170 pptv, with α-pinene, limonene and Δ^3-carene as major compounds, isoprene was detected at levels of 2-35 pptv. From these measurements up to 1.2 km above ground, surface fluxes of biogenic VOCs were derived by a gradient technique and a boundary layer budget method. The resulting afternoon fluxes of monoterpenes varied between 180 and 300 $\mu g m^{-2} h^{-1}$. As a consequence, biogenic VOCs clearly dominated VOC-reactivity at this site.

A footprint-analysis was performed for determining the area of influence for these flux estimates. Depending on the method, the emissions are representative for areas of tens or hundreds of square kilometers. From differences in the results of the two methods it is concluded that emissions nearby are higher than on regional average. This is consistent with information from landcover data, which indicate higher biomass densities close to the site as compared to the regional average. Averaged fluxes derived from our measurements agree reasonably well with modeled biogenic emissions for the area.

The relation of monoterpene oxidation rates and aerosol formation was investigated with a photochemical box model. There was no evident link between monoterpene oxidation throughout the mixed layer and the increases in aerosol mass as observed at the surface. It indicates that biogenic VOC are not the limiting factor for the occurrence of new particle formation. The role of biogenic VOCs in these events therefore remains unclear. However, as chemical analyses of aerosols confirmed, local vegetation significantly contributes to the organic particulate mass, on average.

Tethered balloons were also used to perform first aerosol measurements throughout the mixed layer. The resulting particle profiles showed differing vertical trends for different particle sizes. The sizes relevant for new formation of particles (<100 nm) could not be measured on days with formation events. This type of information may be the missing piece for linking the monoterpene oxidation rates of the mixed layer with the aerosol observations at the surface. Future efforts at this site therefore intend to continue this type of measurements.

The results of both field experiments demonstrated the significance of vertically resolved information for the investigation of ozone and aerosol formation. Tethered balloons proved to be a suitable and cost-effective platform for acquiring such type of data.

Both experiments showed important influences of biogenic VOCs on ozone and aerosol formation. As biogenic VOC can account for a significant fraction of the carbon exchange of ecosystems, their investigation should be included in studies about carbon balance. Because VOC emissions from vegetation depend strongly on temperature and species composition, strong responses on potential changes in climate are expected. From the experience made in these experiments, more measurements on biogenic VOC emissions over seasonal time scales would be valuable. Oxygenated biogenic VOCs should be considered as well, which is now possible thanks to recent developments in measurement techniques.

Zusammenfassung

Die Biosphäre tauscht Spurengase mit der Atmosphäre aus, und übt damit einen bedeutenden Einfluss auf die Luftchemie aus. Bei den flüchtigen organischen Verbindungen (englisch: volatile organic compounds, VOCs) übertreffen die von Pflanzen freigesetzten Mengen die anthropogenen Emissionen global bei weitem. Im Rahmen von zwei grösseren Feldexperimenten wurde die Rolle der VOCs in der Bildung von Ozon und Partikeln untersucht. Dabei wurde den biogenen Quellen besondere Beachtung geschenkt.

Die Wirkungen der flüchtigen organischen Verbindungen in der Ozonproduktion wurden im Rahmen des Experiments PIPAPO (Pianura Padana Produzione di Ozono) in der Poebene erforscht. Ziel von PIPAPO war die Bestimmung der zeitlichen und räumlichen Ausdehnung der VOC- und NO_x-limitierten Ozonproduktion im Gebiet um Mailand.

Die Messungen fanden während zwei Sommersmog-Episoden im Mai und Juni 1998 statt. Bei typischen Wetterlagen, die zu Ozonepsioden führen, wird die Abluftfahne von Mailand nordwärts gegen die Alpen getrieben. Anhand der Messungen von Photooxidantien und verschiedener Vorläuferstoffe an zwei Bodenstationen 5 und 35 km nördlich von Mailand wurden die lokalen Ozonproduktionen berechnet und deren Abhängigkeit von den Konzentrationen der Stickoxide und VOCs bestimmt. Die Ozonproduktion bei der Messtation am Rande Mailands war stärker durch die Menge an VOCs bedingt (d.h. VOC-sensitiv). In Verzago, 35 km nördlich vom Stadtzentrum, wurde vorwiegend NO_x-sensitive Produktion gefunden, mit VOC-sensitiven Abschnitten bei Windlagen mit direkter Advektion der Abluft von Mailand.

Mittels Simulationen eines eindimensionalen photochemischen Modells wurden die Zusammenhänge zwischen lokaler Ozonproduktion und der regionalen Ozonverteilung untersucht. Es konnte gezeigt werden, dass die Ozonkonzentrationen in der Abluftfahne von Mailand während 4-5 Stunden durch VOC-Emissionen limitiert, und danach stärker durch Stickoxide beeinflusst sind. Die Ergebnisse verdeutlichen einige Punkte, die bei derartigen Analysen und Modellrechnungen beachtet werden müssen. 1) Die Verhältnisse am Boden sind nur bedingt repräsentativ für die für die Ozonproduktion relevante Mischungsschicht. Die Ozonproduktion am Boden ist tendenziell stärker VOC-sensitiv als im Rest der Mischungsschicht. 2) In chemischen Transportmodellen ist die Behandlung der vertikalen Mischung von zentraler Bedeutung für die Modellaussagen bezüglich VOC- oder NO_x-Sensitivität. Ungenügende vertikale Auflösung im Modell und zu starke vertikale Mischung ergeben stärkere NO_x-Sensitivitäten.

Es gibt deutliche Hinweise auf die Wichtigkeit der biogenen VOC-Emissionen für die Ozonbildung in der Poebene. Die VOC-Reaktivität in Verzago wurde dominiert von biogenem Isopren. Zudem stiegen die Isoprenkonzentrationen unmittelbar nach dem PIPAPO-Experiment deutlich an, was darauf hinweist, dass die biogenen Emissionen saisonal bedingt im Hochsommer noch an Bedeutung gewinnen. Konzentrationsmessungen am Boden erlauben aber nur beschränkte Aussagen auf die Auswirkungen biogener VOCs. Für eine vollständige Beurteilung des Einflusses biogener VOC wären Flussmessungen von VOCs nötig, am besten mit Methoden, die Aussagen über Emissionen einer möglichst grossen Region ermöglichen.

Solche VOC-Flussmessungen waren das Ziel im zweiten Feldexperiment dieser Dissertation, der Messkampagne im Rahmen des EU-Projekts OSOA (Origin and formation of secondary organic aerosol) im Süden Finnlands. Einige der biogenen VOCs werden in der Atmosphäre zu schwerflüchtigen Produkten oxidiert, die an vorhandenen Partikel kondensieren können. Möglicherweise können sie durch Nukleation sogar neue Partikel bilden.

Mit Fesselballonen wurden die Konzentrationen von VOCs bis in Höhen von 1,2 Kilometer gemessen. Die wichtigsten biogenen Verbindungen über dem Borealen Nadelwald waren

Monoterpene, wobei α-Pinen, Limonen und Δ^3-Caren den Hauptanteil ausmachten. Isopren wurde ebenfalls detektiert. Aus diesen Messungen wurden mit Hilfe einer Gradientenmethode und mit einem Budgetansatz die VOC-Emissionen der Vegetation berechnet., Für die Summe der Monoterpene ergab sich ein Emissionsbereich zwischen 180 und 300 $\mu g m^{-2} h^{-1}$. Damit wird die VOC-Reaktivität an diesem Ort klar von biogenen Verbindungen dominiert.

Mit einer Footprint-Analyse wurde die Fläche bestimmt, für welche diese Flussschätzungen repräsentativ sind. Je nach angewandter Methode zur Bestimmung der Emissionen gelten diese für eine Umgebung von einigen zehn oder hunderten von Quadratkilometern. Aus den Unterschieden wird gefolgert, dass die Emissionen in unmittelbarer Umgebung der Forschungsstation höher sind als im regionalen Durchschnitt. Dies ist im Einklang mit den Informationen aus Vegetationskarten, die eine höhere Biomassendichte in näherer Umgebung zeigen. Die durchschnittlichen Flüsse aus diesen Messungen stimmen gut mit modellierten biogenen Emissionen für das Untersuchungsgebiet überein.

Ein photochemisches Modell wurde benutzt, um die Beziehung zwischen der Oxidation biogener VOCs und der Bildung von Aerosolen zu untersuchen. Die Konzentrationen der Monoterpene in der Mischungsschicht und deren Oxidationsraten zeigten aber keinen offensichtlichen Zusammenhang mit den am Boden beobachteten Neubildungen von Partikeln. Die biogenen VOCs scheinen deshalb nicht der limitierende Faktor für das Auftreten von Partikelneubildungen zu sein. Auch wenn die Rolle der biogenen VOC in diesen Ereignissen weiterhin unklar bleibt, aus chemischen Analysen der Aerosole folgt, dass die lokale Vegetation im Durchschnitt deutlich zur organischen Partikelmasse beiträgt.

Die Ergebnisse aus beiden Feldexperimenten verdeutlichen die Wichtigkeit von vertikal aufgelöster Information für die Untersuchung der Ozon- und Aerosolbildung. Der Fesselballon erwies sich als taugliche und kostengünstige Plattform für die Erhebung solcher Daten.

Die beiden Experimente zeigten bedeutende Einflüsse biogener VOC-Quellen auf die Ozon- und Aerosolbildung. Weil die biogenen VOC-Emissionen einen signifikanten Anteil am Kohlenstoff-Austausch von Ökosystemen ausmachen können, sollten sie auch in Untersuchungen zur Kohlenstoff-Bilanz miteinbezogen werden. Aufgrund der starken Abhängigkeit der pflanzlichen VOC-Emissionen von der Temperatur und der Artenzusammensetzung sind starke Reaktionen auf mögliche Klimaänderungen zu erwarten. Aus den hier gemachten Erfahrungen wird empfohlen, künftige Untersuchungen zu biogenen VOC-Emissionen über längere Zeiträume anzusetzen. Dabei sollten neben Kohlenwasserstoffen auch oxidierte VOCs in die Untersuchung miteinbezogen werden, was dank neuartiger Messtechniken heute möglich ist.

1 Introduction

The air quality in many parts of the world is still not acceptable and often above limit values despite considerable efforts made to reduce the emissions of major pollutants. Among the pollutants exhibiting the most frequent violations of air quality standards are ozone and fine particles. Both adversely affect the health of humans and ecosystems and, furthermore, influence the earth's climate; tropospheric ozone as a greenhouse gas, and particles through their direct and indirect influence on incoming solar radiation (Figure 1).

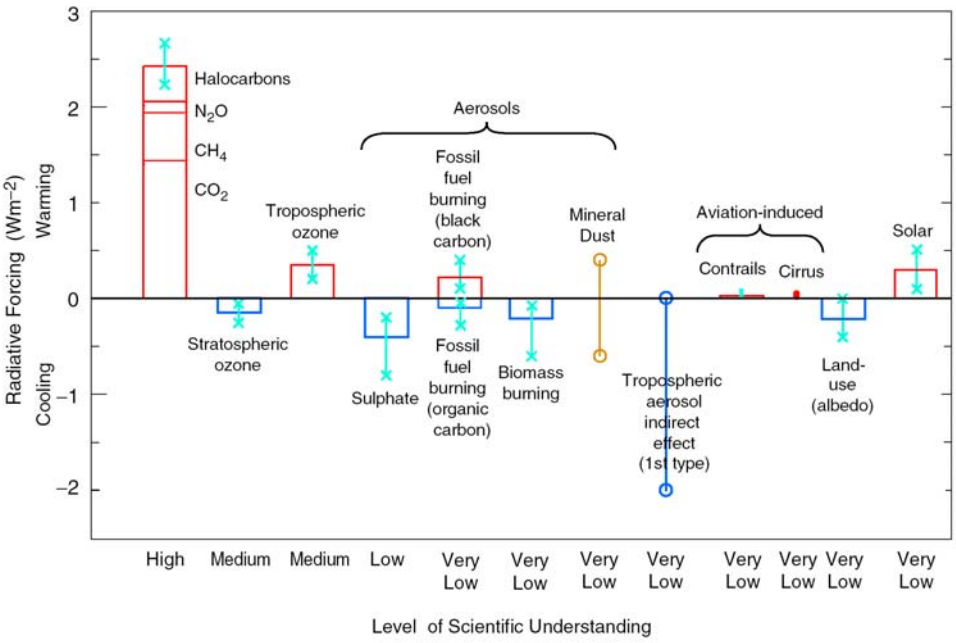

Figure 1: Global, annual mean radiative forcings (bars) of various constituents of the atmosphere (IPCC, 2001). Error bars are estimated uncertainties, mostly based on the range of published values.

As a consequence, strategies have been developed to reduce these pollutants. In both cases, for particles and ozone, a reduction is a complicated task, mainly because they are secondary pollutants (ozone) or have large secondary contributions (particles). Secondary pollutants are formed in the atmosphere upon reactions of directly emitted (primary) pollutants. The mitigation of secondary pollutants can therefore only be achieved indirectly, through reductions of their precursors.

It has been recognized for over 50 years, that ozone is produced from reactions of the precursors nitric oxides (NO_x) and volatile organic carbons (VOCs) if they are exposed to sunlight (Haagen-Smit, 1952). As ozone production is a complex process, depending in a non-linear way on the levels of VOCs and NO_x, it took a few decades of intensive research to gain a sufficiently quantitative understanding of ozone production. Table 1 gives an overview on the history of research on ozone pollution and its control.

With the improving understanding about tropospheric ozone production, it has been recognized that natural sources of VOCs also significantly contribute to ozone formation (Chameides et al., 1988; Trainer et al., 1987a). In the context of developing ozone reduction strategies, the need for information about the nature and control of biogenic VOCs emissions has greatly increased. Today it is known that biogenic VOCs by far surpass anthropogenic sources globally (Guenther et al., 1995). In non-polluted areas, the emissions of reactive biogenic VOCs reduce the levels of OH-radicals, the primary oxidizing agent of the atmosphere (Fehsenfeld et al., 1992; Trainer et al., 1987b). With this impact on the oxidative

capacity of the atmosphere, biogenic VOCs prolong the lifetimes of other substances with relevance for climate, e.g. methane (Poisson et al., 2000). In polluted areas, biogenic VOCs can significantly reduce the effect of anthropogenic VOC controls on ozone (Chameides et al., 1988). Biogenic VOCs, therefore, need to be considered in the development of ozone reduction strategies.

Table 1: Overview on the history of research on ozone pollution and its control.

Year	Milestone	Notes
1840	O_3 molecule discovered, O_3 presence in atmosphere documented	(Schönbein, 1840a,b; Schönbein, 1845)
1874	O_3 shown to be toxic to animals	(Andrews, 1874)
1940s	Photochemical smog found to be causing crop damage	(Middleton et al., 1950)
1950s	O_3 found to be major oxidant in photochemical smog, VOC and NOx shown to be O_3 photochemical precursors	(Haagen-Smit, 1952)
1961	Basic science of O_3 pollution documented in monograph	(Leighton, 1961)
1970	US Clean Air act of 1970: First national program for mitigation of O_3 pollution	
1970s	Initial O_3 reduction strategies tend to emphasize local VOC controls	
1979 (1983 implemented)	UN-ECE (United Nations Economic Comission for Europe Region) Convention on Long Range Transboundary Air Pollution (LRTAP)	Protocols on control of NO_x emissions (1988) and VOC emissions (1991)
1980s	Recognition of importance of biogenic VOCs in tropospheric ozone production	(Fehsenfeld et al., 1992; Trainer et al., 1987a)
1991	US National Research Council: Rethinking the Ozone Problem	(NRC, 1991)
1990s – present	Observation based approaches to characterize ozone production and its limitation. Linking ozone and particle formation	(Kleinman, 1994; Milford et al., 1994; Sillman, 1995) (Meng et al., 1997)

The recognition of the importance of biogenic VOCs contributed to a "rethinking of the ozone problem" (NRC, 1991), and resulted in a modified direction of ozone reduction strategies. While there was previously a tendency to emphasize VOC controls, this new direction saw a more balanced VOC/NO_x control strategy. A majority of more recent research on tropospheric ozone focuses on whether controls in VOCs or NO_x are more effective in reducing the ozone burden.

The EUROTRAC-2 (Transport and Chemical Transformation of Environmentally Relevant Trace Constituents in the Troposphere over Europe) subproject LOOP (Limitation of oxidants production) addressed this question for polluted areas in Europe. Within this project, the urban area of Milan was chosen as an important case study and the field experiment PIPAPO (Pianura Padana Produzione di Ozono) took place in 1998. The first part of this thesis covers the characterization of ozone production during ozone episodes at both local and regional scales and is based on the extensive measurements made during PIPAPO.

Episodes with high ozone levels are typically accompanied with high levels of fine particulate matter. The terms "fine particulate matter" and "aerosol" refer to tiny particles suspended in the air, often measured as the mass concentration of particles with an aerodynamic diameter

<10 µm, denoted as PM10. It has been found that concentrations of these particles in the air are at least as relevant for the health of humans as that of gaseous pollutants. The frequency of respiratory diseases often correlates with the exposure to elevated aerosol concentration (Schwartz et al., 1996).

The significant impacts of aerosols on health and climate are in contrast to a still limited understanding about origin, composition, and transformation processes of particles. A significant fraction of aerosols is of secondary origin, i.e. formed in the atmosphere by gas-to-particle conversion processes. Of this secondary matter, a large part is organic, which tends to be highest during severe urban smog episodes. Like ozone, secondary organic aerosol results from the atmospheric oxidation of reactive volatile organic gases. And, as in the case of ozone, both anthropogenic and biogenic VOC sources contribute to secondary organic aerosol (SOA). Globally, biogenic contributions are estimated to by far exceed the SOA of anthropogenic sources because 1) global emissions of biogenic VOCs are much higher, and 2) the mean fraction of biogenic VOCs converted to aerosols is higher than that of anthropogenic compounds. Figure 2 illustrates the significance of SOA from biogenic sources on the global organic aerosol content.

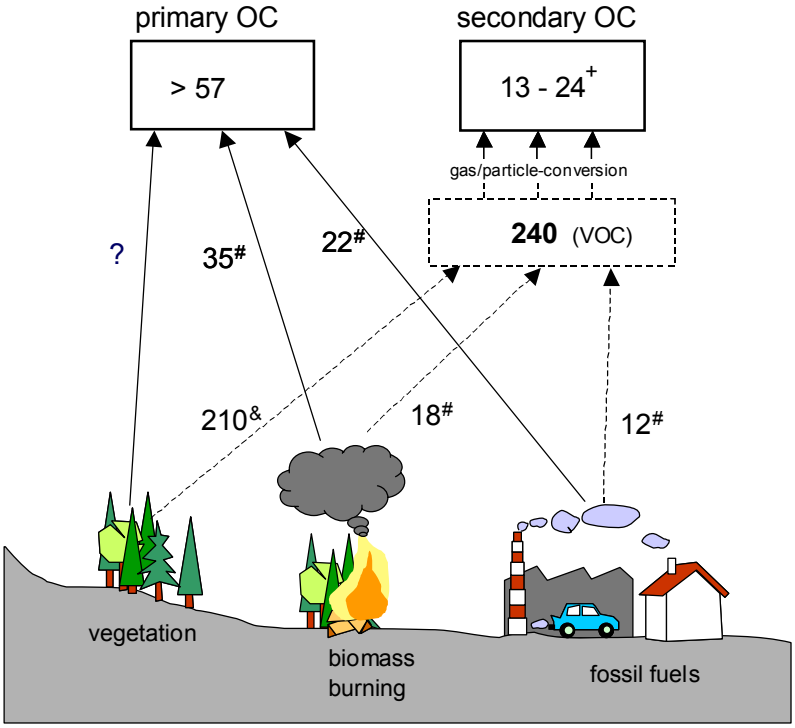

Figure 2: Overview on the global sources of organic carbon (OC) in particles, all numbers in teragrams (10^{12}g) of carbon. (+ Griffin et al. (1999), & Guenther et al. (1995), # IPCC (2001)).

These estimates have large uncertainties, as the current knowledge of chemical pathways and physical processes leading to secondary organic aerosols is still limited. The EU-project OSOA (origin and formation of secondary organic aerosol) was designed to fill some of these gaps. OSOA combined laboratory experiments and field studies with the goal to quantitatively understand the sources and formation mechanisms of secondary organic aerosols. The second part of this thesis encompasses my work in the OSOA field experiment at Hyytiälä in southern Finland. At this site, frequent events of particle formation have been observed throughout the last years, and biogenic VOC are believed to play a major role in these events. The objective of my work was the determination of VOC emissions at the regional level based on measurements of VOC concentrations by tethered balloons.

One common characteristic of the two major topics within this thesis is the task to describe larger-scale phenomena based on local observations. Information on a larger scale can be directly used as input for regional or global chemistry models. These models are currently used to make use of scientific knowledge in decisions on the political level.

1.1 Overview of the thesis

The core of the thesis consists of four papers that arose from my work in the two field experiments PIPAPO and OSOA. The articles for both experiments include one overview paper to which I contributed as co-author, and one paper I am responsible for as principal author. The papers about PIPAPO have been published in the Journal of Geophysical Research in 2002, the articles about OSOA are published in Atmospheric Chemistry and Physics Discussions (.

Chapter 2 provides background information for the main topics of the articles. It is thought as a complementary to the concepts described in more detail in the respective methods section of the papers. Where appropriate, these more theoretical parts are supplemented by some results of my work within the last years that have not been published yet.

Chapters 3 and 4 are the publications of the PIPAPO experiment, the overview (Chapter 3) and the article about VOC or NO_x limitation of ozone production in the Po Valley. The overview introduces the area of investigation, the basic approach of the field campaign as a whole, and summarizes the results of all collaborators. The second article (Chapter 4) characterizes the local ozone production at two observation sites in the Po Valley and relates these results to the regional ozone distribution with help of simulations with a one-dimensional photochemical model.

Chapters 5 and 6 comprise the papers about the OSOA study in southern Finland. The overview paper (Chapter 5) presents the measurement activities of all participating research groups, including the tethered balloon measurements I performed in collaboration with Alex Guenther and Jim Greenberg of the National Center for Atmospheric Research (NCAR) in Boulder, CO. In particular, Chapter 5 also contains the results of our particle measurements on the tethered balloon, which include particle profiles measured by a condensation particle counter. To our best knowledge, this type of measurement has not been made before.

The fourth paper (Chapter 6) discusses the measurements of biogenic VOCs by tethered balloons. These measurements throughout the planetary boundary layer are used to derive estimates of the regional surface fluxes of biogenic VOCs by applying a gradient method and a boundary layer budget approach. The link between biogenic VOC emissions and particle formation is investigated by calculations with a photochemical model. Oxidation rates of biogenic VOCs are interpreted in comparison to the observed increases of aerosol mass.

Chapter 7 summarizes the conclusions of both experiments and ends with a subjective outlook on future directions of research in the area of biogenic VODs.

2 Background

2.1 Tropospheric ozone formation

This section gives a brief overview on the most important processes leading to ozone formation in the troposphere. It is thought as a background and complement to the concepts introduced in more depth within paper I and II. More complete descriptions of the reaction scheme for the formation of tropospheric ozone can be found in (Atkinson, 2000; Finlayson-Pitts and Pitts, 2000; Seinfeld and Pandis, 1998). The last part of this section introduces the situation of the Po Valley, the area of investigation for papers I and II.

2.1.1 Photochemical ozone production

Ozone is produced from molecular oxygen and an oxygen atom (in electronic ground state, i.e. $O\ ^3P$)

$$O_2 + O + M \rightarrow O_3 + M \ (M=air). \qquad (R1)$$

The only source of atomic oxygen ($O\ ^3P$) in the lower troposphere is the photolysis of nitrogen dioxide (requiring light with wavelengths below 430 nm)

$$NO_2 + h\nu \rightarrow NO + O\ . \qquad (R2)$$

R1 is very fast and the ozone production is therefore determined by k_2=J_{NO2}, the rate of NO_2 photolysis. At sufficient levels of nitric oxides (NO_x = NO + NO_2), the major chemical pathway for removal of ozone is the reaction

$$O_3 + NO \rightarrow O_2 + NO_2\ , \qquad (R3)$$

which also reproduces NO_2. The sequence of R1 to R3 therefore results in no net ozone production, and as the interconversion of NO and NO_2 is fast, a photochemical equilibrium (PSS) is established. The ozone concentration in this steady state is given by

$$[O_3]_{PSS} = \frac{J_{NO_2}}{k_3} \cdot \frac{[NO_2]}{[NO]}\ , \qquad (1)$$

and is therefore a function of radiation (J_{NO2}) and the ratio of NO_2/NO. This relationship is not able to reproduce the ozone levels as encountered in urban areas, though. There is an additional process converting NO to NO_2 without consuming ozone, involving the second set of ozone precursors, the volatile organic compounds (VOCs). VOCs (denoted with the term RH, with R representing an organic rest) are oxidized in a process comprising a set of radical species (OH, RO, RO_2, HO_2). It can be described with following reactions:

$$RH + OH + O_2\ (+M) \rightarrow RO_2 + H_2O\ (+M) \qquad (R4)$$

$$RO_2 + NO \rightarrow RO + NO_2 \qquad (R5)$$

$$RO + O_2 \rightarrow HO_2 + CARB \qquad (R6)$$

$$HO_2 + NO \rightarrow OH + NO_2 \qquad (R7)$$

$$(2x)NO_2 + h\nu + O_2 \rightarrow NO + O_3 \qquad (R2)$$

$$\text{net: } RH + 3\ O_2 + h\nu \rightarrow CARB + 2\ O_3 + H_2O\ ,$$

where CARB stands for carbonyl compounds. Carbonyl compounds maybe further oxidized, leading to additional O_3 production, and finally end up as CO_2. The net reaction reveals that VOCs are consumed, while both radical species and NO_x act as catalysts. Figure 3 illustrates this in a simplified picture, leaving out organic peroxy radicals (RO_2).

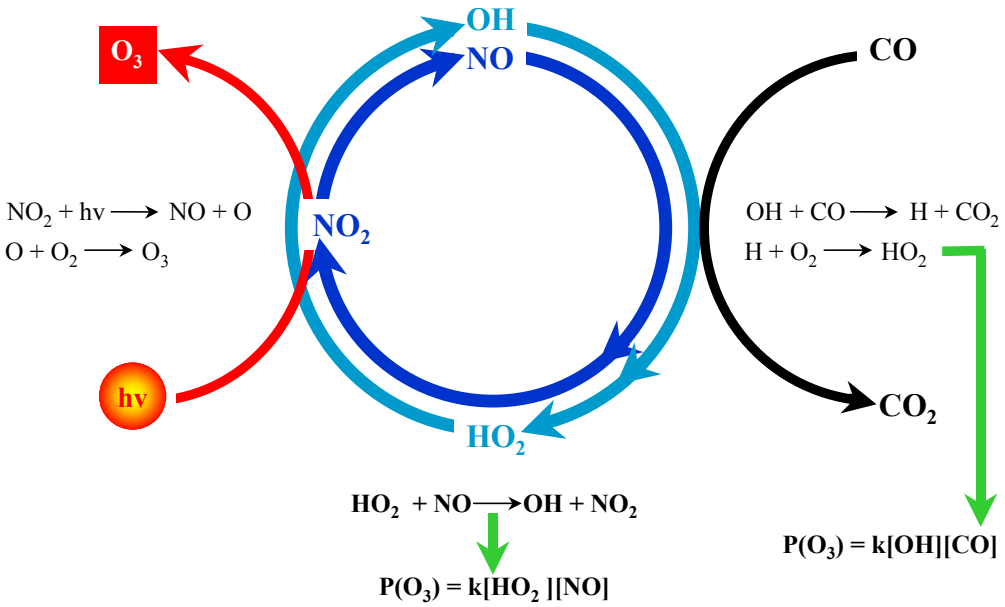

Figure 3: Scheme of ozone production with CO as a surrogate for VOC's. CO is consumed, NO_x and HO_x (OH + HO_2) are recycled.

Ozone formation can be approximated by the rate of reaction (R7) as subsequent NO_2-photolysis and reaction (R1) are fast and produce ozone with nearly a 100% yield. A second approximation for ozone production - valid under most lower tropospheric conditions except very clean situations - is the oxidation rate of CO with OH (Sillman et al., 1990; Sillman, 1995), also shown in Figure 4. [1]

Ozone production is therefore largely determined by the concentration of radicals. As the interconversion between different radical species is fast, a steady state assumption for OH, HO_2 and RO_2 can be made. The relative importance of radical sources and sinks provides a basis to qualitatively understand different regimes of ozone production.

Production of radicals occurs mainly through photolytic reactions:

$$O_3 + h\nu \rightarrow O(^1D) \qquad \text{(R8a)}$$

$$O(^1D) + H_2O \rightarrow 2\,OH \qquad \text{(R8b)}$$

$$HCHO + h\nu \rightarrow 2\,HO_2 \qquad \text{(R9)}$$

Sinks of radicals can be classified by two paths, L_N or L_R:

L_R (radical + radical reactions)

$$HO_2 + HO_2\,(+M) \rightarrow H_2O_2 + O_2\,(+M) \qquad \text{(R10a)}$$

[1] When considering not only CO, but also other hydrocarbons (RH), the approximations of ozone production is accordingly the sum of the rates (R5) and (R7), and the sum of CO- and RH-oxidation by OH, respectively.

$$RO_2 + RO_2 (+M) \rightarrow \text{organic peroxide} + O_2 (+M), \quad \text{(R10b)}$$

or

L_N (radical + NO_x)

$$OH + NO_2 (+M) \rightarrow HNO_3 (+M). \quad \text{(R11)}$$

In general, the rate of O_3 production can be limited by either VOC or NO_x. The existence of these two opposing regimes can be mechanistically understood in terms of the relative sources of radicals and NO_x (Kleinman, 1994). When the OH source is greater than the NO_x source, termination is dominated by L_R, i.e. formation of peroxides (H_2O_2+organic peroxides) >> than formation of HNO_3. In this case, NO_x is in short supply, and as a result the rate of O_3 production is "NO_x limited". On the other hand, when the OH source is less than the NO_x source, termination proceeds predominantly via L_N, and O_3 production is VOC limited.

Figure 4 shows ozone production as function of NO_x for various levels of VOCs. For a given level of VOC, the rate of ozone production will increase with increasing NO_x so long as NO_x is low. Eventually the rate of ozone production reaches a maximum value as the chemistry undergoes a transition from low-NO_x to high-NO_x conditions. At higher NO_x concentrations the rate of ozone production decreases with increasing NO_x but would increase with increasing VOC. The transition from low-NO_x to high-NO_x chemistry is associated with a specific ratio of VOC to NO_x. The exact transition depends on the speciation and reactivity of the VOC mix and not just on the absolute concentration of VOC.

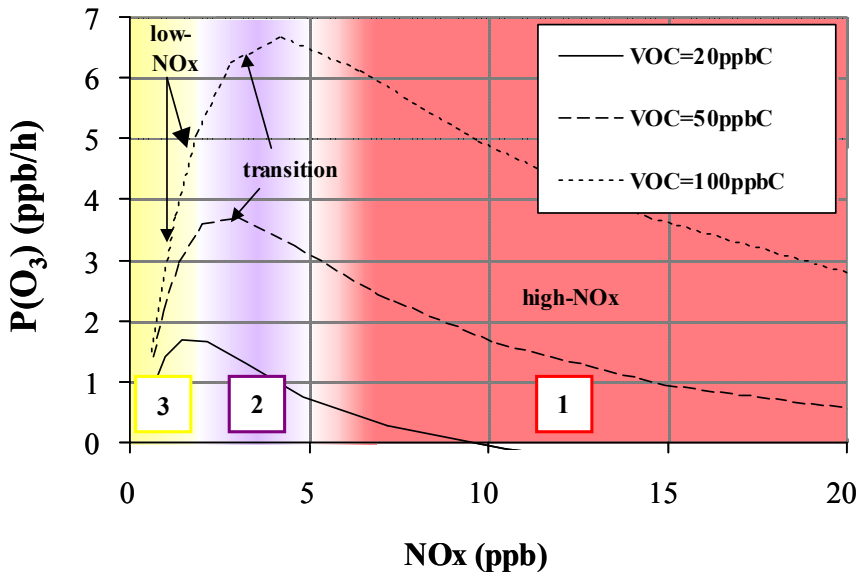

Figure 4: Net rates of ozone production (ppb per hour) as a function of NO_x (ppb), for VOC = 20 ppbC (solid line), 50 ppbC (long dashed line) and 100 ppbC (short dashed line), based on calculations shown in (Milford et al., 1994).

A general feature of the chemical aging of an air mass with a high load of pollutants (e.g. taken up over a large urban area) is also demonstrated within Figure 4. Air with fresh emissions very often starts in the high-NO_x region (label 1). As the air mass travels downwind from an urban area to a region with lower emissions, dilution and chemical reactions reduce the precursor concentrations. NO_x concentrations typically decrease more rapidly than VOC as the air mass ages, because NO_x has a relatively short photochemical lifetime. Thus, the ratio of VOC to NO_x increases as air masses age, and the air mass undergoes a transition from

high-NO_x to low-NO_x chemistry (label 2). The process of transition is hastened if the downwind region includes high emission rates of biogenic VOC, which also shift the VOC-NO_x ratio in the direction of low-NO_x chemistry (label 3). Individual situations vary greatly and there are many exceptions to this rule, but it frequently happens that air undergoes a transition from high-NO_x to low-NO_x chemistry as fresh emissions from an urban plume move downwind. Frequently an aged urban air mass will be recharged with emissions causing a flipping back from NO_x sensitive to VOC sensitive ozone production.

For the development of strategies to improve air quality, the basic question is how a change in precursor emissions VOCs and NO_x will affect the ozone concentration at any location of interest. This obviously complex question was addressed in the PIPAPO experiment for the case of the Po Valley in northern Italy and is coverd in papers I and II of this thesis.

2.1.2 The influence of VOC reactivity

Nearly all VOCs can contribute to photooxidant production, but the impact of the individual species on ozone formation depends on their reactivity (particularly the rate coefficient for their reaction with OH radicals) and their atmospheric degradation mechanism. Within the oxidation of a certain VOC, several steps with formation of peroxy radicals may be involved, which in turn oxidize NO molecules to NO_2 and finally produce O_3 (R1 and R2).

The contribution to ozone formation of a VOC emitted in a certain quantity at a certain place depends significantly on the ambient conditions (meteorology and concentrations of trace gases, particularly NO_x), as well as on the time scale over which the build up of ozone is followed. For example, highly reactive VOCs are most important near the location of their emissions, while the influence of less reactive VOCs will increase with the age of the air mass. The question how much a certain VOC contributes to ozone formation is rather complex, therefore.

The most common approaches to quantify the relative capability of individual VOCs to form ozone are based on simulations by photochemical models. One example is the 'Maximum Incremental Reactivity' (MIR) scale (Carter, 1995; Carter et al., 1995), another is the 'Photochemical Ozone Creation Potentials' (POCP) (Derwent et al., 1998). The MIR scale is based on an urban air quality model developed on the basis of smog chamber experiments. The POCP scale is based on a trajectory model at regional (European) scale. In both cases the increase of ozone due to an increase in the emission of a certain VOC is estimated under conditions with relatively high NO_x levels, where ozone levels are most sensitive to VOC emissions. Table 2 gives the ozone creation potentials according to the MIR scale. Biogenic compounds, isoprene in particular, belong to the most reactive VOCs on this scale. The position on the MIR is determined by the sum of kinetic reactivity (i.e. basically the reaction rate of the initial OH-oxidation) and mechanistic reactivity.

Some important mechanistic aspects that influence the ozone forming potential of a VOC are:

- The number of NO to NO_2 conversions caused immediately by the initial attack of OH on the compound.
- The reactivity of the primary degradation products with respect to the OH radical.
- Formation of reaction products that can provide additional significant radical sources by their photolysis (e.g. formaldehyde).
- Oxidation of olefinic compounds by O3 results in production of OH- and peroxy radicals (Paulson and Orlando, 1996), i.e. a possible mechanism of radical amplification.

Table 2: Ozone production potential of selected anthropogenic and biogenic VOCs. Data from (Carter, 1995; Carter, 2000).

Compound	Maximum Incremental Reactivity (MIR) (g O_3/ g VOC)
Carbon monoxide (CO)	0.057
Ethene	9.07
Propene	11.57
Benzene	0.81
Toluene	3.97
Formaldehyde	8.96
Acetaldehyde	6.83
Methanol	0.69
Isoprene	10.68
a-pinene	4.29
MBO	5.08
US urban mix	3.7

2.1.3 Ozone in the Po valley

Southern Switzerland exhibits the highest ozone concentrations in the country. As part of the BOCCALINO (**B**iogenic **O**rganic **C**arbon **C**ompounds as **L**eading **I**ndicators of **N**on – H_2O_2 Per**o**xides) campaign in 1994, extensive measurements at the ground and aboard an aircraft were performed in southern Switzerland. It was found that elevated O_3 concentrations were generally caused by advection of air from the adjacent area in northern Italy, the Po Valley (Prévôt et al., 1997). The urban area of Milan with its dense road network and large industrial areas provides high emissions of NO_x and VOCs. This source of high precursor emissions and frequent high-pressure weather situations lead to numerous episodes with high ozone levels. The measurement site in Southern Switzerland, about 40 kilometres away from the centre of Milan, was found to have a NO_x sensitive ozone regime (Staffelbach et al., 1997b), with isoprene as dominating VOC compound with respect to OH-reactivity. Based on these measurements it was concluded that emission inventories previously had underestimated biogenic VOC emissions by a factor of 5 (Staffelbach et al., 1997a).

The BOCCALINO results triggered the launch of PIPAPO as a next experiment in this area. In the efforts to investigate the limitation of ozone production in the Po Valley, the measurement sites were chosen closer to the urban area of Milan, in order to capture the expected transition of the VOC- to a NO_x-sensitive ozone production regime downwind of the city.

2.2 Secondary organic aerosol formation

Episodes with high ozone concentrations are typically accompanied by high loads of fine particles (Figure 5). Under these conditions, the levels of ozone or other secondary pollutants correlate well with aerosol concentrations while primary pollutants usually don't (Hering et al., 1998).

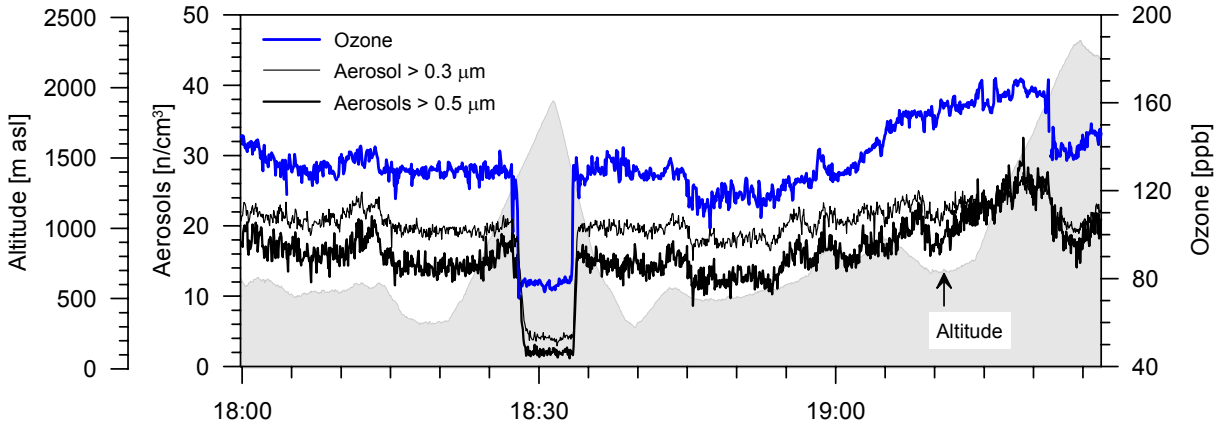

Figure 5: Measurements aboard the MetAir aircraft over the Po Valley on May 13, 1995. Ozone and aerosol concentrations show comparable patterns.

Intense photochemistry during high ozone episodes favors the formation of particles from gaseous precursors. On the other hand, high aerosol loads feed back on photochemistry by reducing radiation, thereby influencing photolysis rates and reducing the production of radicals. An important implication of the feedbacks between particulate matter and ozone production is, that the strategies to reduce these pollutants need to be considered as one task. Otherwise, measures to mitigate the aerosol burden may negatively influence ozone and vice versa (Meng et al., 1997), as a consequence of the high degree of coupling. One evident example of the linking between ozone formation and aerosols is the formation of secondary organic aerosol: VOCs are oxidized by OH, O_3 or NO_3 in the atmosphere. Some of the products formed in these reactions are of very low volatility and they can condense and form particulate matter. Aerosol produced in this way is referred to as secondary organic aerosol.

2.2.1 Gas-particle partitioning theory

Numerous smog chamber studies have proven the potential of certain VOC to form particles (Forstner et al., 1997; Grosjean and Seinfeld, 1989; Hoffmann et al., 1997; Pandis et al., 1991; Wang et al., 1992). From these results, a rule of thumb was derived stating that only compounds with 6 carbon atoms or more do form aerosols (e.g. Seinfeld and Pandis, 1998). Among anthropogenic VOCs, aromatic compounds have the highest potential for aerosol production, monoterpenes (see chapter 2.3.2) have been considered as the most important representatives among the biogenic compounds. There are indications that biogenic compounds like sesquiterpenes or long carbonyls may be at least as important as monoterpenes (Bonn and Moortgat, 2003). As a measure for the particle forming potential of a certain VOC, aerosol yields (Y) were defined as

$$Y = \frac{\Delta M(Aerosol)}{\Delta[VOC]} \quad \left(\frac{\mu g m^{-3}}{\mu g m^{-3}}\right), \qquad (2)$$

with ΔM being the organic aerosol mass produced, and ΔVOC the amount of reacted VOC.

As different experiments showed a great variety of aerosol yields for a certain compound, it has been recognized that these yields cannot be constant, but rather depend on the properties of preexisting aerosol.

The theory for describing secondary organic aerosol (SOA) yields is based on equilibrium partitioning of semi-volatile organic compounds into an absorbing organic aerosol mass (Odum et al., 1996; Pankow, 1994a,b). The equilibrium of a species *i* between the gas phase and an organic aerosol phase is described by (Bowman et al., 1997)

$$p_i = x_i \cdot \gamma_i \cdot p_i^0, \tag{3}$$

where p_i is the gas-phase partial pressure of species *i*, x_i is the mole fraction of species *i* in the organic aerosol phase, γ is the activity coefficient of species *i* in the aerosol-phase organic mixture, and p_i^0 is the vapor pressure of species *i* as a pure liquid (subcooled, if necessary). Or, expressing p_i as gas phase concentration G_i (from Ideal Gas Law),

$$G_i(\mu g m^{-3}) = \frac{p_i \cdot MW_i}{RT} \cdot 10^6 \tag{4}$$

(MW_i = molecular weight of *i* in gmol-1, *R*=ideal gas constant, *T*=temperature), we get

$$G_i = \frac{x_i \gamma_i p_i^0}{RT} MW_i \cdot 10^6 \tag{5}$$

The mole fraction of *i* in the absorbing organic aerosol phase is

$$x_i = n_i / n_{tot} = \frac{\frac{A_i}{MW_i}}{\frac{M_{om}}{MW_{om}}} \tag{6}$$

where A_i is the aerosol mass concentration of species *i*, and M_{om} is the absorbing organic aerosol mass concentration. Combining (5) and (6) yields

$$G_i = \frac{A_i MW_{om} \gamma_i p_i^0}{M_{om} \cdot RT}, \text{ or}$$

$$\frac{A_i}{G_i \cdot M_{om}} = \frac{RT}{MW_{om} \gamma_i p_i^0} = K_{om} \tag{7}$$

where K_{om} ($\mu^3 mg^{-1}$) is defined as the absorption partitioning coefficient of species *i* (Odum et al., 1996). The absorption partitioning coefficient incorporates vapour pressure, activity coefficient, and molecular weight, providing a single equilibrium parameter for each compound. K_{om} is analogous to a Henry's law coefficient in relating gas-phase concentrations of species *i* to the mass fraction of species *i* in the aerosol phase. An important implication of Equation (7) is that a greater fraction of each product must partition to the organic phase as the total organic aerosol concentration increases. K_{om} varies with temperature, as a consequence of the exponential temperature dependence of vapour pressures, i.e. K_{om} increases with decreasing temperature.

2.2.2 Predicting aerosol yields of VOCs

The low volatile products from VOC oxidation are subject to gas-particle partitioning. If partitioning coefficients for all oxidation products are known, the total SOA yield of a VOC can be calculated.

The aerosol fraction of an individual product is

$$A_i = K_{om} \cdot G_i \cdot M_{om}. \quad (8)$$

The mass balance constraint is

$$G_i + A_i = \alpha_i \cdot \Delta VOC, \quad (9)$$

with ΔVOC as the total amount of VOC reacted and α_i as the stoichiometric coefficient for the formation of product *i*. The Aerosol fraction of an oxidation product then becomes

$$A_i = \frac{\alpha_i M_{om} K_{om,i} \cdot \Delta VOC}{\left(1 + M_{om} K_{om,i}\right)}, \quad (10)$$

and the aerosol yield ($Y=A/\Delta VOC$) is the sum of the yields of individual products

$$Y = \sum_i Y_i = M_{om} \sum_i \left(\frac{\alpha_i K_{om,i}}{1 + M_{om} K_{om}} \right). \quad (11)$$

The overall yield is dependent on the organic aerosol mass and also on temperature, as a consequence of the temperature influence on the partitioning coefficients.

There are several difficulties in applying Equation (11) for predicting SOA yields of VOCs in practice. First, the stoichiometric coefficients for the oxidation reactions are assumed to be constant, whereas in practice they will vary in dependence of the concentration ratios of the oxidants. Furthermore, the knowledge about the oxidation pathways of many VOCs is far from complete; typically only part of the oxidation products are known. Even if the products are known, the determination of their partitioning coefficient is a problem of its own. It is likely that no information on vapour pressure are available for this compound. If the boiling point is known, vapour pressures can be estimated with fair accuracy (Schwarzenbach et al., 1993), but often the only information available is the structure of the compound. Vapour pressures derived from the structure of a compound (Fredenslund and Sorensen, 1994) are only order of magnitude estimates.

As a consequence, predictions of aerosol yields still have to rely on experimental data. However, some mechanistic information can be considered by including the dependence of aerosol yields on total organic aerosol mass, according to Equation (11). Aerosol yields observed in smog chamber experiments can adequately be described by Equation (12), with assuming two oxidation products (Odum et al., 1996).

$$Y = M_{om} \left(\frac{\alpha_1 K_{om,1}}{1 + K_{om,1} M_{om}} + \frac{\alpha_2 K_{om,2}}{1 + K_{om,2} M_{om}} \right) \quad (12)$$

Figure 6 shows the observed aerosol yields of smog chamber experiments with α-pinene and the corresponding fit with this two-product model. Such two-product parameters have been derived for a number of VOCs, both of anthropogenic and biogenic origin. Most important anthropogenic representatives for SOA are aromatic compounds (Odum et al., 1997a; Odum et al., 1997b), monoterpenes and sesquiterpenes exhibit the highest yields among the biogenic VOCs. As the yields depend on organic aerosol mass, biogenic and anthropogenic contributions to particles will strongly influence each other. Organic background aerosol (e.g. from biogenic VOC oxidation) can serve as an absorbing organic phase and therefore has a serious impact on the aerosol forming potential of anthropogenic precursors, and vice versa.

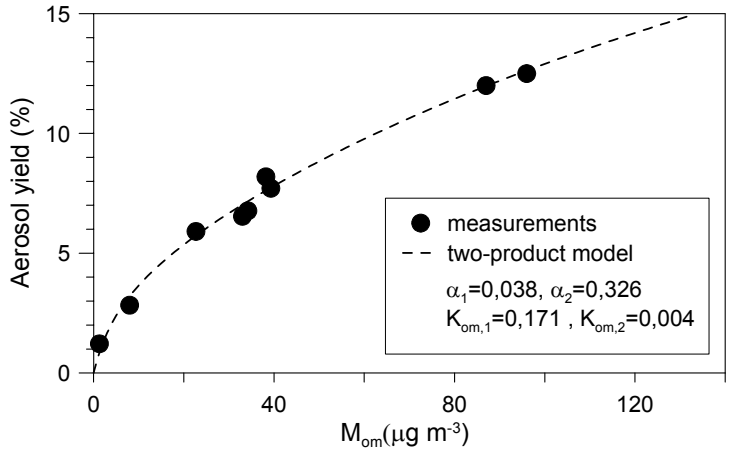

Figure 6: Aerosol Yields of a-pinene from smog chamber experiments and corresponding fit of the two-product model (Hoffmann et al., 1997).

The latest extensions to this gas-particle-partitioning theory include consideration of temperature and humidity effects. Higher relative humidity generally increases the aerosol yields of VOCs. It can be explained by gas-particle partitioning theory (Equations 7, 12) with the effects of increased humidity on MW_{om} (lowered by addition of H_2O to the organic phase) and on the activity coefficients γ (lowered for the often hydrophilic oxidation products) (Seinfeld et al., 2001). Aerosol yields at cold temperatures are higher, as a consequence of decreasing vapour pressures with lower temperatures (see Equation 7). They can be considered in the two-product model by assuming a temperature dependence of the vapour pressures that corresponds to those of the major oxidation product of the VOC of interest. For example, in the case of monoterpene oxidation (see 2.2.3), the temperature dependence of K_{om} is assumed analogous to that of the vapour pressure of pinonaldehyde (Andersson-Sköld and Simpson, 2001):

$$K_{om}(T) = K_{om,SC} \cdot \frac{\exp\left(-\frac{9525}{T_{SC}}\right)}{\exp\left(-\frac{9525}{T}\right)}, \qquad (13)$$

where the indices "$_{SC}$" denote K_{om} value and temperature of the smog chamber experiment.

The temperature dependence of aerosol yields is particularly interesting for the case of biogenic VOCs, as the emission of these precursors is strongly dependent on temperature as well (see 2.3.2). Figure 7 illustrates that the temperature dependencies of emissions and aerosol yields compensate each other to some extent, resulting in a relatively weak overall temperature effect of the product 'emissions × yield'.

The two-product approach is currently the state-of-the-art used in chemical transport models for predicting secondary organic aerosol formation. The results of such calculations show, that SOA from biogenic VOCs is a significant contribution to particulate mass, both at global and local scale. The global production of SOA from biogenic VOC is estimated to be 13 – 24 Tg y^{-1} (Griffin et al., 1999). In these calculations, temperature effects on the gas-particle partitioning were not considered. As temperatures according to the smog chamber experiments were used (room temperatures), the overall estimate can be qualified as conservative, as colder temperatures would favour SOA. Still, using this number, an average mass concentration of tropospheric organic aerosol in the order of 0.5 μg/m^3 was derived (Raes et al., 2000). While the uncertainty of this estimate is large, the magnitude represents an important contribution to typical free tropospheric aerosol concentrations.

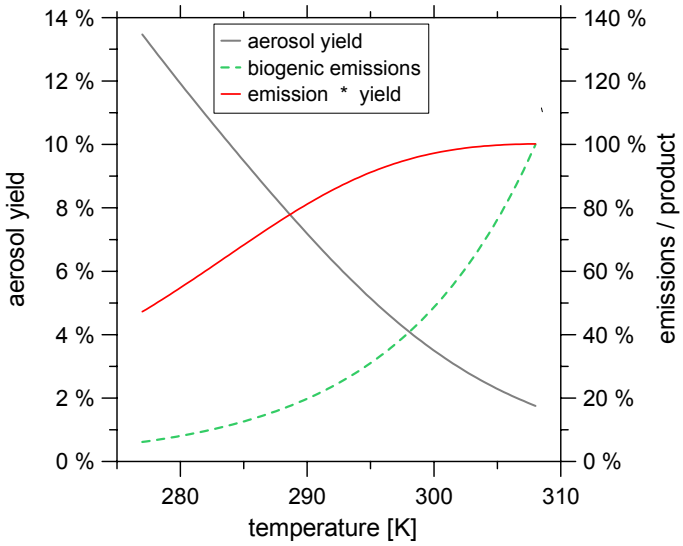

Figure 7: Temperature dependencies of aerosol yields (left axis), biogenic emissions, and their product (right axis). Left axis: Aerosol yield. The emissions and the product are plotted relative to their value at 308K (right axis).

In a model calculation with a gas-particle partitioning mechanism that included temperature effects, SOA accounted for up to 50 % of total aerosol mass in northern Europe. The contribution of SOA from biogenic VOC was far more important than that of anthropogenic sources (Andersson-Sköld and Simpson, 2001).

With a simplified approach based on this model, secondary organic aerosol formation for Switzerland was also estimated to be substantial (Spirig and Neftel, 2002). Relative to primary anthropogenic particle emissions, SOA from biogenic VOCs accounts for 8 % (annual average). During ozone episodes, however, secondary organic aerosol formed from the oxidation of biogenic VOCs may reach 25 % of anthropogenic particle emissions. As a consequence, the organic fraction of aerosols is largely influenced by biogenic VOC emissions under these conditions.

2.2.3 The role of organics in new particle formation

Smog chamber experiments are usually carried out at VOC concentrations in the order of high ppm (ppm=parts per million) mixing ratios. At these levels, oxidation products quickly reach saturation vapour pressure and will homogeneously nucleate (or immediately condense on impurities that may act as nucleating species?). The success of gas-particle-partitioning theory to predict aerosol formation in smog chambers is a consequence of the quick initial formation of an organic aerosol phase that can then act as an absorptive medium. At this point, absorption becomes the dominant mechanism governing the partitioning. As a certain amount of organic aerosol mass is nearly always present in the real atmosphere, it is expected that this mechanism is dominating the overall mass transfer from gaseous to particulate phases. The gas-particle-partitioning theory (Equations 7,11) is therefore a suitable approach for predictions of SOA from biogenic VOCs in the real atmosphere.

Another question is, if the oxidation of biogenic VOC just add to the tropospheric aerosol mass by condensation onto pre-existing particles or if they also contribute to the aerosol number concentration by nucleation of very low-volatile products. Events of new particle formation have been observed at various sites. Most of these locations were remote forested areas (Kavouras et al., 1998; Kulmala et al., 2000; Leaitch et al., 1999; Marti et al., 1997), thus an involvement of oxidation products from biogenic VOCs seems plausible.

For nucleation to occur, the gas phase concentration of the nucleating species has to exceed its equilibrium vapour pressure above the aerosol surface. Some of the oxidation products of monoterpenes may exhibit vapour pressures low enough to be possible candidates to act as nucleating species. Figure 8 shows some of the products that could be identified in reactions of ozone and OH with α-pinene. Compounds as the multifunctional carboxylic acids (pinic acid, norpinic acid, hydroxy pinonic acid) are expected to have extremely low vapour pressures.

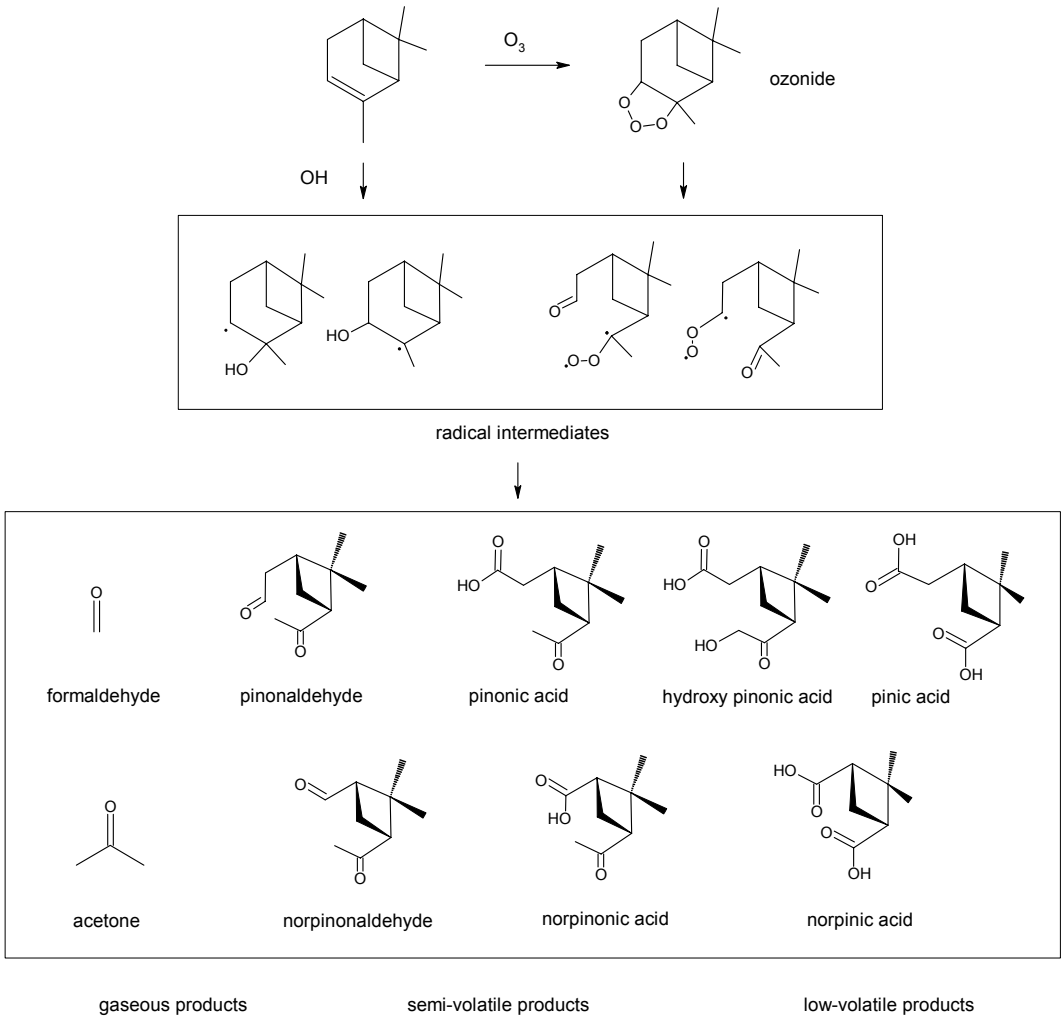

Figure 8: Major products of α-pinene after reactions with OH and O_3 (Hoffmann et al., 1997; Kamens and Jaoui, 2001; Nozière et al., 1999).

The OH- and O_3- reactions lead essentially to the same type of compounds in SOA. The major difference between these two oxidants is the product distribution. O_3 oxidation produces much higher yields of dicarboxylic acids and other low volatiles (totally 1%–9%) than does OH oxidation (totally 0.2%–0.6%) (Larsen et al., 2001). As ambient concentrations of monoterpenes are typically lower than 1 ppb, it is concluded that only the O_3-oxidation can produce condensable vapours in sufficient amounts to be an organic source for new particle formation (Bonn and Moortgat, 2002). The most probable scenario for nucleation from terpene oxidation product seems to be heterogenous nucleation, e.g. through the formation of clusters between different acidic and carbonyl products (Kavouras and Stephanou, 2002). Information about the chemical composition of particles below 10 nm would be needed to confirm these hypotheses. A first instrument allowing such measurements has recently been developed (Voisin et al., 2003a). However, first results from measurements during nucleation

events in an urban area have shown no indication of organic compounds on the smallest particles (Voisin et al., 2003b).

2.2.4 Heterogeneous organic chemistry

Secondary Organic Aerosol (SOA) has been defined as the organic aerosol mass arising from oxidized (primary) VOCs. The definition can be extended to also include that part of the organic aerosol mass originating from secondary reactions in the aerosol phase. There is increasing evidence for the importance of heterogeneous organic chemistry.

First experiments on the uptake of selected VOCs in liquid phases indicate, that the uptake of organics in cloud droplets may be significantly enhanced through further oxidation of the compounds in the aqueous phase (Nozière et al., 2001). There is also evidence on the importance of acid catalyzed reactions of carbonyl compounds in aerosols. The thermodynamic gas-particle-partitioning theory (2.2.1) does not account for heterogeneous reactions. Such processes will decrease the concentration of carbonyls in the aerosol phase, and consequently more carbonyls from the gas phase will be absorbed in order to re-establish partitioning equilibrium. Smog chamber experiments with addition of an acid catalyst demonstrated multifold increases in SOA yields for a number of hydrocarbons (Jang et al., 2002). Under acidic conditions in aqueous aerosols, even oxidation products of lighter hydrocarbons (such as isoprene, for example) can contribute to SOA formation through this mechanism. Sources of atmospheric acids are H_2SO_4 and HNO_3, ultimately associated with the burning of fossil fuels. It is therefore believed that scenarios for high concentrations of inorganic acids are coincident with high SOA formation. Future research needs to consider both inorganic and organic constituents for an accurate explanation of SOA formation. First estimates on the influence of heterogeneous reactions on the total amount of SOA formed indicate, that the already high biogenic contribution as estimated by Griffin et al. (1999) may be low by a factor of two (Kamens et al., 2003).

2.3 Biogenic VOC emissions

The biosphere and plants in particular emit large quantities of reactive organic compounds into the atmosphere. The number of different compounds is estimated to be in the order of several thousands, though only a smaller number is emitted at rates that significantly influence the chemical composition of the atmosphere. Table 3 shows a summary of the major biogenic non-methane volatile organic compounds (VOCs) and their primary sources, demonstrating the dominance of plants in these emissions. Not included in this list are the compounds that are found in flower scent emissions, like alkanes, alcohols, esters, aromatics, nitrogen compounds and sesquiterpenes. These emissions are less significant in the annual budget, but may be important at local scale at certain times.

Table 3: The major biogenic VOCs, data are taken from (Guenther et al., 1995; Rudolph, 1997; Singh and Zimmerman, 1992)

Species	Primary source	Estimated annual global emission (Tg C)
Isoprene	Plants	175 – 503
Monoterpene family	Plants	127 – 480
Other reactive VOCs (e.g. acetaldehyde, 2-methyl-3-buten-2-ol (MBO), hexenal family)	Plants	~260
Other less reactive VOC, (e.g.. methanol, ethanol, formic acid, acetic acid, acetone)	Plants	~260
Ethene	Plants, soils, oceans	8 – 25

The sources of isoprene, monoterpenes and ethene have been investigated extensively and emissions of these species can be predicted with some confidence by biogenic emission models. Much less is known about the controlling factors of the other biogenic VOC emissions, but based on a growing number of measurements their total emission rates are expected to reach similar magnitudes as that of isoprene.

The following chapters give an overview on the most common biogenic VOCs, their sources, the controlling variables of emission, and – where known - their roles in plant physiology and ecology (Fall, 1999).

2.3.1 Isoprene

Isoprene (2-methyl-1,3-butadiene) is the single most common VOC emitted by plants. The majority of the strong isoprene emitting plants are woody species; only a few crop species produce isoprene. Isoprene is produced in many plant families, but there are many cases where a family has both emitters and non-emitters. For example, while all North American species within the oak genus are high isoprene emitters, many European oaks emit monoterpenes rather than isoprene (Bertin et al., 1997). A clear phylogenetic basis for distinction of isoprene emissions in plants has not been found (Harley et al., 1999). With very sensitive measurement techniques, however, even species formerly known as non-emitters were shown to release small amounts of isoprene. It may therefore be true in the strictest sense that most plants emit isoprene.

Although isoprene emissions from plants were discovered as early as in the 1950s (Sanadze, 1957), the reason why plants allocate 1-2% (in certain situations more than 20%) of their C-

fixation to the production of isoprene remains under discussion. One hypothesis explains isoprene's role as a protectant for the photosyntesis apparatus at high temperatures (Sharkey and Singsaas, 1995). Several experiments confirmed a thermoprotective role of isoprene in plants. However, conflicting observations indicate that this hypothesis may not be the definitive explanation (Logan and Monson, 1999).

Isoprene is produced in the chloroplasts by an enzyme (isoprene synthase) exhibiting light- and temperature-dependent activity. A common algorithm to describe its emissions uses a basal emission rate (ε) at standard conditions times an emission activity coefficient (γ_{LT}), which is a product of a light-(C_L) and a temperature-dependent (C_T) factor (Guenther et al., 1999; Guenther et al., 1993):

$$\text{Emission} = \varepsilon \cdot \gamma_{LT} = \varepsilon \cdot C_L \cdot C_T \tag{14}$$

$$C_L = \frac{\alpha \cdot c_{L1} \cdot L}{\sqrt{1+\alpha^2 L^2}} \tag{14a}$$

$$C_T = E_{opt} \cdot \frac{\exp \frac{c_{T_1}(T - T_{opt})}{RT_S T}}{1 + \exp \frac{c_{T2}(T - T_M)}{RT_{opt} T}} \tag{14b}$$

with the empirical coefficients α (=0.0027), c_{L1} (=1.066), c_{T1} (=95'000 J mol^{-1}), c_{T2} (=23'000 J mol^{-1}) and T_M (=314 K), R (ideal gas constant, =8.314 J K^{-1} mol^{-1}), and L= photon flux of photosyntethically active radiation (PAR) (µmol m^{-2} s^{-1}). E_{opt} is the maximum normalized emission capacity, T_{opt} is the temperature, at which E_{opt} occurs. The emission activity as function of light and temperature is illustrated in Figure 9.

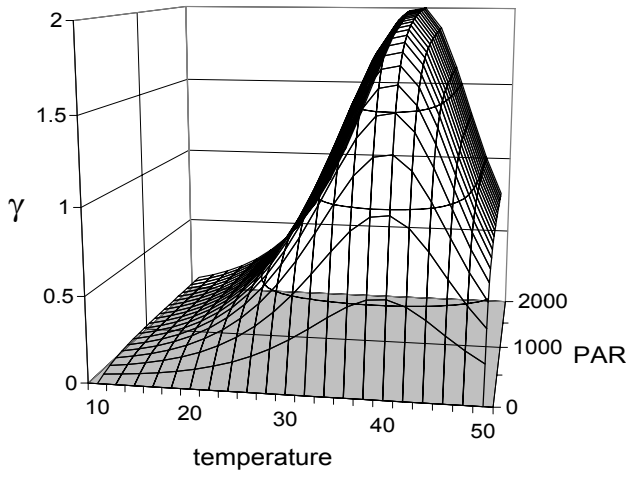

Figure 9: Light- and temperature dependence of isoprene emissions, with E_{opt}=1.9 and T_{opt}=39.5.

This algorithm can sufficiently describe the variation of isoprene emissions at time scales of hours, but it has been found that other factors, such as leaf age or the environmental conditions the plant has been exposed to over the last few days, play a major role as well (Guenther, 1997; Harley et al., 1997; Petron et al., 2001). Young and old leaves emit isoprene at much lower rates than middle-aged leaves, and emissions are strongly dependent on

temperature variations on time scales of days to weeks. These longer-term influences have been incorporated into the newest version of emission algorithms. Long term temperature variation is considered with a correction factor to emission capacity E_{opt} and optimum temperature T_{opt}, in dependence of the mean temperature of the past 15 days, T_d (Guenther et al., 1999):

$$E_{opt} = 1.9 \cdot \exp\left(0.125\left(T_d - 301\right)\right) \quad (15a)$$

and

$$T_{opt} = 312.5 + 0.5\left(T_d - 301\right). \quad (15b)$$

2.3.2 Monoterpenes

Monoterpenes are C_{10} compounds with a great structural diversity: more than 1000 different structures have been determined. However, only few of them are emitted by plants in amounts that are significant for atmospheric chemistry (Geron et al., 2000). The structures of the most commonly emitted terpenes are shown in Figure 10.

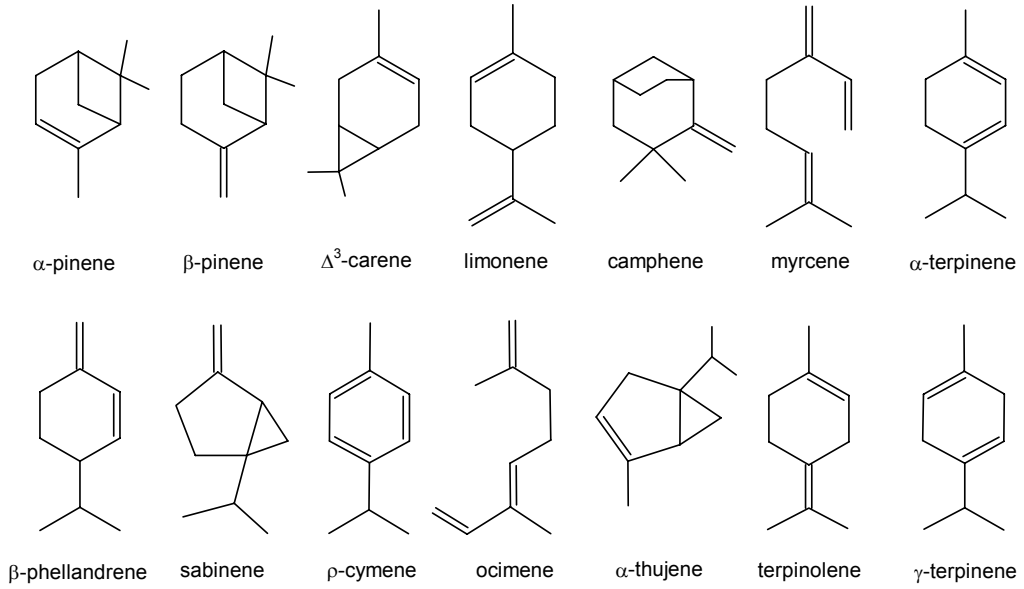

Figure 10: The 14 most commonly emitted monoterpenes from vegetation.

Monoterpene-emitting plants produce a whole mixture of them, however one or two terpenes often dominate this mixture by over 80%. Monoterpenes are often stored in specialized structures of the plants, such as resin ducts (pines) or leaf storage cavities (eucalypts). The role of monoterpenes is as diverse as their structures. Among the ecological functions are defence against herbivores and attraction of pollinators. For example, the rosin of conifers is composed of monoterpenes and diterpene resin acids, both of which are toxic to insects and funghi.

As a consequence of the storage of these compounds, the release of monoterpenes is at least partially a function of their vapour pressure and therefore strongly depends on temperature. However, the increase with temperature is stronger than that of vapour pressure, indicating that other factors are involved as well. Monoterpene emissions can be described as

$$\text{Emission} = \varepsilon \cdot \exp\left(\beta \cdot \left(T_S - T\right)\right) \quad (16)$$

Where ε is again the emission at reference conditions, T_S is the reference temperature and β is an empirical coefficient. (Guenther et al., 1993) found a β value of 0.09 as an average to properly describe the monoterpene emissions of a variety of species.

A few plants emit monoterpenes in both light- and temperature dependence. Regionally important representatives of this class are Mediterranean oaks (e.g. *Quercus ilex*) (Ciccioli et al., 1997; Simpson et al., 1999; Staudt and Seufert, 1995). Quercus ilex shows monoterpene emissions with similar dependences on light and temperature as isoprene emissions and is therefore best predicted with the algorithm in Equations (15).

The temperature response of terpene emissions is of particular significance for their role in secondary organic aerosol formation (Figure 7 in chapter 2.2.2.). Aerosol yields and emissions of monoterpenes exhibit inverse trends with temperature. Aerosol formation from monoterpenes may therefore be important even at low temperatures. Emission estimates for these conditions are highly uncertain, however, as the experiments for deriving emission algorithms and basal emission rates are usually carried out at higher temperatures. In order to look at emissions over a large temperature range, an experiment with typical plants for European coniferous forests was performed at the laboratory of the Biosphere-Atmosphere-Interaction project at the National Center for Atmospheric Research (NCAR). Two trees of Norway Spruce (*Picea abies*) and two Scots Pines (*Pinus sylvestris*) were placed in a climate chamber. By means of 6 cuvettes enclosing sinlge branches, monoterpene emissions of these trees were measured with a gas chromatograph. The climate chamber was held at temperatures between 0 to 30 degrees Celsius. As a summary, the emissions of α-pinene, the most commonly emitted monoterpene from both trees, are plotted against leaf temperature in Figure 11. The results demonstrate that the temperature dependence above and below 15°C is not significantly different. It therefore supports the hypothesis that emission of terpenes from conifers may be of importance for aerosol formation even at cold temperatures. Of course, seasonal effects also need consideration, but a recent report of seasonal measurements in northern Europe confirmed monoterpene emissions even at wintertime (Hakola et al., 2003).

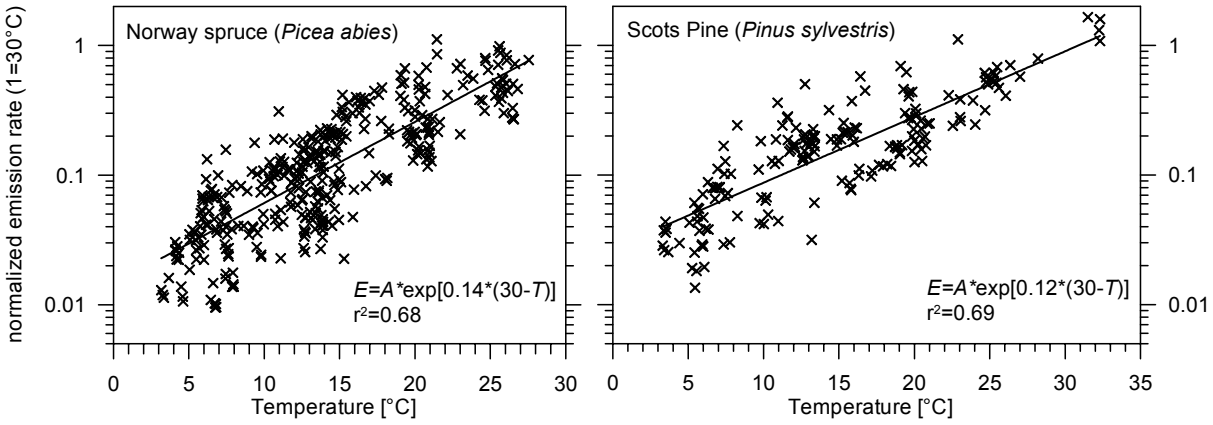

Figure 11: Standardized emission rates versus cuvette temperature from Norway Spruce (4 cuvettes / 365 measurements) and Scots Pine (2 / 185).

Another aspect of these results is the considerably different temperature dependency of these emissions as compared to that recommended by (Guenther et al., 1993) in Equation 16. Other recent experiments on emissions of these trees (Komenda and Koppmann, 2002, Hakola et al., 2003) also found higher exponential factors (β) than 0.09. A higher β factor has important implications for modeling monoterpene emissions. As emissions are calculated in relation to a standard emission rate at 20-30°C, a higher β factor particularly influences emission calculations for regions with relatively cool temperatures. Models assuming a β of 0.09 may

significantly overestimate the emissions in these areas. On the other hand, the model will underpredict emissions at leaf temperatures above the reference temperatures. In perspective of secondary organic aerosol formation, a higher β factor will steepen the slope of the curve "emissions · aerosol yields" in Figure 7. Therefore, model calculations of SOA from biogenic VOCs need to consider the appropriate β factor. Using the value of 0.09 in areas with conifers as dominating tree species may therefore overestimate the significance of SOA from biogenic VOCs at cold temperatures.

2.3.3 Oxygenated compounds

There is a variety of oxygenated VOCs detectable in plant emissions. While the emission rates of single species may be relatively small, their sum reaches the same magnitude as those of isoprene or monoterpenes (Table 3). Oxygenated VOCs in the C_1 to C_3 range have been found as dominant VOC components in forest air at several places (Goldan et al., 1995; Karl et al., 2002). Most abundant are methanol, acetone and acetaldehyde; other investigations found also formic and acetic acid as emissions from European oaks and pines (Kesselmeier et al., 1997). The regulation of production of these C_1-C_3 oxygenated VOCs is still poorly understood with the exception of the emissions of ethanol and acetaldehyde related to well known fermentation processes, e.g. in the roots during anoxic conditions due to flooding (Kreuzwieser et al., 1999). However, ethanol and acetaldehyde emissions have also been seen in fairly dry areas where this mechanism is unlikely to be of importance, suggesting other, yet unknown mechanisms. Methanol is an abundant emission from a variety of plants. Continuous emissions have been found in many ecosystems, including forests and grasslands (Fukui and Doskey, 1998; Holzinger et al., 2000; Karl et al., 2002; MacDonald and Fall, 1993; Nemecek-Marshall et al., 1995; Sharkey, 1996). Methanol and acetone are frequent intermediates of the plant metabolism and found in many tissues of the plants (Fall and Benson, 1996). Therefore these compounds are also released after leaf wounding, or in decomposing plant matter (Warneke et al., 1999).

Another set of oxygenated compounds released mainly after leaf wounding is a group of C_5-C_6 compounds, referred to as the "hexenal family" (Hatanaka, 1993). Virtually all plants seem to produce these compounds (Hatanaka et al., 1987), of which (2E)-hexenal and (3Z)-hexenol are the most important, easily sensed in the typical odor of cut grass.

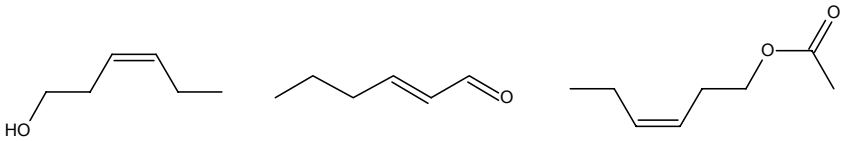

cis-3-hexenol trans-2-hexenal cis-3-hexenyl-acetate

Figure 12: Compounds emitted after leaf wounding

Various compounds of the hexenal family have antibiotic properties. (2E)-hexenal for example inhibits a variety of protozoa, fungi, insects and mites (Croft et al., 1993), supporting the explanation of their physiological role as unspecific defensive agents. Emissions of these compounds have been measured after cutting of grass (Fall et al., 1999; Karl et al., 2001), but also from leaf trees, usually in connection with leaf damages (Hakola et al., 2001).

A compound that is emitted in a similar fashion to isoprene, i.e. light and temperature dependent, is 2-methyl-3-buten-2-ol (MBO). This species is emitted by some of the most common North American pine species (Baker et al., 1999; Harley et al., 1998), and has been found as dominating VOC compound over corresponding forest sites. Explanations for the role of this

emission go in the same direction as those for isoprene, i.e. enhancing thermotolerance of photosynthetic activity (Gray et al., 2003). So far, MBO emissions have not been reported for European tree species.

2.3.4 Modeling biogenic emissions

Global and regional 3D-chemistry and transport models are the current tools of choice for developing effective measures for local and regional air quality. These models require best estimates of VOC emissions, both from anthropogenic and biogenic sources. For regional chemical transport models, emission information is required at spatial scales of tens to hundreds of square kilometres.

Current approaches for predicting biogenic emissions on regional levels start with assigning average emission capacities to landscapes based on species composition and biomass density. These basal emission capacities are then modulated by the environmental parameters that control the emissions (e.g. light and temperature) under consideration of the canopy environment. Trace gas emissions from vegetation is calculated as (Guenther et al., 2000)

$$\text{Emission} = \varepsilon \cdot D_p D_f \cdot \gamma_L \gamma_T \gamma_A \cdot \rho \qquad (17)$$

where ε is the landscape average emission capacity, D_p is the annual peak foliar density, D_f is the fraction of foliage present at a particular time of the year, the γ factors account for the influence of radiation, temperature and leaf age (described in (Guenther et al., 1999)), respectively, and ρ is an escape efficiency that represents the fraction emitted by the canopy that reaches the above-canopy atmosphere. Biogenic emission models therefore depend on the quality of landcover data and on accurate estimates of plant leaf biomass. Considerable uncertainties are associated with estimates for emissions induced by leaf wounding. Usually they are considered with a basal emission rate that is equal for all plant species and assumed temperature-dependent according to Equation (16). An overall uncertainty of a factor of three is reasonable for modelled biogenic emissions, but can be much higher for regions with sparse data availability (Guenther et al., 2000).

Emission measurements are needed for the validation of such models. Of particular value is a combination of techniques to obtain this information on different spatial scales. Enclosures provide data on the leaf-level, micrometeorological techniques give information at the canopy scale. The boundary layer budget and mixed layer gradient approaches deliver flux estimates representative on landscape scale. While information on this scale is directly usable as inputs for regional or larger scale models, it usually has to live with greater uncertainties due to various assumptions included. Paper IV discusses the application of such large-scale methods for estimating fluxes at a Boreal forest site in Finland.

2.3.5 Biogenic VOCs in Switzerland

The base of experimental data on biogenic VOCs in Switzerland is poor. Significant amounts of isoprene were measured in southern Switzerland as part of a field experiment in 1994 (Staffelbach et al., 1997a). Isoprene plays a major role for ozone formation in this part of Europe (Staffelbach and Neftel, 1997). However, total biogenic VOC emissions in Switzerland are dominated by monoterpenes, as coniferous forest accounts for the major part of the total biomass. As a consequence of the limited measurements of biogenic VOCs in Switzerland, the estimates for annual biogenic VOC emissions cover a wide range, from 17’000 t/year to 87’000 t/year (Andreani-Aksoyoglu and Keller, 1995; Simpson et al., 1999). A newer estimate reports an annual emission of 50’000 tons biogenic VOCs, with monoterpenes

as the dominating class (35'000 t), methanol and other oxygenated compounds 10'000 to 15'000 tons, and isoprene 3'000 tons (Spirig and Neftel, 2002).

This number is significantly lower than that of anthropogenic VOC emissions (190'000 t/year), but as a consequence of the aerosol forming potential of monoterpenes and the high reactivity of isoprene they still have an important impact on local air chemistry.

2.3.6 Biogenic VOCs and climate change

As mentioned in the introduction, the oxidative capacity of the atmosphere is significantly influenced by the amount of biogenic VOC emissions. The lifetime of long-lived compounds with relevance for the Earths' radiative balance, such as CH_4, are therefore affected by biogenic VOC emissions (Poisson et al., 2000). Furthermore, natural VOC emissions represent significant fractions of the carbon balance in many ecosystems. Terrestrial ecosystems fix 120 Pg C (Pg=10^{15}g) per year by assimilation of CO_2 (=Gross Primary Production, GPP). Subtracting plant respiration (60 Pg y^{-1}, = autotrophic respiration, R_a) and the amount of C lost through decomposition of plant matter and soil (50 Pg y^{-1}, = heterotrophic respiration, R_h) leaves 10 Pg C y^{-1} net ecosystem production (NEP) (IPCC, 2001). The global biogenic VOC emissions (1150 Tg C y^{-1}, Guenther et al., 1995) are therefore in the order of 12% of global NEP. However, the actual carbon transfer from terrestrial biomass to the atmospheric CO_2 reservoir by biogenic VOCs is difficult to assess, as not all VOCs end up as CO_2 and may be redeposited directly or after transformations to different organic compounds (Figure 12). Current knowledge about biogenic VOC sources and their reaction pathways in the atmosphere is not sufficient to accurately quantify the fraction of biogenic VOC carbon returning to the biosphere. But it is estimated that more than 75% of carbon released as biogenic VOC will end up as CO_2, i.e. about 1 Pg y^{-1} (Guenther, 2002).

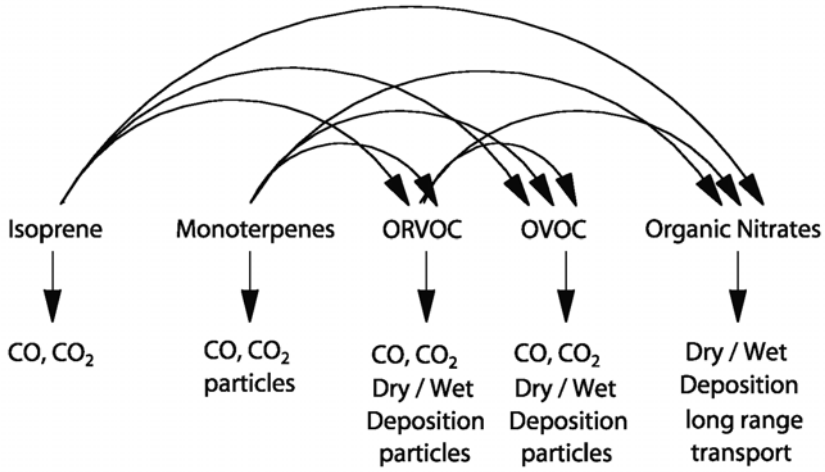

Figure 12: The fate of biogenic VOC emissions, in a schematic view from (Kesselmeier et al., 2002). VOCs can end up as CO_2 or can be transformed to other compounds (other reactive (ORVOC), or less reactive VOCs (OVOC)), which may be subject to deposition.

Biogenic VOC emissions therefore represent a substantial loss of biologically fixed carbon in terrestrial ecosystems. Furthermore, the carbon losses through biogenic VOC emissions are expected to be highly sensitive to future changes in climate. An obvious reason is their strong dependence on temperature, but landcover changes may also dramatically influence the emissions. An evident example is the conversion of forest into agricultural areas. Or, as observed in an area north of Montpellier in southern France, wooded surfaces increased dramatically from 15 % to 60% at the cost of shrublands between 1945 and 1980. The influence of this land use change on monoterpene emissions is dramatic, possibly a 4-fold

increase (Schaab et al., 2000). As biogenic VOC emissions of a certain ecosystem strongly depend on its species composition, even less dramatic changes in vegetation distribution may significantly alter the release of VOCs. It is therefore important to consider biogenic VOC emissions as part of carbon balance studies, especially in the context of global climate change scenarios.

3 Paper I, Overview on the PIPAPO experiment

Sensitivity of photooxidant production in the Milan Basin. Results from a EUROTRAC-2 LOOP field experiment. An overview.

Albrecht Neftel and Christoph Spirig,
FAL Liebefeld-Reckenholz , CH - 3003 Bern, Switzerland

André S.H. Prévôt, and Markus Furger,
Laboratory of Atmospheric Chemistry, Paul Scherrer Institut, CH -5353 Villigen, Switzerland

Jochen Stutz,
Dept. Atmospheric Sciences, UCLA, 7127 Math Sciences, Los Angeles, CA 90095-1565

Bernhard Vogel,
Institut für Meteorologie und Klimaforschung Forschungszentrum Karlsruhe/Universität Karlsruhe D -76021 Karlsruhe, Germany

Jens Hjorth,
Joint Research Centre, Environmental Institute, I-21020 Ispra, Italy

Journal of Geophysical Research, 107 (D22), art.nr. 8188, 2002.

Abstract

The international field experiment Pianura Padana Produzione di Ozono (PIPAPO) studying the VOC / NOx ozone production sensitivity took place in May and June 1998 downwind of the metropolitan area of Milan. The project was embedded in the framework of the EUROTRAC-2 LOOP (Limitation of Oxidant Production) subproject. Several ground stations between the city of Milan and the Alps north of Milan combined with airborne measurements delivered a comprehensive data set suitable for observation based analysis and validation of Chemical Transport Models. The special section devoted to the PIPAPO project contains 10 contributions on the characterization of secondary aerosol formation, and radical precursors, and the characterization of ozone production sensitivity based on field measurements and numerical model simulations. In this paper the scientific background and the major objectives of PIPAPO are described. An overview of the field measurement program, the study site, and the meteorological conditions prevailing during the experiment are given. A general conclusion of the combined results is that under typical summer conditions in the Milan area with clear skies, low wind speeds and high temperatures, the transition from VOC to NOx sensitive ozone production occurs a few tens of km downwind of the strongest emission sources in the city of Milan.

1. Introduction

Over the last twenty years, the understanding of the chemical mechanisms leading to photo-oxidant episodes has been developed and is now on a sound base (see e.g. *NARSTO* [2000]). The degree of photo-oxidant formation in the planetary boundary layer is determined by the meteorological conditions and the emissions of VOC (volatile organic compounds) and NO_x (sum of nitric oxide and nitrogen dioxide). The photo-oxidant formation process is non-linear with respect to emission strength. This makes the development of abatement strategies to meet air quality standards complicated.

High levels of aerosols parallel the occurrence of photosmog episodes. However, photo-oxidants and aerosols have often been studied separately. Air pollution directives are being developed for either one or the other, even though the formation of photo-oxidants and aerosols is tightly linked through atmospheric chemical processes. Emission reduction strategies for photochemical oxidants and aerosols should be evaluated together, as a strategy that is optimum for aerosols may interfere with an ozone reduction strategy, and vice versa [*Meng et al.*, 1997].

The EUROTRAC-2 subproject LOOP studies the VOC and NO_x sensitivity of ozone production and evaluates the temporal and spatial behavior of photo-chemical regimes. We distinguish between two sensitivity measures. The local ozone production sensitivity is defined as the response of the O_3 production rate ($P(O_3)$) to a change in the concentration of either NO_x or VOCs. The integrated ozone concentration sensitivity is the response of O_3 concentration to a change in the emissions of either NO_x or VOCs. For the local ozone production, the transition from one chemical regime to the other (i.e. the transition from VOC sensitive to NO_x sensitive production) is defined as the point at which a relative decrease in both NO_x and VOC concentrations has the same effect on $P(O_3)$ (see e.g. *Kleinman* [1994], *Kleinman et al.* [1997], *Sillman* [1995]).

$$\frac{\partial P(O_3)}{\partial [VOC]} \cdot [VOC] = \frac{\partial P(O_3)}{\partial [NO_x]} \cdot [NO_x] \qquad (1)$$

The sensitivity of the ozone concentration is related to the local sensitivity [*Spirig et al*., this issue] upwind, mixing processes, and deposition integrated over the atmospheric lifetime of ozone. This sensitivity has to be evaluated by varying the emissions in numerical models. The evaluation of abatement strategies also needs to be based on numerical model simulation, ideally with a validated 3-D model.

2. The Pianura Padana Produzione di Ozono Project

Within the Eurotrac-2 subproject LOOP (Limitation of Oxidant Production) we conducted a field campaign in May and June 1998 devoted to the evaluation of the temporal and spatial dynamics of the VOC versus NO_x sensitivity around Milan. Because the Milan region has a photochemical oxidant and aerosol problem, and because the chemistries of these substances are so tightly linked, the LOOP project included a co-operation with the AEROSOL subproject of EUROTRAC-2.

The Milan metropolitan area, located in the Po Basin, the most industrialized and populated area in Northern Italy, is regularly affected by high ozone levels, especially during the late spring and summer months. The entire Milan metropolitan area can be considered as a single urban area, with a population of approximately 3.8 millions. The expansion of the urban area during the last few decades has been paralleled by the development of a dense road network. Inside the area there are about 580 km of highways and 1740 km of secondary roads.

The region between the industrialized area of Milan and the Alps represents a very interesting natural laboratory, with a high variability in emission strength and emission patterns. The region exhibits frequent stagnant meteorological conditions associated with relatively high insulation. In this case, the meteorology of the area is dominated by low wind speeds subject to mesoscale breeze circulations. Winds near the ground typically blow from north to south during the night and in the early hours of the morning. The wind direction changes to southerly in the late morning and remains that way until sunset. Typical residence times of air masses transported between the centre of Milan and the foothills of the Alps some 40 km to the north are 3-5 hours, thus comprising rather short processing times. Concentrations of ozone up to 185 ppb have been reported [*Prévôt et al.*, 1997]. Despite this short time period, field and model studies indicate that integrated ozone production is NO_x sensitive only a few tens of kilometres north of the urban area of Milan [*Staffelbach et al.*, 1997a, 1997b].

Model studies accompanied the experimental activities from the start of the program. A modeling community interested in doing three-dimensional simulations for the Milan area in the Po Basin was established, and had several workshops to coordinate and intercompare their efforts.

The PIPAPO campaign was organized as a pure bottom-up project without central funding. A close co-operation with local authorities was established from the beginning. All information of the PIPAPO project is collected on a CD. This CD contains an ACCESS database with all measurement data as well as a visualization tool.

2.1. Outline of the PIPAPO campaign

2.1.1. The Milan basin as natural photoreactor

The PIPAPO field campaign was basically set up as a lagrangian experiment with several stations within the so-called Milan plume, i.e. downwind of Milan. During two intensive observation periods (IOP's, May 12 and 13, June 1 to 10, 1998), surface station and aircraft measurements were performed. Observational stations at Bresso, Seregno and Verzago were established downwind of Milan, hypothetically located in different chemical regimes according to earlier investigations with a one-dimensional lagrangian model [*Staffelbach et al*., 1997b].

Plate 1 illustrates the evolution of O_3 sensitivity in a typical Milan urban plume as determined by *Staffelbach et al.* [1997b]. The red colour stands for VOC sensitive ozone production, purple for the transition (about equal sensitivity to VOC and NO_x), and yellow for NO_x sensitive ozone production. The calculations are based on an air mass that starts at 7 h LST (local standard time, UTC + 1 h) in Milan and arrives at 15 h LST in Verzago.

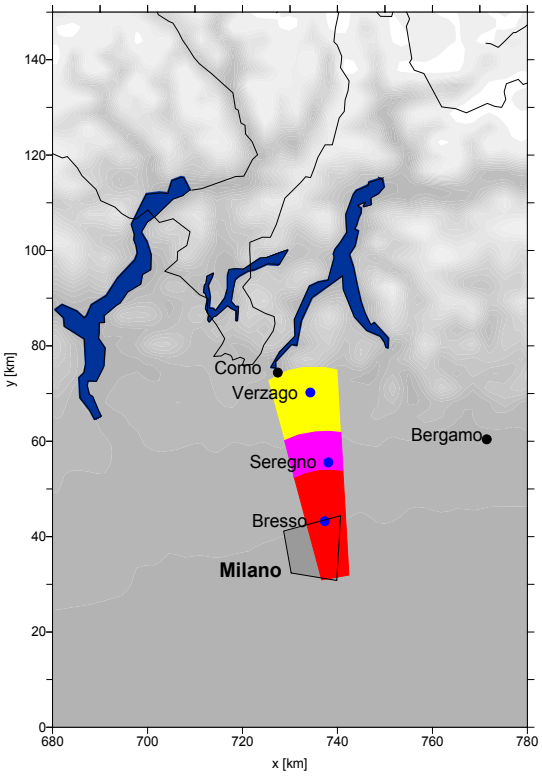

Plate 1: Modeled sensitivity of O_3 concentration to NO_x / VOC emissions in the Milan plume. The red area is VOC sensitivity, purple marks the region with about equal sensitivity and yellow the NO_x sensitive area. The trajectory passed the city of Milan between 07:00 and 10:00 LST.

2.1.2. Intensive observation periods (IOP)

Meteorological criteria for an IOP were i) a high pressure situation lasting for several consecutive days, ii) high insulation producing strong thermally driven circulations and intensive photochemical activity, iii) weak synoptic winds aloft and southerly winds near the surface, and iv) absence of precipitation. Because ozone episodes often occur in spring and early summer, this time of the year was selected over the better-known mid-summer episodes.

The first IOP lasted from May 12 to 13, 1998, and was embedded in a period of exceptionally warm, dry and sunny weather. The synoptic situation showed a stationary high-pressure ridge at 500 hPa extending from northern Africa to southern Scandinavia (Plate 2a and 2b). Milan reported daily maximum temperatures of 31 °C on May 12 and 32 °C on May 13. The Po Basin was free of clouds on both days, while in the afternoon of the second day convective clouds developed in the mountains east of the Lake of Como, which led to thunderstorms that terminated the IOP. A heat low over the Alps was well established on both days. The pressure gradient induced a weak south-to-north flow over the study area, and the ideal flow configuration for PIPAPO was realized on May 13. High insulation and high temperatures were very favourable for photochemistry in the planetary boundary layer (PBL), and the winds supported the transport of polluted air from the basin towards the Alps. Ozone concentrations reached values of 190 ppb during this IOP.

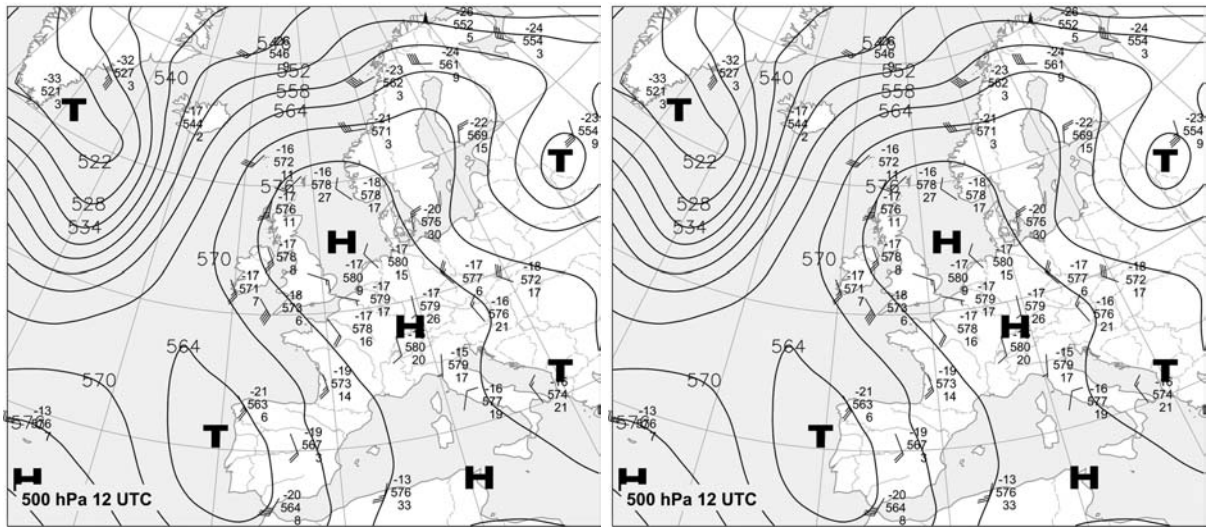

Plate 2a: 500 hPa geopotential height contours, and **b:** surface pressure analysis for 13 May 1998 1200 UTC. Notice that the two charts cover a slightly different geographical area. Charts provided by MeteoSchweiz.

The second IOP took place from June 1 to 10, 1998. The 500 hPa charts show a consistent southwesterly flow across the Alps for the whole period, while the surface charts exhibit various frontal systems which remained north of the Alpine crest.

Winds aloft were mostly southwesterly, while surface winds showed variable directions. Very frequently thunderstorms and scattered intermittent heavy showers developed during the second IOP. In contrast to the first IOP, Milan always reported moderate cloudiness around noon. The ideal flow situation for the second IOP lasted from June 2 to 4, before a cold front approached the Alps (Plate 3a and 3b). The front then became stationary and soon dissolved. The days were warm and sunny, but haze started to accumulate in the PBL, and visibility became poorer with time. In this period, maximum ozone concentrations increased from day to day, reaching peak values of 140 ppb on June 4. Rain was falling in the morning of June 5, and the winds became northerly for a while. Wind speeds were rather low. A frontal system moved across the continent and the Alps on the night of June 7 - 8, thereby interrupting the second IOP. Behind the front, winds turned to northerly directions at all levels for some time.

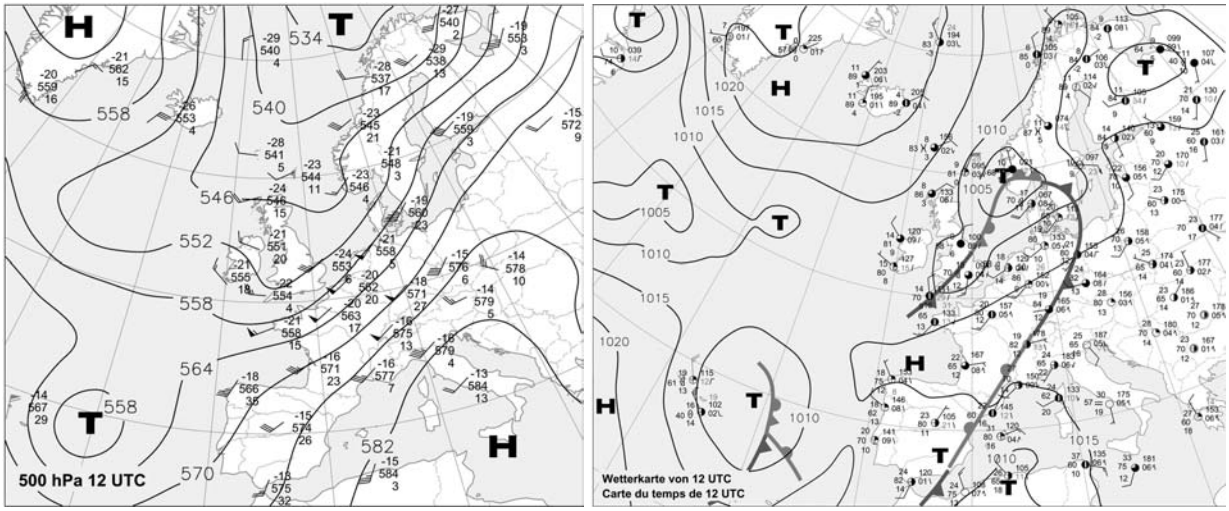

Plate 3a: 500 hPa geopotential height contours, and **b:** surface pressure analysis for 13 May 1998 1200 UTC. Notice that the two charts cover a slightly different geographical area. Charts provided by MeteoSchweiz.

Generally, the surface wind field of the second IOP was quite inhomogeneous.

May 12th and 13th have been chosen as the ideal days for the application of the Eulerian models.

2.1.3. QA/QC of PIPAPO

The quality assurance, quality control (QA/QC) within PIPAPO is based primarily on the conscientiousness of the individual contributors. An overview of the measurements is given in Table 1. The data have been compiled on an MS ACCESS database, including tools for extracting and visualizing of data[2]. Plate 4 shows an example for the representation of the flight data. The user can e.g. scan the flight for any measured species, and then the height above ground, the geographical location and the concentration are shown.

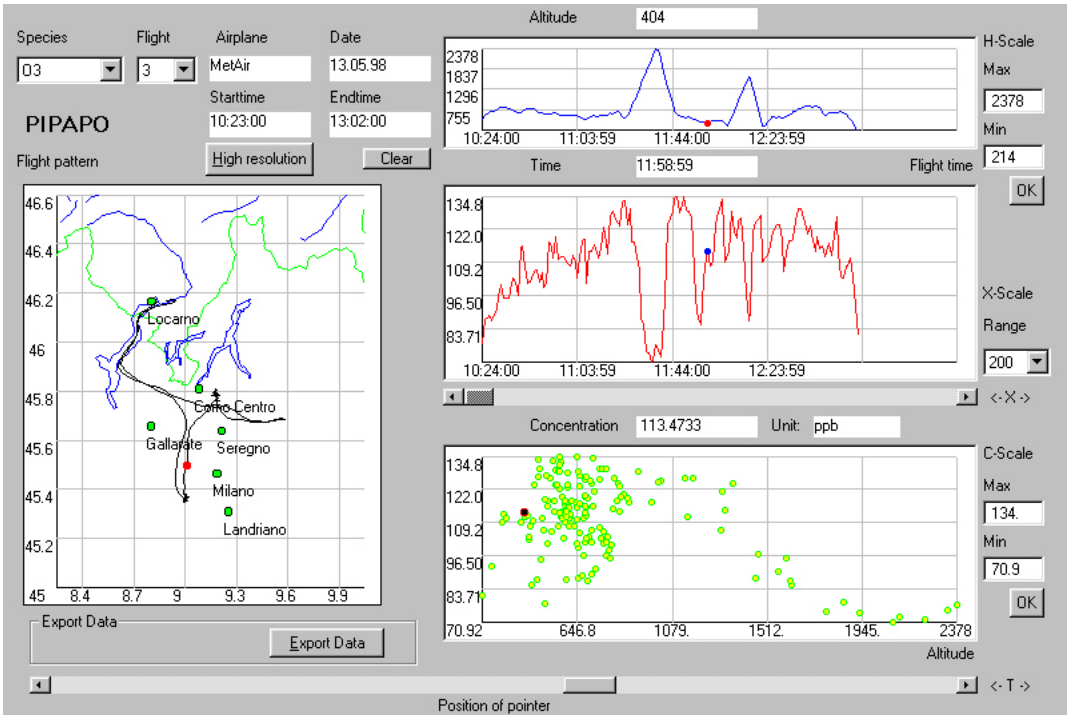

Plate 4: Visualization of aircraft data. On the left panel the flight path is visible. On the right panel time series of the height above ground, the concentration of a selected species, and the vertical profile are represented. The flight can be traced with a ruler (dots in the time series plots).

[2] The CD can be ordered at FAL, P.O. Box ,CH 8046 Zürich

Table 1: Measurements Overview

Species / Parameter	Technique	Reference
Ground Based Measurements		
H_2O_2	Nafion scrubber with fluorescence	e
HCHO	Coil collection with fluorescence	e
HCHO, HONO, O_3, NO_2, SO_2	Differential Optical Absorption Spectrometer (DOAS)	a
Vertical gradients of: HONO, NO_2, SO_2	Differential Optical Absorption Spectrometer (DOAS)	f
HONO, HNO_3	Parallel plate denuder with IC	e
Hydrocarbons (C_4-C_{10})	Gas chromatograph with FID	g
NO, NO_2, NO_y	Chemiluminescence with photolytical/molybdenum converter	h
O_3	UV absorption	h
Peroxy radicals	Chemical amplifier	e
Radiation/J_{NO2}	Radiometer	h
Aerosol compounds	Cellulose and quartz fiber filters in virtual impactors for ionic and carbonaceous species, respectively.	d
Aerosol absorption coefficient	Aethalometer ™	d
Aerosol size distributions	Differential Mobility Analyzers	d
PM2.5	Betameter	b
BC mass concentration	Aethalometer	b
Volatility	Thermodesorber SMPS (scanning mobility particle sizer)	b
Hygroscopic growth	Tandem Differential Mobility Analysis (TDMA)	b
Nitrate, sulfate, gaseous HNO_3	WEDD/AC (wet effluent diffusion denuder/aerosol collector)	b
Aircraft Measurements		
H_2O_2	Chemiluminescence	c
HCHO	Hantch-Fluorescence	c
Hydrocarbons (C_4-C_{10})	Gas chromatograph with FID	c
NO_x	Chemiluminescence	c
O_3	UV-absorption	c

References (this issue, if not specified)

a Alicke et al.: Impact of Nitrous Acid Photolysis on the Total Hydroxyl Radical Budget During the LOOP/PIPAPO Study in Milan

b Baltensperger et al.: Urban and rural aerosol characterization of summer smog events during the PIPAPO field campaign in Milan, Italy

c Dommen et al.: Characterization of the photo-oxidant formation in the metropolitan area of Milan from aircraft measurements

d Putaud et al.: Submicron aerosol mass balance at urban and semi-rural sites in the Milan area (Italy)

e Spirig et al.: NOx versus VOC limitation of O3 Production in the Po Valley: Local and integrated view based on observations

f Stutz et al.: Nitrous acid formation in the urban atmosphere: Gradient measurements of NO2 and HONO over grass in Milan, Italy

g Thielmann et al. (2001): Empirical ozone isopleths as a tool to identify ozone production regimes, Geophys. Res. Letters, 28, 2369-2372

h Thielmann et al.: Sensitivity of ozone production derived from field measurements in the Italian Po Basin

2.2. Emissions

The emission inventory for the LOOP project was compiled by *Maffeis et al.* [1999]. Unfortunately, different methodologies were used for the Italian and Swiss part of the domain. In the small Swiss part of the domain, a spatial disaggregation of only 5 km x 5 km gridding was available. The Swiss inventory includes two source categories, traffic and industry.

The pollutants considered in the Italian inventory are sulphur dioxide (SO_2), nitrogen oxides (NO_x), carbon monoxide (CO), and non-methane volatile organic compounds (NMVOC), while the Swiss inventory considers VOC speciation into 32 classes. Lombardy and Piedmont VOC estimates were speciated in SAROAD classes on the basis of eleven different profiles (eight anthropogenic and three biogenic, [*Carter*, 1995, *Derwent et al.*, 1996]). The Swiss part of the inventory considers a typical summer profile for the temporal distribution of emissions. In Piedmont and Lombardy, the emission estimate algorithms used meteorological parameters that are specific to the hour, day, and area considered. This means that the calculation of isoprene (and other biogenic compounds) in a certain hour of the simulation and in a certain town is based on interpolated temperature and radiation. The same applies for traffic, and evaporative emissions.

It should be noted that the inventories are based on indicators and emission factors referenced to the year 1995. This introduces other sources of uncertainty including:

- new important infrastructure construction (e.g. the Malpensa airport);
- strong car fleet renewal during the past few years;
- changes in industry processes and their decentralisation from the main cities.

3. Occurrence of photosmog episodes in the Milan area

Occurrences of elevated ozone concentration in the region between Milan and the Alps are strongly related to the meteorological conditions. As an example, Plate 5 shows the variability of late afternoon concentration in Verzago as a function of the prevailing meteorological conditions. Daily average global radiation and daily temperature maxima were calculated from representative ground stations. The prevailing wind conditions were derived from wind profiler measurements at Seregno, which is located between Milan and Verzago. The best correlation is found between temperature and ozone concentrations in Verzago in the late afternoon (17.30 Central European Daylight Time, = LST + 1 h = UTC+2 h) during the PIPAPO campaign. Ozone increases from around 45-70 ppb at 20°C to 80-145 ppb at 30°C. The main reasons for this relationship are higher biogenic emissions, higher chemical reaction rates, and usually higher global radiation at higher temperatures, yielding higher ozone production. However, taking only temperature into account, a great part of variability in the ozone concentration remains unexplained. Ozone does not exhibit a consistent dependence on global radiation. On days with low radiation (lower than 2/3 of typical clear days), ozone concentrations do not exceed 80 ppb (crosses in Plate 5). Assuming the wind profiler data to be representative for the region around Milan, we can deduce the influence of the air mass origin on the ozone concentrations in Verzago. The highest concentrations in a particular temperature range are found for the cases when southerly winds prevail, transporting the Milan plume to Verzago (round circles in Plate 5). In the case of strong winds (several hundred kilometers transport distance within 10 hours) and no development of thermally induced winds towards the Alps, low ozone concentrations are found in the according temperature range (squares in Plate 5). On days with thermally induced winds not

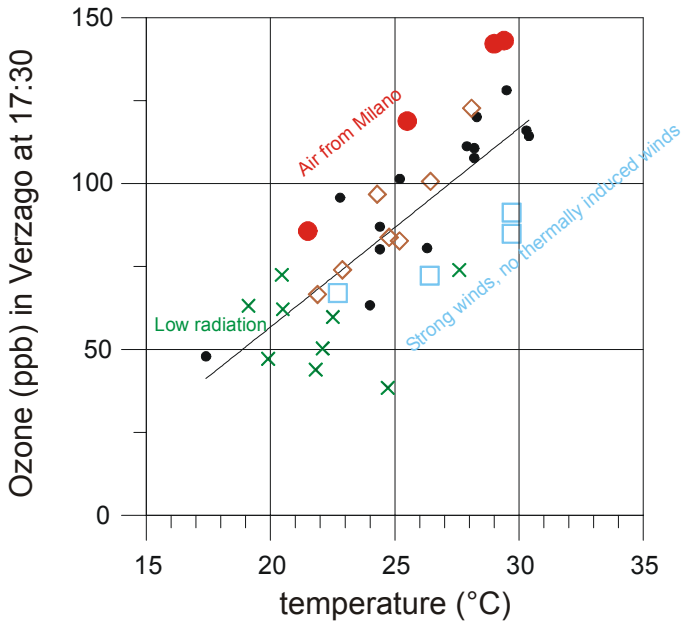

Plate 5: Late afternoon ozone concentrations in May and June 1998 in Verzago versus the daily maximum temperature in Milan. The crosses are days with low global radiation. The big circles are cases with air masses originating from Milan. The small circles are days with incomplete or missing data from the wind profiler. The squares are days with very high wind speeds or no thermally induced southerly winds. The diamonds are cases with thermally induced winds, not originating from Milan.

originating from Milan (usually southwesterly or southeasterly wind directions), the ozone concentrations were close to the linear correlation fit (diamonds in Plate 5).

In summary, the ozone concentrations in Verzago in the late afternoon typically increase by about 6 ppb ozone per 1 °C daily maximum temperature. On days with low global radiation ozone concentrations do not exceed 80 ppb. When the air originates from Milan, we find around 20-30 ppb higher ozone concentrations than the concentration typical for the prevailing temperature. This is similar to what was found in cross-sections of the plumes, where the maximum ozone concentrations are often 20-40 ppb higher than in the adjacent air masses [*Dommen et al.*, this issue]. For conditions with strong winds or no development of southerly thermally induced winds, ozone concentrations are 20-30 ppb lower than typical for the prevailing temperature.

4. Overview of scientific outcomes

In this section we give a short overview on the most important scientific findings of the papers of this special section.

4.1. Aerosol measurements

Two papers discuss the aerosol measurements that have been performed in Bresso and Verzago. Primary aerosols in Bresso are strongly related to traffic density, with peak values during the morning rush hour. A large fraction consists of hydrophobic organic material. PM 2.5 values, on the other hand, do not show a diurnal variation and are therefore not directly linked to primary aerosols. There is a higher percentage of secondary aerosols in Verzago compared to Bresso, in accordance with a generally higher photochemical age of the air masses in Verzago. However, secondary aerosol formation cannot be described using a simple flow reactor picture during transport to Verzago. Both dilution and additional emission influence the level of secondary aerosols in the plume. *Baltensperger et al.* showed that a

large part of the HNO_3 formed over Milan during the morning hours was transformed rapidly to aerosol nitrate, and was transported away by thermally induced winds.

Putaud et al. showed that ammonium nitrate and ammonium sulfate contribute roughly 50% to the submicron aerosol fraction; particulate organic matter 32% in the urban site and 39% in the rural site. They conclude also that NH_3 is not the limiting factor for NH_4NO_3 production in the Po Basin in summer.

4.2. Gas phase measurements in Bresso, Verzago, and by aircraft

Three papers present in detail the measurements of gas phase species at the urban site of Bresso. *Alicke et al.* and *Stutz et al.* report DOAS measurements of the important odd-H radical precursors HCHO and HONO, together with O_3, NO_2, SO_2, and NO measurements. In the heavily polluted area of Milan, photolysis of HONO and HCHO are the most important OH sources at ground level for clear days, more important than the photolysis of ozone. DOAS was also used to determine fluxes with the gradient technique. With this approach it can be shown that for HONO an equilibrium between deposition and emission - a kind of compensation point, related to the $HONO/NO_2$ ratio - is established. The measurements show a HONO formation rate in the order of a few percent of the NO_2 concentration, as a consequence of NO_2 dry deposition. *Thielmann et al.* discuss the sensitivity of the ozone production rate based on time series of O_3, NO, NO_2, HNO_3, NO_y and H_2O_2 measurements in Bresso and Verzago. The analysis shows a predominantly VOC sensitive ozone chemistry in Bresso and both VOC and NO_x sensitive ozone chemistry in Verzago. VOC sensitive ozone chemistry in Verzago is always associated with polluted air masses from the Milan area.

Spirig et al. determined the odd-H radical levels and the local ozone production from measurements in Verzago and Bresso. Based on a steady state analysis, the VOC/NO_x sensitivity was determined. In cases where air masses have been advected directly from south the local production in Verzago during the afternoon was determined to be VOC sensitive. The measurements suggest an additional strong emission source between the city of Milan and Verzago that is not adequately represented in the numerical simulations. In other air masses the ozone production was NO_x sensitive

A similar approach was taken by *Dommen et al.* using measurements from the MetAir aircraft. Their analysis shows that the core of the Milan plume is highly VOC sensitive with a downwind extension of about 40 km and a width of 10 to 20 km. Peroxide and ozone productions rates were calculated from the measurements and also deduced from a local steady state photochemical analysis. The intercomparison of these two approaches yielded reasonable agreement for peroxide and lower ozone productions for the steady state analysis. *Dommen et al.* concentrated on measurements in the Milan plume due to their rather high uncertainty for low NO_2 concentrations.

Based on previous field campaigns, a gradual increase of biogenic VOC emission in the Milan plume going north was postulated. Isoprene emissions were expected to have the largest influence on the ozone production. According to the VOC measurements taken from the aircraft, isoprene contributes only moderately to the total VOC reactivity in the layers where the aircraft was flying, with no clear increase towards the Alps over the Po Basin.

4.3. Model simulations

Three contributions are based on simulations with chemical transport models. *Dosio et al.* and *Martilli et al.* used the TVM-LCC model to simulate the conditions in the Po Basin for May 13th. *Hammer et al.* used the KAMM/DRAIS model. *Dosio et al.* concentrate on the meteorological aspects and the associated ozone dispersion in the Po Basin. The mountain-

induced circulation extends for about 1000 m in the vertical. The simulations show that at higher altitudes a return current is present that subsides in the middle of the Basin.

Martilli et al. focus on the VOC/NO_x sensitivity of the ozone production rate and discuss the influence of the formation of nitrate aerosols on the indicator values. The detailed comparison with field data shows a series of systematic deviations between modeled and measured concentrations. There are two main reasons for this: i) deviations of the real emissions for May 13 from those used as emission input, and ii) a too low vertical exchange during the night between the first few model layers. We believe that these deviations have only a minor influence on the NO_x/VOC sensitivity in the model. This is supported by observation-based analysis of the local ozone production rate from the field data (see *Spirig et al.* and *Dommen et al.*). Also, the scaling up of the local analysis with simple box and one-dimensional lagrangian models are giving the same picture of a rapid changeover from VOC to NO_x sensitive ozone production 20 to 40 km downwind of the city of Milan. The absence of a detailed NH_3 emission inventory and atmospheric measurements (NH_3 concentrations were only measured in Verzago) prevents a quantitative validation of the aerosol formation in the TVM-LCC model.

Hammer et al. used the KAMM/DRAIS model to investigate the applicability of the indicator H_2O_2/HNO_3 to separate NO_x sensitive and VOC sensitive regions in the polluted planetary boundary layer on a regional scale. Three dimensional model runs were performed for two model domains in Germany and one domain in the Po valley. These domains differ significantly in the spatial distribution of the emissions, in the absolute values of the emissions, and in the composition of the VOC. The domains also differ in their meteorological conditions and therefore in the involved transport processes. Nevertheless, the transition value of H_2O_2/HNO_3 found for the individual domains differs by less than 30 % from each other. The VOC sensitive area is larger in the KAMM/DRAIS model compared to the TVM-LCC model run. The reason for this deviation is the differences in the windfields of the two models.

5. Summary of scientific findings and outlook

The main goal of the PIPAPO field campaign was to describe the spatial and temporal dynamics of the NO_x/VOC sensitivity in the plume of the Milan metropolitan area. This can only be reached with models that have been proven not only to reproduce well the ozone distribution in space and time, but also the correct sensitivity to changed emission rates However, a comparison with experimental data has to be based only on the base case model run. Sensitivity runs are thus simulating situations that do not correspond to the real situation, and can therefore not be validated with measurements. This situation is a dilemma, as a validation of sensitivity runs with field data cannot be performed.

Reasons for deviations between modeled and measured values must be assessed, and it must be evaluated whether the causes for the deviations are affecting the sensitivity. We carefully investigated whether the models are producing the right ozone level just by a combination of wrong assumptions that are canceling each other.

Photochemical smog episodes are accompanied by high aerosol loads, with an important contribution from secondary aerosols. The high radical level associated with photochemical smog favors the formation of secondary aerosols, both inorganic and organic. The aerosol measurements have confirmed the large contribution from secondary aerosols. However, a simple description of the aerosol in a kind of a flow reactor downwind of Milan cannot be expected due to the patchy emissions. Fresh emissions are always mixed into chemically aged air masses. The NH_3 emissions are one of the driving forces for the inorganic aerosol

formation. However, an adequate spatially and temporally resolved emission inventory was not available, and atmospheric NH_3 concentration measurements to validate the plausibility of such an inventory do not exist.

Aerosol formation in the model world has a very minor influence on ozone formation. The two most important processes that couple the photooxidant and aerosol formation are not yet in the models: there is no feedback of the aerosol levels on the radiation properties, and there is no reaction of radicals with aerosol surface or within water droplets. E.g., the plume that arrived in Verzago in the early afternoon caused a 10% drop of the jNO_2 values at the surface [*Thielmann et al.*, this issue].

The representation of the vertical mixing in the models has an important influence on the VOC/NO_x sensitivity. In the analysis of *Spirig et al.*, model calculations predicted a NO_x sensitive O_3 production in the residual layer earlier in the day. LIDAR measurements on the ARAT aircraft confirm that there was an increase in O_3 concentration above the mixing layer: The analysis of the flight in the morning of June 2 (0930 LST to 1030 LST) indicates a mean net ozone production decreasing from 10 to 2 ppb/h, going from 700 m asl to 1200 m asl. However, these increases are not significant due to the large scatter of the data. We cannot determine whether the ozone production in the residual layer is due to remaining precursors or due to fresh emissions, because we have no direct information on the vertical profiles of the parameters driving the ozone formation, i.e. NO and the ODD-H levels. But it is evident that ozone produced in the residual layer earlier in the day would influence the sensitivity of the O_3 concentration at the surface in the afternoon, most likely in an accentuation of NO_x sensitivity.

The indicator concept introduced by *Sillman* [1995] and *Milford et al.* [1994] uses simple combinations of concentrations of reasonably long-lived species, such as O_3, NO_z, HNO_3 and H_2O_2, to discriminate between VOC and NO_x sensitive integrated ozone production. These species are well mixed in the PBL in the afternoon. Ground based measurements can therefore be regarded as representative for the whole boundary layer. The transition values found by the different Eulerian models essentially confirm the values *Sillman* [1995] derived from runs for the eastern part of the USA. But the transition values are sensitive to the dry removal mechanism in the model that has to be improved in a next model generation. In particular, the transition value of the ratio H_2O_2/HNO_3 is probably shifted to slightly lower values due to an overestimation of the indicator ratio at the inflow borders.

The PIPAPO field campaign showed that the relevant spatial scale for the ozone production in the Milan plume is 10 to 30 km. Peak values of ozone, secondary aerosols, and other photooxidants are reached within a few 10 km from the major emission sources. It is on this scale that reduction strategies have to be assessed. PIPAPO looked at two periods of only a few days. Extrapolation of the analysis to the seasonal scale relevant for reduction strategies and application was not in the scope of the PIPAPO activity. Nevertheless, we are convinced that the model approaches used in the PIPAPO studies can be extended to longer time scales to get the integrated NO_x/VOC sensitivity for the whole summer. The analysis also shows that the measuring network in the Po Basin could be complemented by indicator species in order to get an independent approach of the spatial and temporal variability of the ozone production sensitivity based on field measurements.

The PIPAPO field campaign has reached its main goal: a consistent description of the VOC/NO_x sensitivity of the ozone production in the Milan plume for typical summer conditions. The findings have to be expanded in five directions.

1. Model simulations must include an aerosol module that treats aerosol – photochemistry – radiation feedbacks, especially the modifications to global radiation due to the aerosol loading.
2. Model simulations must cover a full year in order to get the sensitivities for seasonal averages of ozone and aerosol levels.
3. For the validation of the aerosol module, field data on aerosol speciation and vertical profiles especially of radiation properties in the lowest layers must be available.
4. The investigations on the role of biogenic emissions, both VOC's and NO_x must be improved. Approaches for obtaining regionally integrated fluxes of isoprene, related oxidation products of isoprene, terpenes and carbonyl compounds have to be implemented.
5. Emission inventories must be improved. In particular, spatially highly resolved NH_3 inventories are a prerequisite for a reliable simulation of the aerosol level.
6. The situation in the Milan area calls for a second project focused on the interaction of secondary aerosol formation and photo-oxidant production. Because the highest aerosol levels are found during the stagnant winter conditions, the measurements should also include winter campaigns.

Acknowledgements

Marx Stampfli, Stampfli Mathemathics, CH-3018 Bern developed the visualization tools for the ACCESS database. We are grateful to all participants of the PIPAPO filed campaign that made this poor bottom-up project a scientific success. We especially thank Thomas Staffelbach, Matteo Tamponi, Guido Lanzani for their enthusiastic support of the PIPAPO field project. Financial support through the commission for technology and industry (KTI , project 3261.1) is greatly acknowledged.

List of papers of PIPAPO special section:

Alicke, B., Platt, U. and Stutz, J.: Impact of nitrous acid photolysis on the total hydroxyl radical budget during the LOOP/PIPAPO study in Milan.

Baltensperger, U, Streit, N., Weingartner, E., Nyeki, S.,., van Dingenen R., Virkkula, A., Raes, F., and Gäggeler, H.W.: Urban and rural aerosol characterization of summer smog events during the PIPAPO field campaign in Milan, Italy.

Dommen, J., Prévôt, A.S.H., Neininmger, B. and Bäumle, M.: Characterization of the photooxidant formation in the metropolitan area of Milan from aircraft measurements.

Dosio, A., Galmarini, S. and. Graziani, G: Simulation of the circulation and related photochemical ozone dispersion in the Po plains (Northern Italy) comparison with the observation of a measuring campaign.

Hammer, M., Vogel, B. and Vogel, H.: Findings on NOy and H2O2/HNO3 as Indicators for Ozone Sensitivity in the vicinity of Milan, Berlin and in Baden-Württemberg based on Numerical Simulations.

Martilli, A., Neftel, A., Favaro, G., Kirchner, F, Sillman, S. and Clappier, A.: Simulation of the ozone formation in the Northern Part of the Po Basin.

Puteaud, J.P., Van Dingenen, R. and Raes, F: Submicron aerosol mass balance at urban and semi-rural sites in the Milan area (Italy).

Spirig, C., Neftel, A., Kleinman, L., and Hjorth, J.: NOx versus VOC limitation of ozone production in the Po Basin: Local and integrated view based on observations.

Stutz, J, Alicke, B. and Neftel, A.: Gradient measurements of NO2 and HONO over grass in the urban atmosphere.

Thielmann, A., Prévôt, A.S.H., Neftel, A. and Staehelin, J.: Sensitivity of Ozone Production derived from Field Measurements in the Italian Po Basin.

References:

Carter, W. P. L., Computer modeling of environmental chamber measurements of maximum incremental reactivities of volatile organic compounds, Atmos. Environment, 29: 2513-2527, 1995.

Derwent, R. G., M. E. Jenkin and S. M. Saunders, Photochemical ozone creation potentials for a large number of reactive hydrocarbons under European conditions. Atmos. Environment, 30, 181-199, 1996.

Kleinman, L. I., Low and high-NOx tropospheric photochemistry, J. Geophys. Res., 99, 16831-16838, 1994.

Kleinman, L.I., P.H. Daum, J.H. Lee, Y. Lee, L.J. Nunnermacker, S.R. Springston, and L. Newman, Dependence of ozone production on NO and hydrocarbons in the troposphere, Geophys. Res. Letters, 24 (No.18), 2299 - 2302, 1997.

Kleinman, L. I., P. H. Daum, D. G. Imre, J. H. Lee, Y-N. Lee, L. J. Nunnermacker, S.R. Springston, J. Weinstein-Lloyd, and L. Newman, Ozone production in the New York City urban plume, J. Geophys. Res., 105, 14495-14511, 2000.

Maffeis, G., M. Longoni, A. De Martini and M. Tamponi, Emissions estimate of ozone precursors during PIPAPO campaign in Proceedings of "Photochemical Oxidants and Aerosols in Lombardy Region" (Milan, Italy, June 1999) 1999."

Meng, Z., D. Dabdub, and J. H. Seinfeld, Chemical coupling between atmospheric ozone and particulate matter, Science, 277,116-119, 1997.

Milford, J., D. Gao, S. Sillman, P. Blossey, and A. G. Russell, Total reactive nitrogen (NOy) as an indicator for the sensitivity of ozone to NOx and hydrocarbons, J. Geophys. Res., 99, 3533-3542, 1994.

NARSTO Synthesis Team, An Assessment of Tropospheric Ozone Pollution July 2000, http://odysseus.owt.com/Narsto/

Prévôt, A. S. H., J. Staehelin, G. L. Kok, R. D. Schillawski, B. Neininger, T. Staffelbach, A. Neftel, H. Wernli, and J. Dommen, The Milan photooxidant plume, J. Geophys. Res., 102, 23375-23388, 1997.

Sillman, S., The use of NOy, H2O2 and HNO3 as indicators for O3-NOx-VOC sensitivity in urban locations, J. Geophys. Res., 100, 14175-14188, 1995.

Staffelbach, T., A. Neftel, A. Blatter, A. Gut, M. Fahrni, J. Staehelin A. S. H. Prévôt, A. Hering, M. Lehning, B. Neininger, M. Bäumle, G. L. Ko, J. Dommen, M. Hutterli and M. Anklin, Photochemical oxidant formation over southern Switzerland, part I: Results from summer, 1994, J. Geophys. Res., 102, 23345-23362, 1997a.

Staffelbach, T., A. Neftel and L. W. Horowitz, Photochemical oxidant formation over southern Switzerland, part II: Model results, J. Geophys. Res., 102, 23363-23374, 1997b.

Thielmann, A., A. S. H. Prévôt, F. C. Grüebler, and J. Staehelin, Empirical ozone isopleths as a tool to identify ozone production regimes, Geophys. Res. Letters, 28, 2369-2372, 2001.

4 Paper II, Limitation of ozone production

NO_x versus VOC limitation of O_3 production in the Po Valley: Local and integrated view based on observations

Christoph Spirig, Albrecht Neftel

Swiss Federal Research Station for Agroecology and Agriculture, Zürich-Reckenholz and Liebefeld-Bern, Switzerland.

Lawrence I. Kleinman

Atmospheric Sciences Division, Department of Environmental Science, Brookhaven National Laboratory, Upton, New York.

Jens Hjorth

Environment Institute, Joint Research Center of the European Commission, Ispra, Italy.

Journal of Geophysical Research, 107 (D22), art.nr. 8196, 2002

Abstract

We characterize the local O_3 production at an urban and a rural site in the northern part of the Po Valley (Italy) during the Pianura Padana Produzione di Ozono experiment (PIPAPO). A steady state calculation based on observations is performed to determine the local O_3 production rate, $P(O_3)$, and its sensitivity to precursor concentrations. The urban site exhibited a strongly VOC sensitive O_3 production rate while both VOC and NO_x sensitive conditions were observed at the rural site. In addition to the local steady state analysis, we performed 1D Lagrangian model calculations that simulate conditions in the Po Valley. These calculations show that the $P(O_3)$ at the surface tends to be more VOC sensitive than the average in the mixed layer. The Lagrangian calculations are also used to determine the response of O_3 concentration to an emissions change. We compare emission control information with information on sensitivities from the local analysis. It is concluded that a local analysis of $P(O_3)$ within the mixing layer offers useful qualitative information but tends to overestimate VOC sensitivity as judged by a comparison with an emissions based Lagrangian model.

1. Introduction

Tropospheric ozone concentrations are known to be highest downwind of large cities. The Po Valley in Northern Italy often exhibits ozone levels that are among the highest concentrations observed in Europe. The ingredients for the production of high ozone levels: nitrogen oxides (NO_x), volatile organic compounds (VOC) and solar radiation are abundant in this region. The highly industrialized and densely populated Milan metropolitan area and the extended road network around supply high emissions of VOC and NO_x [*Heymann et al.*, 1994; *Klimont et al.*, 1993]. In addition, the meteorological situation during summer months is often characterized by high pressure conditions with high solar radiation. Wind directions are then dominated by a mesoscale breeze induced by a heat low over the Alps, leading to a southern wind direction during daytime and a flow from north to south during the night [*Lehnig et al.*, 1996].

Earlier investigations in the area observed a plume originating from Milan, in which the production of photooxidants was highly effective. *Prévôt et al.* [1997] found ozone concentrations up to 185 ppb 4-5 hours downwind of Milan. Differences in ozone concentrations between air masses within and outside the plume were as high as 100 ppb, indicating that the Milan plume can add enormously to the regional background.

The PIPAPO field experiment [*Neftel et al.,* 2002] aims to describe the spatial and temporal dynamics of the VOC versus NO_x sensitivity of the ozone production in the northern part of the Po Valley. In this work we present an observation based approach to get information about the limitation of ozone formation. A steady state calculation driven by observations gives the local O_3 production rate, $P(O_3)$ and its sensitivity to NO and VOCs, $d\ln P(O_3)/d\ln[NO]$ and $d\ln P(O_3)/d\ln[VOC]$. These quantities describe the instantaneous chemistry at the time and place where the measurements were taken. In this case, we characterize the chemistry at two surface sites.

We study how this local and instantaneous information can be related to the regional context of ozone control strategies. With a 1 D Lagrangian photochemical model, we simulate a situation that is representative for summer smog conditions in the Po Valley. The results of these model runs are treated in the same way as the observations and used as inputs for steady state calculations. We thus get the local characteristics of the chemistry as a function of altitude. This allows us to address, if the conditions of ozone production through the depth of the boundary layer can be assessed based on surface observations.

The 1D model is also used to investigate the effects of emission changes on the ozone concentrations. This combination of local analyses and 1D model calculations allows us to discuss the relations between local quantities that are accessible to observations and the integrated perspective, the sensitivity of O_3 concentration to its precursor emissions.

2. PIPAPO field experiment

2.1. Scope

Earlier field experiments and model studies on the chemistry of the Milan plume indicated that the transition from VOC to NO_x sensitive regime in the plume occurs within a relatively short time [*Staffelbach and Neftel*, 1997; *Staffelbach et al.*, 1997*a*]. The PIPAPO experiment took place in early summer 1998 and was designed based on this experience: Major ground stations were placed along the prevailing wind direction. One was located upwind of the strongest emission sources, while the others were situated between 5 and 40 km downwind of the major emission source. According to earlier model calculations, these stations were expected to be located in different O_3 production regimes [*Neftel et al.*, 2002].

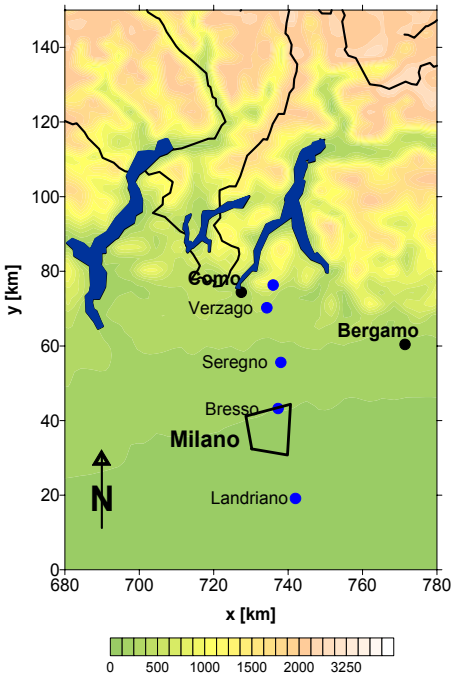

Figure 1: PIPAPO ground stations, color scale indicates altitude above sea level (m).

2.2. Measurement sites

Results from two PIPAPO measurement sites, Bresso and Verzago, will be discussed in this work. At these two sites, extensive sets of parameters were measured which allows an observation based characterization of the local ozone production.

2.2.1. Verzago

Verzago is located approximately 35 km north of downtown Milan (Figure 1). This station has a rural character and is located slightly higher than its surroundings. The nearest major emission source is a highly congested road one kilometer northeast, connecting the cities of Como and Bergamo. There are no major emission sources nearby to the south. Therefore it is expected that the air reaching the site under prevailing southern wind directions during smog episodes is relatively undisturbed by recent emissions.

2.2.2. Bresso

The second station considered is situated on a military airfield in Bresso, in the northern outskirts of Milan (5 kilometers north of downtown Milan). North of this site lies a major highway axis and just 50 m west there is another very busy street (Vialle A. Grandi). For a detailed description of this site see *Alicke et al.*, [2002]. Bresso is expected to exhibit a strongly VOC-limited ozone production regime due to the emission sources nearby.

2.3. Measurement Methods

Most of the measurements we will discuss here were performed with the same techniques at both sites and instruments are identical with those described in *Staffelbach et al.* [1997*a*].

New additions for this campaign were a modulated chemical amplifier (MCA) for peroxy radical measurements at the Verzago site and differential optical absorption spectrometers (DOAS) for measurements at the Bresso site. [*Alicke et al.*, 2002].

Table 1 summarizes the measured parameters that were used in our analyses. O_3, NO and NO_2 were measured with a commercially available system (Cranox, Ecophysics, Switzerland). O_3 was measured by UV absorption, NO by ozone chemiluminescence. NO_2 and NO_y were determined as NO by means of a photolytic and a molybdenum converter, respectively. Details about this system and calibration procedures are given in *Thielmann et al*. , [2002].

HNO_3 and HONO were collected using a parallel plate denuder (PPD) and subsequently

Table 1: Instrumentation at the Verzago and Bresso Sites.

Species	Analytical Method	Detection Limit	Time Resolution [a]
Verzago			
O_3	UV absorption	3 ppb	20 sec.
NO	Chemiluminescence	23 ppt	20 sec.
NO_2	Chemiluminescence with photolytical converter	23 ppt	20 sec.
NO_y	Chemiluminescence with molybdenum converter	23 ppt	20 sec.
Hydrocarbons (C4-C11)	Gas chromatograph with FID	20 ppt (C4)	30 min.
H_2O_2	Monitor based on gas injection	100 ppt	2 min.
HNO_3	Parallel plate denuder with IC	10 ppt	60 min.
HONO	Parallel plate denuder with IC	5 ppt	60 min.
PAN	GC combined with Luminol detection	100 ppt	30 min.
HCHO	Coil collection with fluorescence	0.5 ppb	60 min.
CH_3CHO	DNPH cartridges and HPLC	0.5 ppb	200 min.
Acetone	DNPH cartridges and HPLC	0.5 ppb	200 min.
CO	Non dispersive IR absorption	50 ppb	1 min.
Peroxy radicals	(see text, Section 2.3)		
Bresso			
O_3	UV absorption	2 ppbv	20 sec.
NO	Chemiluminescence	50 ppt	20 sec.
NO_2	Chemiluminescence with photolytical converter	50 ppt	20 sec.
NOy	Chemiluminescence with molybdenum converter	50 ppt	20 sec.
Hydrocarbons (C_4-C_{11})	Gas chromatograph with FID	20 ppt (C4)	30 min.
HCHO	DOAS	1.6 ppb	5 min.
HONO	DOAS	0.2 ppb	5 min.
CO	Non dispersive IR absorption	50 ppb	1 min.

[a] Hourly means were used as inputs for steady state calculations.

analyzed by ion chromatography. The denuder was designed for a quantitative stripping of soluble gases [*Neftel et al.*, 1996; *Staffelbach et al.*, 1997*a*].

Peroxyacetyl nitrate (PAN) was measured with a commercial system (LPA-4 PAN analyzer, Scintrex Unisearch, Canada), a gas chromatograph combined with a Luminol chemiluminescence detector, measuring thermally decomposed PAN as NO_2.

H_2O_2 was collected with a Nafion denuder and measured with fluorescence detection. The system has a built-in gas phase calibration source and is described in detail by *Sigg et al.*, [1992].

At the Verzago site, HCHO was collected in a Nafion membrane diffusion scrubber and analyzed with fluorescence detection. At the Bresso site, HCHO was measured by DOAS [*Alicke et al.*, 2002].

Acetone and acetaldehyde were sampled on cartridges containing 2,4-dinitrophylhydrazine (DNPH) coated silica and analyzed a few days after collection by the Norwegian Institute for Air Research (NILU), Kjeller, Norway, by reversed phase HPLC using UV detection.

Hydrocarbons (C_4-C_{11}) were measured with a commercial gas chromatograph (airmoVOC 1010, Airmotec, Switzerland). The instrument was run in a quasi-continuous mode. Hydrocarbons (HC) were first preconcentrated on Carbosieve/Carbotrap cartridges at ambient temperature, then thermally desorbed, cryofocused on a short column containing Carbopack B at temperatures below O°C and finally injected onto a BGB 2.5 capillary column. Details about the hydrocarbon measurements at both sites are given in *Grüebler*, [1999].

HONO was measured with a DOAS system at the Bresso site. The instrument and the significance of HONO at this site are discussed in detail by *Alicke et al.* [2002] and *Stutz et al.* [2002].

Peroxy radicals were measured with a modulated chemical amplifier (MCA) instrument that has been described in detail elsewhere [*Cantrell et al.*, 1984; *Hastie et al.*, 1991]. The method is based on a chain reaction producing NO_2, initiated by the reaction of HO_2 radicals with NO in a CO/NO/air system; NO_2 is then measured as a proxy of the HO_2 radicals. Since most organic peroxyradicals produce HO_2 by their reaction with NO and O_2, the instrument will also respond to these radicals. The MCA used in this study was built at the Institute of Environmental Physics at the University of Bremen, Germany, and uses detection of NO_2 by measurement of the chemiluminescence of its reaction with a luminol solution. The concentrations of NO and CO applied in this system were 4 ppmV and 9%, respectively.

The sensitivity of the chemical amplifier depends on the reaction chain length, which was determined using a known radical concentration generated by the photolysis of water in air to form HO and HO_2 radical as described by [*Schultz et al.*, 1995]. The average measured chain length during the campaign was 182 with a standard deviation of 26. Chain length and NO_2 calibrations were performed daily, apart from June 5, where the data of the subsequent calibration were used.

It has recently been shown that the response of the MCA to HO_2 as well as to organic peroxy radicals decreases significantly with increasing humidity of the air that is sampled, apparently due to a combination of increased wall losses and a water dependence of the gas phase chemistry [*Mihele and Hastie*, 1998]. The relationship between chain length and relative humidity is temperature dependent. In order to allow a correction of measured data for this humidity effect, the chain length calibration of the MCA was performed at different temperatures and relative humidity levels. For typical daytime relative humidity and temperature at Verzago during the measurement period (40-60% RH, 26 ^{0}C), this correction is in the range between a factor of 2 and 2.5.

The random error on the RO_2 measurements is mainly due to fluctuations in the detected NO_2 signal (most of the NO_2 arriving at the detector comes from the titration of ozone by NO in the instrument). For the measurements reported here, this random 'noise' level corresponds typically to approximately 10 pptV [RO_2] (data are averaged over 10 minutes). The size of other, potential sources of measurement errors can only be tentatively estimated. Based on the observed variations, we estimate that changes in chain length during a day and uncertainties on the chain length calibration will cause a 20% uncertainty on the measurements, and that the uncertainty on the correction for the effects of humidity will be approximately 30%. It must also be taken into account that the response of the MCA to organic peroxy radicals is not exactly the same as the response to HO_2 radicals. A recent study [*Ashbourn et al.*, 1998] has shown that the response of an MCA instrument to a series of organic peroxy radicals was between 6 and 38% higher than the response to HO_2. This difference in sensitivities may add another 15% uncertainty. Thus the overall measurement uncertainty is estimated to be a 10 pptV baseline noise combined with an uncertainty, proportional to the measured concentrations, of ~39% (calculated as the geometric mean of the three contributions).

2.4. Intensive Observation Periods

Two intensive observation periods (IOP) took place. They were chosen to cover high ozone episodes, i.e. days with high solar radiation and low wind speeds. For details about the weather conditions see *Neftel et al.*, [2002]. May 12 and 13 were the last days of a longer period with warm and sunny weather. Wind directions on these days corresponded almost

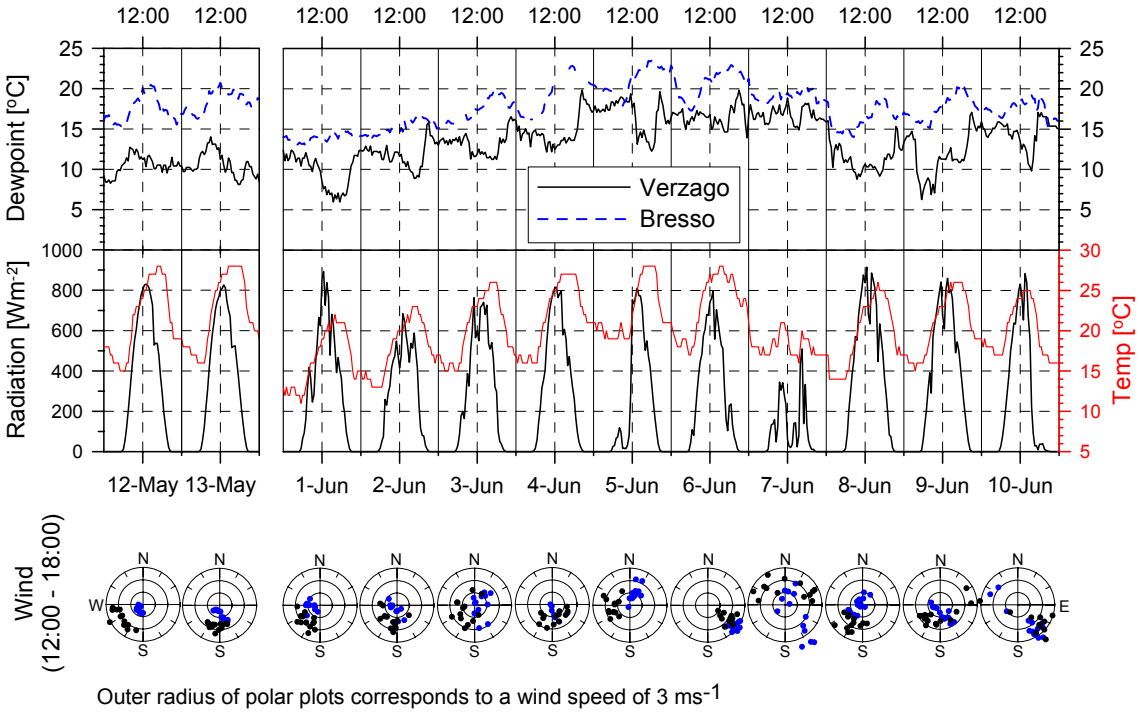

Figure 2: Humidity, Temperature (red), incoming radiation, and afternoon winds during the IOPs. Temperature and radiation are shown for Verzago only.

ideally to the situation desired for the PIPAPO experiment. Especially on May 13, winds blew directly from the South and the measurement sites were in a line downwind of the strongest emission sources. Clear sky and high temperatures led to an effective photochemistry in the boundary layer and a maximum ozone concentration of 195 ppb (half hour mean) was reached at Verzago.

The second IOP from 1st to 10th of June showed a somewhat unsteady situation with wind directions that often differed from the desired flow from south to north. The days were warm, but not always cloudless. Nevertheless, ozone production in the Po Valley was still considerable from 2nd till 4th of June, when ozone maximums up to 150 ppb were measured in the foothills of the Alps, 40 km north of Milan. The second IOP was not a continuous high ozone episode. Showers occurred in the morning on June 5th north of Milan and an almost continuous rainfall on June 7th terminated the first half of this IOP. From the 8th through the 10th of June, weather conditions were again favorable for high ozone production, although somewhat limited by clouds. Figure 2 gives an overview on the meteorological situation during the two IOPs.

As can be seen in Figure 3, the different character of the two sites in terms of pollution is evident; the urban site Bresso with strong variations in concentrations of primary emissions and the rural station of Verzago with generally lower concentrations in VOC, NO_x and CO, but higher levels of ozone.

In the afternoon on May 13th, June 4th , and June 9th, the rural site at Verzago exhibited slightly higher concentrations of VOC and NO_y for a short time period. Since the NO_x concentrations at Verzago do not show this behavior, it is an indication that a heavily polluted and photochemically aged air mass arrived at Verzago at those periods. This observation was particularly pronounced in the afternoon of May 13, the day with the highest ozone concentration at Verzago during the whole measurement campaign. Note that there are a few occasions (mainly during the night or in the early morning) at Bresso where NO_x measurements exceed the values of NO_y. The reason is probably an incomplete conversion in the molybdenum converter [*A. Thielmann*, pers. communication] at very high NO_x concentrations. The data of interest for this study, i.e. daytime concentrations, are free of such artifacts [*Thielmann et al.*, 2002].

3. Models

We use two model tools for our analyses about the limitation of ozone production: Steady state calculations for the characterization of local and instantaneous quantities and a 1D photochemical model for studying the relation between emission changes and regional ozone concentration.

3.1. Steady State Approximation (SSA)

Concentrations of odd-H radicals (odd hydrogen = OH + HO_2 + RO_2, whereas RO_2 stands for any organic peroxy radicals) were estimated with a radical steady state approximation (SSA) [*Staffelbach et al.*, 1997*a*]. Due to their short lifetimes, the radical species OH, HO_2 and RO_2 are assumed to be in a steady state and their concentrations can be determined using a system of equations:

$$\frac{d[OH]}{dt} = P_{OH} - [OH]\cdot\sum_i k_i\cdot[S_i] = 0 \qquad (1)$$

$$\frac{d[HO_2]}{dt} = P_{HO_2} - [HO_2]\cdot\sum_j k_j\cdot[S_j] - 2k_{peroxid}\cdot[HO_2]^2 = 0 \qquad (2)$$

$$\frac{d[RO_2]}{dt} = P_{RO_2} - [RO_2]\cdot\sum_j k_j\cdot[S_j] - 2k_{o\_peroxid}\cdot[RO_2]^2 = 0 \qquad (3)$$

where P_{OH}, P_{HO2} and P_{RO2} are the production rates of OH, HO_2 and RO_2, respectively. S_i, S_j, and $S_{j'}$ denote (radical or non-radical) species that act as reaction partners in sink reactions of OH, HO_2 and RO_2, respectively. The concentrations of the non-radical reaction partners were constrained to measured concentrations. The steady state equations (1-3) were solved by iteration for OH, HO_2 and RO_2. Table 2 shows all radical reactions that were considered in this SSA. Details about the choice of reaction rates are given in [*Staffelbach et al.*, 1997*a*]. Some minor modifications were made for this work and are briefly described here.

The SSA was performed in two variations; with NO and NO_2 input concentrations fixed to the measured values, and with only NO taken from measurements. In the later case, NO_2 was determined by including it in the iteration, where it was calculated as

$$[NO_2] = [NO]\cdot\left([O_3]\cdot k_{O_3} + [HO_2]\cdot k_{HO_2} + [RO_2]\cdot k_{RO_2}\right)\Big/ j_{NO_2} \qquad (4)$$

with k_{O3}=1.8E-12·exp(-1370/T) cm^3 $molecules^{-1}$ s^{-1}, and other rate constants according to Table 2.

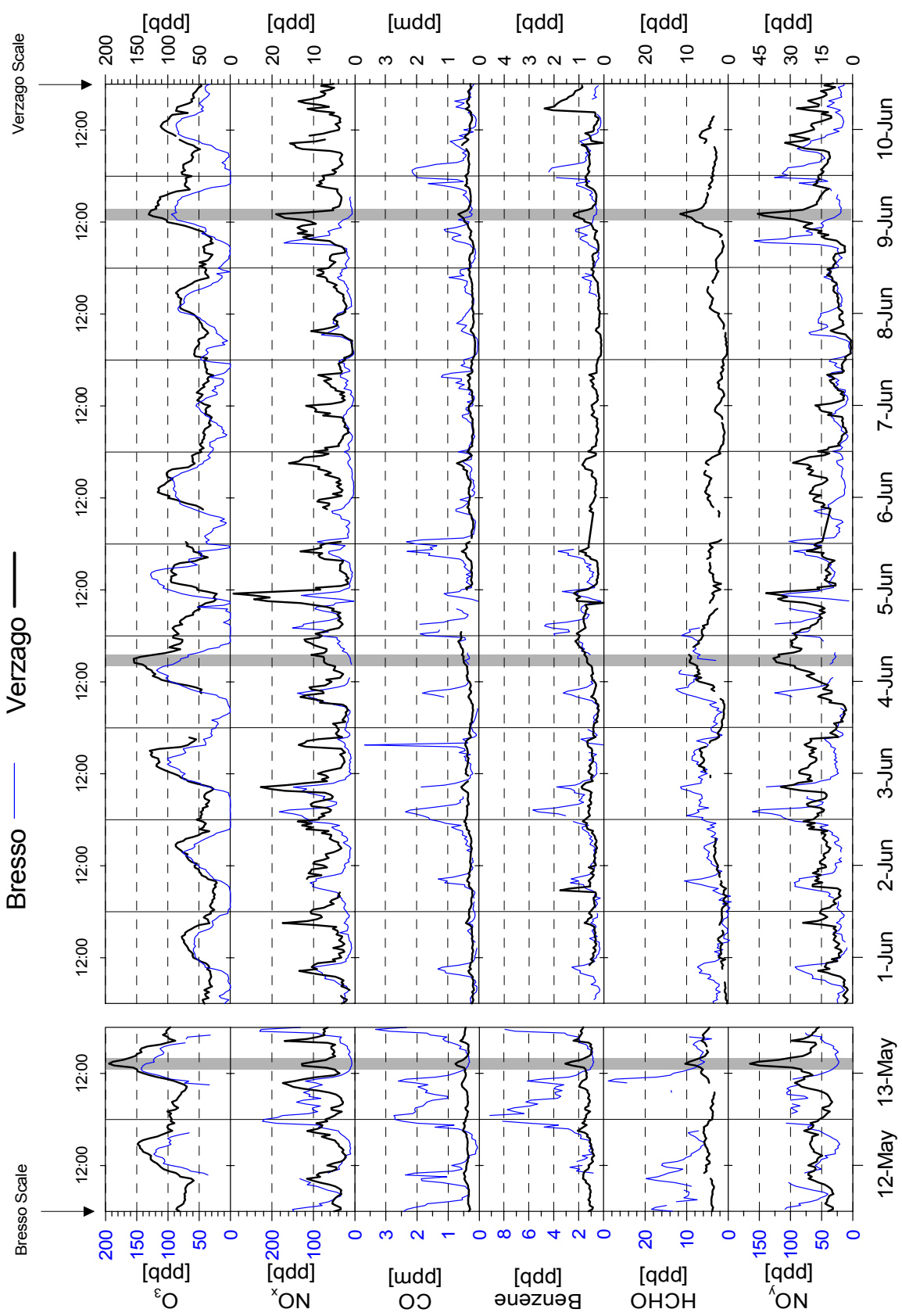

Figure 3: Selected measurements at Bresso and Verzago during both IOPs. Note the different scales at the two sites for NO_x, NO_y and Benzene. NO_x concentrations at Bresso during the afternoons of May 13, June 4, and June 9 are 35 to 40% of NO_y, whereas at Verzago the NO_x to NO_y ratio is 20 to 25%.

$$[NO_2] = [NO] \cdot \left([O_3] \cdot k_{O_3} + [HO_2] \cdot k_{HO_2} + [RO_2] \cdot k_{RO_2}\right) / j_{NO_2} \quad (4)$$

with k_{O3}=1.8E-12·exp(-1370/T) cm^3 $molecules^{-1}$ s^{-1}, and other rate constants according to Table 2.

Photolysis rates were calculated with the Tropospheric Ultraviolet and Visible Radiation model (TUV, V4.1a) [*Madronich and Flocke*, 1999]. We calculated clear sky photolysis rates for the Po Valley with consideration of total ozone concentrations as obtained from measurements of Earth Probe TOMS (NASA). At Verzago, J_{NO2} measurements were available for the first IOP [*Thielmann et al,* 2002]. These observed values were used to calculate j values for other photolysis reactions (j_x) by scaling the clear-sky TUV model predictions (j_x(TUV)), i.e.;

$$j_x = j_x(TUV) \cdot \frac{j_{NO_2}(obs.)}{j_{NO_2}(TUV)} \quad (5)$$

When j_{NO2} observations were not available, TUV photolysis rates were scaled by the ratio of measured to theoretical total solar irradiance as derived from zenith angles.

For the rate of the reaction VOC + OH, a mean of $1.2 \cdot 10^{-12}$ mol. $cm^{-3}s^{-1}$ (Verzago) and $1.5 \cdot 10^{-12}$ $mol.cm^{-3}s^{-1}$ (Bresso) was chosen. These values correspond to the averaged reactivities of the VOC mix (with VOC expressed in units of carbon concentration) as estimated from the HC measurements at Verzago and Bresso. Reaction rate constants of individual HCs were taken from *Atkinson et al.*, [1992]. Since the HC measurements at these sites included only C_4-C_{11}, an approximation was made for the contribution of C_2 and C_3 hydrocarbons. Based on measurements of these compounds at the nearby site of Colma del Piano, we estimated an addition of 20% to the total OH reactivity from this group. Because of its high reactivity and unique emission source, isoprene is included explicitly in our SSA and not as part of the VOC group. Among the oxygenated VOCs, formaldehyde, acetaldehyde and acetone were treated explicitly in our SSA. Since the VOC group does not include the contribution of other oxygenated VOC, our reaction rate for this lumped group certainly reflects a lower limit estimate.

Of the peroxides included in the SSA, (H_2O_2 and CH_3OOH), only H_2O_2 was continuously measured in this campaign. Considering the small influence of CH_3OOH on the results of the SSA, we used a constant concentration of 330 ppt, a value based on the experience of detailed peroxide measurements in an earlier experiment in the area. [*Staffelbach et al.*, 1997*a*].

Table2: List of Reactions Considered in the Steady State Approximation (SSA)

Reaction												Reaction rate constant [b]
OH sources												
HO_2	+	NO			→	OH	+	NO_2				8.5E-12
O_3	+	HO_2			→	OH	+	$2O_2$				2.1E-15
O_3	+	*hν*			→	2 OH	+	O_2				2.31E-5
HONO	+	*hν*			→	OH	+	NO				1.77E-3
H_2O_2	+	*hν*			→	2 OH						5.71E-6
CH_3OOH	+	*hν*	+	O_2	→	HCHO	+	HO_2	+	H_2O		4.41E-6
CH_3OOH	+	OH			→	HCHO	+	H_2O	+	OH		2.2E-12
OH sinks												
Isoprene	+	OH			→	RO_2	+	products				1.0E-10
VOC	+	OH			→	RO_2	+	products				1.5E-12
HCHO	+	OH			→	CO	+	HO_2	+	H_2O		1.0E-11
CO	+	OH	+	O_2	→	CO_2	+	HO_2				2.4E-13
NO_2	+	OH	+	M	→	HNO_3	+	M				1.1E-11
HO_2	+	OH			→	O_2	+	H_2O				1.1E-10
CH_4	+	OH	+	O_2	→	RO_2	+	H_2O				6.7E-15
O_3	+	OH			→	O_2	+	HO_2				7.0E-14
OH	+	NO	+	M	→	HONO	+	M				4.8E-12
OH	+	H_2	+	O_2	→	HO_2	+	H_2O				7.2E-15
H_2O_2	+	OH			→	H_2O	+	HO_2				1.7E-12
CH_3OOH	+	OH			→	RO_2	+	H_2O				5.2E-12
CH_3OOH	+	OH			→	HCHO	+	H_2O	+	OH		2.2E-12
CH_3COCH_3	+	OH	+	O_2	→	RO_2	+	H_2O				2.1E-13
HONO	+	OH			→	NO_2	+	H_2O				4.9E-12
CH_3CHO	+	OH	+	O_2	→	RO_2	+	H_2O				1.6E-11
HNO_3	+	OH			→	NO_3	+	H_2O				1.4E-13
HO_2 sources												
CO	+	OH	+	O_2	→	CO_2	+	HO_2				2.4E-13
RO_2	+	NO	+	O_2	→	NO_2	+	HO_2	+	products		7.7E-12
HCHO	+	*hν*	+	$2\ O_2$	→	$2\ HO_2$	+	CO				2.37E-5
OH	+	H_2	+	O_2	→	HO_2	+	H_2O				7.2E-15
HCHO	+	OH	+	O_2	→	CO	+	HO_2	+	H_2O		1.0E-11
CH_3OOH	+	*hν*	+	O_2	→	HCHO	+	HO_2	+	H_2O		6.71E-7
CH_3CHO	+	*hν*	+	O_2	→	RO_2	+	HO_2	+	CO		4.19E-6
RO_2	+	RO_2	+	$2\ O_2$	→	$2\ HO_2$	+	products				3.5E-13 x 0.5
O_3	+	OH			→	O_2	+	HO_2				7.0E-13
H_2O_2	+	OH			→	H_2O	+	HO_2				1.7E-12
HO_2 sinks												
O_3	+	HO_2			→	OH	+	$2\ O_2$				2.1E-15
NO	+	HO_2			→	OH	+	NO_2				8.5E-12
RO_2	+	HO_2			→	products						6.0E-12
OH	+	HO_2			→	O_2	+	H_2O				1.1E-10
HO_2	+	HO_2			→	H_2O_2						5.0E-12
RO_2 sources												
Isoprene	+	OH			→	RO_2	+	products				1.0E-10
VOC	+	OH			→	RO_2	+	products				1.5E-12
CH_4	+	OH	+	O_2	→	RO_2	+	H_2O				6.7E-15
CH_3COCH_3	+	OH	+	O_2	→	RO_2	+	H_2O				2.1E-13
CH_3OOH	+	OH	+	O_2	→	RO_2	+	H_2O				5.2E-12
CH_3CHO	+	OH	+	O_2	→	RO_2	+	H_2O				1.6E-11
PAN					→	RO_2	+	NO_2				5.9E-04
CH_3CHO	+	*hν*	+	O2	→	RO_2	+	HO_2	+	CO		4.19E-6
RO_2 sinks												
RO_2	+	NO	+	O_2	→	NO_2	+	HO_2	+	product		7.6E-12
RO_2	+	RO_2	+	$2\ O_2$	→	$2\ HO_2$	+	products				3.5E-13
					→	products						3.5E-13
RO_2	+	HO_2			→	products						6.0E-12
RO_2	+	NO_2			→	products						1.1E-11 [c]

[b] Read 8.5E-12 as 8.5×10^{-12}, Rate constants at 298 K, in cm^3 $molecule^{-1}$ s^{-1} for bi-molecular reactions and in s^{-1} for photolysis reactions. Photolysis rates are given for May 12 1200 UTC, clear sky conditions.

[c] Actual rate was fixed to the thermal decomposition rate of PAN.

3.1.1. Instantaneous sensitivity of ozone production rate to NO_x and VOCs

The radical concentrations estimated by SSA were used to calculate instantaneous ozone production rates at both measurement sites. Ozone production, $P(O_3)$, is assumed to be determined by the reactions,

$$NO + HO_2 \xrightarrow{k_1} NO_2 + OH \qquad \text{(R 1)}$$

$$NO + RO_2 \xrightarrow{k_2} NO_2 + RO \qquad \text{(R 2)}$$

since subsequent NO_2 photolysis and the reaction of $O(^3P)$ atoms with oxygen are reasonably fast. With the peroxy radical concentrations obtained from the SSA, $P(O_3)$ is thus calculated as

$$P(O_3) = [NO] \cdot (k_1[HO_2] + k_2[RO_2]) \qquad (6)$$

The sensitivity of the instantaneous O_3 production on NO_x and VOC concentrations can be described by comparing radical sinks and sources. *Kleinman et al.*, [1997] showed that the sensitivity can be derived from a single parameter L_N/Q, where Q denotes the odd-H production and L_N is the loss rate of free radicals caused by reactions with NO_x.

In our calculations, Q consists of the photolysis reactions of O_3, HCHO, H_2O_2, HONO and CH_3CHO (acetaldehyde). L_N is approximated by the reaction $OH+NO_2 \rightarrow HNO_3$. Formation of organic nitrates from reaction of RO_2 radicals with NO is a minor channel averaged over the observed mixture of VOCs and is ignored. PAN is assumed to be in steady state so that it is neither a source or sink of radicals. The effects of this approximation are discussed in Section 5. Relative sensitivities of the ozone production ($dlnPO_3/dln\,[NO_x]$ and $dlnPO_3/dln[HC]$) can then be expressed as simple functions of L_N/Q [*Kleinman et al.*, 1997]:

$$\frac{dlnP(O_3)}{dln[NO_x]} = \frac{1 - 3/2\,\frac{L_N}{Q}}{1 - 1/2\,\frac{L_N}{Q}} \qquad (7)$$

$$\frac{dlnP(O_3)}{dln[HC]} = \frac{1/2\,\frac{L_N}{Q}}{1 - 1/2\,\frac{L_N}{Q}} \qquad (8)$$

VOC-sensitive conditions are characterized by a value of L_N/Q greater than 0.5 whereas a NO_x sensitive ozone production exhibits a ratio smaller than 0.5. Relative sensitivities have a value of 1 if an n% change in $[NO_x]$ or [VOC] results in an n% change in the ozone production [*Kleinman*, 2000].

3.2. 1-D Lagrangian model

3.2.1. Model description

We conducted our calculations with the Harvard photochemical trajectory model. This model has been applied before to various tropospheric chemistry situations [*Fan et al.*, 1994; *Jacob et al.*, 1995; *Staffelbach et al.*, 1997*b*]. The chemical mechanism is identical with the one used by *Staffelbach et al.*, [1997*b*] and is based on the compilation of kinetic and photochemical data by *Atkinson et al.*, [1992] and *Moore et al.*, [1992]. It includes more than 200 species and 600 reactions. Dry deposition of O_3, NO_y species, peroxides, carbonyls, and SO_2 were parameterized by specifying deposition velocities [*Staffelbach et al.*, 1997*b*]. Radiation is

calculated with a six-stream code for the Rayleigh scattering atmosphere at 45.7°N (latitude of Verzago = 45.77 °N). The solar declination was set to 18.2° corresponding to May 13. The model simulates the atmospheric boundary layer with six layers, which have increasing dimensions with altitude. The tops of the six layers are at 40, 105, 225, 500, 950 and 1800 m above ground. Movement of an air mass is simulated by varying emissions and vertical mixing. Mixing layer depth was set to 200 m at nighttime and increases during the day to 1700 m as shown in Figure 4. The estimates of the mixing layer heights from 8:00 to 18:00 hours compare reasonably well with the heights determined from measurements with a windprofiler, which was operated at Seregno (by the Swiss Meteorological Institute, SMI). Vertical exchange between the layers is simu-lated with eddy diffusion coefficients, also shown in Figure 4.

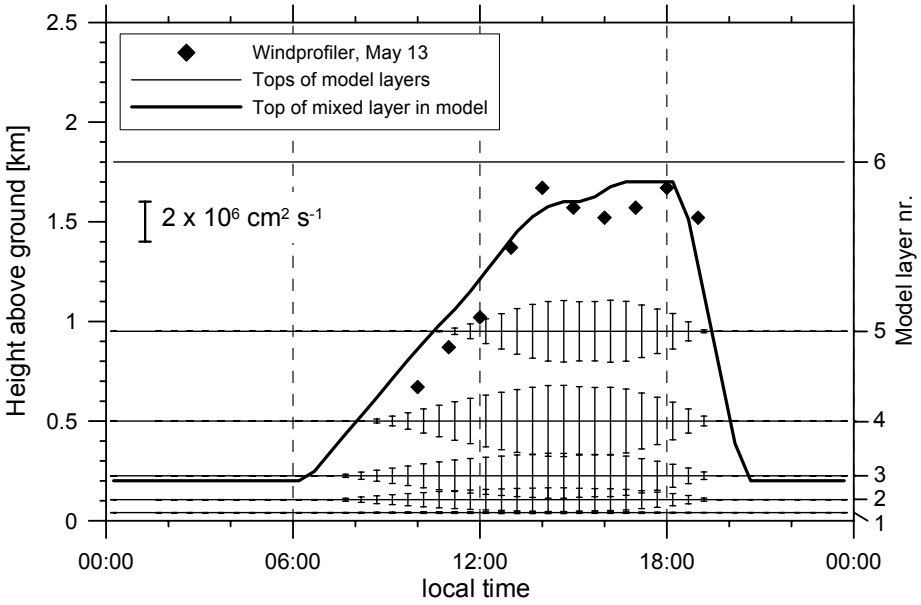

Figure 4: Mixing layer height and eddy coefficients (vertical bars) as applied in 1D-model runs. Diamonds are mixing layer heights as derived from windprofiler measurements at Seregno on May 13.

3.2.2. Emission Data

Regione Lombardia Network prepared an hourly resolved emission inventory for the Milan area with a grid size of 3 by 3 km [*Martilli et al*., 2002]. The inventory contains emissions of NO_x, CO, SO_2 and 32 classes of VOC. From this data base, we calculated the emissions along pathways of air masses reaching the site of Verzago on May 13. A total of 7 model runs were made simulating air masses arriving at Verzago between 10:30 and 18:30 (local time). The routes of the air masses were approximated by a backwards integration of hourly wind measurements. Two representative surface observations were used for this purpose, data from Verzago and the Brera tower in downtown Milan. Since these surface measurements would represent too low velocities for the boundary layer, measurements at 400 m above ground from the wind profiler in Seregno were included as a third wind data set. The horizontal speed of the air parcel at time *t* was calculated as the weighted mean of the 3 measured wind vectors.

The weighting of each measurement was taken inversely proportional to the distance between air parcel and measurement station. I.e.

$$V_{emp}(t) = \sum_{i=1}^{3} f_i \cdot \begin{pmatrix} u_i(t) \\ v_i(t) \end{pmatrix},$$

with

V_{emp} empirical speed of air parcel at time t

f_i weighting factor for wind measurement at site i, $\Sigma f_i = 1$

u_i, v_i horizontal wind components from measurements

We averaged the emissions over 3 x 3 grid cells, leading to an effective emission resolution of 9 x 9 km to take into account horizontal diffusion. An overview on the emission strengths of the trajectories is shown in Figure 5.

Model runs lasted 48 hours and were started at midnight. Initial concentrations were taken in accordance to earlier model studies in this area [*Staffelbach et al.*, 1997*b*]. The simulation of

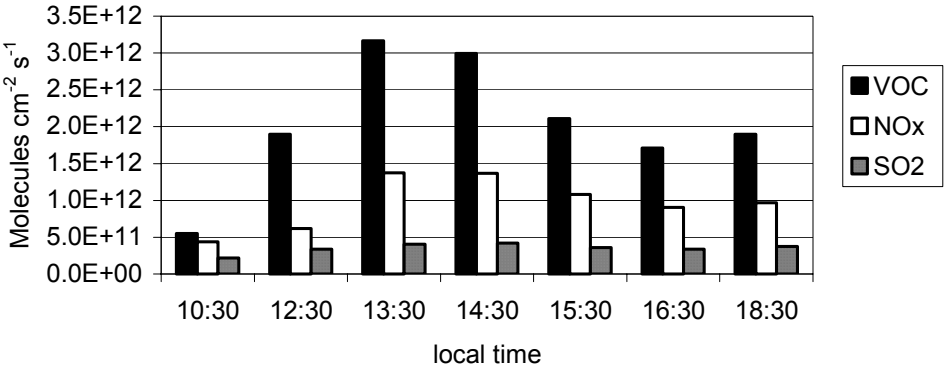

Figure 5: Mean emission strengths used in model trajectories. The trajectories are denoted by the arrival times at the Verzago site.

the first day was not used for interpretation, but served as a prerun in order to get a consistent field of initial concentrations for the second day.

4. Model predictions for Verzago and Bresso

We start with the description of the local ozone production rate at both ground stations. These are results of calculations with the SSA. The 1D photochemical model is afterwards used to study the relation between these local quantities and the regional and integrated perspective of ozone concentration sensitivities.

4.1. Local analysis

4.1.1. Radical concentrations

Figure 6 shows the calculated OH-radical concentrations of Verzago and Bresso. Mean noon OH concentrations are $1.2 \cdot 10^7$ molecules cm^{-3} at Verzago and $9 \cdot 10^6$ molecules cm^{-3} at Bresso. The OH -radical levels in relation to the NO_x concentrations at these two sites are within the range of results from measurements or estimates in other experiments [*Daum et al.*, 2000; *Volz-Thomas and Kolahgar*, 2000].

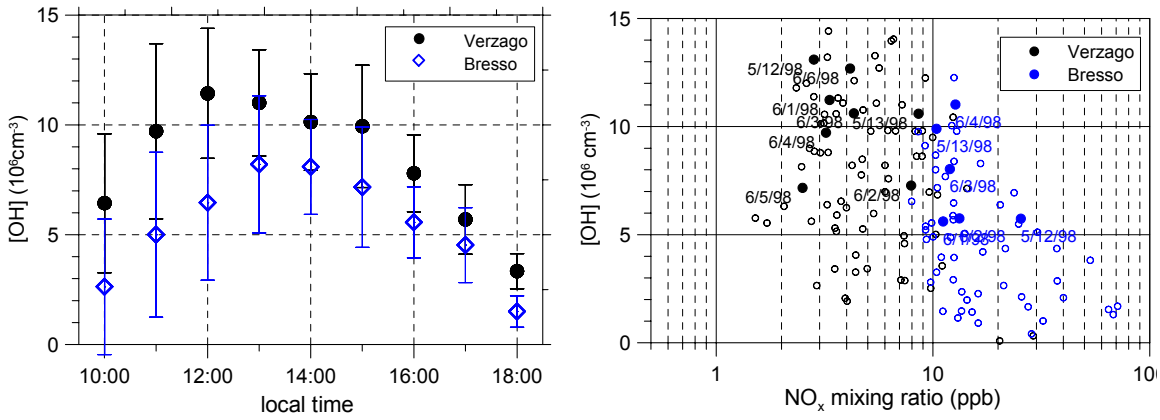

Figure 6: OH concentrations as calculated with SSA for Verzago and Bresso. Left: Average over 6 days (Error bars are standard deviations). Right: OH concentrations in dependence of NO_x concentration, filled symbols denote noon values.

Sensitivity analyses showed that HONO is a rather important parameter in our calculations. As described by *Stutz et al.*, [2002], the HONO concentrations recorded at Bresso can be reasonably explained by steady state calculations and it is unlikely that HONO exceeds 5% of NO_2 concentration during daytime. At the Verzago site, measurements of HONO were performed with a denuder instrument. Since these measurements often exceeded 5% of the NO_2 concentration during daytime, we assume that this HONO measurement suffered from artifacts. We therefore calculated HONO concentrations according to *Alicke et al.*, [2002] and used these values as inputs for the SSA.

A comparison was made between SSA calculations which used observed NO and NO_2 as inputs with calculations that used only observed NO. Observed NO_2 is close to the calculated steady state value. The two types of calculations yield nearly identical predictions for other calculated quantities such as $P(O_3)$. Furthermore, box model calculations were performed for testing our steady state assumption: Using measured concentrations as initial conditions for the box model, the NO to NO_2 ratio did not change significantly. We interpret it as meaning that the air at Verzago was close to being in steady state for radicals and NO_2.

The comparison of measured and calculated peroxy radical concentrations (Figure 7) gives an ambiguous picture, mainly because the amount of data for comparisons is limited. June 1, 5 and 8 are the only days where MCA data and complete input data sets for the SSA were avai-

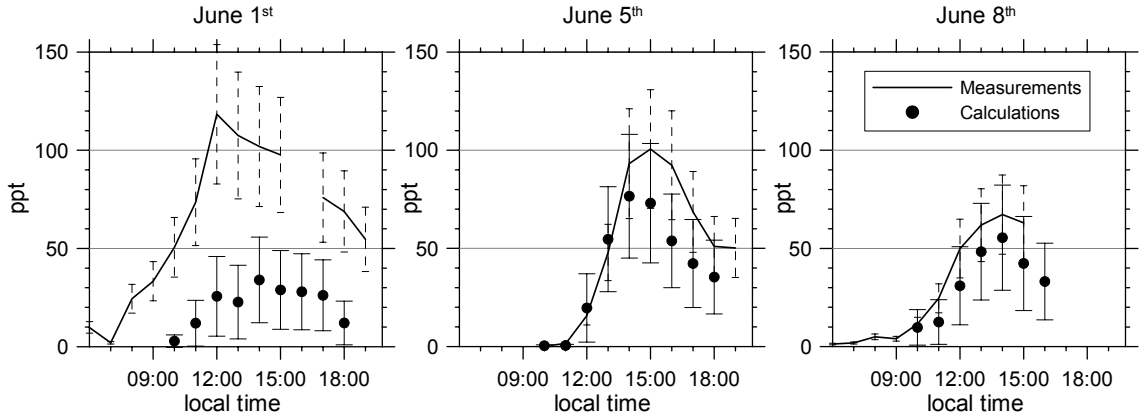

Figure 7. Comparison of peroxy radical measurements (lines) and calculations (symbols) at Verzago. Measurement uncertainties are 39%, error bars of the calculations were determined from errors of the concentrations used as input for the SSA by assuming standard error propagation.

lable. On the morning of June 5 and on June 8, calculated and observed peroxy radical concentrations are within the measurement and calculation errors. On June 1, observed peroxy radicals are approximate-ly 3 to 5 times of calculated values, a discrepancy that is much greater than expected based on a consideration of experimental and model errors. A maximum ozone production rate of 14 ppb/h is predicted from Eq (6) using calculated SSA values for peroxy radical concentration. An ozone production rate in excess of 50 ppb/h is predicted from observed peroxy radical concentration. June 1 was a day with a relatively low O_3 concentration as compared with other IOP days, and on this basis the measured peroxy radical concentration appears to be too high. We suspect interferences in the peroxy radical measurement as suggested by *Stevens et al.* [1997], who applied comparable measurement and calculation methods and found similar discrepancies in environments with relatively high NO_x levels (NO > 100 ppt).

4.1.2. Sensitivity of O_3 production to NO_x and VOC

For all datasets, we calculated the relative change of the ozone production rate due to a small change (5%) in the concentrations of NO_x and VOC (including CO, biogenics and CH_4). In Figure 8, these relative ozone production sensitivities ($dlnP(O_3)/dln\ [NO_x]$ and $dlnP(O_3)/dln[VOC]$) are plotted against the parameter L_N/Q.

The L_N/Q values calculated from observations (circles and squares) follow the theoretical pattern (lines) quite well, except at higher L_N/Q values, where the 'observed' relative sensitivity of VOC-changes is somewhat lower than in theory. However, the transition between NO_x and VOC sensitive O_3 production occurs almost exactly at the theoretical L_N/Q value of 0.5. L_N/Q is therefore used in the following to distinguish between NO_x- and VOC sensitive ozone production. Calculated L_N/Q values for the sites of Bresso and Verzago reveal that ozone production at the urban site of Bresso is VOC sensitive, while Verzago exhibited both VOC and NO_x sensitive conditions.

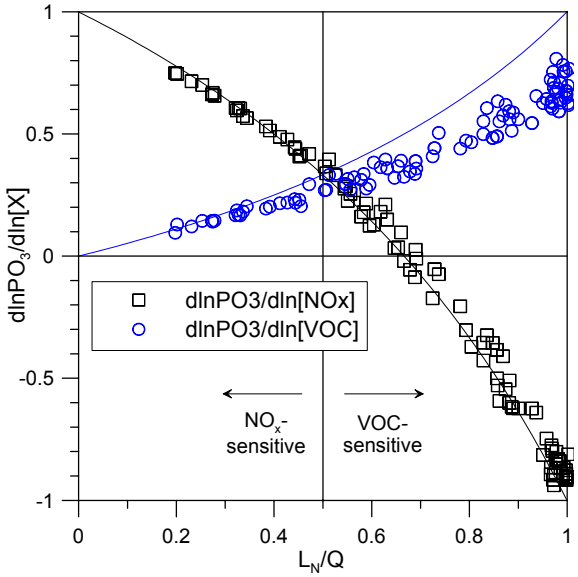

Figure 8. Relative sensitivities of local ozone production as determined from measurements between 10:00 and 18:00 at Bresso and Verzago.

The VOC sensitivity at Bresso is not surprising due to the various strong emission sources nearby. The situation in Verzago is more complex. Ozone production and its sensitivity is influenced by the diurnal variation of radiation, vertical mixing and horizontal transport

processes. Figure 9 shows the ozone productions and their sensitivities at Verzago for 6 IOP days. In the morning, ozone production is generally VOC sensitive. Lower radiation results in a smaller radical production and the lower height of the boundary layer limits vertical mixing. Therefore, there is a large amount of NO_x relative to radical production, most radicals will be removed by NO_x – radical reactions, and L_N/Q will be close to 1 and O_3 production will be VOC sensitive.

May 12 and 13 were similar days considering the solar radiation (sunny, no clouds), but the local ozone production at Verzago shows a rather distinctive behavior. At 14:00, it was NO_x sensitive on 12th of May but VOC sensitive on 13th of May. The maximum O_3 production rate on May 13th occurred significantly later than the radiation maximum and was between 5 and 10 ppb higher than the day before. For most of the measured species at Verzago, a dramatic increase in concentration was observed between 13:00 and 14:00 local time, indicating the arrival of a heavily polluted air mass (Figure 3). Wind measurements by the wind profiler in Seregno reveal that the wind directions were directly from the South on 13th of May, but more western on May 12 (Figure 2). It appears that a strong emission source south of Verzago (other than Milan) causes this difference between the situations on May 12 and 13. A comparison of the quasi conservative tracers, CO and NO_y, registered during May 13 in Bresso, Seregno and Verzago also points to a substantial emission source between Bresso and Verzago in addition to the strong emissions in the metropolitan area of Milan (compare *Martilli et al.*, [2002]). Our local analysis reveals that this plume caused an additional ozone production of 5-10 ppb/h. Furthermore, the sensitivity of ozone production during this event was more VOC sensitive (higher L_N/Q) than at the same time on other IOP days. In the absence of a pronounced plume, O_3 production at Verzago was NO_x limited on cloudless days. Recall that the sum of VOC and the reaction rate of VOC + OH as used in our calculation represent lower limit estimates. An increase in VOC concentrations and reactivity would shift the results towards more NO_x sensitivity.

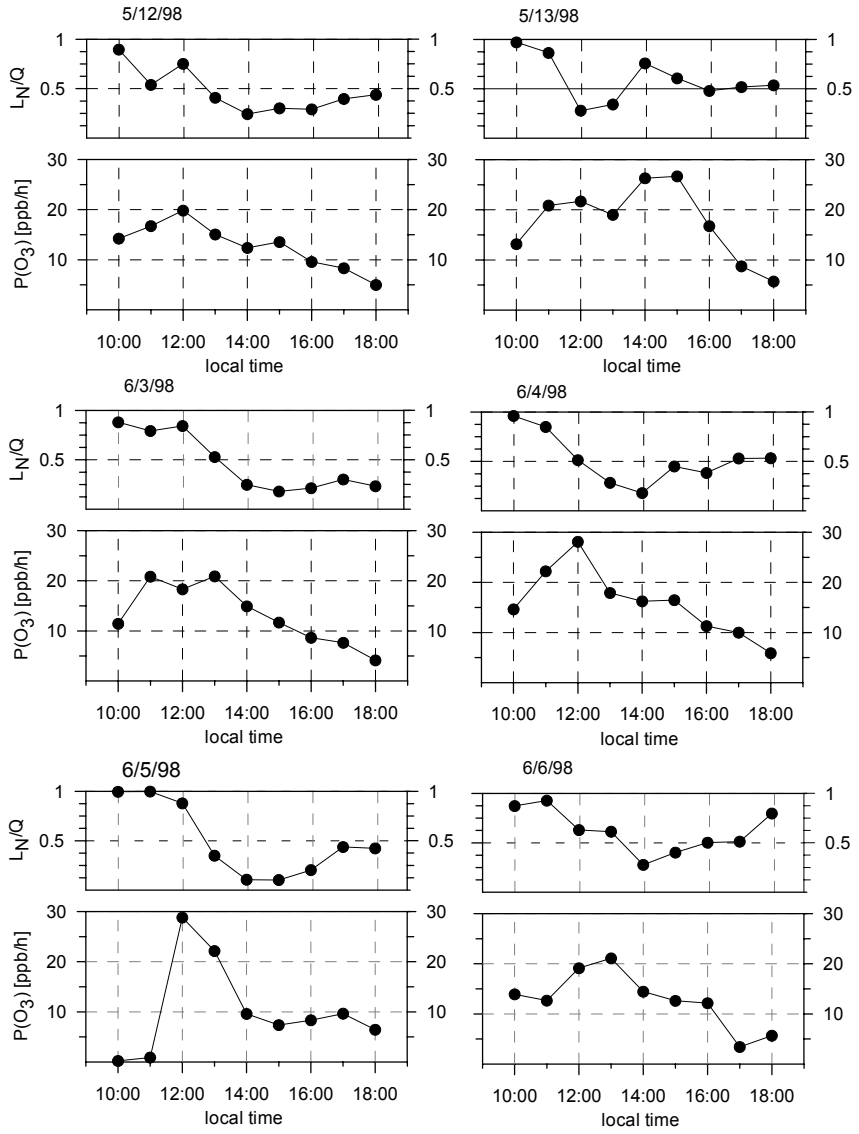

Figure 9. Instantaneous ozone productions and their sensitivities (expressed by L_N/Q) to NO_x and VOC concentrations. SSA results from measurements at Verzago.

4.2. Lagrangian model runs

In the previous section we presented an analysis of the instantaneous state of an air parcel. For the development of an O_3 control strategy, the sensitivity of O_3 concentration to an emissions change has to be considered. This quantity will depend on the history of the air mass. With the help of model calculations we will discuss how representative our surface based analysis can be and whether statements about the local ozone production rate can be linked to the regional question of the effects of emission controls.

The Lagrangian model described in Section 3 was used to simulate the concentrations observed at Verzago on May 13. A comparison between model results and measurements at Verzago is shown in Figure 10. The model simulates reasonable O_3 concentrations and captures approximate levels of other photooxidants. However, a 1-D model cannot accurately simulate 3-D transport and there are known deficiencies in model inputs. For example, the difference in CO is most likely a consequence of insufficient emissions in the inventory, as pointed out by *Thielmann*, [2000]. On the other hand, SO_2 emissions seem to be much too high [*Martilli et al.,* 2002]). The model reproduces similar NO_x and VOC levels but fails to

simulate the high concentrations observed in the early afternoon. These differences might be explained by the modest spatial resolution of emissions (9*9 km) used for these model calculations. But there is also evidence from ground and airborne measurements, that there are some hot spots in the emissions that are not sufficiently resolved in the inventory.

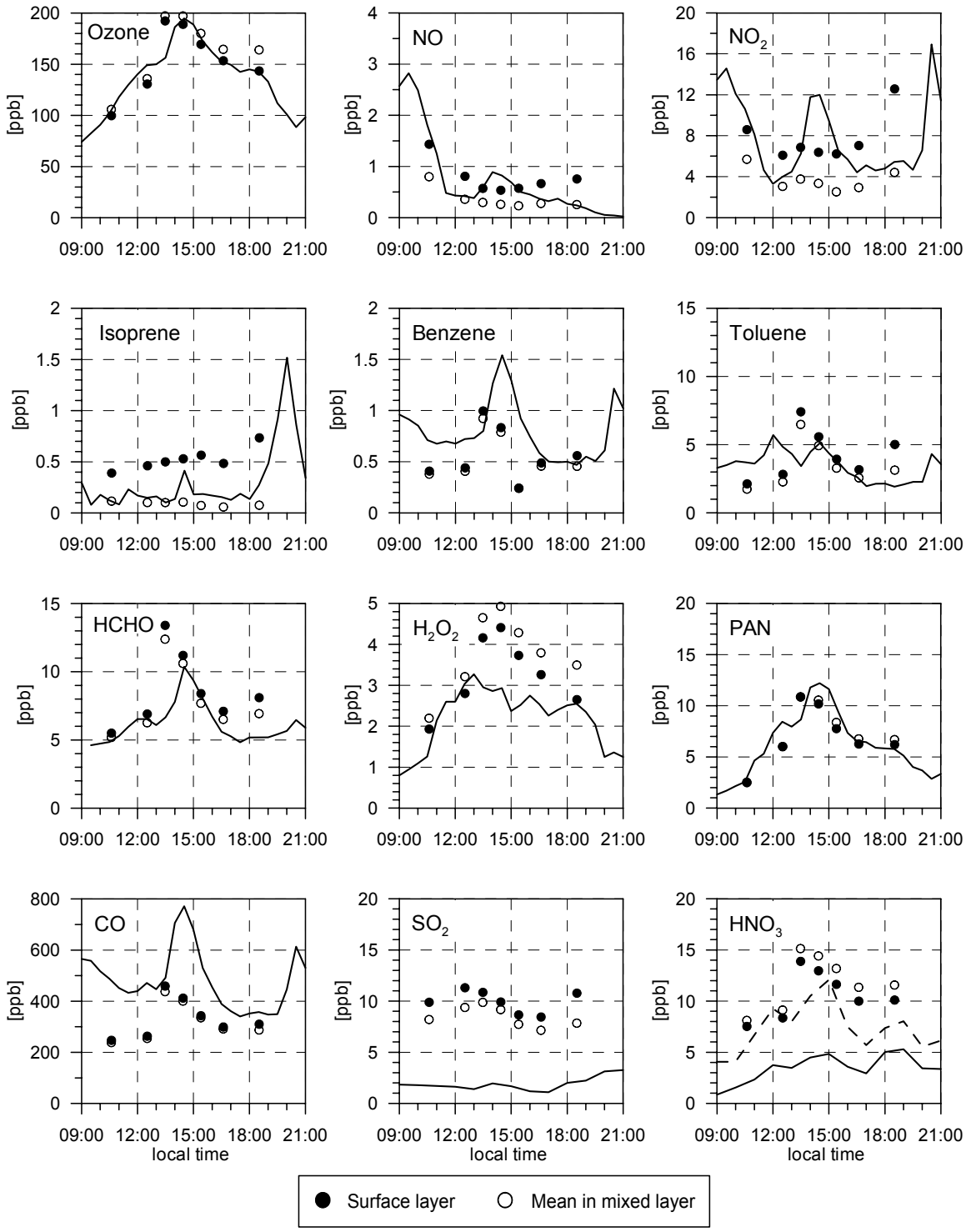

Figure 10. Simulation of the situation on May 13 1998: Measurements (lines) at Verzago and concentrations predicted by the Lagrangian model (symbols) at the arrival of the 7 trajectories at Verzago.

HNO_3 concentrations are much higher in the model, since it doesn't include aerosol formation. If the sum of HNO_3 and aerosol NO_3^- measurements (dashed line in Figure 10) are compared to modeled HNO_3 values, the agreement is reasonable.

Isoprene measurements taken at the surface are known to be representative for only a very limited area [*Staffelbach et al.*, 1997*a*]. Because of its high reactivity towards OH, isoprene is quickly removed and concentrations are dominated by local emissions. Isoprene measurements taken on an aircraft 500 m above ground agree well with mean mixing layer concentrations in the model. It is therefore concluded that the isoprene emissions of the emission inventory are realistic. Since the modeled concentrations are higher than the surface measurements, it is likely that the measurement site exhibited lower isoprene emissions nearby than the average of the corresponding grid cell in the emission inventory. The evening peak of isoprene was a repeatedly observed phenomenon at the Verzago site. We rule out an anthropogenic origin, since there is no correlation between the concentrations of toluene and isoprene or benzene and isoprene during the evening hours (whereas there is a correlation between toluene and benzene). Elevated isoprene concentrations during the evening at surface sites have been observed at various locations [*Stroud et al.*, 2001, *Starn et al.*, 1998, and references therein]. We assume a similar explanation for the Verzago site: The development of a shallow nocturnal boundary layer in combination with a higher lifetime of isoprene due to reduced OH levels in the evening leads to elevated concentrations even though emissions are lower than in the middle of the day. Again, this phenomenon is beyond the resolution of our Lagrangian model and can therefore not be realistically represented in the simulation.

Since the measured NO_x and VOC levels compare well to the afternoon concentrations modeled for the mean of the mixing layer, it is concluded that Verzago is a station representing well the conditions of the mixing layer. This is supported by NO_x measurements at 200 to 700 m above ground on the French ARAT aircraft. When flying directly above Verzago, the NO_x levels recorded on the aircraft are in the range of those registered at the surface (Figure 11).

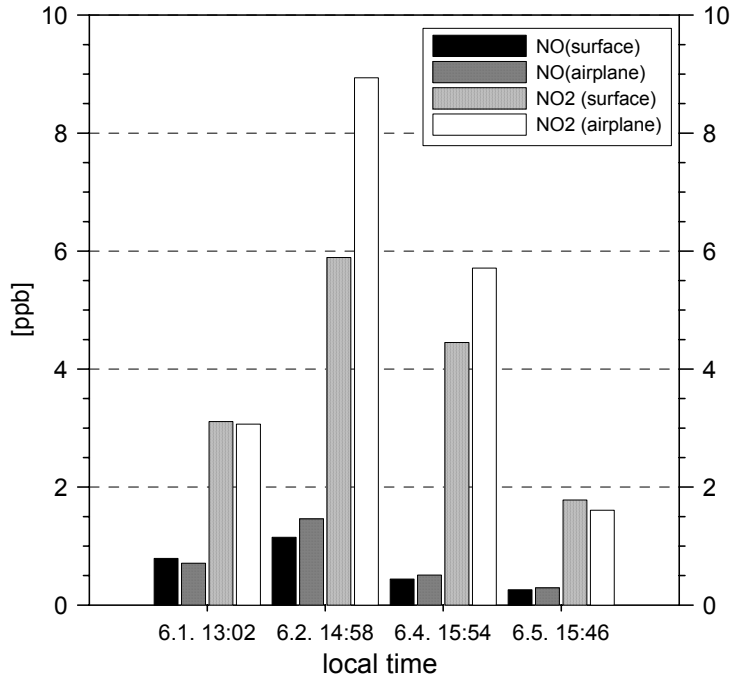

Figure 11. Comparison of surface and airplane NO_x measurements at Verzago.

In order to examine the treatment of vertical mixing in the model, radon was included as a modeled species and compared to measurements. For radon, a decay constant of $2.1 * 10^{-6}$ s^{-1} (i.e a half-life period of 3.82 days) and a constant emission rate of 72 Bq/m^2 was used. Figure 12 shows modeled and measured radon values for May 13, and indicates that vertical mixing in the model was simulated reasonably well.

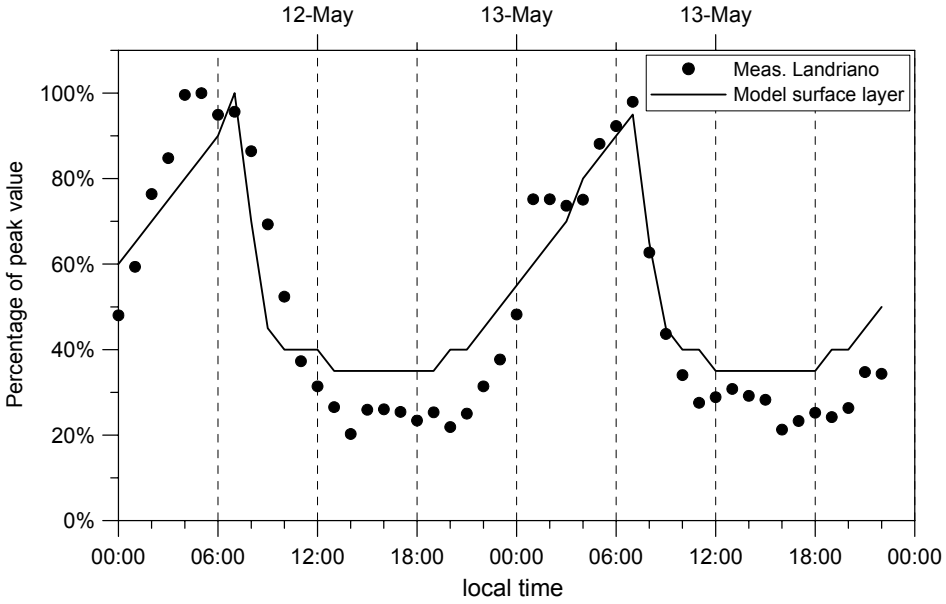

Figure 12. Radon concentrations measured at Landriano on May 13 and in surface layer of the 1D model. Concentrations are scaled to daily peak values.

The comparisons between model runs and measurements demonstrate that the model simulated a situation that is realistic for the Po Valley. It is therefore a useful tool for considering the relations between local and integrated ozone production sensitivities.

5. O_3 and $P(O_3)$ along a trajectory

In this section the Lagrangian model is used to show how the sensitivity of O_3 concentration to an emissions reduction of NO_x or VOCs varies as a function of time and altitude as an air mass is advected along a trajectory. As a case study, we choose the trajectory simulating the air mass reaching Verzago at 15:30 local time. The response of O_3 to an emissions change is determined by comparing a base case calculation with a calculation having either a 35% NO_x or VOC (including CO, CH_4 and biogenic VOC) reduction.

A steady state analysis has also been done following the methods of Section 3, but using Lagrangian model output in place of real observations. The SSA yields predictions of the sensitivity of $P(O_3)$ to NO_x and VOCs. We compare the local sensitivity of $P(O_3)$ to NO_x and VOC with the integrated sensitivity of O_3 concentration to NO_x and VOCs emissions. The purpose of this comparison is to determine the ability of the local analysis to predict the effects of an emissions change.

5.1. Response of O_3 to an emissions change

Figure 13 shows the calculated near-surface O_3 concentration in an air parcel that is advected to the north from Milan to Verzago. In the morning the air parcel is over downtown Milan; it reaches Verzago at 15:30 and at later times it is north of Verzago. The three lines in Figure 13 are for base case emissions and for NO_x and VOC emissions reduced by 35%. Before 13:00 a NO_x reduction is seen to cause a higher near surface (model layer 1) O_3 concentration. At

about 14:30, when the air mass is 30 km north of downtown Milan, the NO_x and VOC reduction curves cross. Before this time O_3 is VOC sensitive and after this time NO_x sensitive. Thus the air parcel displays the expected transition from VOC sensitive chemistry near a source region to NO_x sensitive chemistry downwind.

The dependence of NO_x versus VOC sensitivity on altitude is illustrated in Figure 14. When $[O_3]$(NO_x reduction) - $[O_3]$(VOC reduction) is greater than zero, a VOC emissions reduction

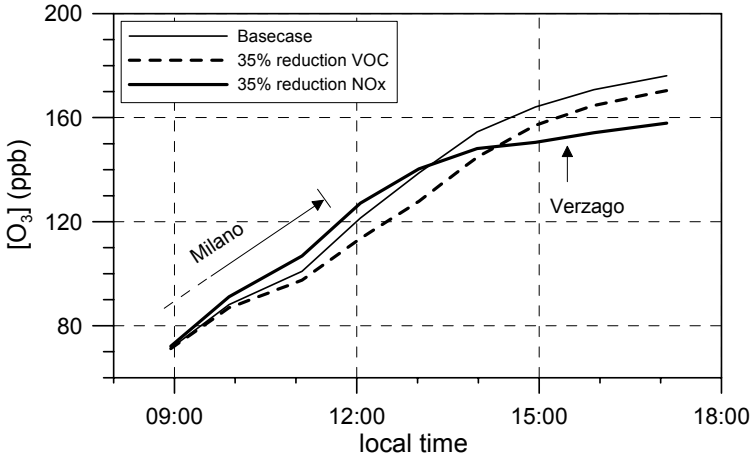

Figure 13. Ozone as predicted by the Lagrangian model: Surface concentrations of an air column advected northward from Milan towards Verzago. It moves over the urban area of Milan from 8:00 to 11:30 and then heads north with a speed of 8 to 10 km/h.

is more effective than a NO_x emissions reduction in reducing O_3. By definition O_3 is then VOC sensitive. At all times NO_x sensitivity increases with altitude. In the uppermost layer, the ozone concentration remains NO_x sensitive throughout the whole trajectory. The switch from VOC to NO_x sensitivity occurs about 30 minutes later at the surface than in the middle of the mixed layer. Later in the day, the sensitivity in all six model layers converge. Convective mixing aided by the absence of a strong surface emission source leads to a well mixed atmosphere.

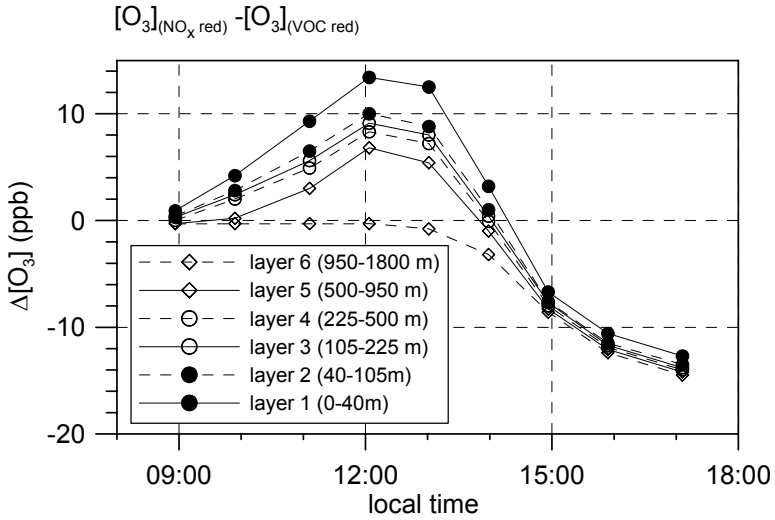

Figure 14. Modeled ozone concentrations at different altitudes: Difference between scenarios with 35% reduced NO_x and VOC emissions.

5.2. Base case ozone production rate

Output from the Lagrangian model was used to calculate $P(O_3)$. Two ways of doing this were explored. In one method Lagrangian model results (for non-radical species) were used as input to an SSA calculation identical to that described in Section 3.1. The SSA calculation then yields predicted values for radical concentrations. In the other approach radical concentrations are obtained directly from the Lagrangian calculation. In both cases $P(O_3)$ is calculated from [NO], [HO_2] and [RO_2] using Eq. (6). A comparison between these two methods is discussed at the end of this section.

$P(O_3)$ calculated from Lagrangian model output using the SSA method is shown in Figure 15. The SSA calculations also yield values for L_N/Q, which according to (7-8) and Figure 8, are directly related to $P(O_3)$ sensitivities. Figure 15 illustrates how the instantaneous ozone production rates depend on altitude and how they evolve as the air mass is advected from a source region to a cleaner downwind region.

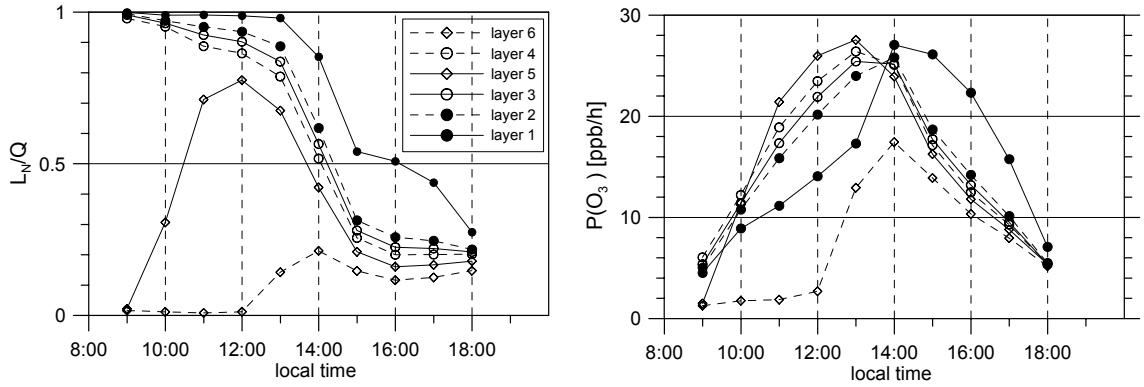

Figure 15. Characterization of instantaneous ozone productions along the model trajectory. Results of the SSA using concentrations of the 1-D model as inputs. 15a: O_3 production, 15b: Sensitivity of O_3 production expressed by L_N/Q.

In model layers 1-4, $P(O_3)$ starts the day VOC sensitive ($L_N/Q > 0.5$) and becomes NO_x sensitive ($L_N/Q < 0.5$) later in the day. Model layers 5 and 6 (500 – 1800 m above ground level) represent the residual layer early in the day. Because of low pollutant concentrations (in particular low NO_x concentrations), ozone production in layers 5 and 6 is very NO_x sensitive at the start of the day. When the boundary layer reaches heights within these model layers (see Figure 4), ozone production increases and gets more sensitive to the VOC concentration (i.e. L_N/Q increases). Later in the day when vertical mixing is well established, layers 2-6 exhibit rather similar conditions of ozone production, while the surface layer still exhibits a more VOC sensitive O_3 production. Part of the more VOC sensitive ozone production in the lowest layer is a consequence of the fact that the model receives its emission inputs continuously into that layer. NO_x levels in the surface layer are thus consistently higher than the average in the mixed layer. Test runs with anthropogenic emissions interrupted for 30 minutes show only a negligible difference between surface layer and the other layers within the mixing layer.

The SSA calculation predicts that $P(O_3)$ is always NO_x limited in layer 6 and that the transition between VOC and NO_x sensitivity occurs at about 14:00 for model layers 2-5 and at 16:00 for the surface layer. In the presence of surface emission sources, a prediction of $P(O_3)$ sensitivity based on surface data is thus different than a prediction based on the bulk of the boundary layer. Note also, the height of each of the model layers increases with altitude so that the amount of ozone produced in the upper layers is greater than that produced in the lower layers even if the effective production rate (ppb/h) is lower.

The analysis of $P(O_3)$ in different layers also allows us to demonstrate that the vertical model resolution can play a major role in the sensitivity of ozone production. Recall that turbulent mixing is parameterized by means of eddy coefficients between the model layers. Within the layers, complete and instantaneous mixing is assumed. When the boundary layer rises above the altitude of a model layer, mixing from underneath into the upper model layer will occur and any pollutants lifted up are distributed homogeneously within this layer. As a consequence, vertical mixing at certain altitudes will be faster in the model than in reality. This difference rises with increasing layer dimensions of the model. In our case, this effect becomes particularly pronounced when the boundary layer grows through the uppermost layer (which has a vertical dimension of 850 m). This occurs between 11:00 and 14:00. NO_x and VOC transported into this layer with its strongly NO_x sensitive ozone production leads to a significant increase in the ozone production. Considering the total ozone production in the column, the poor vertical resolution of the model thus has the effect, that more ozone is produced under NO_x sensitive conditions. Even though the modest vertical resolution of our model unrealistically exaggerates this effect, it demonstrates that entrainment is an important factor in the study of ozone production sensitivities. That a model is successful in reproducing the conditions for O_3 production at the surface, does not necessarily imply that it is equally skilled at simulating conditions in the upper part of the mixed layer. Model studies about the limitation of ozone production therefore should be carefully tested not only against surface measurements, but also against observations throughout the boundary and the residual layer. Measurements of entrain-ment fluxes would be very helpful in future field studies addressing the limitation of ozone production.

5.3. Comparisons between $P(O_3)$ and O_3

Calculations presented in the last 2 sub-sections yield predictions for 1) O_3 concentration and production rate $P(O_3)$, 2) the sensitivity of $P(O_3)$ to changes in the concentration of NO_x and VOCs, and 3) the change in O_3 concentration due to a change in emissions. We are now in a position to offer some qualitative observations about how these quantities are related.

In the Lagrangian calculation O_3 concentration is affected by chemical production and loss, mixing between model layers and, surface deposition. Leaving aside mixing as not affecting the total amount of O_3 and noting that chemical loss and surface loss are relatively small, the amount of O_3 formed over the calculation (between initial time t_0 and ending time t) should be approximately equal to the amount of O_3 chemically produced, or

$$[O_3(t)] - [O_3(t_0)] = \int P(O_3)dt \qquad (9)$$

Equation (9) can be differentiated with respect to the NO_x or VOC emission rate, E_{NOx} or E_{VOC}, yielding

$$\frac{d[O_3]}{dE} = \int \frac{dP(O_3)}{dE} dt \qquad (10)$$

where E is either E_{NOx} or E_{VOC}. Although $P(O_3)$ can be calculated from local observations, $dP(O_3)/dE$ cannot. This derivative represents the response of the instantaneous state of the atmosphere to an emissions change which took place at a different location and at an earlier time. We can attempt to simplify (10) by expanding the derivatives using the chain rule.

$$\frac{d[O_3]}{dE} = \int \left(\frac{\partial P(O_3)}{\partial [NO_x]} \cdot \frac{\partial [NO_x]}{\partial E} + \frac{\partial P(O_3)}{\partial [VOC]} \cdot \frac{\partial [VOC]}{\partial E} + \frac{\partial P(O_3)}{\partial Q} \cdot \frac{\partial Q}{\partial E} \right) dt \qquad (11)$$

The chain rule expansion is done assuming that there are 3 independent variables, NO_x, VOCs, and Q (odd-H production) that provide a complete description of local

photochemistry. An actual evaluation of the integrand in (11) would be problematic as, for example, HCHO is both a radical source and a VOC. Rather than deal with the exact form of (11) we consider some general features. Equation (11) contains terms like $\partial[NO_x]/\partial E_{NOx}$ and $\partial[VOC]/\partial E_{NOx}$ which express how an emission change affects $[NO_x]$ and [VOC] downwind. In the simplest case an emission change of (for example) NO_x would cause a proportionate change in NO_x downwind and no change in [VOC] or Q. Then:

$$\frac{d[O_3]}{dE_{NO_x}} = \int \frac{\partial P(O_3)}{\partial [NO_x]} dt \qquad (12a)$$

$$\frac{d[O_3]}{dE_{VOC}} = \int \frac{\partial P(O_3)}{\partial [VOC]} dt \qquad (12b)$$

Equations (12) suggest that, to a first approximation, O_3 concentration sensitivity depends on the time integral of local ozone production sensitivity. If (12a and 12b) are correct, then the transition of $[O_3]$ from being VOC sensitive to NO_x sensitive should occur at a time when, roughly speaking, the VOC sensitive contribution of $P(O_3)$ balances the NO_x sensitive contribution. Since $P(O_3)$ is VOC sensitive at the beginning of the trajectory and switches to NO_x sensitive at about 14:00 (see Figure 15 for layers 2-5, where most of the O_3 is produced), we would anticipate that the change from VOC to NO_x sensitivity for ozone concentration would occur several hours later, at a time when enough O_3 is formed under NO_x sensitive conditions at the end of the trajectory to balance the O_3 formed under VOC sensitive conditions at the start of the trajectory. However, in this case the shift of the ozone concentration sensitivity occurs about at the same time (14:00), as can be seen from Figure 13. Adding in the effects of level 6, which remains NO_x sensitive throughout the day, gives us a somewhat earlier layer-average transition time for $P(O_3)$ to become NO_x sensitive. Even still, it is clear that at 14:00 (when O_3 makes the transition) less than half of the O_3 has been formed under NO_x sensitive condition according to the base case calculation. Therefore, $P(O_3)$ from the base case calculation yields a prediction that $[O_3]$ is more VOC sensitive than it actually is.

$P(O_3)$ along a trajectory does not give us a quantitative prediction of the VOC to NO_x sensitive transition of $[O_3]$ because Eq. (12) is only an approximation. NO_x and VOC concentration depend in a nonlinear way on their emissions. A certain reduction of NO_x emissions will not only result in a different decrease in its concentration, but it will also influence the VOC concentration (and vice versa). Because of the complicated and non-linear dependence of $[NO_x]$ and [VOC] on emissions, $d[O_3]/dE_{NOx}$ and $d[O_3]/dE_{VOC}$ cannot be described as simple functions of $P(O_3)$ as written in Equations (12).

We can explicitly demonstrate the effects of the non-linear relation between $[NO_x]$ and [VOC] and their emissions by examining $P(O_3)$ for the calculations in which emission rates of NO_x and VOCs were reduced by 35%. Figure 16a shows the difference in O_3 production rate (calculated with the SSA method) for the 2 emission reduction scenarios,

$$\Delta P(O_3) = P(O_3)_{NO_x \text{ reduction}} - P(O_3)_{\text{VOC reduction}} \quad (13)$$

A comparison of the zero-crossing in Figure 16a with the $L_N/Q = 0.5$ line in Figure 15, shows

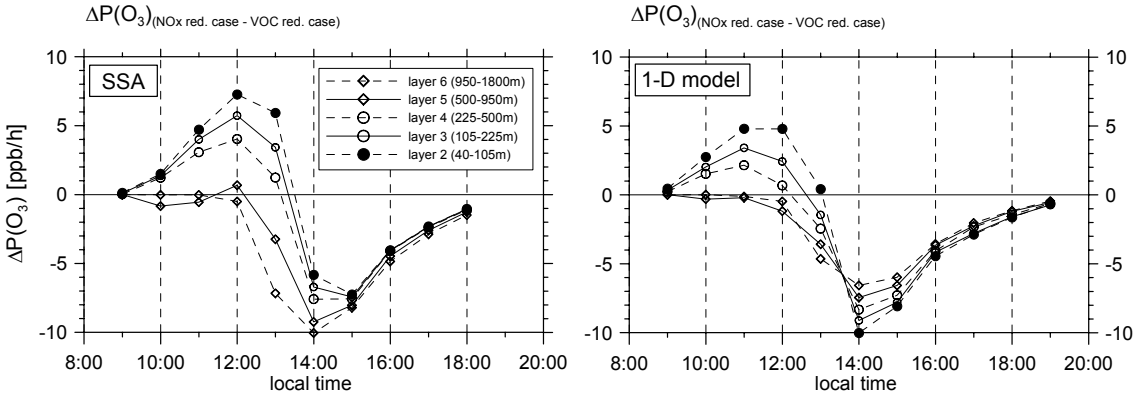

Figure 16. Differences in ozone production between runs with 35 % reduction of NO_x and VOC emissions. 16a: Steady state calculations with 1-D model concentrations a s inputs, 16b: 1-D model results.

that the $P(O_3)$ transition from VOC to NO_x sensitivity occurs almost an hour earlier in the day when the effect of emissions reduction on $[NO_x]$ and [VOC] is taken into account.

In Figure 16b, $\Delta P(O_3)$ is calculated directly from the Lagrangian model using predicted values for for [NO], $[HO_2]$, and $[RO_2]$. Ideally, this method would yield the same results as the SSA method but there are differences because of approximations made in the SSA method. The most serious of these approximations is the assumption that PAN is in steady state. Figure 10 shows that PAN concentrations are high and therefore its formation and eventual dissociation, both of which are not part of a steady state calculation, can have a significant influence on local photochemistry. Figure 16b indicates that an earlier transition time is obtained when $P(O_3)$ is calculated directly from the Lagrangian model. Near the transition time, the Lagrangian calculation predicts that the atmosphere is more NO_x sensitive than does the SSA calculation. We have traced this effect to the importance of PAN chemistry: At the time that model levels 2 to 4 make a transition from VOC to NO_x sensitive behavior, the production rate of PAN is positive, which implies that fewer radicals are available for forming HNO_3. As *Sillman* [1995] has noted, the transition point from VOC to NO_x sensitivity depends on $P(HNO_3)$ and not on P(PAN). This result is also implicit in the derivation given by *Kleinman et al.* [1997] in which analytic equations for NO_x and VOC sensitivity (equations (7) and (8) of this paper) follow from an argument in which L_N is approximated as $P(HNO_3)$. The SSA calculation by neglecting the PAN formation pathway for removing radicals, over-estimates $P(HNO_3)$ and $P(HNO_3)/Q$ in regions where PAN is being formed. It therefore over-predicts VOC sensitivity. In regions where PAN is dissociating, the SSA calculation over-predicts NO_x sensitivity.

6. Conclusions

As part of the 1998 PIPAPO field campaign to study the Milan urban plume, comprehensive sets of trace gas measurement were made downwind at Bresso and Verzago. These observations were used as input to a steady state calculation for the purpose of determining the concentration of free radicals, the production rate of O_3, $P(O_3)$, and the sensitivity of $P(O_3)$ to NO_x and VOCs.

The SSA calculations show that $P(O_3)$ at Bresso was VOC sensitive. In contrast $P(O_3)$ at Verzago exhibited both VOC and NO_x sensitive behavior, usually starting out in the morning as VOC sensitive and becoming NO_x sensitive in the early afternoon. Maximum rates for O_3 production were about 30 ppb/h at Verzago.

This observation based analysis allows us to determine how $P(O_3)$ is affected by changes in NO_x and VOC s, but it does not give us an answer to the question of how O_3 concentration depends on emissions. A study with a Lagrangian model was performed to address the later problem. By looking at the instantaneous ozone productions along this model case, we could illustrate how local ozone production sensitivities relate to ozone concentration sensitivities.

We found a vertical gradient in $P(O_3)$ sensitivity with model layers near the ground being more VOC sensitive than layers in the mid-boundary layer. Since ozone production at the surface accounts only for a fraction of the ozone concentration, local analyses based on surface observations need careful interpretation. Conditions at a surface site will only be representative for a large part of the ozone production if the site is not affected by local emissions and at times when strong vertical mixing is established.

The non-linear relationships between emissions and concentrations prevent a direct derivation of ozone concentration sensitivity from local sensitivities of ozone production. Calculations with chemical transport models are necessary for predictions about the sensitivity of ozone concentrations. In our simulation of the situation on May 13, $P(O_3)$ in mid of the mixed layer makes a transition from VOC sensitive behavior to NO_x sensitive behavior at about the same time as O_3 concentration changes from being VOC sensitive to NO_x sensitive. Recalling the results of the local analyses at the Verzago site on this day, it is plausible that ozone concentration during the plume arrival was VOC sensitive, but NO_x sensitive later in the afternoon.

This finding fits with other analyses during the PIPAPO campaign [*Martilli et al.*, 2002, *Thielmann et al.*, 2002]. The Milan area exhibits only a limited area of VOC sensitive ozone concentration during summer smog episodes, the transition from VOC to NO_x sensitive regime downwind of Milan occurs within 4-5 hours.

Acknowledgements

We thank all participants who contributed their data to build the PIPAPO database. The help of various institutions of the Lombardy region for the organization of the campaign is highly appreciated. We thank Thomas Staffelbach for his commitment during the field experiment and his valuable inputs to our analyses. Financial support through the Swiss Agency for the Environment, Forests and Landscape (SAEFL) (Project "Biogene Aerosole"), and through the commission for technology and industry (KTI) (Eurotrac-2 supproject LOOP) is greatly acknowledged. The National Center for Atmospheric Research is sponsored by the National Science Foundation.

References

Alicke B., U. Platt, and J. Stutz, Impact of nitrous acid photolysis on the total hydroxyl radical budget during the LOOP/PIPAPO study in Milan, J. Geophys. Res., 107 (D22), art. no.-8196, 2002.

Ashbourn, S.F.M., M.E. Jenkin, and K.C. Clemishaw, Laboratory Studies of the Response of a Peroxy Radical Amplifier to HO2 and a Series of Organic Peroxy Radicals, J. Atmos. Chem., 29, 233-266, 1998.

Atkinson, R., D.L. Baulch, R.A. Cox, R.F.H. Jr., J.A. Kerr, and J. Troe, Evaluated kinetic and photochemical data for atmospheric chemistry, J. Phys. Chem. Ref. Data, 21, 1125 - 1600, 1992.

Cantrell, C.A., D.H. Stedman, and G.J. Wendel, Measurements of atmospheric peroxy radicals by chemical amplification, Anal. Chem., 56, 1496-1502, 1984.

Daum, P.H., L. Kleinman, D.G. Imre, L.J. Nunnermacker, Y.-N. Lee, S.R. Springston, and L. Newman, Analysis of the processing of Nashville urban emissions on July 3 and July 18, 1995, J. Geophys. Res., 105, 9155-9164, 2000.

Fan, S.M., D.J. Jacob, D.L. Mauzerall, J.D. Bradshaw, S.T. Sandholm, R.D. Blake, H.B. Sing, R.W. Talbot, G.L. Gregory, and G.W. Sachse, Origin of tropospheric NOx over subarctic eastern Canada in summer, J. Geophys. Res., 99, 16867 - 16878, 1994.

Grüebler, F.C., Reactive hydrocarbons in the Milan area: Results from the PIPAPO campaign, PhD thesis, Swiss Federal Institute of Technology (ETH), Zürich, 1999.

Hastie, D.R., M. Weissenmayer, J.P. Burrows, and G.W. Harris, A calibrated chemical amplifier for atmospheric ROx measurements, Anal. Chem., 63, 2048-2057, 1991.

Heymann, M., Y. Kasas, and R. Friedrich, European emission data with high temporal and spatial resolution, in Proceedings of EUROTRAC Symposium 1994, pp. 437 - 443, SPB Academic Publishing, Den Haag, The Netherlands, Garmisch-Partenkirchen, 1994.

Jacob, D.J., L.W. Horowitz, W. Munger, B.G. Heikes, R.R. Dickerson, R.S. Artz, and W.C. Keene, Seasonal transition from NOx- to hydrocarbon-limited conditions for ozone production over the eastern United States in September, J. Geophys. Res., 100, 9315 - 9324, 1995.

Kleinman, L.I., Ozone process insights from field experiments, part II: Observation based analysis for ozone production, Atmos. Environ., 34, 2023-2033, 2000.

Kleinman, L.I., P.H. Daum, J.H. Lee, Y. Lee, L.J. Nunnermacker, S.R. Springston, and L. Newman, Dependence of ozone production on NO and hydrocarbons in the troposphere, Geophys. Res. Letters, 24 (No.18), 2299 - 2302, 1997.

Klimont, Z., M. Amann, J. Cofala, F. Gyarfas, G. Klaassen, and W. Schöpp, An emission inventory of the cnetral European initiative 1988, Atmos. Environ., 28, 235 - 246, 1993.

Lehnig, M., H. Richner, and G.L. Kok, Pollutant transport over complex terrain: Flux and budget calculations for the POLLUMET field campaign, Part A, Atmos. Environ., 30, 3027 - 3044, 1996.

Madronich, S., and S. Flocke, The role of solar radiation in atmospheric chemistry, in The Handbook of Environmental Chemistry, edited by P. Boule, pp. 1-26, Springer-Verlag Berlin Heidelberg New York, Berlin, 1999.

Martilli, A., A. Neftel,, G. Favaro, F. Kirchner, S. Sillman, and A. Clappier, Simulation of the ozone formation in the Northern Part of the Po Basin, J. Geophys. Res., 107 (D22), art. no.-8195, 2002..

Mihele, C.M., and D.R. Hastie, The sensitivity of the radical amplifier to ambient water vapour, Geophys. Res. Letters, 25, 1911-1913, 1998.

Moore, W.B.D., S.P. Sander, D.M. Golden, R.F. Hampson, M.J. Kurylo, C.J. Howard, A.R. Ravishankara, C.E. Kolb, and M.J. Molina, Chemical kinetics and photochemical data for use in stratospheric modling: Evaluation 10, JPL Publ., 92 - 20, 1992.

Neftel, A. , A. S. H. Prévôt, M Furger, and B. Vogel, Overview paper PIPAPO special section, J. Geophys. Res., 107 (D22), art. no.-8188, 2002..

Neftel, A., A. Blatter, R. Hesterberg, and T. Staffelbach, Measurements of concentration gradients of HNO2 and HNO3 over a semi-natural ecosystem, Atmos. Environ., 30, 3017-3025, 1996.

Prévôt, A.S.H., J. Staehelin, G.L. Kok, R.D. Schillawski, B. Neininger, T. Staffelbach, A. Neftel, H. Wernli, and J. Dommen, The Milan photooxidant plume, J. Geophys. Res., 102, 22375 - 23388, 1997.

Schultz, M., M. Heitlinger, D. Mihelcic, and A. Volz-Thomas, A calibration source for peroxy radicals with built-in actinometry using H2O and O2 photolysis at 185 nm, J. Geophys. Res., 100, 18811-18816, 1995.

Sigg, A., A. Neftel, and P.K. Dasgupta, A miniaturized battery powered H2O2 monitor for airborne measurements in a motor glider, Air Pollut. Res. Rep., 41, 111-117, 1992.

Sillman S., The use of NOy, H2O2 and HNO3 as indicators for ozone-NOx-hydrocarbon sensitivity in urban locations, J. Geophys. Res., 100, 14175-14188, 1995.

Staffelbach, T., and A. Neftel, Relevance of biogenically emitted trace gases for the ozone production in the planetary boundary layer in Central Europe, Swiss Federal Research Station for Agroecology and Agriculture (FAL), Zuerich-Reckenholz, 1997.

Staffelbach, T., A. Neftel, A. Blatter, A. Gut, M. Fahrni, J. Staehelin, A. Prévôt, A. Hering, M. Lehning, B. Neininger, M. Bäumle, G.L. Kok, J. Dommen, M. Hutterli, and M. Anklin, Photochemical oxidant formation over southern Switzerland, 1. Results from summer 1994, J. Geophys. Res., 102, 23345 - 23363, 1997a.

Staffelbach, T., A. Neftel, and L.W. Horrowitz, Photochemical oxidant formation over southern Switzerland, 2. Model results, J. Geophys. Res., 102, 23363 - 23373, 1997b.

Starn, T. K., P. B. Shepson, S. B. Bertman S. B., D. D. Riemer, R. G. Zika, and K. Olszyna, Nighttime isoprene chemistry at an urban-impacted forest site, J. Geophys. Res., 103, 22437-22447, 1998.

Stevens, P. S., J.H. Mather, W.H. Brune, F. Eisele, D. Tanner, A. Jefferson, C. Cantrell, R. Shetter, S. Sewall, A. Fried, B. Henry, E. Williams, K. Baumann, P. Goldan, and W. Kuster, HO2/OH and RO2/HO2 ratios during the Tropospheric OH Photochemistry Experiment: Measurement and theory, J. Geophys. Res., 102, 6379-6391, 1997.

Stroud, C.A., J.M. Roberts, P.D. Goldan, W.C. Kuster, P.C. Murphy, E.J. Williams, D. Hereid, D. Parrish, D. Sueper, M. Trainer, F.C. Fehsenfeld, E.C. Apel, D. Riemer, B. Wert, B. Henry, A. Fried, M. Martinez-Harder, H. Harder, W.H. Brune, G. Li, H. Xie, and V.L. Young, Isoprene and its oxidation products, methacrolein and methylvinyl ketone, at an urban forested site during the 1999 Southern Oxidants Study, J. Geophys. Res., 106, 8035-8046, 2001.

Stutz J., B. Alicke, and A. Neftel, Gradient measurements of NO2 and HONO over grass in the urban atmosphere, J. Geophys. Res., 107 (D22), art. no.-8192, 2002..

Thielmann, A., A. S. H. Prévôt, A. Neftel, and J. Staehelin, Sensitivity of ozone production derived from field measurements in the Italian Po basin, J. Geophys. Res., 107 (D22), art. no.-8194, 2002..

Thielmann, A., Sensitivity of ozone production derived from field measurements in the Po basin, PhD thesis, Swiss Federal Institute of Technology (ETH), Zürich, 2000.

Volz-Thomas, A., and B. Kolahgar, On the budget of hydroxyl radicals at Schauinsland during the Schauinsland Ozone Precursor Experiment (SLOPE), J. Geophys. Res., 105, 1611-1622, 2000.

5 Paper III, Overview on the OSOA experiment

Overview of the field measurement campaign in Hyytiälä, August 2001 in the frame of the EU project OSOA

M. Boy[1], T. Petäjä[1], M. Dal Maso[1], Ü. Rannik[1], J. Rinne[1], P. Aalto[1], M. Kulmala[1], A. Laaksonen[2], P. Vaattovaara[2], J. Joutsensaari[2], T. Hoffmann[3], J. Warnke[3], M. Apostolaki[4], E. G. Stephanou[4], M. Tsapakis[4], A. Kouvarakis[4], C. Pio[5], A. Carvalho[5], A. Römpp[6], G. Moortgat[6], C. Spirig[7], A. Guenther[7], J. Greenberg[7], P. Ciccioli[8]

[1] {Dept. of Physics, University of Helsinki, P.O. Box 64, FIN-00014, Finland (UHEL)}

[2] {University of Kuopio, Kuopio, Finland (UKU)}

[3] {Institut für Specktrochemie, Dortmund, Germany (ISAS)}

[4] {Environmental Chemical Processes Laboratory – University of Crete, GR-71409 Heraklion, Greece (ECPLUC)}

[5] {Universidade de Aveiro, Departamento de Ambiente e Ordenamento, Portugal (UVAR)}

[6] {Max-Planck-Institut für Chemie, Atmospheric Chemistry Division, D-55020, Germany (MPG)}

[7] {Atmospheric Chemistry Division, National Center for Atmospheric Research, Boulder, CO, USA (NCAR)}

[8] {Instituto di Metodologie Chimiche, Area della Ricerca del CNR di Montelibretti, Italy (CNR)}

Atmospheric Chemistry and Physics Discussions, 3, 3769-3831, 2003.

http://www.copernicus.org/EGU/acp/

Abstract

In the frame of the OSOA project a field campaign with intensive chemical and physical experiments were carried out in Hyytiälä, Finland between the 1st and 16th of August 2001. During this period clear particle formation could be observed on three days and in a not so clear way on another three days. The investigation of the meteorological and physical situation divided the period into two parts. During the first three days of August relatively cold and clean air masses (condensation sink - CS: < 0.002 s^{-1}, NO_x: < 0.5 ppb) from northwest passed over the station and we monitored for nucleation mode aerosols (3-10 nm) daily particle bursts with number concentrations between 600 – 1200 particles cm^{-3}. After this period warmer and more polluted air from south-west to south-east arrived at the station (CS: 0.002 - 0.01 s^{-1}, NO_x: 0.5 – 4 ppb) and during these 13 days only three more unclear events were observed. The chemical analyses from different institutes of PM_2 and PM_{10} particles corroborate the presumption that organic matter from the oxidation of different terpenes contributed to the formation of secondary organic aerosols (SOA). Concerning these conclusions among others, ratio between formic (oxidation product of isoprene and monoterpenes by ozone) and acetic acid (increased by anthropogenic emissions) (ratio = 1 to 1.5) and concentration of different carboxylic acids (up to 62 ng m^{-3}) were investigated. Gas/particle partitioning of five photo-oxidation products from α- and β-pinene led for pinonic, nor pinonic and pinic acids to higher concentrations in the particle phase than in the gas phase, which indicates preference of these compounds to the particle phase. The growth factors (GF) from 100 nm particles in water vapour gave diurnal pattern with a maxima during daytime and values between 1.2-1.7 (oxidation products of α-pinene: GF = 1.1). In average the amount of secondary organic carbon reached values around 19 % of the sampled aerosols and the results indicate that formation of SOA with the influence of photo-oxidation products from terpenes was the reason for the monitored particle bursts during the campaign. However, correlations between the precursor gases or the favourable condensing species with the monitored nucleation mode particles were not found. For the investigated time period other factors like the CS, temperature and solar irradiance seem to be more important steering parameters for the production of new aerosols.

Another open question concerns the vertical distribution of the formation of SOA. For this reason measurements gained through a tethered balloon platform with particle sampling and particle counting equipment together with particle flux measurements at 23 m high level were explored. The results gave first indications that the process of the production of new aerosols happens throughout the PBL, whereby different parameters e.g. temperature, CS, solar irradiance or concentration of monoterpenes are responsible for the location of the vertical maxima.

1. Introduction

The purpose of the EU project OSOA (Origin and Formation of Secondary Organic Aerosols) was to quantitatively understand the sources and formation mechanisms of secondary organic aerosols applying a combination of laboratory studies, chemical analysis of particulate matter, modelling and field observations. In the frame of this project an extensive field campaign was carried out in Hyytiälä, Finland between the 1st and 16th of August 2001. Altogether eight institutes from five different countries participated in this experiment with partly new developed analytical instrumentation and methodologies to reach a better scientific knowledge about the sources and chemical composition of this organic fraction of atmospheric aerosols.

Up to this day we know that the total organic carbon can comprise 25-65% of the fine aerosol (diameter < 2.5 μm) mass in some regions (Chow et al., 1994 and Novakov et al., 1997) and that the emission by vegetation of volatile organic compounds (VOC) is approximately 1150 C Tg per year (Guenther et al., 1995). Further we know that bursts of newly formed aerosols appear in various rural areas (i.e. continental boundary layer: Kulmala et al., 2001a, Nilsson et al., 2001a and Birmili et al., 2002). However the exact understanding of the pathways from emission of VOCs to the particle phase still includes many unknowns.

Secondary organic aerosols are formed when the saturation vapour pressure of the gas-phase oxidation products is sufficiently low so that these species can condense on existing particles or even form new particles by themselves through homogeneous nucleation. Hoppel et al., 2001 observed in Calspan's 600 m^3 environmental chamber aerosol formation and growth from the reaction products of α-pinene and ozone, utilizing relatively low concentration of α-pinene (15 ppb) and ozone (100 ppb). The nucleation in this α-pinene/ozone system could not be explained by classical nucleation theory. So the authors suggest, that the nucleation rate in the α-pinene/ozone system may be limited by the initial nucleation steps (i.e. dimer, trimer or adduct formation). This would be a possible pathway how organic species formed out of gas-phase reactions from monoterpenes could contribute to the formation of new aerosols by homogeneous nucleation. However the concentrations of α-pinene used in this experiment are still one order of magnitude higher than observed in the rural area of central Finland, for example. Another theory, which would explain the nucleation events or the time of particle bursts, is ternary nucleation of H_2O, NH_3 and H_2SO_4 (Korhonen et al., 1999). According to the suggestions of Kulmala et al. (2000) ternary nucleation can occur at typical tropospheric conditions leading to a reservoir of thermodynamically stable clusters (TSCs, diameter ≅ 1 nm), which under certain conditions grow to detectable sizes. In this case organic compounds with low volatility could be the condensing species, which bring the particles to that stage where present state-of-art instrumentation can detect them.

The aim of the OSOA project and the field campaign in Hyytiälä was to get more detailed information about the precursor gases, the condensing species and the reaction mechanisms involved. Out of these reasons gas-phase and particle phase measurements were carried out in a rural area with low anthropogenic impact.

2. Instrumentation

SMEAR II (UHEL)

Data were collected at the Station for Measuring Forest Ecosystem-Atmosphere Relations (SMEAR II) in Hyytiälä, Finland. The station is located in Southern Finland (61°51' N, 24°17' E, 181 m asl), with extended areas of Scots Pine (Pinus sylvestris) dominated forests. The conditions at the site are typical for a background location; however, occasionally measurements were polluted by the station buildings (0.5 km away) and the city of Tampere (60 km away) both located in a west-south-west direction (215 – 265 degree) from the instruments.

A Differential Mobility Particle Sizer (DMPS) system (located in the cottage) monitored aerosol size distributions at 2 m height from ground level. This gave a continuous view of the distribution and evolution of sub-micrometer aerosol particles. The DMPS system used here actually consists of two systems. The first system includes a TSI 3025 UFCPC and a Hauke-type short DMA (Differential Mobility Analyzer) and measured particles between 3 and 20 nm in dry diameter. The second system included a TSI 3010 CPC and a Hauke-type medium DMA capable of measuring particles between 20 and 500 nm. Particle size distribution is recorded every 10 minutes.

Concentrations of H_2O, NO_x, SO_2 and O_3 were measured with an URAS gas analyzer, chemiluminescence gas analyzer (TEI 42S), fluorescence analyzer (TEI 43BS) and an Ozone analyser (API 400), respectively. Air samples were collected from the mast at 4.2 m, 16.8 m and 67.2 m height levels every 5 minutes. Temperature (measured with PT-100-sensors, platinum resistance thermometers) and horizontal wind speed (measured with cup anemometers) were collected every 50s at these three heights as well. Wind direction was measured every 50 s by wind vanes at 16.8 m and 50.4 m heights.

A Sensitron AB monostatic 2.3 kHz doppler Sound Detection and Ranging system (SODAR) was used to measure the stability of the air (echo strength) and the means and standard deviations of the horizontal and vertical wind components as well as wind direction up to 500 m height in 25 m intervals. Raw echo measurements were achieved in 8-second cycles between three antennas. The vertical antenna echo strength was averaged and stored every 3 minutes. Average and standard deviations of wind speed were then derived and averaged over 30 minutes periods.

Spectral solar irradiance in the range from 280 to 580 nm and a step width of 1 nm was measured with a Bentham DM150 double monochromator. The scans were performed every half hour and lasted approximately 11 minutes. A detailed description of this instrument is given by Boy and Kulmala (2002a).

The aerosol particle number fluxes were measured by the eddy covariance (EC) technique at 23 m height, approximately 10 m above the forest canopy. The fast response measurements of wind speed and particle number concentration were performed by a sonic anemometer (Solent Research R3, Gill Instruments, Lymington, UK) and a condensational particle counter (CPC) TSI model 3010 (TSI Incorporated, Shoreview, MN, USA). The particle sizes detected by the EC system included particles bigger than 10 nm in diameter (lower cut-off size 14 nm). Particle fluxes were calculated for half-hour averaging period. More details of the particle eddy covariance system and various aspects of its application and operation can be found in Buzorius et al. (2000).

For a more detailed description of SMEAR II station and instrumentation, we refer to Kulmala et al. (2001a) and http://www.honeybee.helsinki.fi/smear.

HTDMA and OTDMA

As a part of the physicochemical characterization of aerosol during the Hyytiälä campaign, hygroscopic properties of sub-micron particles as well as their ability to absorb ethanol were monitored using Tandem Differential Mobility Analyzers (TDMA). A Hygroscopicity TDMA (HTDMA) and an Organic TDMA (OTDMA) were set up in a container close to the mast and they used the same sample inlet, which drew air from the height of 16 meters through a steel tube (diameter 2.5 cm). The flow rate was approximately 17 L min^{-1} in order to minimize particle losses due to long residence time inside the inlet tube. The samples to the individual instruments were drawn through 10 mm OD copper tubes from the main inlet line near the container.

The HTDMA system consists of two Vienna type DMAs (Winklmayr et al. 1991) in series and one TSI-CPC 3010 particle counter for concentration measurements. In addition there is also humidification unit, which generates desired relative humidity inside the second DMA. The system is built following the guidelines set by Hämeri et al. (2000) to measure also in the ultra-fine size range (10-20 nm). As an output, HTDMA gives the ratio of particles diameter at elevated RH and at dry conditions, denoted as growth factor (GF).

The hygroscopicity measurements of the particles were conducted at ~90 % ± 4% relative humidity. Size changes in elevated relative humidity were monitored for the particles of 20,

30, 50, 100 and 150 nm in diameter. Concentrations in HTDMA were not corrected with respect to losses inside the system and sampling inlet. Fluctuations of RH during the measurements were not taken into account either. The functionality of HTDMA was daily checked by measuring growth factor for a known substance, pure ammonium sulphate aerosol. It was generated from liquid solution with TSI 3076 Constant Output Atomizer. Hygroscopicity data was obtained every 10 minutes for one dry size. Taking into account the number of dry sizes measured, hygroscopic properties were measured ca. once per hour for each dry size. HTDMA was in operation continuously, 24 h a day.

The main features of the OTDMA are similar to those of the HTDMA with the exception that the humidification unit is used to generate a constant ethanol saturation ratio inside the second DMA. Also the aerosol line before DMA-2 can be humidified with ethanol. The details of the instrument are described in Joutsensaari et al. (2001). Growth in ethanol vapour was mainly determined for particles of 20, 30, 50, 80 and 100 nm in diameter. Saturation ratio (S) of ethanol vapour was kept at 0.90 ± 0.02 during the experiments. The OTDMA measurements were mainly carried out during daytime (9 a.m. - 8 p.m.) because the system is not fully automatized and supervision is needed during measurements. Only a few nighttime experiments (15.8, 16.8 and 17.8.2001) were carried out. An external treatment unit at the inlet of the DMA-2 was used some times to treat particles with ethanol before DMA-2. In most of the experiments, aerosol particles were only treated inside DMA-2 by ethanol-rich sheath air.

Atmospheric aerosol is often an external mixture, i.e. it consists of particles which have different chemical compositions. Their water and ethanol uptake properties may therefore vary, which is observed in the HTDMA and OTDMA as distinct peaks.

Tethered balloon platform measurements (NCAR)

Measurements on tethered balloon platforms can be used to derive gas fluxes averaged over large areas (20 to < 200 km^2) (Davis et al., 1994, Greenberg et al., 1999 and Helmig et al., 1998). For this purpose, two tethered helium balloons (9 m^3 Vol., Blimp Works, Statesville, NC) were flown at heights between 2 m and 1.2 km above ground during OSOA 2001. The launch site was the soccer field at the Hyytiälä station, located 0.9 km southeast of the SMEAR II mast.

VOCs were collected onto adsorbent cartridges (combinations of Carbotrap®, and Carbosieve S-III®) by miniaturized air samplers. The sampling packages also include sensors for temperature and pressure, and can be attached to any position on the tether line. Details about these samplers are given in Greenberg et al. (1999). Analysis of VOC samples was performed in the laboratory at NCAR (Boulder, CO), with gas chromatography and mass spectrometry detection (GC-MS). The procedure for the analysis of the cartridges is described by Greenberg et al. (1995).

In addition to VOC sampling, in-situ particle counters were attached to the tethered balloons. Two handheld particle counters were used, an optical particle counter (OPC) (ABACUS, Particle Measurement Systems, Boulder, CO) and a condensation particle counter (CPC) (Model 3007, TSI Inc., Shoreview, MN). The OPC quantifies particle number concentrations in 4 size bins (0,3-0,5 μm, 0,5 – 1 μm, 1-5 μm, and > 5 μm diameter), the CPC measures the total particle number in the size range of 10 nm -1 μm.

Tethered balloons were flown during daytime from August 2 to August 12, in two basic configurations.

VOC sampling package and particle sensor attached 0.5 m below the balloon with continuous measurement during ascent and descent. This setup generates vertical profiles of temperature,

humidity and particles, as well as an integrative VOC measurement from ground to the maximum height of the balloon. With time resolutions of 30 s (OPC), 10 s (CPC, averaged data of originally 1Hz) and 2 s (temperature and humidity) at ascent and descent rates of 0,5 – 1 ms^{-1}, the resulting vertical resolutions were 30 and 10 m for particle measurements and 1-2 m for meteorological data, respectively.

Three VOC sampling packages attached on the tether line at heights of about 120 m, 250 m and 550 m. The packages sampled air at those heights during 30 min., delivering a mean VOC vertical profile of the lowest 550 m.

Measuring on tethered balloons was limited by weather conditions. Rain and high wind speeds prevent a safe operation and reduced the data coverage during the OSOA campaign. A total of 48 successful balloon flights were performed as summarized in Table 1.

All gas and particle samplings described below were taken on an extra tower approximately 15 m away from the mast at 16 m height level (2 m above the canopy).

Collection of formic and acetic acids with an annular denuder system (UVAR)

Formic and acetic acid were collected for 12 hours, day and night, using an annular denuder system. The denuders were extracted using ultra-pure water, and the extract was analysed by isocratic ion chromatography (Lawrence and Koutrakis, 1994; Zervas et al, 1999). Gaseous carbonyls were collected during 12 hours periods (day and night) by drawing air through (DNPH)-coated Sep-Pak silica cartridges (Waters Assay Milford), (Sirju and Shepson, 1995), after removal of ozone in a KI impregnated copper tube coil. The cartridges were extracted with acetonitrile and the extract was analysed by binary gradient HPLC with diode-array detection.

Gas- and particle-phase collection of photo-oxidation products and formic and acetic acids (ECPLUC)

Carbonaceous aerosol samples were collected, using a novel sampling device (Kavouras et al., 1999a), for 12-h sampling periods from July 31 to August 8, 2001 in the forest of Hyytiälä in Finland. Details on sampling device and sampling procedures are given in Kavouras et al. (1999b). The polar and acidic fractions of all samples were analysed according to Kavouras et al. (1999b) using a GCQ Finnigan ion trap gas chromatograph-mass spectrometer. Gaseous formic and acetic acids were collected by using an annual denuder equipped with a filter pack system (Lawrence and Koutrakis, 1996). The analyses of the denuder extracts were performed by ion chromatography (Mihalopoulos et al., 1997).

High-volume samplers and analysis by thermal-optical method (UVAR)

The particulate matter collection was carried out by means of high-volume samplers, over Whatman QMA quartz filters. Both size segregated and non-segregated samples were obtained. A fraction of each aerosol sample was analysed for black and organic carbon (BC and OC, respectively) by means of a thermal-optical method (Pio *et al.*, 1994). The remaining parts of the filters were extracted with dichloromethane (DCM) and ultra-pure water. The obtained extracts were analysed by a thermal-chemical method and GC-MS. (Alves *et al.*, 2001 e 2002; Carvalho *et al.*, 2003).

High-volume samplers and LC-TOF-MS (MPG)

PM_2 aerosol samples were collected on preheated quartz filters using a Digitel high volume sampler at flow rates of $1m^3$/min. Terpene oxidation products were measured with 12h sampling time between August 1 and 10. The filters were extracted with 10% methanol and

were analyzed by LC-TOF-MS (Applied Biosystems, Langen, Germany) (Römpp and Moortgat, 2000).

Quartz fibre filters and HPLC-ESI-MS-Analysis (ISAS)

For $PM_{2.5}$ particle sampling quartz fibre filters with a diameter of 70 mm were used, mounted in stainless steel filter holders. A sampling flow rate of 2.3 m^3 h^{-1} was applied. During the Hyytiälä-campaign a backup filter was placed behind the front filter to determine possible sampling artefacts. The duration of the sampling was about 12 hours, usually divided in day and night samples. Prior extraction the filters were spiked with a standard (camphoric acid) for determination of the recovery rate. Afterwards the filters were extracted in an ultrasonic bath using methanol as solvent. The analysis was done by a capillary-HPLC-ESI-IT-MS system (ThermoFinnigan, San Jose, USA) (Warnke et al. 2003).

3. Results and discussion

The results of the experiments will be divided into five sub-chapters. Sub-chapter one contains the characteristics and the vertical fluxes of aerosols. In chapter two precursor measurements of different gases will be discussed and chapter three will present the gas/particle partitioning of some photo-oxidation products. In sub-chapter four chemical aerosol analyses from different institutes will be introduced and in the last sub-chapter we will give an overview of the meteorology including solar radiation during the time of the field campaign in Hyytiälä.

3.1. Characterisation of the aerosols

3.1.1. Time of particle bursts and condensational sink (UHEL)

Nucleation events or particle bursts measured at a detection limit > 3 nm were observed on the first three days and in more unclear patterns on the 7th, 10th and 14th of August (Figure 1). On all event days beside the 7th and the 10th we view high number concentrations (600 – 1300 # cm^{-3}) of nucleation mode particles (3 – 10 nm) followed by a continuous growth to the Aitken and sometimes even accumulation mode. The 7th and the 10th of August are objectively difficult to declare as an event or a non-event day, however, for a wider discussion field we keep both of them in this publication as nucleation days. In the single subplots thin red lines mark the onset and the end of the particle bursts, chosen when the number concentration of the nucleation mode exceeds or falls below 200 particles cm^{-3}. Also we know that a new cluster needs time to grow to 3 nm in size and that this timing will vary under different atmospheric situations, we use for a better understanding these times as nucleation start and nucleation end.

Further we calculated for all days of the campaign the condensational sink by

$$CS = \sum \beta_i \cdot r_i \cdot N_i \qquad (1)$$

where r_i is the radius of the i:th size class, N_i is the respective number concentration and β_i the transitional correction factor, given by Fuchs and Sutugin (1970). In the calculations the molecular mass and the diffusion volume of the condensing vapour was used from sulphuric acid. Figure 2 gives for the whole campaign period 30 minutes average values of the number concentration of the nucleation mode particles, the calculated condensational sink and the nucleation event time discussed above. At all events we recognise a clear decrease of the condensational sink short time before or at the start of the particle bursts. This phenomenon was observed on most off the events in Hyytiälä during the last years and could be explained by the onset of turbulent mixing of quite clear air masses from the residual layer and more

polluted air from the surface layer at the evolution of the mixed layer (Boy and Kulmala, 2002b and Nilsson et al. 2001b). Further the values of the condensational sink on the clear events in the beginning (CS ≅ 0.001 s^{-1}) were two to three times smaller than on the other event days (CS ≅ 0.002 – 0.003 s^{-1}). The 7th of August with the lowest number concentration of nucleation mode particles also shows the highest condensational sink values. These results indicate that high number concentration of existing aerosols reduce or prevent the formation of new particles by acting as sinks for the condensing vapours or for the very small new formed particles (D_p < 3 nm).

3.1.2. Growth rate of particles and calculated gas concentrations (UHEL)

The growth rates of the newly formed particles during the early stages (first few hours) of growth were obtained from the DMPS surface plots, according to the change in the maximum diameter the new particles had reached by the end of formation. Assuming that the growth rate is constant during the formation period, condensation theory enables us to estimate the amount of condensable vapour present. For the condensable vapour we can write a simple differential equation

$$\frac{dC}{dt} = Q - CS * Q \qquad (2)$$

where Q is the vapour source rate and CS the condensation sink caused by the existing aerosol. Assuming that the vapour concentration changes slowly, we can use a steady-state approximation and estimate the source rate by setting dC/dt = 0. A detailed description of this method can be found under Dal Maso et al. (2002). The results of this analysis are given in Table 2. The growth rates observed and further the calculated vapour concentrations (8-15 10^7 cm^{-3}) and sources (1-5 10^5 cm^{-3} s^{-1}) are rather high compared to the long-term mean observed in Hyytiälä, but are quite comparable with earlier summertime observations. However the 14th of August with about four times higher values than the other event days seems to be questionable: event or advection of polluted air masses. We will continue to discuss this day in the next chapters.

3.1.3. Water and ethanol vapour uptake properties of aerosols (UHEL and UKU)

The hygroscopic properties of the ambient aerosol during this campaign were found to be quite similar as measured by Hämeri et al. (2001) in earlier campaigns. On average, the ambient aerosol in Hyytiälä is quite inert in terms of water uptake, and it can mostly be classified to the less hygroscopic mode based on their growth factors (GF = 1.1-1.4). According to laboratory measurements, e.g. oxidation products of alpha-pinene (biogenic VOC, GF = 1.1, Virkkula et al., 1999) and toluene (anthropogenic VOC, GF = 1.2, Petäjä et al., 2002) belong to this group.

In order to study diurnal variations in water uptake, concentration weighed averages of measured hygroscopic growth factors in water were calculated. For internally mixed aerosol this is just the observed growth factor but in case of externally mixed aerosol, averaging process ensures that the dominant hygroscopic fraction is weighed more and thus affects the average hygroscopic properties more. External mixing with respect to water uptake prevails for sizes larger than 50 nm in diameter. Growth factors in ethanol were more internally mixed and only one growth factor was observed most of the time. This indicates same ethanol uptake for all particles in the ambient aerosol population.

The diurnal variation of the hygroscopic properties is clear in Hyytiälä. Considering hourly averages of all days of the campaign (Figure 3), the growth factors are usually larger and

more variable during daytime than during nighttime. Roughly between 8 a.m. and 8 p.m. growth factors are larger than 1.4 for 100 nm particles. Maximum growth factors above 1.6 as hourly averages are observed during afternoon hours. During nighttime, growth factors are quite stable and between roughly 1.3 and 1.4.

When nucleation days and the days with no nucleation burst are considered separately (Figure 3), it can be noticed that the daily maximum is somewhat higher during nucleation days, whereas non-nucleation days exhibit more stable water uptake throughout the day and night. Slight decrease in water uptake prior to sunrise is present during all days, but hourly averaged growth factors are lower in advance of nucleation burst than during the days, when nucleation does not take place.

Figure 4 shows the average growth factors of 100 nm particles in ethanol vapour with saturation ratios of 0.90 ± 0.02 for event days and non-event days. A maximum value of around 1.3 - 1.35 is reached in the morning, after which the GF gradually decreases to values closer to 1.2 by 8 p.m. There are only 3 nighttime measurement series, showing somewhat different behaviour; in one series after a nucleation event day (14.8.2001) the GF decreases rapidly from above 1.35 at midnight to 1.2 at 3.30 a.m. and in the other series after non-event days the GF remains at a nearly constant value of 1.15 throughout the night. Figure 4 also reveals that, unlike with the hygroscopicity, the daytime behaviour of ethanol GF's is very similar during nucleation event and non-event days.

Figure 5 shows two time series which compare the behaviour of 50 nm and 100 nm particles in both water and ethanol vapours. The hygroscopic growth factors of 50 nm particles are most of the time somewhat smaller than those of 100 nm particles with the average of the fraction GF(50 nm)/GF(100 nm) close to 0.9. The difference is mostly too large to be explained (at least solely) by the Kelvin effect, indicating that the compositions of the 50 nm and 100 nm particles are usually somewhat different. A further proof of this is the similar time series for the fraction of 50 to 100 nm particle growth factors in ethanol vapour. It can be seen that the 50 nm particles grow more in ethanol than do 100 nm particles, with the average of GF(50 nm)/GF(100 nm) close to 1.02. Note, that if the Kelvin effect could be accounted for, this number should be even slightly higher. A possible explanation for the data shown in Figure 5 is that the 100 nm particles contain a somewhat higher fraction of inorganic salts and a somewhat lower fraction of organic materials than do the 50 nm particles. However, this interpretation cannot be considered conclusive without a chemical analysis of the particles. In any case, it is interesting to note that both the hygroscopicity and ethanol growth data shown in Figure 5 exhibit trends such that the 50 and 100 nm growth factors appear to become more similar toward the end of the campaign.

3.1.4. Aerosol flux measurements (UHEL)

The particle flux measurements were performed throughout the campaign. However, during most of the days unfavourable wind direction conditions for particle flux observation prevailed (see Figure 6): under South-westerly wind (215 – 265^{o}) the forestry field station buildings act as a source of aerosol particles and corresponding fluxes do not correspond to background conditions (Buzorius et al., 2001). Under such conditions the particles emitted from the station will be seen as upward fluxes accompanied with erratic pattern in flux time series, in contrast to normal background conditions when particle deposition into forest occurs.

During the first three days in August when particle formation was observed the wind direction was different than the sector corresponding to field station. During these day's particle number concentration decreased at night prior to particle formation (Figure 7). The nights

were moderately stable, but turbulent transport of heat and momentum (friction velocity around 0.2 m s^{-1}) did not cease. However, particle fluxes were very small as typically observed at the measurement site (Buzorius et al., 2001). During the particle bursts period's rapid increase in particle concentration together with very large downward fluxes were observed. The very high flux values during particle formation events result from elevated particle number concentration as well as domination of small nucleation mode particles in size spectrum, which have very high deposition velocities (e.g., Peters and Heiden, 1992). Similar behaviour but with more variation in fluxes can be seen on the other three event days. In addition to non-stationary, rapid changes in particle concentration, meteorological reasons such as horizontal advection and circulation in convective mixed layer can cause significant variation in observed fluxes (Nilsson et al., 2001b).

The fluxes obtained from measurements present average fluxes of particles larger than 10 nm in diameter. During nucleation events these fluxes indicate mainly the vertical motion of small particles: deposition of these particles into forest was observed. The result implies also existence of higher concentration of these particles up in the atmospheric boundary layer.

3.1.5. Vertical aerosol profiles (NCAR)

The optical particle counter (OPC) was operated on the balloon described in chapter 2 from August 2 throughout August 12, whereas the CPC instrument was flown from August 7 (start 3 p.m.) till August 12, only. As a consequence, CPC data cover exclusively days without obvious particle formation events.

Profiles as obtained by this method represent instantaneous snapshots of the vertical particle distribution. This is documented by large variations in particle numbers at comparable heights between individual profiles. Variations from one profile flight to the next (time gap of at least 2 hours) or even between ascent and descent of the same flight (30 min) are large.

Some distinct features could be observed by looking at the vertical distribution of particles in a relative way, by looking at number concentrations normalized to the averaged concentration over the mixed layer. As can be seen in Figure 8, there was a different vertical trend in particle concentrations (>300 nm) on 3rd of August as compared to the average profile recorded on non-event-days. On 3rd of August, particle concentrations above the planetary boundary layer (PBL) were small and no significant gradient within the PBL could be observed, whereas increasing aerosol concentrations with height were observed on the other days.

During three flights, CPC and OPC were run in parallel. Of the resulting 10 profiles, some show different vertical trends for different particle sizes (Figure 9). It indicates that particles of the sizes most interesting for nucleation events may have an opposite gradient than larger particles.

Summarising both figures no indication for preferred particle formation above the surface layer or in the free troposphere appears, contrariwise the results lead to the conclusion that the formation of new particles happens throughout the boundary layer in a more or less homogenous pattern.

More information of this type (especially measurements of particles < 300 nm) during nucleation events may provide valuable data for the interpretation of particle formation. As the results indicate, such efforts ideally would include not only measurements of particle numbers, but also information about the size distribution.

3.2. Precursor measurements

3.2.1. Ozone, SO2 and NOx (UHEL)

The concentrations of different gases (O_3, NO_x and SO_2) monitored continuously in Hyytiälä SMEAR II were analysed for the time of the OSOA field campaign (at 16m level) and plotted as half-hour average values in Figure 10. During the experiment the ozone concentrations were varying between 10 and 40 ppb with a clear diurnal profile. However there is no trend of higher or lower values at time of new particle formation, neither in the daily maxims nor in the time gradients in front of the particle bursts ($d[O_3] / dt$) visible.

NO_x and SO_2 concentrations were varying during the campaign between 0.068 to 2.98 ppb and below detection limit to 1.34 ppb, respectively. If we compare the number concentrations from NO_x with the wind-direction from Figure 6 we recognise higher values during the times, when probably more polluted air masses from Southwest (also with high values in condensational sink – see Figure 2) arrived at the station. So the first three clear event days in the beginning of August show the lowest concentrations of NO_x and also SO_2. The other events later on are more polluted with 2 to 4 time's higher values for both gases. Gao et al. (2001) found in four chamber experiments concerning the reaction of ozone with α-pinene including SO_2 ([Ozone] = 95, 110, 110 and 100 ppb, [α-pinene] = 16, 15, 15 and 15 ppb and $[SO_2]$ = <0.1, 0.5, 2.5 and 6 ppb) a direct correlation between increasing SO_2 concentrations and measured number concentration of new-formed particles (N = 14, 73, 187 and 380 * 10^3 cm^{-3}). This result stands in contradiction to our measurements. Although SO_2 (or the oxidised form H_2SO_4) is involved through binary or ternary nucleation in the formation of TSCs in the real atmosphere the influence of other parameters like for example the number concentration of existing particles may be more important for the formation of new aerosols than the varying in SO_2 concentration.

3.2.2. VOC measurements on tethered balloons (NCAR)

During the OSOA field campaign a total of 80 VOC samples were collected onto cartridges from balloon platforms. In addition, VOC probes were taken on the SMEAR II mast at heights between 23 and 43 m above ground. The goal of these measurements was to determine fluxes of biogenic VOC, terpenes in particular, at both local and regional scales.

The analyses of the balloon samples focused on monoterpenes and isoprene. Terpene concentrations in the PBL during that period were in the order of a few ppts, with α-pinene, limonene, Δ_3-carene and camphene as the major compounds. Isoprene was also found in most samples, although at lower concentrations than monoterpenes. In comparison to earlier measurements at Hyytiälä, the contribution of α-pinene to the sum of terpenes was smaller in these PBL-measurements (Figure 11a). Averaged VOC profiles within the PBL showed a decreasing trend with height, as would be expected for gases with a source at the surface (Figure 11b).

Daily averages of all VOC samples taken within the PBL are shown in Figure 12. Days with particle formation events (Aug 2., 3. and 7.) had low terpene concentrations. Note however, that a direct comparison of days is difficult, as the temporal coverage with balloon soundings varies significantly from day to day.

The VOC measurements from balloons were used to derive fluxes of biogenic VOC (Spirig et al., manuscript in preparation). The footprints of fluxes obtained from measurements in the PBL are of the order from tens to hundreds of square kilometers, depending on the method applied. Uncertainties of fluxes determined in this way are large due to the various assumptions included (Guenther et al., 1996). For example, homogenous emissions are

assumed within the footprint area, a condition that is most commonly violated in practice. Landscape fluxes therefore need to be determined from averaged VOC profiles reflecting various conditions and wind directions. As a consequence, the advantage of deriving a flux representative for the scale of a whole landscape is accompanied by limited temporal information about the flux.

The mean terpene fluxes as derived from balloon measurements between August 2 and August 12 were between 140 and 300 μgC m^{-2} h^{-1}, depending on the method applied (Spirig et al., manuscript in preparation). Assuming the discrepancy is mainly a consequence of the different footprints of the methods, we conclude that terpene emissions averaged over a region of several hundreds of km^2 surrounding Hyytiälä are less than those of the region covering tens of km^2 close to the site. The same trend of lower emissions with increasing footprint area exists in the comparison of balloon results with measurements from the mast. The average of the terpene fluxes determined from gradients on the mast on August 15 was 330 μgC m^{-2} h^{-1}. This corresponds to a basal emission rate (30°C) of 900 μgC m^{-2} h^{-1}; a value similar to earlier flux measurements on the tower (Rinne et al., 2000).

3.2.3. Carboxylic acids and carbonyls (ECPLUC and UVAR)

The concentrations of gas-phase carboxylic acids observed during the campaigns were measured by two independent groups (ECPL-UOC and UVAR). The results are shown in Figure 13 and Table 3. The data collected by ECPL, concerning the gaseous concentration of small carboxylic acids support the hypothesis that biogenic emissions are the main sources of atmospheric formic and acetic acid. The concentration of formic acid ranged from 0.52 up to 5.04 μg m^{-3}, while the corresponding concentration for acetic acid ranged from 0.41 up to 4.06 μg m^{-3}. The general trends in both formic and acetic were similar showing a high degree of correlation (Figure 13A) suggesting that their sources should be closely related. The formic to acetic ratio varied from 1.04 to 1.43, indicating thus predominance of formic acid in the forested area of Hyytiälä. This comes in accordance with the observations by Chebbi et al. (1996) that formic acid is the main product of isoprene and monoterpenes (emitted by trees) oxidation by ozone. The same trend has been observed in a previous study in a Eucalyptus forest in Portugal (Kavouras et al., 1998). Photochemical production (that favours formic acid) seems to play a more important role than direct emissions from vegetation (that favour acetic acid). Acetic acid concentrations can be increased by anthropogenic emissions (Kawamura et al., 1985) and/or biomass burning (Talbot et al., 1987) this seems not to happen in the investigated area. Measurements of the same acids conducted by UVAR resulted to lower concentration ranges, namely from 0.15 up to 1.26 μg m^{-3} for formic acid and from 0.21 up to 1.82 μg m^{-3} for acetic acid. The UVAR measured concentrations of formic acid mostly lower than acetic acid, but in some samples with low acidic content, the levels of formic acid were also higher than acetic acid. The highest concentrations occurred between 4^{th} and 13^{th} August. Both laboratories observed a predominance of maxima during daytime and minima during nighttime (Figure 13A).

Formaldehyde presented a smooth diurnal variation with maxima during daytime and minima during nighttime. Acetaldehyde and acetone exhibited also a predominance of daytime maxima. Nevertheless these carbonyl compounds presented the highest concentrations during nighttime. Acrolein exhibited a strong daily variation of concentrations with maxima during nighttime and minima during daytime. The most pronounced variation occurred between the 7^{th} and 11^{th} of August. Propionaldehyde didn't present a characteristic diurnal variation and the highest concentrations of hexanaldehyde were observed mainly at night.

3.3. Gas/particle partitioning of photo-oxidation products (ECPLUC)

The volatile and semi-volatile of the polar and acidic fractions in both particulate and gas phase were analysed. A series of monoterpene-skeleton photo-oxidation carbonyl and acidic compounds were detected and quantified in both gas and particles over the Hyytiälä forest. In particular, 6,6-dimethyl- bicyclo[3.1.1]heptan-2-one (reported as nopinone) and 2,2-dimethyl-3-acetyl-cyclobutyl-ethanal (reported as pinonaldehyde), 2,2-dimethyl-3-acetyl-cyclobutyl-formic acid (reported as *nor*-pinonic acid), 2,2-dimethyl-3-acetyl-cyclobutyl-acetic acid (reported as pinonic acid), and *cis*-2,2-dimethyl-3-carboxy-cyclobutyl-acetic acid (reported as pinic acid) were identified on the basis of their CI and EI mass spectra and comparison with authentic standards (Figure 13B-F). These compounds have been determined as characteristic products of the photo-oxidation of α- and β-pinene with ozone, OH and NO_3 radicals, in laboratory studies. Pinonaldehyde and nopinone have shown for most of the sampling days higher gas phase than particle concentrations. Nighttime reactions of pinenes with NO_3 radicals eventually contributed to the relatively elevated concentration of pinonaldehyde in the particulate phase. For pinonic, nor pinonic and pinic acids, particle concentrations were higher than the corresponding concentrations in the gas phase. Pinonic acid is produced through the reaction of α-pinene with both OH radicals and ozone, and pinic acid is mainly formed through the reaction of α- and β-pinene with ozone. The concentration levels of pinonic acid and pinic acid show that the first is produced faster and in higher amounts than the second under real conditions. Thus, it is clear that the atmospheric concentration of OH radicals and ozone has an effect on the composition of organic aerosol produced through the atmospheric photo-oxidation reactions. These data show the preference of these compounds to the particle phase and eventually their ability to condense under certain atmospheric conditions.

3.4. Chemical aerosol characterisation

Chemical analyse of the particle-phase matter were performed by three groups with different sampling and analytical techniques, which gave the chance to compare the results of some measured species.

3.4.1. Particle analysis by UVAR

Carbonaceous aerosol was one important component of the aerosol at the studied locations. Organic carbon accounted for 27 % of the PM_{10} mass concentration in Hyytiälä. Adding the contribution of black carbon, the share of total carbon reaches 34 %. Using the dichloromethane-extraction procedure 31 % of the organic carbon could be extracted. The addition of the water-extract increased this ratio to 52 %, which is comparable to the 48 % obtained during the short-term experiment (Alves *et al.*, 2002).

On average the fraction of secondary carbon in the Finnish aerosol accounted for 71 % of the organic carbon, which corresponds to 19 % of the PM_{10} mass concentration. Secondary organic carbon was calculated by subtracting primary organic carbon from total organic carbon, considering that the ratio between primary organic carbon and black carbon is 1.1 (Castro *et al.*, 1999). In some periods the fraction of secondary organic carbon showed clear maxima during daytime and minima during nighttime. This is an obvious indication of local or regional formation of secondary aerosol, because even the interference of wood burning emissions, which is higher at night, did not cause the rise of the values calculated for night periods.

The total concentration ranges and carbon preference indexes (CPI) for n-alkanes, n-alkanols and n-monocarboxilic acids are presented in Table 4. CPI is a diagnostic parameter, where a

value higher than 3 indicates the major incorporation of recent biological constituents into the aerosol sample. The input of anthropogenic contaminants reduces the CPI, such that values of approximately 1 reflect the significant introduction of contaminants with human origin. C_{max} can also give an indication of relative source input and serves as a regional parameter of vascular plant contributions to the atmosphere (Abas and Simoneit, 1996). The distribution of the n-alkanes ranged from C_{16} to C_{34}, with C_{max} equal to 27. Odd carbon number predominance was found, especially in range $C_n > 23$, wherein odd carbon number alkanes represent a primary major contribution of vascular plants waxes (Abas and Simoneit, 1996). The isoprenoid hydrocarbons derived from petroleum (pristane and phytane) were also detected.

The most representative PAH in the sampling site was indeno[1,2,3-cd]pyrene, benzo[b+k]fluoranthene, benzo[a]anthracene, benzo[e]pyrene and benzo[a]pyrene. On average in the Finnish samples the total concentrations of PAH (8.9 ng m^{-3}) was lower than those from the previous short-experiment in Finland (17 ng m^{-3}, Alves *et al.*, 2002).

Carbonyl compounds including linear homologues were detected. However, the discontinuity of the series makes impracticable the application of the CPI parameter for linear compounds. Table 5 presents the biogenically derived compounds detected in the samples, which includes some carbonyl compounds. Pinonaldehyde, 6,10,14-trimethyl-2-pentadecanone and abieta-8,11,13-trien-7-one presented the highest concentrations in Hyytiälä. During the previous short-term experiment in Hyytiälä, pinonaldehyde was more abundant (6.6 ng m^{-3}; Alves *et al.*, 2002) and trimethylpentadecanone was not a ubiquitous component of the aerosol. Nopinone and monoaromatic carbonyls, including benzaldehyde, were detected in all the experiments.

The homologous compound series of n-alkanols ranges from C_{11} to C_{30} in the Finnish site. The most abundant homologue was C_{26} and strong primary contributions of vascular plants waxes were found. Sterols were also present in the samples (Table 5).

The n-alkanoic acids are one of the dominant components in the extractable lipids. The homologous compound series range from C_8 to C_{32} with an even carbon number predominance. The samples present a predominance of C_{max} at n-C_{16} that may reflect an enhanced primary microbial component and a less pronounced variable maxima for carbon number higher than 22. Alkanedioic acids were present in the aerosol samples from the finish forest in a discontinuous series ranging from hexanedioic acid to docosanedioic. Nonanedioic was the most abundant constituent of this class and it has been suggest to be formed by photo-oxidation of oleic and linoleic acids (Yokouchi and Ambe, 1986; Kawamura and Gagosian, 1987, Stephanou and Stratigakis, 1993), which were also detected in the samples. Acids resulting from the photo-oxidation of pinene were also present in the aerosol phase (Table 6). Resin acids were also detected.

The compounds detected in the water-extract were polyhydroxy-, mono- and dicarboxylic acids, polyhydric alcohols (polyols) and sugars. The most representative individual compounds were malic acid, mannitol, arabitol, glucose and sucrose. Levoglucosan (1,6-anhydro-ß-D-glucopyranose) was also detected in the water-extract, thought it is extracted predominantly by dichloromethane in the first extraction stage. This anhydrosugar is considered a specific tracer of biomass burning, which results from the depolymerization of cellulose at temperatures above 300 ºC (Simoneit *et al.*, 1999). Table 6 also shows the concentration ranges for some water-extractable organic compounds. A more detailed discussion on the sources and size distributions of water-extractable organic compounds can be found elsewhere (Carvalho *et al.*, 2003).

3.4.2. Particle analysis by ISAS

In aerosol samples from the Hyytiälä measurements station a series of organic acids, which originated from terpene (α-pinene) oxidation, were detected and quantified. The results are shown in Figure 14. These acids, verified by commercially available standards, were norpinic, pinic and pinonic acid. Since their volatile precursors are of biogenic origin these low volatile substances can be used as marker compounds for the natural fraction of the tropospheric secondary organic aerosol. The concentrations of these compounds are mostly between 0.2 and 8 ng m^{-3}. The C_{10}-ketocarboxylic acid - pinonic acid - is often higher concentrated as the C_9-dicarboxylic acid - pinic acid. Norpinic acid - a C_8-dicarboxylic acid - is found at the lowest concentration levels, often below the detection limit.

Correlation analysis was done to get an indication of the source, biogenic or anthropogenic, of known and unknown compounds. The source can be meant as source of primary emissions, a source of the precursor substances and/or the mechanism of formation (e.g. oxidation by ozone). As an example, one correlation analysis is shown for pinic and pinonic acid in Figure 15. As can be expected the concentration of pinic and pinonic acid shows a good correlation, since both compounds are formed from the same precursor compound and both originate from identical degradation mechanisms. Furthermore, it can be seen that the average concentration of pinonic acid is almost 2 times higher than pinic acid.

Identification of compounds: Within the samples from Hyytiälä a signal was observed which indicated the presence of a molecule with a molecular mass of 232 g mol^{-1}. This compound was also observed in chromatograms from oxidation experiments of α-pinene with NO_x done in the CEAM-laboratory in Valencia as well as in samples from other laboratory experiments. Warscheid and Hoffmann (2002) suggested a structure based on online MS^n experiments made during ozone oxidation experiments in a smog chamber, as shown in Figure 16. The molecule contains a carboxylic acid and per-ester function and consequently can be supposed to have a very low vapour pressure.

3.4.3. Particle analysis by MPG

Pinic and pinonic acid were identified and quantified by the corresponding standards. Sabinic, caric and limonic acid were measured for the first time in ambient aerosol samples (Table 7). They were identified by comparison with the laboratory experiments. Sabinene, limonene and carene were reacted with ozone in a smog chamber and the particles were collected. Sabinic acid could be quantified in the Hyytiälä samples. But caric and limonic acid coeluted in the HPLC, so the concentrations stated are the sum of both acids. Sabinic, limonic and caric acid were quantified using pinic acid as a standard. Their concentrations exceeded the concentrations of pinic, pinonic and norpinic acid on several days. This shows that they have to be taken into account when assessing the contribution of terpene oxidation to secondary organic aerosol production.

3.5. Meteorology and solar radiation (UHEL)

The last point from the results presented in this publication gives an overview of the meteorological situation during the campaign including the solar radiation. Figure 17 shows the half-hour average values of relative humidity, vertical wind variance and short wavelength irradiance (300 – 340 nm) for all the events and table 8 contains characteristic values of these parameters for all days of the campaign including temperature. In agreement with the results presented by Boy and Kulmala (2002b) for a one-year data analyse at Hyytiälä, Finland the relative humidity is lower during periods of particle bursts or decreases in front of the nucleation start. The same result concerning the influence of water molecules was

investigated by Bonn et al. (2002) in laboratory experiments: Ozonolysis of monoterpenes and special of exocyclic monoterpenes (β-pinene and sabinene).

According to Boy and Kulmala (2002a) we choose short wave length irradiance (E_s) measured with a radiospectrometer as the determinant radiation factor in this analysis. All event days show roughly the same behaviour with the appearance of the particle bursts after $E_s > 6$ W m^{-2}. If we include in our consideration the time a new cluster needs to grow to the detectable size of 3 nm (approximately 20 minutes with the growth rates from table 2 - thin black line in Figure 17) then the nucleation would start at all event days during the ascending part of the irradiance curve. Furthermore these estimated nucleation start times are coinciding with the onset of vertical wind variance and so the start of mixing different air masses from the residual and the surface layer.

In the end we will also include the temperature in our considerations. Although the solar radiation reaches higher values during the first three days of August compared to the rest of the campaign the diurnal mean values of the temperature especially on the 1st and 2nd of August are about 5 K lower than on the other days. Without analysing any weather maps we can conclude that relatively clean and cold air from northwest passed over the station during this period (see Figures 2, 6 and 10). According to Nilsson et al. (2001a) nucleation in Hyytiälä occurs in arctic and to some extent in polar air masses, with a preference for air in transition from marine to continental air masses. The results from Nilsson et al. established during BIOFOR campaign in Hyytiälä, Finland agree complete with the first three events. However the other event days show different meteorological situations.

4. Summary and conclusions

The main results of the OSOA field campaign are briefed in chapter 3. Obviously two different kind of meteorological situations appeared during this period. In the beginning of August (1st to 3rd) clean cold air masses – nucleation favouring conditions - from northwest passed over the station (low values of NO_x, SO_2 and CS). During these days clear particle formation events with number concentrations between 600 and 1200 particles cm^{-3} for nucleation mode particles (3-10 nm) were monitored. Later in August the dominating wind sector was south to east and the above mentioned parameters increased clearly. Still we observed three days with indications of particle bursts during this period. However, the 14th of August is difficult to declare: Event or pollution. All parameters calculated in chapter 3.1.2 (growth rate, vapour concentration, vapour source and formation rate) are 4 to 5 times higher than during other event days and a clear peak in NO_x between the formation start and end was measured. Furthermore the particle number concentrations of nucleation mode particles and total particle number (3-500 nm) show the same ascent with a peak at 1.15 p.m. of 1257 and 10889 particle cm^{-3}, respectively. These results tend more to the conclusion that polluted air masses probably from the station building or the town Tampere were blown over the measuring site.

The analysis of precursor measurements from chapter 3.2 showed an opposite trend for the sum of terpenes than the number concentration of the nucleation mode particles. However, the high variation in the temporal coverage and the large scattering of the measurements during single days limit final conclusions. Nevertheless a direct correlation between the concentration of monoterpenes and the ongoing of nucleation can be excluded. The same result is valid for the concentrations of the carboxylic acids, the photo-oxidation products from monoterpenes with the lowest saturation vapour pressures (chapter 3.2.3 and 3.3). In this case the highest concentrations of formic and acetic acids were measured between the 4th and 13th of August, excluding the three clear event days in the beginning of August. Further the sum of gas- and particle-phase concentrations of nor-pinonic or pinonic acids measured

during the first eight days in August leads to the same result. Summarising this paragraph brings the conclusion, that at least during the time of the campaign the concentrations of the supposed precursors and the condensing species aren't limiting factors for the formation of new particles in Hyytiälä, Finland. This fact is also supported by comparing the calculated vapour concentrations of the condensing species from chapter 3.1.2 with the measurements. For the first five events we calculated necessary concentrations for the condensing species between 8-15 10^7 molecules cm^{-3} and the measured concentration of pinonic acid for example was between 1-8 10^6 molecules cm^{-3} during the first 3 event days. Including all the other carboxylic acids with low volatilities which are in consideration to participate in the formation of new particles the comparison supports our conclusion.

The chemical analyses discussed in chapters 3.3 and 3.4 of PM_2 to PM_{10} particles done by four institutes independently with different sampling and analytical methods and the results of the HTDMA and OTDMA measurements from chapter 3.1.3 gave the following results:

- The fraction of secondary organic carbon reaches 19 % of the particle material in average with maxima during daytimes, which obviously indicates local or regional formation of secondary organic aerosols.
- The concentrations of the identified carboxylic acids (formic, acetic, pinonic, pinic, norpinic, sabinic, limonic and caric acids) reached values up to 62 ng m-3.
- The formic to acetic ratio varied from 1.04 to 1.43, indicating thus predominance of formic acid in the forested area of Hyytiälä. Formic acid is the main product of isoprene and monoterpenes oxidation by ozone, whereas acetic acid comes from direct emission from vegetation and partly from biomass burning and/or anthropogenic emissions.
- The calculated carbon preference indexes (CPI) for the whole range (C16-C34) gave values for the n-alkanes, n-alkanols and n-monocarboxylic acids of 2.69 ± 1.0, 8.52 ± 4.16 and 6.86 ± 1.67 respectively, where a CPI number higher than 3 indicates a major incorporation of recent biological constituents into the aerosol sample.
- The average growth factors in ethanol vapour and in water vapour for 100 nm particles show a diurnal variation with maxima during daytime. However the aerosols monitored during the campaign were less hygroscopic with GF between 1.2 and 1.7. According to laboratory experiments oxidation products of alpha-pinene or toluene belong to this group.
- The ratio of 50 and 100 nm particles in ethanol and water vapours (~1.05 and ~0.85 respectively) during the three clear events in the beginning of August indicate that the smaller particles contain a somewhat higher fraction of organic materials and a somewhat lower fraction of inorganic salts.

Summarising these points we recognise a clear contribution of organic matter originating from the oxidation of terpenes from the local biosphere to the sampled aerosols. However, the fact that state-of-the-art technique is not able to analyse nucleation mode particles separately still leaves a lack of information about the composition of these newly formed particles and to what extent the species with the lowest volatility (dicarboxylic acids) are responsible for the growing of the newly formed clusters.

One question still not answered concerning the formation of SOA is: "Where in the PBL are the particles formed?" The analysis of particle flux measurements indicates that during all formation events the dominating fluxes were downward. However, high uncertainties in this data set as mentioned in sub-chapter 3.1.4 and zero or even small upward fluxes during some event days prevent direct conclusions. Furthermore the vertical profiles of monoterpenes concentrations showed as expected for gases with only ground-sources the highest values in

the surface layer and the vertical profiles of aerosols in the PBL give some indications that the formation of newly formed particles is homogenous in the PBL (see chapter 3.1.5). Summarizing, the question could not be answered in the frame of this project. However, we can assume that the particles are formed throughout PBL whereas different parameters (temperature, humidity, solar irradiance and concentration of different gases like monoterpenes, SO_2, OH and others) with varying vertical profiles shifting the maxima of the formation rate in connection with the available conditions. To gain detailed information about this mechanism we would need vertical profiles of aerosols throughout the day with size and number distributions and simultaneous measurements of concentrations of different gas-species.

Acknowledgements

We thank the "Fundação para a Ciência e a Tecnologia" for financial support through the grant PRAXIS XXI / BD / 18450 / 98 to A. Carvalho. The Ministry of Education of Greece (EPEAEK Program) is acknowledged for financial support to Maria Apostolaki. We would also like to thank the personnel of the SMEAR II station and the Hyytiälä Forestry Field Station for help and support during the campaign.

References

Aalto, P., Hämeri, K., Becker, E., Weber, R., Salm, J., Mäkelä, J., Hoell, C., O'Dowd, C. D., Karlsson, H., Hansson, H.-C., Väkevä, M., Koponen, I., Buzoius, G. and Kulmala, M.: Physical chracterization of aerosol particles during nucleation events, Tellus, Volume 35B, Number 4, 344-358, 2001.

Abas, M. R. B. and Simoneit, B. R. T.: Composition of extractable organic matter of air particles from Malaysia: initial study, Atmos. Environ. 15, 2779-2793, 1996.

Alves, C., Pio, C. and Duarte, A.: Composition of extractable organic matter of air particles from rural and urban Portuguese areas, Atmos. Environ. 35, 5485 – 5496, 2001.

Alves, C., Carvalho, A. and Pio, C.: Mass balance of organic carbon fractions in atmospheric aerosols, J. Geosphys. Res., 107 (D21), ICC7 1-9, 2002.

Birmili, W., Berresheim, H., Plass-Dülmer, C., Elste, T., Gilge, S., Wiedensohler, A. and Uhrner, U.: The Hohenpeissenberg aerosol formation experiment (HAFEX): a long-term study including size-resolved aerosol, H2SO4, OH and monoterpenes measurements, Atmos. Chem. Phys. Discuss., 2, 1655-1697, 2002.

Bonn, B., and Moortgat, G. K.: New particle formation during α- and β-pinene oxidation by O_3, OH and NO_3, and the influence of water vapour: particle size distribution studies, Atmos. Chem. Phys. Discuss., 2, 469-506, 2002.

Bonn, B., Schuster, G. and Moortgat G.K.: Influence of water vapour on the process of new particle formation during monoterpene ozonolysis, The Journal of Physical Chemistry A, 106 (12), 2869-2881, 2002.

Boy, M. and Kulmala, M.: The part of the solar spectrum with the highest influence of the formation of SOA in the continental boundayr layer, Atmos. chem. phys., 2, 375-386, 2002a.

Boy, M. and Kulmala, M.: Nucleation events in the continental boundary layer: Influence of physical and meteorological parameters, Atmos. chem. phys., 2, 1-16, 2002b.

Buzorius, G., Rannik, Ü., Mäkelä., J. M., Keronen, P., Vesala, T. and Kulmala, M.: Vertical aerosol fluxes measured by the eddy covariance method and deposition of nucleation mode particles above a Scots pine forest in southern Finland, J. Geophys. Res., 105, 19905-19916, 2000.

Buzorius, G., Rannik, Ü., Nilsson, D. and Kulmala, M.: Vertical fluxes and micrometeorology during aerosol particle formation events, Tellus, 53B, 394-405, 2001.

Carvalho, A., Pio, C. and Santos, C.:. Water-soluble hydroxylated organic compounds in German and Finnish aerosols, in press: Atmos. Environ., 2003.

Castro, L., Pio, C., Harrison, R. and Smith D.: Carbonaceous aerosol in urban and rural European atmospheres: Estimation of secondary organic carbon concentrations, Atmos. Environ., 33, 2771 – 2781, 1999.

Chebbi, A. and Carlier, P.: Carboxylic acids in the troposphere, occurrence, sources and sinks: A review, Atmos. Environ. 30, 4233-4249, 1996.

Chow, J. C., Watson, J. G., Fujita, E. M., Lu, Z. Q., Lawson, D. R. and Ashbaugh, L.: Temporal and spatial variations of PM2.5 and PM10 aerosol in Southern California Air Quality Study, Atmos. Environ., 28, 2061-2080, 1994.

Christoffersen T. S., Hjorth J., Horie O., Jensen N. R., Kotzias D., Molander L. L., Neeb P., Ruppert L., Winterhalter R., Virkkula A., Wirtz K. and Larsen B. R.: Cis-Pinic acid, a possible precursor for organic aerosol formation from ozonolysis of a-pinene, Atmos. Environ. 32, 1657-1661, 1998.

Dal Maso, M, Kulmala, M., Lehtinen, K. E. J., Mäkelä, J. M., Aalto, P. and O'Dowd, C. D.: Condensation and coagulation sinks and formation of nucleation mode particles in coastal and boreal forest boundary layers, J. Geophys. Res., 107, PAR 2, 1-10, 2002.

Davis, K.J., Lenschow, D.H. and Zimmerman, P.R.: Biogenic Nonmethane Hydrocarbon Emissions Estimated from Tethered Balloon Observations, J. Geophys. Res., 99, 25587-25598, 1994.

Gao, S., Hegg, D. A., Frick, G., Gaffrey, F., Pasternack, L., Cantrell, C., Sullivan, W., Ambrusko, J., Albrechcinski, T. and Kirchstetter, T. W.: Experimental and modelling studies of secondary organic aerosol formation and some applications to the marine boundary layer, J. Geophys. Res. 106, D21, 27619-27634, 2001.

Greenberg, J., Lee, B., Helmig, D. and Zimmerman, P.: Fully automated gas chromatograph-flame ionization detector system for the in situ determination of atmospheric non-methane hydrocarbons at low parts per trillion concentration, J. Chromotography, 676, 389-398, 1995.

Greenberg, J.P. et al.: Tethered balloon measurements of biogenic VOCs in the atmospheric boundary layer, Atmos. Environ., 33, 855-867, 1999.

Guenther, A., et al.: A global model of natural volatile organic compound emissions, J. Geophys. Res. 100, 8873-8892, 1995.

Guenther, A. et al.: Isoprene fluxes measured by enclosure, relaxed eddy accumulation, surface-layer gradient, mixed-layer gradient, and mass balance techniques, J. Geophys. Res., 101, 18555-18568, 1996.

Hämeri, K., Väkevä, M., Hansson, H.C. and Laaksonen, A.: Hygroscopic growth of ultrafine ammonium sulphate aerosol measured using an ultrafine tandem differential mobility analyser, J. Geophys. Res., 105, 22231-22242, 2000.

Hämeri, K., Väkevä, M., Aalto, P., Kulmala, M., Swietlicki, E., Zhou, J., Seidl, W., Becker, E., and O´Dowd C.: Hygroscopic and ccn properties of aerosol particles in boreal forests, Tellus, 53B, 359-379, 2001.

Hämeri, K., Koponen, I. K., Aalto, P. and Kulmal, M.: The particle detection efficiency of the TSI-3007 condensation particle counter, Aeros. Science, 33, 1463-1469, 2002.

Helmig, D. et al.: Vertical profiling and determination of landscape fluxes of biogenic nonmethane hydrocarbons within the planetary boundary layer in the Peruvian Amazon, J. Geophys. Res., 103, 25519-25532, 1998.

Hoffmann T., Odum J. R., Bowman F., Collins D., Klockow D., Flagan R. C. and Seinfeld J. H.: Formation of organic aerosols from the oxidation of biogenic hydrocarbons, J. Atmos. Chemistry 26, 189-222, 1997.

Hoppel, W., Fitzgerald, J., Frick, G., Caffrey, P., Pasternack, L., Hegg, D., Gao, S., Leaitch, R., Shantz, N., Cantrell, C., Albrechcinski, T., Ambrusko, J. and Sullivan, W.: Particle formation and growth from ozonolysis of α-pinene, J. Geophys. Res., 106, 27603-27618, 2001.

Joutsensaari, J., Vaattovaara, P., Vesterinen, M., Hämeri K. and Laaksonen, A.: A novel tandem differential mobility analyzer with organic vapor treatment of aerosol particles, Atmos. Chem. Phys., 1, 51-60, 2001.

Kamens, R. M., and Jaoui, M.: Modeling Aerosol Formation from α-Pinene + NOx in the Presence of Natural Sunlight Using Gas-Phase Kinetics and Gas-Particle Partitioning Theory, Environ. Sci. Technol., 35, 1394-1405, 2001.

Kavouras, I., Mihalopoulos, N. and Stephanou, E. G.: Formation of atmospheric particles from organic acids produced by forests, Nature 395, 683-686, 1998.

Kavouras, I., Mihalopoulos, N. and Stephanou, E. G.: Formation and Gas/Particle Partitioning of Monoterpenes Photo-oxidation Products over Forests, Geophys. Res. Lett. 26, 55-58, 1999a.

Kavouras, I., Mihalopoulos, N. and Stephanou, E. G.: Secondary aerosol formation vs. primary organic aerosol emission: In situ evidence for the chemical coupling between monoterpene acidic photo-oxidation products and new particle formation over forests, Environ. Sci. Technol. 33, 1028-1037, 1999b.

Kawamura, K., Lai-Ling Ng and Kaplan, I. R.: Determination of Organic acids (C1-C10) in the atmosphere, Motor exhausts, and Engine oils, Environ. Sci. Technol. 19, 1082-1086, 1985.

Kawamura, K. and Gagosian R. B.: Implication of w-oxocarboxylic acids in the remote marine atmosphere for photo-oxidation of unsaturated fatty acids, Nature 325, 330-332, 1987.

Koch, S., Winterhalter, R., Uherek, E., Kolloff, A., Neeb, P. and Moortgat, G.: Formation of new particles in the gas-phase ozonolysis of monoterpenes, Atmos. Environ. 32, 4031-4042, 2000.

Korhonen, P., Kulmala, M., Laaksonen, A., Viisanen, Y., McGraw, R. and Seinfeld, J.H.: Ternary nucleation of H2SO4, NH3 and H2O in the atmosphere, J. Geophys. Res., 104, 26349-26353, 1999.

Kulmala, M., Pirjola, L. and Mäkelä, J.M.: Stable sulphate clusters as a source of new atmospheric particles, Nature, 404, 66-69, 2000.

Kulmala, M., Hämeri, K. K., Aalto, P., Mäkelä, J., Pirjola, L., Nilsson, E. D., Buzorius, G., Rannik, Ü., Dal Maso, M., Seidl, W., Hoffmann, T., Jansson, R., Hansson, H.-C., O`Dowd, C. and Viisane, Y.: Overview of the international project on biogenic aerosol formation in the boreal forest (BIOFOR), Tellus B, 53, 324-343, 2001a.

Kulmala, M., Dal Maso, M., Mäkelä, J.M., Pirjola, L., Väkevä, M., Aalto. P., Miikkulainen, P., Hämeri, K. and O'Dowd, C.: On the formation, growth and composition of nucleation mode particles, Tellus B, 53, 479--490, 2001b.

Larsen, B. R., Di Bella, D., Glasius, M., Winterhalter, R., Jensen, N. R., and Hjorth, J.: Gas-phase OH oxidation of monoterpenes: Gaseous and particulate products, J. Atmos. Chem., 38, 231-276, 2001.

Lawrence J. E. and Koutrakis P.: Measurement of atmospheric formic and acetic acids: Methods evaluation and results from field studies, Environ. Sci. Technol., 28, 957-964, 1994.

Lawrence, J. and Koutrakis, P.: Measurement and speciation of gas and particulate phase organic acidity in an urban environment. I. Analytical, J. Geophys. Res. 101, 9159-9163, 1996.

Leaitch, W. R., Bottenheim, J. W., Biesenthal, T. A., Li, S.-M., Liu, P. S. K., Asalian, K., Dryfhout-Clark, H., Hopper, F., and Brechtel, F.: A case study of gas-to-particle conversion in an eastern Canadian forest, J. Geophys. Res., 104, 8095 - 8111, 1999.

Marti, J. J., Weber, R. J., McMurry, P. H., Eisele, F., Tanner, D., and Jefferson, A.: New particle formation at a remote continental site: Assessing the contributions of SO2 and organic precursors, J. Geophys. Res., 102, 6331 - 6339, 1997.

Mihalopoulos, N., Stephanou, E.G., Kanakidou, M., Pilitzidis, S. and Bousquet, P.: Tropospheric aerosol ionic composition in the Eastern Mediterranean region, Tellus B 49, 314-326, 1997.

Nilsson, E.D., Paatero, J. and Boy, M.: Effects of air masses and synoptic weather on aerosol formation in the continental boundary layer, Tellus, 53B, 2001a.

Nilsson, E.D., Rannik, Ü., Kulmala, M., Buzorius, G. and O'Dowd, C.D.: Effects of continental boundary layer evolution, convection, turbulence and entrainment, on aerosol formation effects of the continental boundary layer evolution, convection, turbulence and entrainment on aerosol formation. Tellus, 53B, 441-461, 2001b.

Novakov, T., Hegg, D. A. and Hobbs P. V.: Airborne measurements of carbonaceous aerosols on the East Coast of the United States, J. Geophys. Res., 102, 30023-30030, 1997.

Nozière, B., Barnes, I., and Becker, K. H.: Product study and mechanisms of the reactions of alpha-pinene and of pinonaldehyde with OH radicals, J. Geophys. Res., 104, 23645-23656, 1999.

Petäjä, T., Aalto, P. and Hämeri, K.: Hygroscopicity of toluene oxidation products, Abstracts of the Sixth International Aerosol Conference in Taipei, 851-852, 2002.

Peters, K. and Eiden, E.: Modelling of the dry deposition velocity of aerosol particles to a spruce forest, Atmos. Environ., 26A, 2555-2564, 1992.

Pio, C., Castro, L. and Ramos, M.: Differentiated determination of organic and elemental carbon in atmospheric aerosol particles by a Thermal-optical method, in: G. Angeletti, G. Restelli (eds). Proc. Sixth European Symp. on Physico-chemical Behaviour of Atmospheric Pollutants, Report EUR 15609/2 EN, pp 706-711, 1994.

Rinne, J., Hakola, H., Laurila, T. and Rannik, Ü.: Canopy scale monoterpene emissions of Pinus sylvestris dominated forests, Atmos. Environ., 34: 1099 – 1107, 2000.

Römpp, A. and Moortgat, G.: Analysis of Oxygenated Compounds in Ambient Aerosol by LC-MS-TOF. Proceedings of EUROTRAC 2002, 2002.

Rogge W. F., Hildemann L. M., Mazurek M. A., Cass G. R. and Simoneit B. R. T.: Sources of fine organic aerosol. 1. Charbroilers and meat cooking operations, Environ. Science and Technology 25, 1112-1125, 1991.

Simoneit B. R. T., Cox R. E. and Standley L. J.: Organic matter of the troposphere-IV. Lipids in Harmattan aerosols of Nigeria, Atmos. Environ. 22, 983-1004, 1988.

Simoneit B. R. T.: Organic matter of the troposphere - V: Application of molecular analysis to biogenic emissions into the troposphere for source reconciliations, J. Atmos. Chemistry 8, 251-275, 1989.

Simoneit, B., Schauer, J., Nolte, C. Oros, D., Elias, V., Fraser, M., Rogge, W. and Cass, G.: Levoglucosan, a tracer for cellulose in biomass burning and atmospheric particles, Atmos. Environ., 33, 173 – 182, 1999.

Simoneit B. R. T.: Biomass burning – a review of organic tracers for smoke from incomplete combustion, Applied Geochemistry 17, 129-162, 2002.

Standley L. and Simoneit B. R. T.: Characterization of extractable plant wax, resin, and thermally maturated components in smoke particles from prescribed burns, Environ. Science and Technology 21, 163-169, 1987.

Standley L. and Simoneit B. R. T.: Resin diterpenoids as tracers for biomass combustion aerosols, J. Atmos. Chemistry 18, 1-15, 1994.

Stephanou, E., and Stratigakis, N.: Determination of anthropogenic and biogenic organic compounds on airborne particles: flash chromatographic fractionation and capillary gas chromatographic analysis, J. Chromatogr. A 644, 141-151, 1993.

Sirju A.-P. and Shepson P. B.: Laboratory and field investigation of the DNPH cartridge technique for measurement of atmospheric carbonyl compounds, Environ. Sci. Technol., 29, 384-392, 1995.

Stratman, F., Siebert, H., Spindler, G., Wehner, B., Althausen, D., Heintzenberg, J., Hellmuth, O., Rinke, R., Schmieder, U., Seidel, C., Tuch, T., Uhrner, U., Wiedensohler, A., Wandinger, U., Wendisch, M., Schell, D. and Stohl, A.: New-particle formation events in a continental boundarylayer: First results from the SATURN experiment, Atmos. Chem. Phys. Discuss., 3, 1693-1731, 2003.

Talbot, R.W., Beecher, K.M., Harris, R.C. and Coferr, W.R. III J.: Atmospheric chemistry of formic and acetic acids at a mid-latitude temperate site. J. Geophys. Res. 93, 1638-1652, 1988.

Virkkula, A., Van~Dingenen, R., Raes, F. and Hjort, J.: Hygroscopic properties of aerosol formed by oxidation of limonene, alpha-pinene, and beta-pinene, J. Geophys. Res., 104, 3569-3579, 1999.

Voisin, D., Smith, J. N., Sakurai, H., McMurry, P. H., and Eisele, F. L.: Thermal desorption chemical ionization mass spectrometer for ultrafine particle chemical composition, Aerosol Sci. Technol., 37, 471-475, 2003.

Warnke, J., Bandur, R. and Hoffmann, T.: Characterisation of boreal forest aerosols by HPLC/MS, submitted to J. Aerosol Sci., 2003.

Warscheid, B. and Hoffmann, T.: Direct analysis of highly oxidised organic aerosol constituents by on-line ion trap mass spectrometry in the negative ion mode, Rapid. Commun. Mass Spectrom., 16, 496-504, 2002.

Winklmayr, W., Reischl, G., Lindner, A. and Berner, A.: A new electromobility spectrometer for the measurement of aerosol size distributions in the size range from 1 to 1000 nm, J. Aerosol Sci., 22, 289-296, 1991.

Winterhalter R., Neeb P., Grossmann, Kolloff A., Horie O. and Moortgat G.: Products and mechanism of the gas phase reaction of ozone with b-pinene, J. Atmos. Chemistry 35, 165-197, 1999.

Yokouchi Y. and Ambe Y.: Aerosols formed from the chemical reaction of monoterpenes and ozone, Atmos. Environ. 19, 1271-1276, 1985.

Yokouchi Y. e Ambe Y.: Characterization of polar organics in airborne particulate matter, Atmos. Environ. 20, 1727-1734, 1986.

Zervas E., Montagne X. and Lahaye J.: Collection and analysis of organic acids in exhaust gas. Comparison of different methods, Atmos. Environm., 33, 4953-4962, 1999.

Tables

Table 1 Data collected on tethered balloons at Hyytiälä during the OSOA campaign 2001.

Date	VOC profiles	integrative VOC	OPC profiles	CPC profiles	Met. Profiles (Temp./RH)
2. Aug	1		2		3
3. Aug	4	4	8		8
4. Aug		2	6		6
5. Aug	2	3	4		
6. Aug	2	1	6		
7. Aug	3	3	6	2	
8. Aug	3	4	8	8	
9. Aug	2	1	8	6	
10. Aug					4
12. Aug	3	2		10	
Total	20	20	48	26	76

Table 2: Growth rates, estimated vapour concentrations, source rates and particle formation rates at observed particle formation bursts during OSOA field campaign.

Day	Growth rate	Vapour conc.	Vapour source	Formation rate
	[nm/h]	10^7 cm^{-3}	10^5 cm^{-3} s^{-1}	cm^{-3} s^{-1}
1. Aug	6,24	8,79	1,08	0,24
2. Aug	10,74	15,22	1,27	0,38
3. Aug	10,41	14,74	2,64	0,17
7. Aug	9,59	13,38	4,93	0,31
10. Aug	9,37	13,13	4,73	0,18
14. Aug	37,95	54,58	19,14	1,72

Table 3: Organic compounds measured in the gas-phase.

Compound name	Formula	Concentration Range (μg m^{-3})		
Low weight carboxylic acids				
Formic acid	HCOOH	< 0,15	-	1,26
Acetic acid	CH_3COOH	< 0,21	-	1,82
Aldehydes and Ketones				
Formaldehyde	HCHO	0,18	-	0,98
Acetaldehyde	CH_3CHO	0,12	-	3,24
Acetone	CH_3COCH_3	0,24	-	1,80
Acrolein	CH_2CHCHO	< 0,01	-	1,33
Propionaldehyde	CH_3CH_2CHO	0,02	-	0,38
Hexanaldehyde	$CH_3(CH_2)_4CHO$	< 0,01	-	0,31

Table 4: The total concentration ranges and carbon preference indexes for some of the detected homologue compounds series

Compounds Class	Concentration Range ($ng\ m^{-3}$)	C_{max}	CPI Whole range (Petroleum) C_{10}-C_{34}	CPI Split range (Bacterial) C_{10}-C_{25}	CPI Split range (Plant wax) C_{21}-C_{34}
n-Alkanes	7,2 - 95,2	C_{27}	2,69 ± 1,05	1,83 ± 0,69	5,85 ± 2,54
n-Alkanols	1,0 - 17,4	C_{26}	8,52 ± 4,16	3,33 ± 1,82	18,98 ± 8,44
n-Monocarboxylic Acids	39,0 - 192,0	C_{16}	6,86 ± 1,67	7,00 ± 2,18	4,72 ± 1,10

C_{max} - Carbon number with the highest peak in the chromatogram; CPI - Sum of the odd carbon number homologues divided by the sum of the even carbon number homologues over the range indicated for n-alkanes and the inverse for n-alkanols and n-alkanoic acids (Abas and Simoneit, 1996).

Table 5: Some primary and secondary compounds derived from biogenic sources.

Compound name	Max. conc. ($ng\ m^{-3}$)	Proposed sources and References
6,10,14-trimethyl-2-Pentadecanone	15,0	Degradation product of phytol found in plant wax (Simoneit *et al.*, 1988)
Triterpenones $C_{30}H_{48}O$ (isomers)	2,7	Angiosperm wood burning or plant wax weathering (Standley and Simoneit, 1987; Simoneit 2002)
Cholesterol	1,4	Wood burning or plant wax weathering (Simoneit, 1989 and 2002); Cholesterol from meat cooking (Rogge et al., 1991)
Stigmasterol	2,4	
ß-Sitosterol	25,0	
Pina ketone (Nopinone)	0,2	Photo-oxidation of alpha- and/or beta-Pinene (Yokouchi and Ambe, 1985; Hoffmann et al., 1997; Christoffersen *et al.*, 1998; Winterhalter et al., 1999; Koch *et al.*, 2000)
Pinonaldehyde	5,5	
Pinonic acid	2,6	
Pinic acid	5,0	
Dehydroabietinal	0,2	Degradation of resinous components by coniferous wood burning or natural weathering (Standley and Simoneit, 1987 and 1994; Simoneit 1989 and 2002)
Abieta-8,11,13-trien-7-one	2,1	
6-Dehydrodehydroabietic acid	0,5	
Dehydroabietic acid	2,3	
7-Oxodehydroabietic acid	0,1	

Table 6: Some organic compounds detected in the water-extract

Compound name	Formula	Concentration Range (ng m^{-3})		
Malic acid (Hydroxibutanedioic)	$C_4H_6O_5$	0,1	-	8,0
2-Hydroxiglutaric acid	$C_5H_8O_5$	0,1	-	2,6
Arabitol	$C_5H_{12}O_5$	1,4	-	241
Mannitol	$C_6H_{14}O_6$	< 0,5	-	88
Glucose	$C_6H_{12}O_6$	1,3	-	41
Sucrose	$C_{12}H_{22}O_{11}$	0,3	-	10

Table 7: Aerosol concentrations of terpene oxidation products

	Min (ng/m^{-3})	Max (ng/m^{-3})	Average (ng/m^{-3})
Pinic acid	2,0	21	5,6 (n=16)
Pinonic acid	5,2	14	8,1 (n=16)
Norpinic acid	n.q.	1,0	0,3 (n=16)
Sabinic acid	0,7	4,1	1,9 (n=16)
Limonic and caric acid	1,7	62	10 (n=16)

n.q.: below limit of quantification

n: number of samples

Table 8: Characteristic values from relative humidity, vertical wind variance, temperature and short wavelength irradiance (300 – 340 nm).

Date	RH [%]		Vert. wind variance [m s^{-1}]		Irradiance [W m^{-2}]		Temp. [°C]	
	Mean	Min.	Mean	Max.	Mean	Max.	Mean	Max.
1. Aug	55,3	48,3	1,01	1,24	5,0	9,3	13,4	14,7
2. Aug	48,6	38,8	0,97	1,23	5,0	9,4	11,8	13,7
3. Aug	44,8	33,3	0,84	1,11	5,9	9,2	14,7	18,0
4. Aug	61,9	48,1	0,95	1,37	3,8	7,6	15,4	17,6
5. Aug	77,5	54,0	0,64	1,00	4,1	8,6	17,9	20,8
6. Aug	76,1	56,9	0,50	0,83	3,2	7,5	15,5	17,8
7. Aug	61,1	45,4	0,64	0,90	4,2	8,1	16,6	18,8
8. Aug	57,8	43,9	0,73	1,01	4,9	8,7	16,9	19,1
9. Aug	73,0	52,7	0,78	1,03	3,1	7,0	17,3	20,4
10. Aug	58,9	44,8	0,88	1,19	4,7	8,8	17,3	19,1
11. Aug	81,6	56,3	0,49	0,79	2,2	6,9	13,8	17,8
12. Aug	75,8	60,9	0,60	0,85	3,2	7,8	14,3	16,2
13. Aug	76,8	58,3	0,56	0,89	3,3	8,0	15,2	17,9
14. Aug	63,8	52,2	0,59	0,90	4,8	8,1	15,8	18,5
15. Aug	62,7	48,2	0,65	0,86	4,8	7,8	19,4	22,4
16. Aug	73,0	47,9	0,75	1,07	3,9	7,9	19,9	24,0

Figures

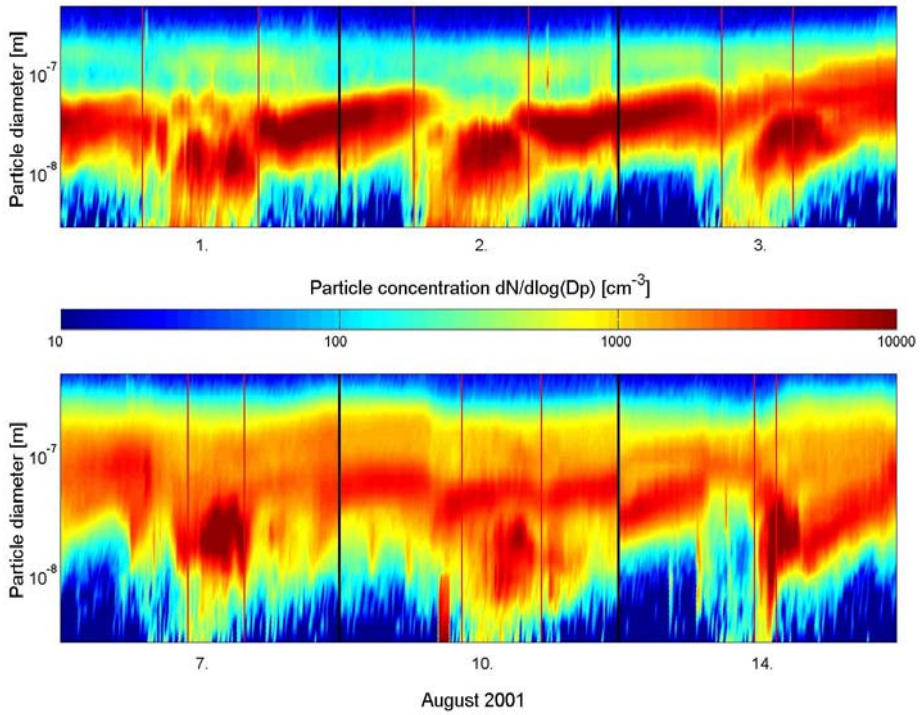

Figure 1: Aerosol number size distributions from the DMPS system at 2 m height in Hyytiälä, Finland for all the event days during the OSOA field campaign. Included as thin red lines are the start and end times of the particle bursts (times: $[N_{3\text{-}10nm}]$ > or < 200 particles cm^{-3}).

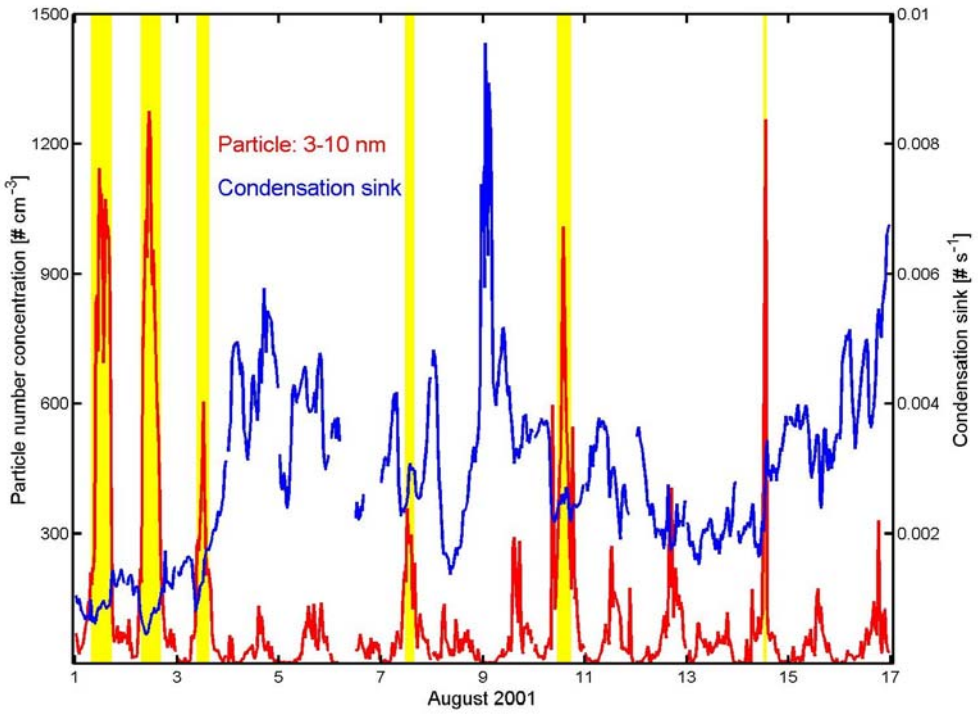

Figure 2: Half hour average values for the number concentration of the nucleation mode particles (3-10 nm) and condensational sink. The yellow areas mark the periods when bursts of nucleation mode particles were observed.

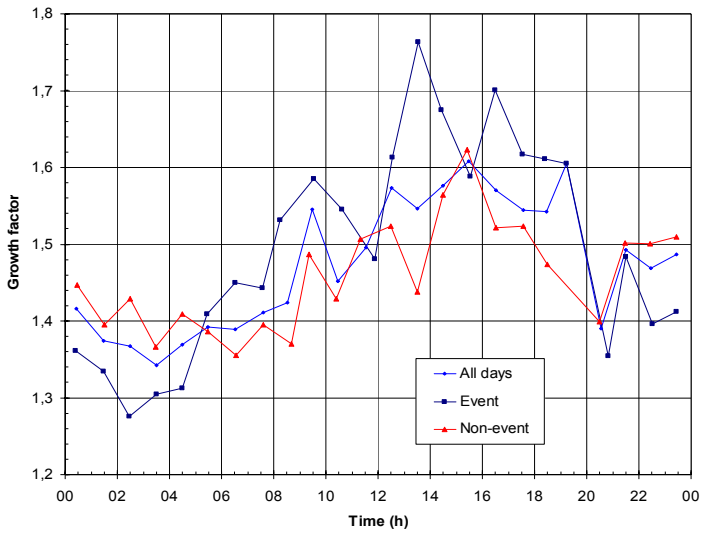

Figure 3: Hourly averages of hygroscopic growth factors in water vapour of all days, nucleation event and non-event days (dry particle size 100 nm).

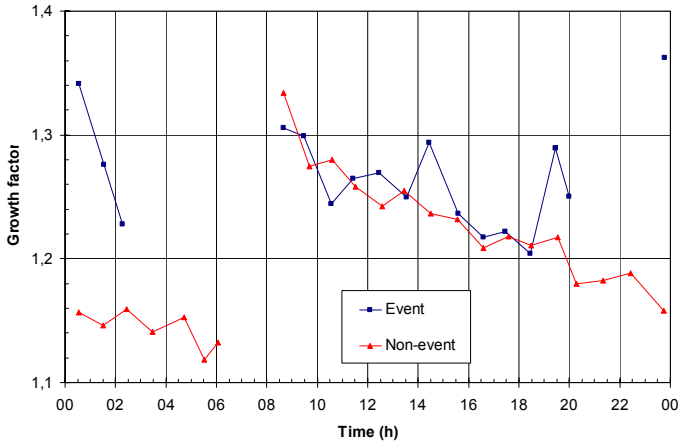

Figure 4: Hourly averages of hygroscopic growth factors in ethanol vapour for nucleation event and non-event days (dry particle size 100 nm).

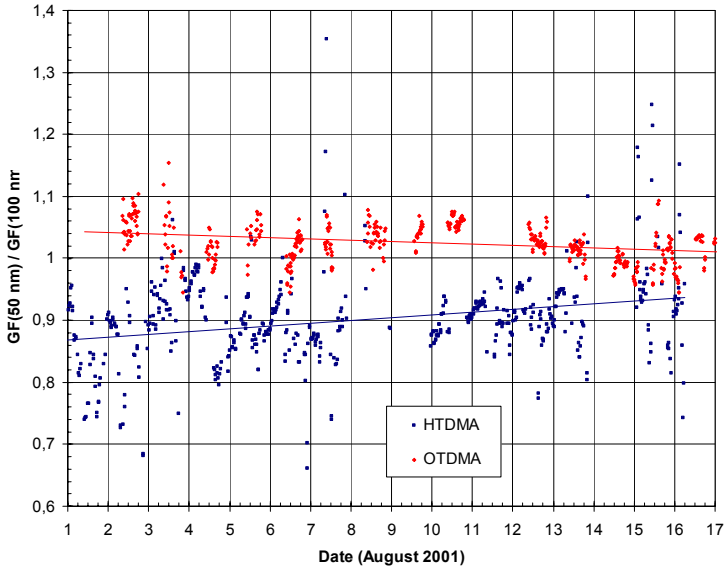

Figure 5: Time series for the fraction of 50 to 100 nm particle growth factors (GF(50 nm)/GF(100 nm)) in water (HTDMA) and ethanol (OTDMA) vapours.

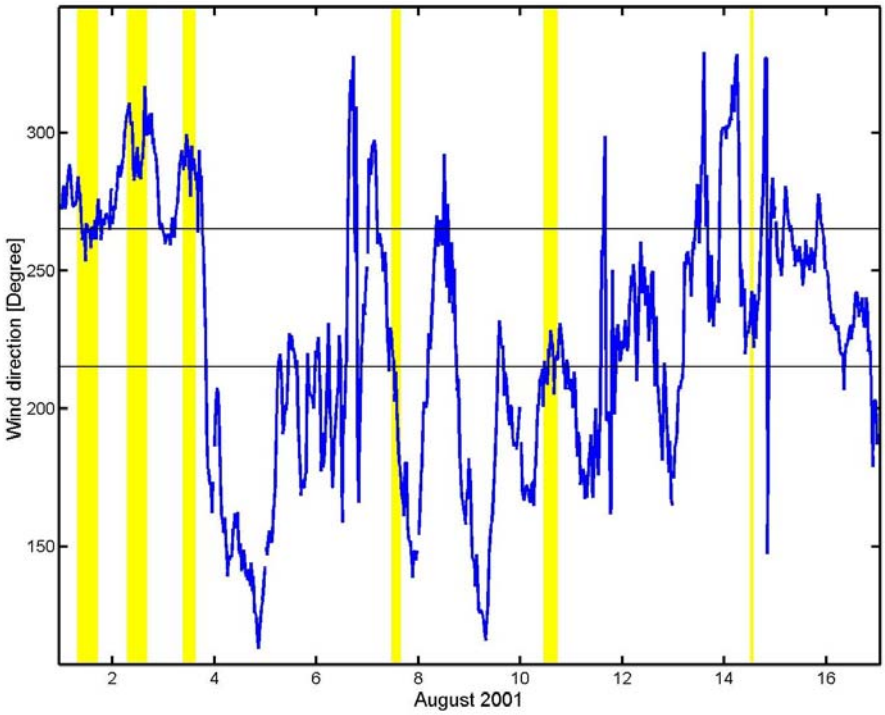

Figure 6: Half hour average values of the wind direction. The yellow areas mark the periods when bursts of nucleation mode particles were observed and the thin black line is the wind-sector from Tampere and the station building.

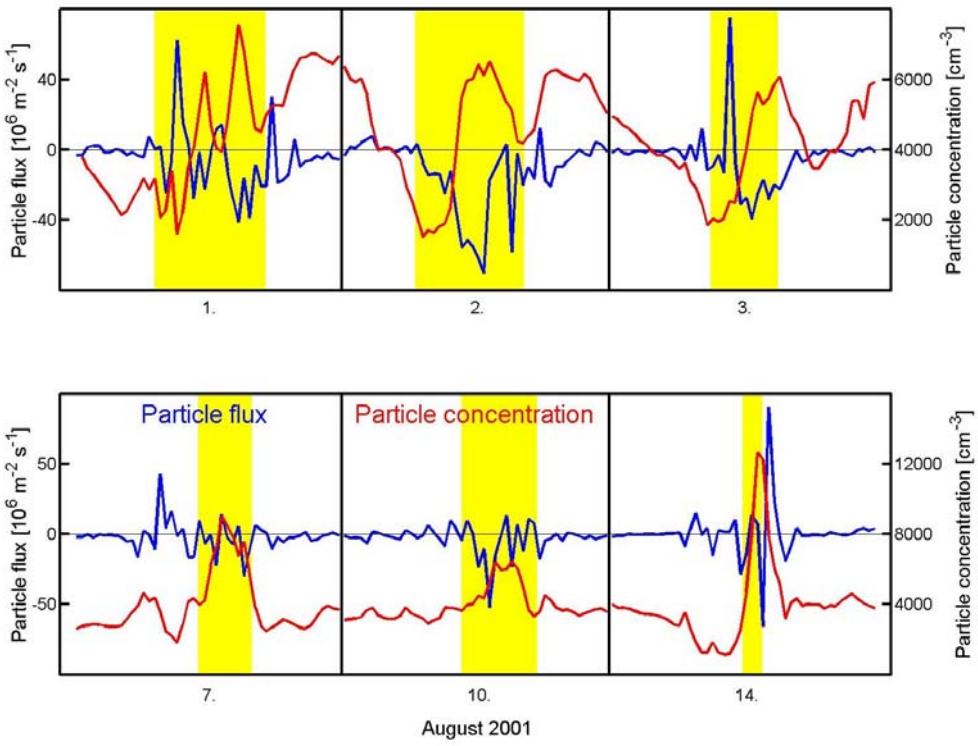

Figure 7: Half hour average values for the particle number concentration measured by the CPC from the EC system at 23 m and calculated particle fluxes. The yellow areas mark the periods when bursts of nucleation mode particles were observed.

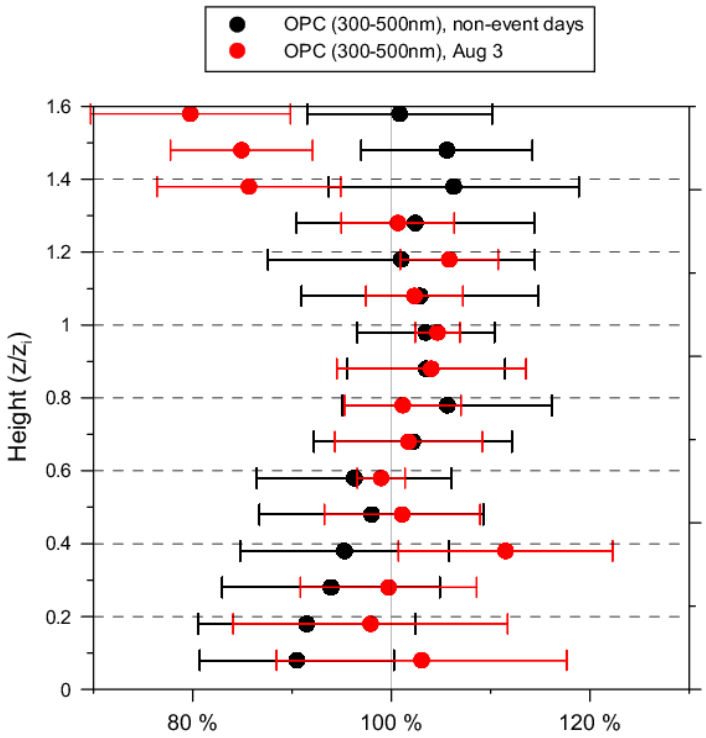

Figure 8: Vertical profiles of particle number concentrations. Concentrations are normalized to the average in the mixed layer, altitude is given as height above ground divided by boundary layer depth (z/z_i). Only profiles with measurements both in the mixed layer ($z/z_i<1$) and above ($z/z_i>1$) are included; error bars denote standard deviations of the sample (Aug 3, n=6, other days n=33).

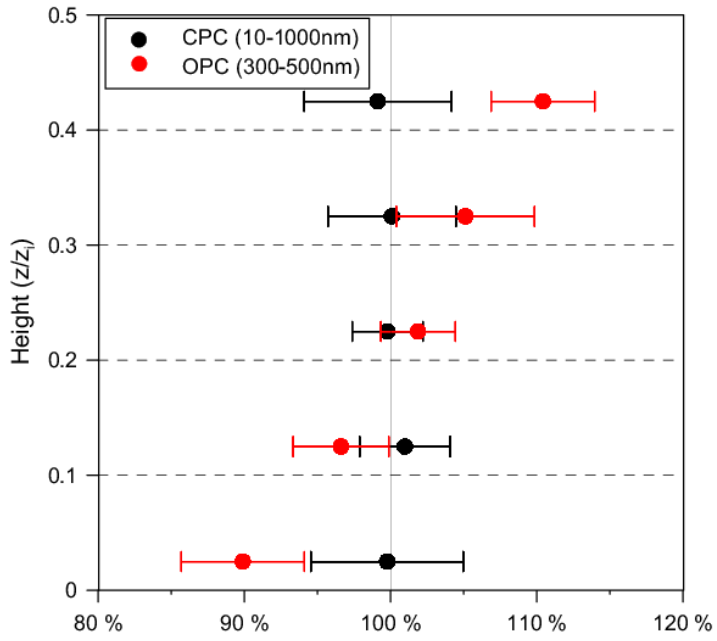

Figure 9: Vertical particle concentration gradients for different sizes, plotted in the same way as in Figure 8; average of 4 profiles measured on Aug 8, 14:30 – 15:30.

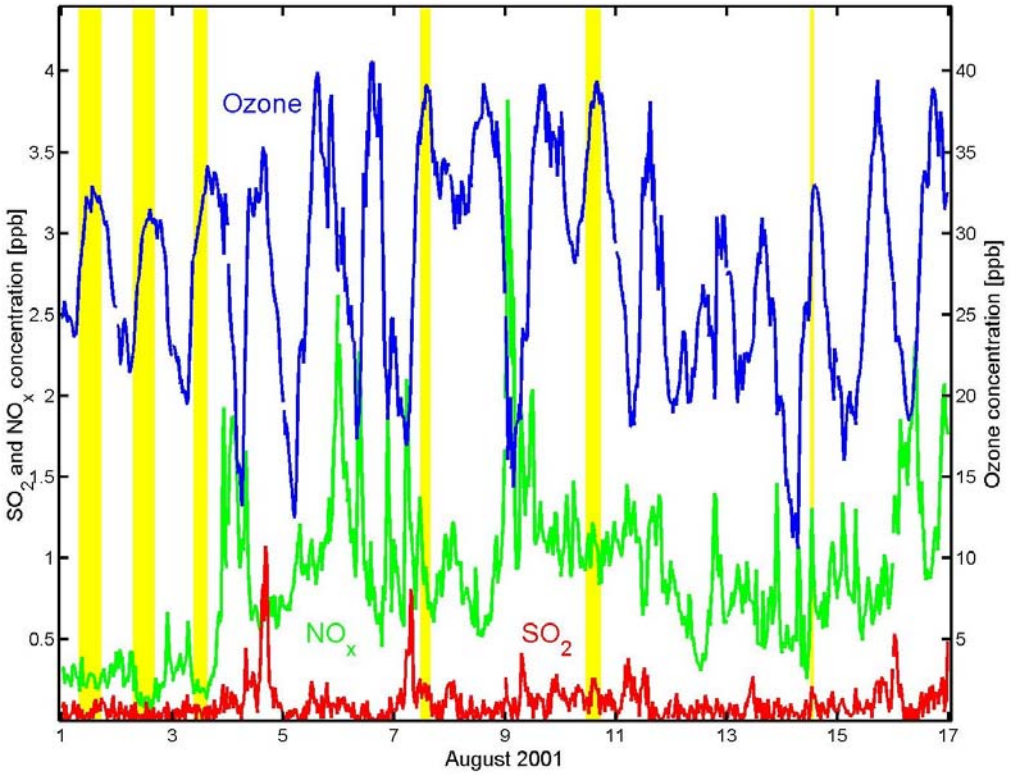

Figure 10: Half hour average values of O_3, NO_x and SO_2. The yellow area marks the periods when bursts of nucleation mode particles were observed.

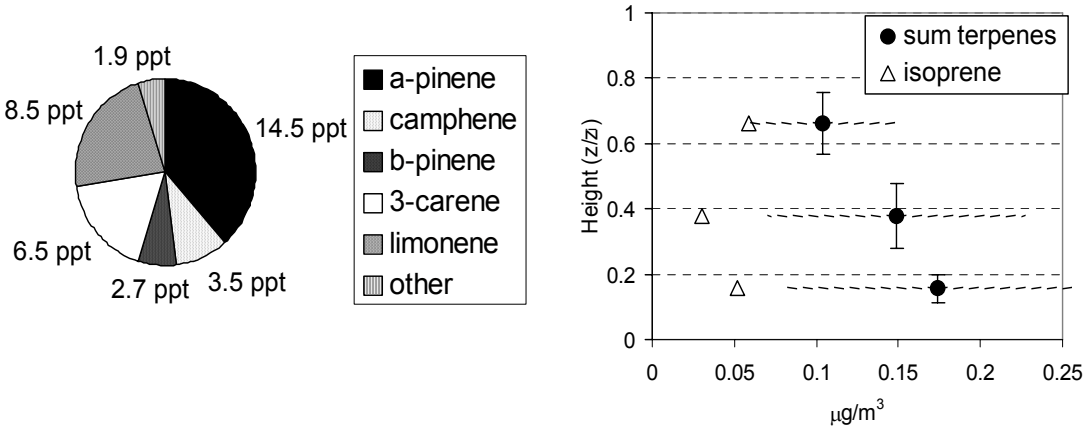

Figure 11: Averaged monoterpene concentrations from balloon samples, a) mean composition, b) profile of medians (error bars are interquartile ranges).

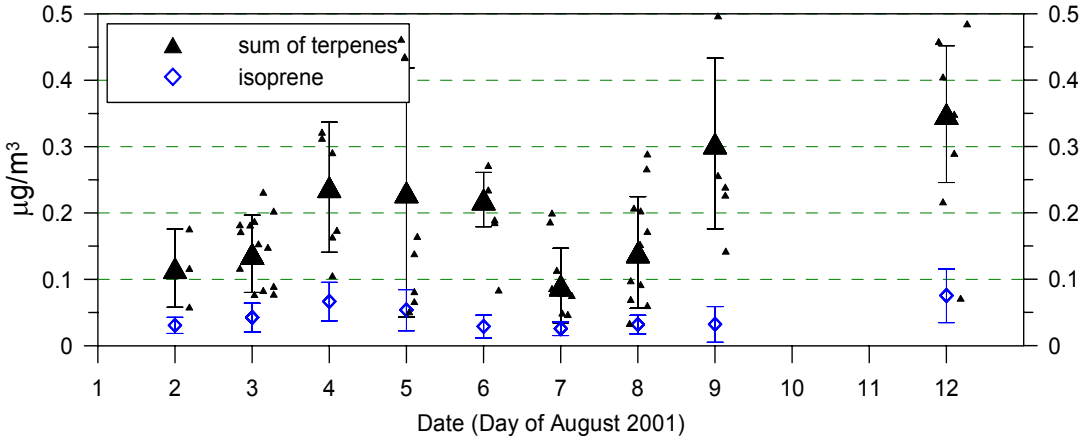

Figure 12: Biogenic VOC concentrations during the OSOA campaign 2001. Large symbols are daily averages (error bars are standard deviations) of all measurements taken within the PBL (small symbols).

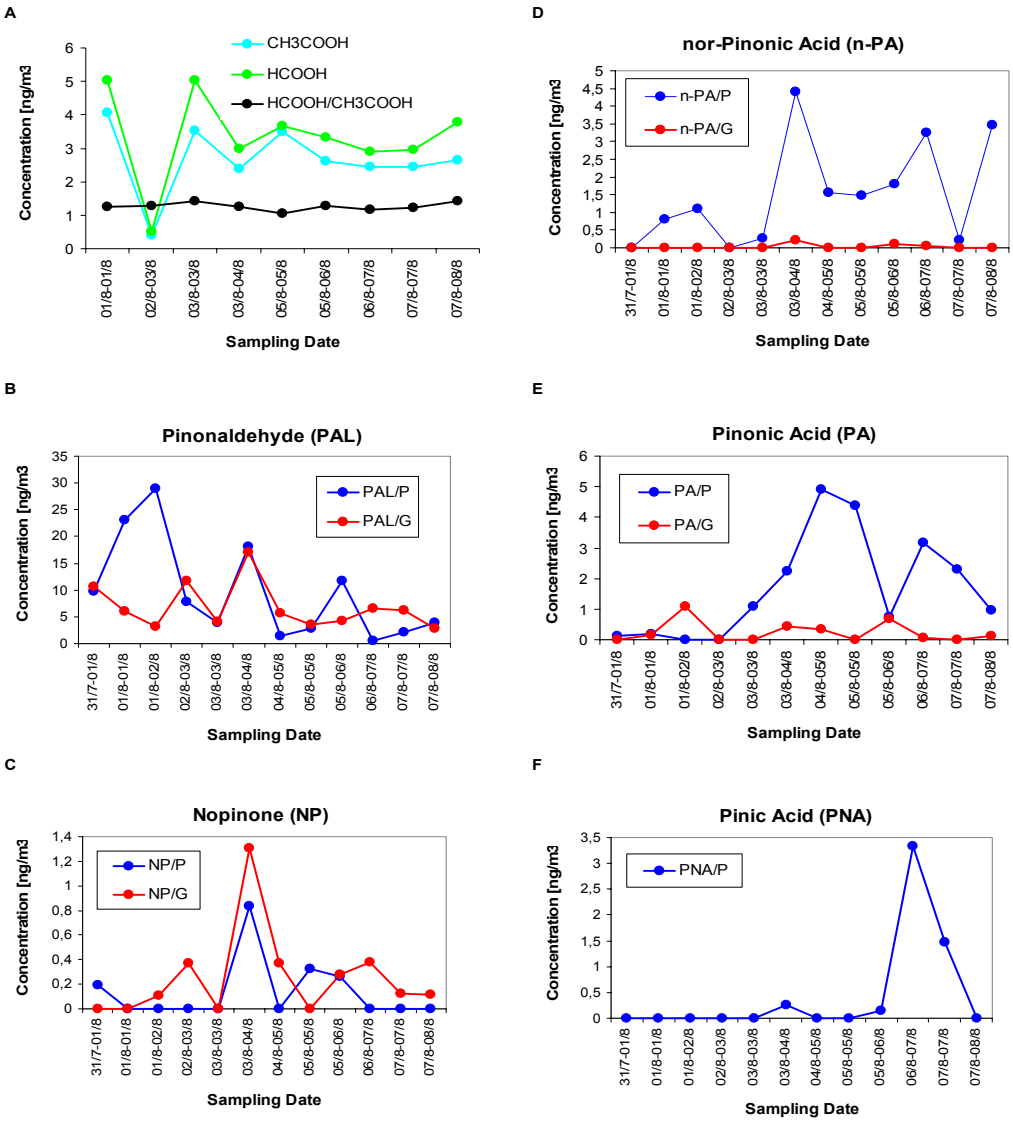

Figure 13: Gas- and particle-phase concentrations of some photo-oxidation products for the first eight days in August 2001 with a sampling time of 12 hours and start times at 6 p.m. and 6 a.m. respectively.

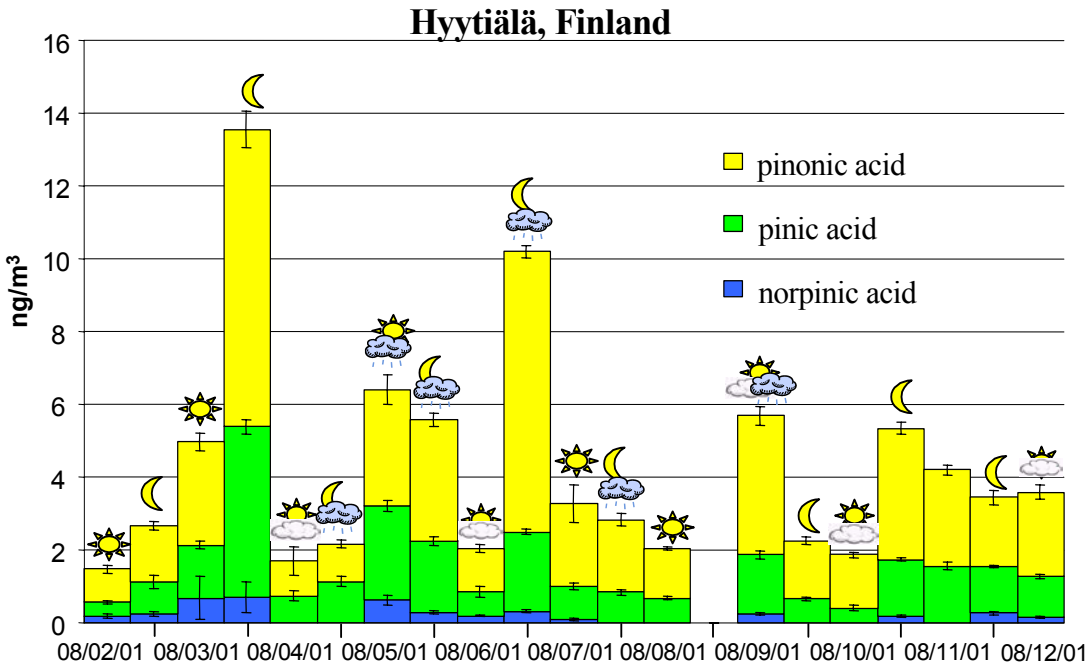

Figure 14: Acids of biogenic origin quantified in samples from Hyytiälä, Finland. The symbols are indicating the meteorological conditions during the sampling period.

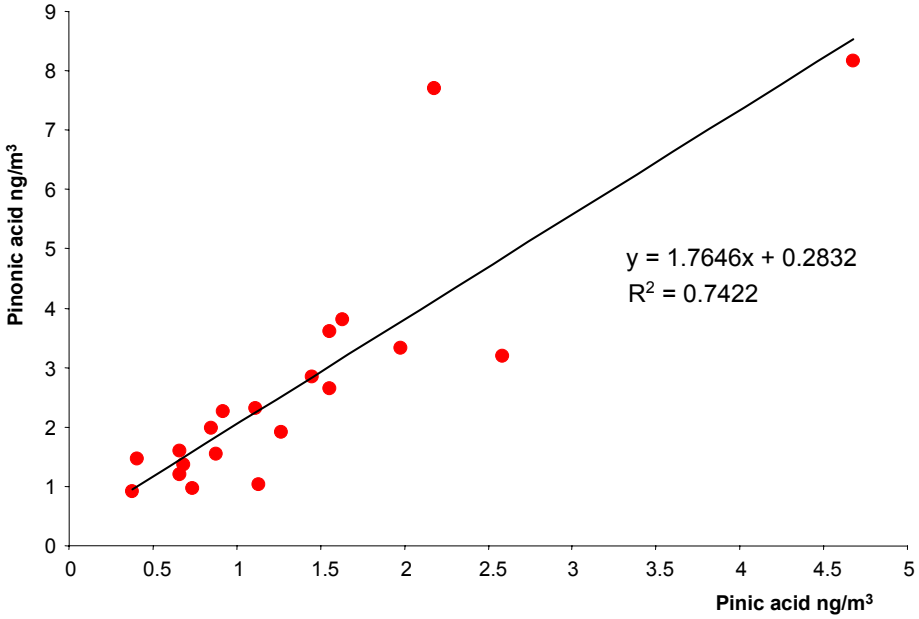

Figure 15: Concentration of pinic acid vs. pinonic acid in atmospheric aerosol samples.

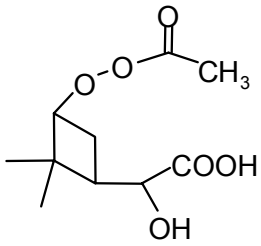

Figure 16: Structure of "m/z 231"

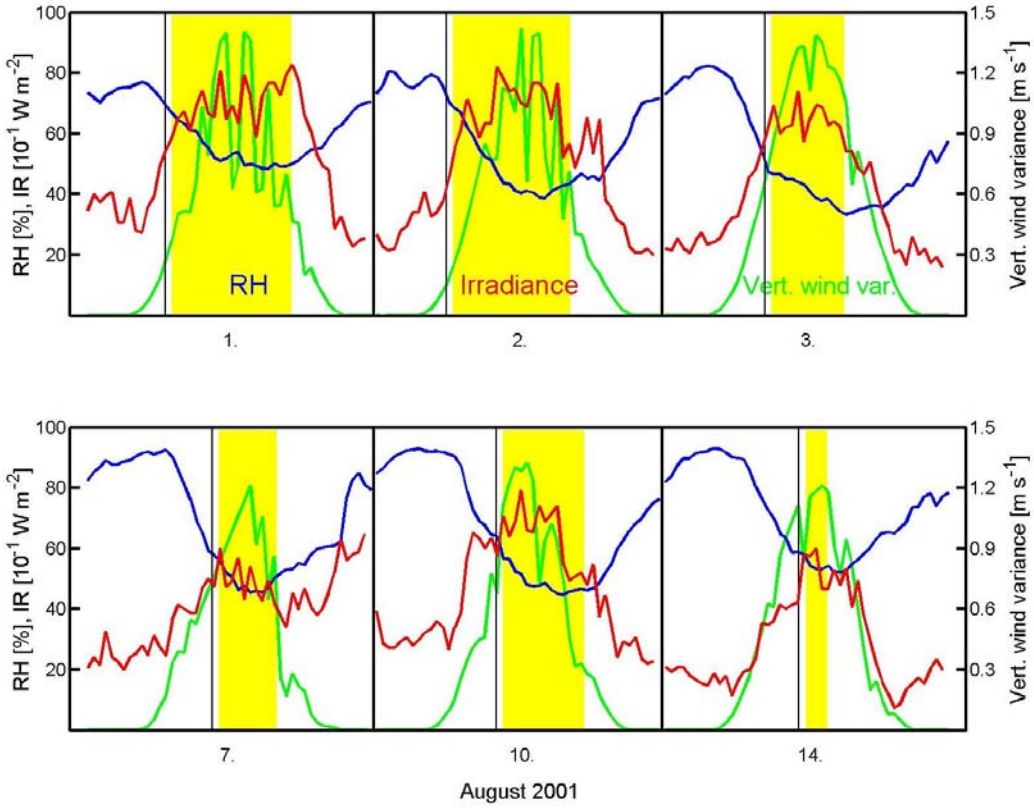

Figure 17: Half hour average values of relative humidity, solar short wavelength irradiance (300-340 nm) and vertical wind variance. The yellow area marks the periods when bursts of nucleation mode particles were observed.

6 Paper IV, Tethered Balloon Measurements of Biogenic VOCs

Tethered balloon measurements of biogenic volatile organic compounds at a Boreal forest site

Christoph Spirig[1,2], Alex Guenther[2], James P. Greenberg[2], Pierluigi Calanca[1], and Virpi Tarvainen[3]

[1]{Swiss Federal Research Station for Agroecology and Agriculture, Zürich, Switzerland}

[2]{National Center for Atmospheric Research, Boulder, USA}

[3] {Finnish Meterological Institute, Helsinki, Finland}

Atmospheric Chemistry and Physics Discussions, 3, 5357-5397, 2003

http://www.copernicus.org/EGU/acp/

Abstract

Measurements of biogenic volatile organic compounds (VOCs) were performed at Hyytiälä, a Boreal forest site in Southern Finland as part of the project OSOA (origin and formation of secondary organic aerosol) in August 2001. At this site, frequent formation of new particles has been observed and the role of biogenic VOCs in this process is still unclear. Tethered balloons served as platforms to collect VOC samples within the planetary boundary layer at heights up to 1.2 km above ground during daytime. Mean mixed layer concentrations of total monoterpenes varied between 10 and 170 pptv, with α-pinene, limonene and Δ^3-carene as major compounds, isoprene was detected at levels of 2-35 pptv. A mixed layer gradient technique and a budget approach are applied to derive surface fluxes representative for areas of tens to hundreds of square kilometres. Effects of spatial heterogeneity in surface emissions are examined with a footprint analysis. Depending on the source area considered, mean afternoon emissions of the sum of terpenes range between 180 and 300 $\mu g\ m^{-2}\ h^{-1}$ for the period of Aug 2 to Aug 12, 2001. Surface fluxes close to Hyytiälä were higher than the regional average, and agree well with mean emissions predicted by a biogenic VOC emission model. Total rates of monoterpene oxidation were calculated with a photochemical model. The rates did not correlate with the occurrence of new particle formation, but the ozone pathway was of more importance on days with particle formation. Condensable vapour production from the oxidation of monoterpenes throughout the mixed layer can only account for a fraction of the increase in aerosol mass observed at the surface.

1. Introduction

The biosphere and plants in particular release a variety of reactive volatile organic compounds (VOCs) that are of importance for atmospheric chemistry. Among the major biogenic emissions are those of monoterpenes, C_{10}-compounds that are readily oxidized in the atmosphere by OH-, NO_3-radicals or ozone. Several products of these reactions are of low volatility and partition between gas and particulate phases and accordingly may contribute to organic aerosol mass. Through this pathway of secondary organic aerosol (SOA) formation, biogenic VOCs are estimated to significantly add to the load of aerosols on a global scale (Griffin et al., 1999).

Various smog chamber studies have proven the potential of monoterpenes to form aerosols upon oxidation (Hoffmann et al., 1997; Kamens et al., 1999). Several field studies have also indicated the links between the oxidation of biogenic VOCs and formation of organic aerosol under environmental conditions (Kavouras et al., 1998; Kavouras et al., 1999; Leaitch et al., 1999). While it seems clear that biogenic VOC contribute to organic aerosol mass, their role in the process of new particle formation is still uncertain, however. There is also evidence from observations that monoterpene oxidation products are rather linked to growth than to new formation of particles (Janson et al., 2001).

At Hyytiälä, a Boreal forest site in Southern Finland, extensive particle measurements have been carried out in recent years and formation of new particles has been observed on a regular basis (Kulmala et al., 2001; Mäkelä et al., 1997). These nucleation events are postulated to occur on a large horizontal scale in the order of hundreds of km, as they were detected simultaneously at sites in distances of more than one hundred km (Nilsson et al., 2001).

In summer 2001, we participated in a field campaign at Hyytiälä as part of the EU project OSOA (origin and formation of secondary organic aerosol formation). The aim of this project was to quantitatively understand the sources and formation mechanisms of secondary organic aerosols with both laboratory and field experiments.

In order to judge the impact of biogenic VOCs during particle formation events, one important piece of information is the quantification of their surface flux. Past measurement efforts at the site confirmed the emission of various biogenic VOCs, terpenes in particular, with the use of chamber and micrometeorological gradient techniques (Janson et al., 2001; Rinne et al., 2000; Spanke et al., 2001). As a result of these studies, monoterpene emissions close to the SMEAR II site could be characterized. However, it is desirable to verify larger scale fluxes with measurements as well. This is of particular interest for biogenic VOC fluxes at the Hyytiälä site since the particle formation events are believed to occur on large spatial scale. This work aims to determine if the VOC fluxes on a larger scale are consistent with those near the tower. For this purpose, we performed VOC measurements throughout the atmospheric boundary layer (up to about 1km above ground) using a tethered balloon sampling platform. From these measurements we derive surface flux estimates representative for areas of tens to hundreds of square kilometres by means of a gradient method and a boundary layer budget approach.

2. Experimental

2.1. Site description

The experiment took place in Southern Finland at Hyytiälä (61°51'N, 24°17'E, 181 m asl), a research site operated by University of Helsinki (SMEAR II, Station for Measuring Forest Ecosystem-Atmosphere Relations). The station is surrounded by Boreal coniferous forest, dominated by Scots pine (*Pinus sylvestris*) and Norway spruce (*Picea abies*). According to landuse data encompassing 20 × 20 km around the station, 72% of the surface is covered with forest (Figure 1). Water bodies (12%), open fields (10%) and clear cuts account for most of the remainder. Of the forest area, 37% are pine dominated, 16% by spruce, 18% is covered by deciduous forest, the remainder is mixed coniferous and broadleaf forest (29%). There is no major source of anthropogenic trace gases nearby; the nearest city is Tampere, located 60 km in South-western direction. The terrain around the site exhibits only modest terrain height variation, with 95% of the area within 20 × 20 km between 100 and 220 m asl.

At SMEAR II, aerosols size distribution, gaseous pollutants (SO_2, O_3 and NO_x) and (micro) meteorological parameters have been measured on a routine basis for several years. The sensors are installed at several levels on a 67 m high tower, located 0.8 km northeast of the research site buildings. The tethered balloons were launched from a soccer field next to these buildings, about 100 m east of a lake (Figure 1).

2.2. Measurements by tethered balloons

Two 9 m^3 helium balloons (Blimp Works, Statesville, NC) served as platforms to collect VOC samples and meteorological data at heights between 100 m and 1.3 km above ground. Three tether lines and winch systems were employed during the campaign. Two were commercially available electric winches (model TS-3-AW, Air Instrumentation Res. Inc., now Vaisala, Boulder CO) that can either be operated with a 12 V DC car battery or on AC-power. The lines on these winches were of 700 m and 800 m length, respectively. A third system, with a 1500 m line, was a custom built spool driven by an electric drill.

2.2.1. Sample collection and temperature measurements

VOCs were collected using miniaturized sampling packages that were attached at several different points on the tether line (for a detailed description, see Greenberg et al. (1999a)). They are operated by timers and provide flow controlled air sampling onto adsorbent cartridges (adsorbent was a two-stage combination of Carbotrap®, and Carbosieve S-III® by

Supelco, Inc., Bellefonte, Pennsylvania). The flow rates were 200 ml/min yielding sampling volumes between 6 and 10 litres for pumping times between 30 and 50 minutes. In addition to collecting trace gases on cartridges, the packages also record pressure, temperature and humidity, all of them logged at 0.5Hz. In front of the cartridge, glass wool filters (Acrodisc, Pall Corp., Ann Arbor, MI) soaked with potassium iodide were installed in order to remove ambient ozone and avoid VOC losses through ozone (Helmig, 1997). Cartridges were conditioned in the week before the experiment and stored at ~ - 30°C. At Hyytiälä, cartridges were in a freezer at ~-10°C, during transport to and from Finland (approximately 20 hours) cartridges were kept in an ice chest (0-5°C). All samples were stored at –30°C and analyzed within 30 days after the experiment.

The sampling packages were attached to the tether line in two configurations. (1) Setup for integrative VOC measurement with one package right below (1-2 m) the balloon, operating during ascent and descent. This arrangement delivers temperature and humidity profiles (vertical resolution usually 1-2 m) and an integrative VOC measurement from ground to the maximum height reached.

(2) Profile setup, three VOC sampling packages are attached to the tether line at heights of about 120 m, 250 m and 500-600 m. The packages sampled air at those heights during 30 min., delivering a mean VOC profile of the lowest 500-600 m.

Altitudes were determined from pressure data recorded during sampling. Pressure and temperature readings of the different sampler packages were referenced daily against the official pressure measurement in the SMEAR II station. Considering the precision of pressure sensors and variability due to up and downdrafts of the balloon during sampling, height accuracy is estimated to be within 20 m.

2.2.2. Analysis of VOC samples

The contents of the adsorbent cartridges were analysed by a gas chromatograph with a mass spectrometry detector (GC-MS, Hewlett Packard model HP5890/5972). Transfer of the samples onto the chromatographic column (30 m × 0.32 mm I.D., 1μm-film DB1-column, J&W Scientific, Folsom, CA) was achieved by an automated inlet system described in detail by Greenberg et al. (1996; 1999a). The key steps can be summarized as follows: Water trapped during sampling is first removed by purging with helium at 40°C. VOCs are then desorbed from the cartridge at 325° (purge flow of 20-30 ml He for 30 min), and focused in a cryogenic freeze-out loop (2 mm ID × 100 mm length stainless steel tubing packed with 60/80 mesh glass beads). Finally, the cryotrap is rapidly heated to 150°C and the sample is transferred onto the column, which is held at –50° for 2 min after injection, then heated to 200°C at 4°C min^{-1}. In regard to the low VOC concentrations encountered in the experiment, the detector was operated in selective ion mode. Isoprene was quantified from m/z 67 and monoterpenes from m/z 93.

Response factors were determined by calibration against pressurized gas standards. Primary standard was a cylinder with 201 ppb 2,2-dimethylbutane from the National Institute of Standards and Technology (Boulder, CO), a cylinder with 10 ppb camphene and 11 ppb isoprene (custom made by E. Apel, NCAR, Boulder CO) was used as secondary standard. Runs with the secondary standard were performed daily, by collecting volumes of 500-1000 ml onto identical cartridges as used in the field experiment. Several halogenated hydrocarbons were introduced into each sample as internal standards, to allow for the estimation of any variations in mass spectrometer sensitivity: chloropropane, which eluted just after isoprene, and 3-fluorotoluuene and decahydro-naphthalene (decalin), which elute before and after monoterpenes, respectively. Considering these uncertainties and including errors during

sampling and storage as mentioned above, accuracy and precision are estimated to be approximately 20 ppt for isoprene at 50 ppt and for monoterpenes at 100 ppt.

2.3. Flux calculation methods

Concentration measurements of monoterpenes and isoprene at different heights within the boundary layer are used to derive corresponding surface fluxes. We applied two methods, a technique deducing surface fluxes of a scalar from its mixed layer gradient and a boundary layer budget approach.

2.3.1. Mixed layer gradient technique (MLG)

Gradient methods have widely been applied to determine fluxes from measurements within the surface layer. The flux is described in analogy to molecular diffusion by the product of a gradient and a diffusion coefficient, whereas it is a turbulent exchange coefficient rather than a diffusion coefficient in case of the surface layer gradient theory. In similar genre, Wyngaard and Brost (1984) proposed a flux gradient relationship for the mixed layer, whereas the mixed layer encompasses that part of the convective boundary layer (CBL) dominated by convective eddies whose scales are comparable to the depth of the entire CBL:

$$\frac{\partial C}{\partial z} = -g_b\left(\frac{z}{z_i}\right)\frac{\overline{wc_0}}{z_i w^*} - g_t\left(\frac{z}{z_i}\right)\frac{\overline{wc_{z_i}}}{z_i w^*}, \tag{1}$$

with w^* denoting the convective velocity scale within the CBL ($w^*=(g(\overline{w\theta_v})_0 z_i / \theta_{v0})^{1/3}$), $\overline{(w\theta_v)_0}$ is the surface virtual temperature flux, z_i the depth of the CBL, $\overline{wc_0}$ and $\overline{wc_{z_i}}$ are the turbulent scalar surface and entrainment fluxes, respectively, z is the altitude above ground, C is the mean scalar mixing ratio, and g_b and g_t are dimensionless bottom-up and top-down gradient functions of height within the CBL.

Moeng and Wyngaard (1984; 1989) determined the gradient functions from large eddy simulations of scalar transport within the CBL. From the results of these simulations, Davis (1992) derived following fits for the gradient functions:

$$g_b = 0.4\cdot\left(\frac{z}{z_i}\right)^{-3/2} \text{ and } g_t = 0.7\cdot\left(1-\frac{z}{z_i}\right)^{-2} \tag{2}$$

Given these gradient functions g_b and g_t, and measurements of CBL depth z_i and the convective velocity scale, two unknowns remain in equation (1), the surface and entrainment flux. Being interested in the surface flux, one can integrate and resolve the equation if the concentration gradients over two height intervals are known, or, alternatively if only one value for $\partial C/\partial z$ and the entrainment flux are known. The latter can be estimated by a simple jump model, describing the entrainment as the product of the concentration difference ('jump') across the boundary layer top and the entrainment rate:

$$\overline{wc_{z_i}} = -w_e\left(C_{ML} - C_F\right) \tag{3}$$

C_{ML} and C_F are the mean concentrations of the scalar in the upper mixed layer (ML) and the atmosphere above the ML, respectively. The entrainment velocity (w_e) is the rate at which air is drawn into the ML from above, and can be determined from observations of mixed layer depth growth.

The calculation of scalar surface fluxes by the MLG technique therefore requires the scalar concentrations at two or more heights within the CBL, information about the strength of

convective mixing (w^*), and the CBL depth. Measurements with the tethered balloon provide mixed layer concentrations and the height of the convective boundary layer. Values for w^* are calculated from measurements of potential temperature fluxes at the SMEAR II tower. Finally, surface fluxes for single VOC profiles collected at Hyytiälä are obtained by fitting the MLG equation to the measured concentrations with a least square method.

When applying the MLG technique for flux estimates, the validity of the MLG assumptions needs careful evaluation (Davis et al., 1994; Guenther et al., 1996; Helmig et al., 1998). In short, the critical requirements are 1) Sufficiently rapid convective mixing for maintaining a quasi-steady profile, i.e. convective turnover time (z_i/w^*) is smaller than variations in surface heat flux and convective layer growth. 2) Lifetime of species is large compared to the timescale of vertical mixing. 3) Sufficient integration time of concentration measurements in order to average over at least a few eddies. Finally, MLG theory assumes a horizontally homogenous system, implying spatial homogeneity in emissions and vertical mixing.

In typical midday conditions at Hyytiälä, convective turnover times were about 10-15 min (z_i = 1200-1600 m, w^*= 1.5-2 ms^{-1}). This turnover time is sufficiently short compared to the timescale of midday variations in mixed layer depth, as well as to the lifetime of most biogenic VOCs. During the increase of the CBL in the morning, however, the changes in surface heat flux may occur on a comparable time scale as z_i/w^* and profiles during these times may not be suitable for MLG calculations. The sampling time of 30 minutes in the profile measurements is long enough to represent a mean mixed layer gradient and should be sufficient to encompass the average over several eddies.

2.3.2. Mixed box technique (MB)

In this budget approach, the convective boundary layer is treated as a well-mixed box. A simplified conservation equation for the mean scalar in this box can be written as

$$\frac{\partial C}{\partial t} = -U\frac{\partial C}{\partial x} + \frac{\overline{wc_0} - \overline{wc_{z_i}}}{z_i} + S\,. \tag{4}$$

C is the mean scalar mixing ratio, U is the mean horizontal wind, $\partial C/\partial x$ is the local concentration gradient along the mean horizontal wind direction, $\overline{wc_0}$ and $\overline{wc_{z_i}}$ are the turbulent fluxes at the surface and at the top of the mixed layer (z_i), respectively. The term S denotes either a sink or source of the scalar in the mixed box. This representation neglects turbulent horizontal advection and mean vertical advection, and premises a linear vertical flux profile in the mixed layer. All these assumptions are commonly satisfied in the well-mixed convective boundary layer (Guenther et al., 1996). Resolving this equation for the surface flux yields

$$\overline{wc_0} = \overline{wc_{z_i}} + z_i\left(\frac{\partial C}{\partial t} + U\frac{\partial C}{\partial x} - S\right). \tag{5}$$

To calculate the surface flux of biogenic VOCs, we assume their concentration has reached a steady state ($\partial C/\partial t$ = 0), is homogenous in space ($\partial C/\partial x$ = 0), and that entrainment can be neglected. The surface flux is then given by the product of $z_i \cdot S$, whereas S is the total loss rate due to chemical reactions in this case.

We briefly address the relevance of these mixed box assumptions here, a more detailed discussion is provided by Guenther et al. (1996). Neglecting entrainment results in an underestimate of the actual surface flux, whereas the effect of omitting horizontal advection cannot be uniquely qualified. However, the magnitude of both terms can usually be estimated

from the balloon profiles. Entrainment fluxes can be assessed with help of the jump model (Equation 3), and the temporal variations in mean mixed layer concentrations throughout the day provide an estimate for the importance of horizontal advection.

The overall uncertainty of box model flux estimates is usually dominated by the uncertainty in quantifying the chemical sink term. For biogenic VOCs, the total loss rate during daytime can be approximated by the sum of their reactions with OH-, NO_3-radicals and ozone (O_3).

The final equation for calculating the flux of a particular VOC is then

$$\overline{wc_0} = z_i \cdot [\mathrm{VOC}] \cdot \left(k_{OH} \cdot [\mathrm{OH}] + k_{O_3} \cdot [\mathrm{O_3}] + k_{NO_3} \cdot [\mathrm{NO_3}]\right) \quad (6)$$

with k_{OH} , k_{O3} and k_{NO3} being the second order rate coefficients of the VOC with OH, O_3, and NO_3, respectively. The surface flux calculation by the MB method therefore requires measurements of the boundary layer depth and the mean concentration in the mixed layer, as well as estimates for the total chemical loss rates of VOCs.

2.4. Photochemical Model

Chemical VOC degradation within the mixed layer was quantified with a photochemical box model. The chemical mechanism of the model consists of about 3340 gas phase reactions among 1200 species, as described by Aumont et al. (1999) and Hauglustaine et al. (1999). Photolysis rates are calculated with the tropospheric ultraviolet-visible (TUV 4.1) model (Madronich and Flocke, 1999). An albedo of 10% was assumed for these calculations and total ozone columns (310-340 Dobson Units) were taken according to data of the NASA Earth Probe TOMS satellite.

As in previous applications of the model for planetary boundary layer (PBL) cases (Greenberg et al., 1999b; Karl et al., 2002), entrainment of air during the growth of the PBL was represented as a first-order source or sink for chemical species in the PBL, depending on the concentration difference between background and PBL

$$\left(\frac{dX_{PBL}}{dt}\right)_{entrainment} = -K_{entrainment}\left(X_{PBL} - X_{bg}\right) \quad (7)$$

X_{PBL} is the concentration of the species in the PBL, X_{bg} is the concentration above the PBL (background), first-order rate constants $K_{entrainment}$ (>0 during growth of the PBL and zero at all other times) were chosen specifically for each day, derived from maximum PBL heights and duration of PBL growth. Background concentrations X_{bg} were kept constant with time and set to zero for all VOCs with tropospheric lifetimes shorter than 5 hours (corresponding to simple dilution during PBL growth).

Measurements of O_3, NO_x, VOCs, and radiation are used to constrain the box model. For this purpose, biogenic VOC concentrations are taken from the balloon measurements, anthropogenic VOCs are set to mean concentrations as measured on the tower during the second week of the experiment or as reported in earlier campaigns at this site (Janson et al., 2001; Spanke et al., 2001); total non-methane VOC levels measured were below 5 ppb. Ozone and NO_x levels are constrained to the half hourly measurements at 67 m above ground on the SMEAR II mast. Finally, the clear sky photolysis rates calculated by the model were scaled with help of UVA-measurements taken above the forest canopy.

2.5. Footprint modelling

Deriving fluxes from boundary layer measurements has the advantage of delivering estimates representative for large areas. Each of the methods we apply has its own area of influence.

For concentration measurements, this area can be estimated from the footprint function. It can be understood as a probability function that describes how strongly an emission from a given elemental source downwind affects the measurement point (Figure 1). The footprint of the MLG technique corresponds to the actual footprint of the profile measurements. Under strongly convective conditions with mean wind speeds up to 5 ms^{-1}, it typically encompasses an upwind range of 0.2 to 10 km, yielding footprint areas in the order of tens of square km.

The fluxes derived by the MB technique are representative for even larger areas. For a given VOC, the upwind range of the footprint is approximately mean wind speed multiplied by the time until this compound has reached a steady state concentration. For terpenes with usual lifetimes between 2-3 hours, this results in a footprint in the order of hundreds of square kilometres.

Spatial variation in surface emissions violates the assumptions of horizontal homogeneity in the boundary layer flux calculation methods. For the Hyytiälä site this may be an issue as the balloon launch site was located close to a lake. We therefore model the footprints of our profile measurements, for the purpose of determining the impact of heterogeneous surface emissions on the results of our flux estimates. The footprint model is described in detail by Kljun et al. (2002) and is based on a three-dimensional Lagrangian stochastic particle dispersion model (De Haan and Rotach, 1998). The model has been shown to produce valid footprint predictions under a wide range of stratifications and for receptors at heights from the surface to the mixed layer (Kljun et al., 2003).

3. Results and Discussion

3.1. Balloon measurements

From August 2 till August 12, 2001, we collected a total of 80 VOC samples from tethered balloons. Weather conditions were variable during this period, August 3rd, 7th and 8th were mostly sunny, other days were often cloudy and rainy. Operation of the balloon had to be interrupted several times by rain and high wind speeds that resulted in unsafe tethered balloon operating conditions.

Temperature and humidity profiles obtained from flights with continuous sampling during ascent and descent were used to determine boundary layer depths. Part of the flights did not exceed the top of the boundary layer and their depths were estimated. In these cases, they were approximated with the flux-ratio method (Stull, 2000), based on continuous measurements of the surface heat flux on the tower and potential temperature differences across the boundary layer top as derived from balloon profiles early in the day.

Figure 2 gives an overview on the meteorological conditions and averaged VOC concentrations in the mixed layer. The integrative VOC measurement during the ascent and descent of the balloon is considered as a representative sample of the mean boundary layer concentration. From three-level-profiles, mean concentrations are derived by fitting the MLG profile to the three measurements and building the average over the whole profile. With our choice of heights for the three samplers, these mixed layer averages did not significantly differ from the arithmetic means of the measurements. Total monoterpene concentrations in the mixed layer during OSOA 2001 were of the order of 10-100 ppt, with α-pinene (38%), limonene (23%), Δ_3-carene (20%) and camphene (9%) as the major compounds. Isoprene was also found in all samples, although at lower concentrations than the sum of monoterpenes.

Highest concentrations of biogenic VOCs were recorded on days with reduced radiation, apparently as a consequence of reduced vertical mixing and shallower boundary layer heights. Note however, that a day-by-day comparison of these concentrations is problematic as data coverage on single days varied significantly due to weather conditions. Winds were from a sector between 120 and 300 degrees during the balloon flights, at speeds up to 7 ms^{-1} (wind measurements at 50.9 m height on the tower). Maximum mixed layer heights varied between 1 and 2.2 km and were in agreement with results from earlier studies at Hyytiälä (Nilsson et al., 2001).

The concentration dependence with height above ground showed the expected behaviour for gases with a source at the surface. In general, concentrations decrease with height (Figure 3). The maximum height of the uppermost samplers in our profile measurement was 600 – 750 m, wherefore sample collection above the mixed layer was limited to situations with a shallow mixed layer, usually early in the day. Comparing the concentrations within and above the mixed layer from these flights (total of 7 profiles), the ratio of concentrations within the mixed layer (ML) and above the mixed layer (AML) was greater than one in nearly all cases for terpenes (Table 1). For isoprene, this trend was still observed in average, however with several inverse cases. Myrcene, tricyclene and sabinene were also detected in several samples, with greater concentrations in the mixed layer than above. The comparison of absolute concentrations within and above the mixed layer is more ambiguous, apparently as a consequence of large variations between concentrations of individual profiles.

Earlier VOC studies in the area found α-pinene, Δ^3-carene and β-pinene as the dominating monoterpenes, limonene proportions were significantly lower than in our measurements. Based on leaf-level measurements of the dominating tree species in the area, Scots Pine and Norway Spruce (Komenda and Koppmann, 2002), limonene in such high proportions is surprising.

We considered the possibility of an analytical artefact in our VOC measurements. A general background problem is unlikely, as limonene concentrations correlated with those of the other terpenes. The use of KI traps for removal of ozone prior to sampling is known to produce artefacts (iodine-containing VOCs, though none shown to be derived from monoterpenes),, but they can easily be distinguished from terpenes based on the EI-mass spectrum (Helmig and Greenberg, 1995). Finally, two VOC samples taken in parallel to our measurements, using different adsorbent media were analysed at CNR laboratories in Rome, Italy. The limonene concentrations determined there are consistent with the results of our measurements (Ciccioli et al., 2002). Limonene has also been detected in earlier measurements at this and other Boreal forests sites in Finland (Hakola et al., 2000; Rinne et al., 2000). It has been shown that the composition of terpenes emitted by Scots Pine exhibits significant plant to plant variation and can also vary with season (Janson et al., 2001; Komenda and Koppmann, 2002). Results of a recent study (Hakola et al., 2003) on seasonal variations of monoterpene concentrations at Hyytiälä indicate that the proportions of limonene in emissions of Norway Spruce increase from early to late summer. Limonene has also been measured as a major compound emitted from soils (Hayward et al., 2001), and during decomposing of coniferous needles (Kainulainen and Holopainen, 2002). Finally, limonene concentrations are low enough to be caused by emissions from single plant species that may not be accounted for in the regional vegetation database. Given the lack of evidence for analytical artefacts and the above possibilities for the higher than expected limonene concentrations, we proceed with the measured concentrations in the following analyses.

3.2. Flux estimates from mixed layer gradients

As pointed out in section 2.3.1, several conditions need to be fulfilled in order to derive fluxes from a gradient within the mixed layer. For compliance with sufficiently strong convective conditions, morning profiles before 1100 local time were excluded. From the remaining data set we also removed profiles with measurements exclusively above heights of z/z_i=0.3. The MLG equation predicts only small concentration differences in dependence of the surface flux at these heights. As a consequence, concentration gradients above this height do not contain sufficient information about the surface flux. After this screening, 12 profiles comprised of 32 individual VOC samples remained for flux calculations with the mixed layer gradient method.

The MLG equation was then fitted to the measured profiles, both with and without assumptions for entrainment fluxes. In all cases, varying assumptions of entrainment fluxes did not result in significant differences of the surface fluxes (less than 10%). This is not surprising, as we chose the concentration measurements at heights where gradients are influenced by the surface flux rather than the entrainment flux. Furthermore, our data selection includes midday to afternoon profiles exclusively, without cases of strong mixed layer growth, and concentration jumps across the boundary layer height were too small to result in significant entrainment fluxes. For simplicity, only results with entrainment fluxes set to zero are presented.

Figure 4 shows the median fluxes of those VOC that were detected in every single measurement within the profiles. The median of the sum of monoterpene fluxes is 278 μg m^{-2} h^{-1}. If the median terpene flux is calculated from the gradients of total terpene concentrations of individual profiles, the resulting median flux of terpenes is 312 μg m^{-2} h^{-1}. The higher number in the latter case is attributed to the very low concentrations of terpenes that could often be detected at the lowest altitude only and consequently pronounced the gradients of total terpenes. For isoprene, the MLG method derives a median deposition flux for this selection of profiles, while the average shows a small emission of 15 μg m^{-2} h^{-1}.

As biogenic VOC emissions depend strongly on temperature, it is useful to normalize emission rates to a standard temperature. The temperature dependency of monoterpene emissions can be described by the equation

$$E = E_{30} \cdot \exp\left[\beta\left(T - 30°C\right)\right], \tag{8}$$

where E_{30} is the emission rate normalized to 30°C, β is an empirical coefficient (=0.09) and T is temperature in degrees Celsius (Guenther et al., 1993). Normalizing the monoterpene fluxes to 30°C according to this algorithm yields an emission potential of 832-927 μg m^{-2} h^{-1}.

As documented by the large interquartile ranges, the variation of fluxes between individual profiles is considerable in spite of the preceding data selection. The following section addresses uncertainties and the effects of potential violations of the MLG assumptions in our flux calculations.

3.2.1. Error and footprint discussion

MLG estimates heavily rely on accurate measurements of mixing ratio differences. With the small VOC levels encountered at Hyytiälä, the differences for single terpene concentrations were close to the detection limit. The uncertainty of terpene measurements at these levels is estimated to be ± 30 %, propagating into large uncertainties of the flux estimates.

Non-homogeneity in surface emissions is one of the most common violations of the MLG assumptions in practice. Our balloon launch site was located close to a lake (Figure 1) and often downwind of this lake during the measurement period. This severe inhomogeneity in surface emissions may influence our profiles. With the help of a footprint analysis, we evaluate how strongly the lake affects the flux estimates. The footprints of individual profile measurements are calculated with a footprint model (section 2.5). By combining them with detailed land use data of 20×20 km around the site, we assess differences in the source areas of individual profile measurements. The footprint model is run under the assumption of an infinite homogenous forest surface and a homogenous mean wind field. This implies that potential stratification effects due to the lake cannot be represented. In cases with the receptor downwind of the lake, the modelled footprint function may therefore overemphasize the surface elements close to the receptor, as stratification has the tendency to shift the footprint farther upwind. In our effort to assess the impact of the nearby lake as a non-emitting spot within the source area, the model result therefore will reflect an upper limit estimate of its influence.

As an example for the model results, Figure 1 illustrates the footprint of the measurement at 150 m on Aug 3 13:00 local time. Fetches for the profile measurements were calculated as the distance upwind where the crosswind-integrated footprint accumulates to 95%. Typical fetches in the afternoon were 7 to 12 km, yielding footprint areas in the order of 20 to 40 km^2. With increasing measurement altitude, the fetches get larger and the maximum of the crosswind-integrated footprint function shifts further upwind. For measurements at 150 m above ground, the function peaks between 0.4 and 0.8 km upwind, the corresponding maxima for receptor heights around 600 m are less pronounced and occur at about 5 km. As a consequence, the proportion of the nearby lake within the footprints is most pronounced for measurements at lower levels. Figure 5 is a box plot (medians, quartiles and extremes) showing the proportions of forested area within the footprints for the three sampling altitudes. The forest proportion is systematically smaller at the lowest measurement level. However, the variation of forest areas between different heights is within 15% of the average, a range considerably smaller than the error range due to the uncertainties in the concentration measurements.

A systematic error in the MLG calculations is introduced by neglecting chemical degradation. For very reactive VOCs like limonene and isoprene, chemical sinks are large enough to pronounce the vertical profile and the surface flux may be overestimated. In order to assess how strongly this accentuation of the gradient may influence the fluxes, we adjusted the profile concentrations to correct for chemical degradation. The concentration decrease at a certain height is approximated by the typical duration of vertical transport (w^* × height of measurement) times the total chemical loss rate of the VOC. The later was obtained from the photochemical model results (3.3). Flux estimates from such modified profiles resulted in 5-15% lower fluxes in the median. Effects were most pronounced for limonene and only minor for other terpenes. The uncertainty associated with neglecting chemical sinks is therefore well within the overall uncertainties. Furthermore, this overestimate due to neglecting chemistry approximately compensates for the potential underestimate due to the spatial inhomogeneities in emissions.

Some variability is introduced by calculating mean fluxes from individual profiles that were collected at differing temperatures and wind directions. Examining the rotation of selected footprints around the launch site, we conclude that the proportions of the forested surface do not vary by more than 15% for wind directions as observed during the campaign. Varying wind directions can therefore not explain the observed differences in fluxes. Surface temperatures during the selected profile measurements were also in a narrow range. With the

exception of two profiles at 14°C, surface temperatures were between 17.5 and 21.4° C. As there is no evident correlation between fluxes from single profiles and corresponding temperatures, we acknowledge that other influences must dominate the overall variation.

An important issue violating the MLG assumption of a horizontally homogenous boundary layer is partial cloud cover. Most of the days within the OSOA campaign exhibited partly cloudy weather. It is impossible to quantify the error associated to variability in cloudiness, but it can be qualified as non-systematic.

Summarising this analysis, we conclude that systematic errors like the uncertainties as a consequence of footprint anomalies within single profiles or due to negligence of chemical degradation are small compared to non-systematic errors. These are dominated by uncertainties in the concentration measurements and by violations of the assumption of a horizontally homogenous boundary layer. Given these errors are random in nature, the averaged terpene flux derived from the ensemble of profiles can be considered meaningful. On the other hand it is problematic to interpret fluxes from single profiles. The MLG method is not sensitive enough to determine the surface flux of isoprene or the emissions of single terpenes at this site, with the exception of that of α-pinene. A plot of the MLG concentration profile for α-pinene as predicted for the median flux from all individual profiles illustrates the large overall variation, but also the plausibility of the median flux as the fit lies within the observed concentrations of individual profiles (Figure 6).

3.3. Fluxes from mixed box calculations

While the MLG technique relies on theoretically firmer assumptions, flux estimates by the mass balance approach have the advantage of being based on the more robust measurement of mean mixed layer concentrations as compared to concentration differences from profile measurements. The balloon flights during OSOA delivered 40 mean mixed layer concentrations suitable for flux calculations with the mixed box technique. The median flux of total terpenes derived from these data is 100 and 186 $\mu g/m^2/h$ for all measurements and the selection of afternoon data, respectively (Figure 7). Normalized to 30°C (equation 8) the total monoterpene emissions are 575 $\mu g/m^2/h$.

We first evaluate the magnitude of errors due to neglecting entrainment and horizontal advection in the MB approach. Mixed layer growth rates during the day were up to 0.05 ms^{-1}, and the concentration difference of short-lived VOCs across the boundary layer top corresponds to the mean mixed layer concentrations, at most. This translates (Equation 3) into a maximum entrainment rate of 35 $\mu g/m^2/h$ for typical monoterpene concentrations (0.19 $\mu g/m^3$) at Hyytiälä. While this may be a substantial fraction of the calculated surface flux during mixed layer growth before noon, the afternoon flux calculations are only slightly affected. The underestimate of MB fluxes due to the neglect of entrainment is therefore 20 %, at most.

Typical changes of mean monoterpene concentrations with time were 0 ± 0.03 μg/h. The random nature of these changes indicates that advection is dominating, but also supports that neglecting advection in average is reasonable (Equation 4). From observed time changes of concentration and with typical mixed layer heights of 1500 m, the uncertainty in box model surface flux estimates due to negligence of advection becomes ± 30 $\mu g\ m^{-2}\ h^{-1}$.

The uncertainty in quantifying the chemical sink term in equation (6) usually dominates the overall uncertainty of box model flux estimates (Greenberg et al., 1999a). However, with the measurements of NO_x, O_3, VOCs and radiation available at Hyytiälä, it was possible to reasonably constrain the photochemical box model. The constraint of a box model

representing the mixed layer with O_3 and NO_x measurements taken at the surface may be problematic in areas with strong local emissions of NO_x (Spirig et al., 2002). At Hyytiälä however, there are no major NO_x emissions upwind within several turnover times of the mixed layer, measurements were taken at 67 m above ground, reducing any influence of near-surface gradients.

Among the input data used for the photochemical box model, we consider the concentrations of VOCs other than biogenic compounds as those with the highest uncertainty. The sensitivity of the radical levels on anthropogenic VOC concentrations was evaluated by running the model with double and half anthropogenic VOC levels. The resulting maximum changes in OH levels at daytime were – 18 % and + 13%, for doubled and half anthropogenic VOC concentrations, respectively. This limited sensitivity is a consequence of the severe constraints with measurements, but also of the general characteristics of this rural site, which was not affected by significant pollution events during our measurements. We estimate the overall uncertainty for the quantification of the chemical loss rate for terpenes as ± 30%. The determination of mixed layer heights from balloon profiles or estimates is associated with a 20% error. Assuming standard propagation of these errors in mixed layer depth and loss rate yields an uncertainty of ±36%.

Overall, the error range of the MB calculations is estimated to ±50 % for the averaged fluxes, and even higher for fluxes from single profiles, as a consequence of the influence of horizontal advection that accounts for an additional uncertainty of 20-30%.

3.4. Comparison of flux estimates

The surface flux derived by the mixed box (MB) technique is lower in average than that calculated by the mixed layer gradient (MLG) method, even when the selection of MB fluxes is reduced to an ensemble comparable to that of the MLG estimates (encompassing fluxes after 1100 local time, exclusively).

The two techniques yield flux estimates representative for different areas. As calculated with the footprint model, fetches for the profile measurements and the MLG method were 7 to 12 km, and footprints in the order of 30 to 50 km^2. For comparison, the fetch of the MB technique can be estimated from the mean wind speed in the PBL times the lifetime of the substances. MB fetches for monoterpenes were between 50 and 100 kilometres, resulting in footprint areas of 200 to 500 km^2 (assuming the same ratio of lateral and longitudinal dimension of the footprint as in the case of the modelled footprint functions). The different flux estimates from the two methods therefore indicate that monoterpene emissions close to the site are higher than the regional average.

Previous measurement efforts at Hyytiälä include the determination of fluxes with the surface layer gradient technique. Emissions derived from those measurements, representing the immediate surroundings of the SMEAR II tower, were between 200 and 450 $\mu g/m^2/h$ for comparable temperature conditions in August 1998 (Rinne et al., 2000; Spanke et al., 2001). The fluxes derived by the MLG technique are in the same range, whereas the MB method with its significantly larger footprint observes a lower emission, again supporting our conclusion of lower emissions on regional scale.

Such a trend should also be reflected in the landcover data, so it is useful to look at modelled biogenic emissions for the Hyytiälä site. Lindfors et al. (2000) calculated biogenic emissions for European Boreal forests based on land cover information from satellite data and meteorological observations. Using the same emission model, terpene and isoprene emission rates were calculated for the areas 1×1 km and 10×10 km around the SMEAR II site. Figure 8 shows model emissions and the flux estimates from our balloon measurements. The

selection of model data includes the emissions between 11 and 18 local time for Aug 2 – Aug 12. The larger of the model areas is comparable to the footprint size of the MLG technique, while the MB method estimates surface fluxes for even a larger area. On average, modelled and observationally derived emissions agree well. Furthermore, the trend of higher monoterpene emissions close to the site is also predicted in the emissions model. The trend of higher emissions near SMEAR II as compared to the regional average is therefore in agreement with the landuse data around Hyytiälä.

Model and observations also agree for emissions of isoprene. As noted earlier, the MLG method proved not sensitive enough for the relatively low fluxes of isoprene, possibly because of rather inhomogeneous distribution of isoprene emissions within the mostly coniferous forest. For the budget technique with its larger footprint, this effect would be of less importance. The isoprene fluxes from this method are similar to the model results.

3.5. Production of condensable vapours

The results of the photochemical modelling are also used to look at the monoterpene oxidation rates on different days. As terpene oxidation is considered as an important source of condensable vapours, this analysis attempts to look at the links between monoterpene emissions and particle formation. Figure 9 shows the oxidation rates representing mean mixed layer conditions from Aug 2 to Aug 12 for the days with VOC measurements from tethered balloons. Total oxidation rates (terpene + OH-, O_3-, and NO_3-reactions) were between 1-8·10^5 molecules cm^{-3} s^{-1}. The days with particle formation events (highlighted yellow in Figure 9) exhibit rates of 2·10^5 molecules $cm^{-3}s^{-1}$ or lower.

The oxidation products of monoterpene are expected to partition between the gas and aerosol phase according to gas/particle partitioning theory (Odum et al., 1996). For the conditions at Hyytiälä with rather low amounts of pre-existing organic aerosol mass, an upper aerosol yield from terpene oxidation of 5% can be assumed. Using this fraction as an estimate for the amount of condensable products formed upon oxidation, the degradation of monoterpenes produces condensable compounds at a rate of 1·10^4 molecules cm^{-3} s^{-1} or less on days when particle formations were observed. This rate is close to those derived in a similar way from VOC measurements in August 1998 on the tower, which were 1.2·10^4 molecules cm^{-3} s^{-1} in average (Spanke et al., 2001). This production of condensables is too low to explain the observed aerosol growth during those days. From aerosol size distribution measurements, the production of condensable vapours necessary to explain the observed growth of particles can be derived. For the period of interest here, these source rates were between 1 - 2.6·10^5 molecules cm^{-3} s^{-1} on days with particle formation (Boy et al., 2003). Comparing these results with our calculations, at most 10% of the condensable vapours necessary to account for the newly formed aerosol could be explained by oxidation of monoterpenes.

However, our oxidation rates are representative for conditions within the mixed layer, whereas the amounts of condensable vapours were calculated from aerosol measurements at two metres above ground. Monoterpene concentrations and oxidation rates close to the surface may be significantly higher than the average in the mixed layer. This was observed during a field campaign in 1998, where terpene oxidation rates derived from measurements at two metres height were found high enough to explain most of the observed aerosol growth (Janson et al., 2001). One might now speculate that particle production occurs mainly close to the surface. On the other hand, from all measurements carried out at Hyytiälä in 2001, including particle measurements throughout the mixed layer, there are no indications that particle formation would occur close to the surface exclusively. A definite answer can therefore not be given at this point, but these findings indicate that it would be valuable to have more vertically resolved measurements of particle distributions in future.

Another aspect of biogenic VOC and particle formation is the question, if monoterpene oxidation products play a role in the nucleation process. In this perspective, we looked at the different oxidation pathways. Hoffmann et al. (1997), and Jang and Kamens (1999) showed that oxidation by ozone yields higher amounts of low volatile products than the reaction with OH, and ozonolysis is considered as the only pathway to generate nucleating species from terpene oxidation under atmospheric conditions (Bonn and Moortgat, 2002). The upper panel in Figure 9 shows the relative contribution of the O_3-pathway to the total oxidation rate. Because OH sources are of photolytical origin mainly, the relative importance of O_3-oxidation exhibits a strong diurnal variation in opposite to radiation. For the purpose of the day-to-day comparison in Figure 9, data points prior to 11 and later than 17h local time were therefore excluded. It can be seen that the relative importance of the O_3 channel tends to be higher on the days when new particle formations were observed. The same trend cannot be seen in the absolute amount of monoterpenes oxidized by O_3, though, as a consequence of the lower concentrations of terpenes on event days. The trend of pronounced O_3 oxidation on event days in a relative but not in an absolute way may be an indication that ozone-oxidation of VOCs not considered here could play an important role. Possible compounds could be sesquiterpenes, biogenically emitted VOCs that are especially reactive with ozone and have very high yields of condensable vapours.

4. Conclusions

Observations from tethered balloon platforms were used to derive monoterpene and isoprene fluxes on landscape scales around Hyytiälä for the period of Aug 2 to Aug 12, 2001. The analysis of error sources in both methods revealed that the averaged surface fluxes derived from a number of profiles represent a robust order of magnitude estimate for regional emissions. On the other hand, flux estimates from single profiles are heavily influenced by non-systematic errors, especially for the low to moderate emission levels of single compounds encountered at Hyytiälä. For these conditions, the methods are not useful for providing temporal resolution, but can characterize regionally averaged emissions.

Total monoterpene fluxes representative for areas of tens and hundreds square kilometres around Hyytiälä were 278 and 186 $\mu g\ m^{-2}\ h^{-1}$, respectively, at a mean surface temperature of 17.5°C. The mean level of biogenic VOC fluxes and the tendency of higher emissions close to the site are in agreement with the results of a biogenic VOC emission model. It gives confidence in the approaches of biogenic emission models combining experimental information about single plants emissions and landuse data to derive surface fluxes of larger areas.

The links between biogenic VOC emissions and particle formation events remain ambiguous. Chemical analyses of aerosols clearly show a contribution of monoterpene oxidation products (Boy et al., 2003). On the other hand, our modelled oxidation rates of monoterpenes in the mixed layer are too low to account for the observed aerosol growth during the nucleation days alone, a significant fraction of condensing vapours needs to arise from a different source. One possibility could be components directly emitted from conifer leaf epicuticular wax, as recent analyses of organic aerosol matter in forested areas have shown significant contributions of such primary compounds (Kavouras and Stephanou, 2002).

Insufficient information about the vertical distribution of aerosols made it difficult to relate VOC measurements within the boundary layer to aerosol observations close to the surface. It would therefore be interesting to collect more information about the temporal evolution and the differences in aerosol and gas concentrations within the forest canopy and the layers above.

Future work on biogenic VOCs and aerosols should also include measurements of sesquiterpenes and oxygenated VOCs. However, the methods applied in this work cannot be used to estimate sesquiterpene fluxes from boundary layer measurements because of their short atmospheric lifetimes in the range of a few minutes.

Acknowledgements

The authors thank Toivo Pohja for his technical and logistic assistance at the Hyytiälä site. We are grateful to Paasi Aalto, Michael Boy and Petri Keronen of University of Helsinki for their support on the site and for providing us with landcover and measurement data of the SMEAR II site. Brian Lamb of Washington State University and Air Research Inc., Boulder CO (now Vaisala) kindly lent us two electric winches. Christoph Spirig acknowledges funding through the Swiss National Science Foundation (Grant No. 21-61573.00). NCAR is sponsored by the National Science Foundation.

References

Aumont, B., Madronich, S., Ammann, M., Baltensperger, U., Hauglustaine, D., and Brocheton, F.: On the NO_2 + soot reaction in the atmosphere, J. Geophys. Res., 104, 1729-1736, 1999.

Bonn, B., and Moortgat, G. K.: New particle formation during α- and β-pinene oxidation by O3, OH and NO3, and the influence of water vapour: particle size distribution studies, Atmos. Chem. Phys. Discuss., 2, 469-506, 2002.

Boy, M., Petäjä, T., Dal Maso, M., Rannik, Ü., Rinne, J., Aalto, P., Kulmala, M., Laaksonen, A., Joutsenaari, J., Hoffmann, T., Warnke, J., Apostolaki, M., Stephanou, E. G., Tsapakis, M., Kouvarakis, A., Pio, C., Carvalho, A., Römpp, A., Moortgat, G. K., Spirig, C., Guenther, A., Greenberg, J., and Ciccioli, P.: Overview of the field measurement campaign at Hyytiälä, August 2001 in the frame of the EU project OSOA, Atmos. Chem. Phys. Discuss., 3, 3769-3831, 2003.

Ciccioli, P., Possanzini, M., Brancaleoni, E., Frattoni, M., Di Palo, V., and Brachetti, A.: OSOA-Scientific Report of the second year, C.N.R., Roma, Italy, 2002.

Davis, K. J.: Surface fluxes of trace gases derived from convective-layer profiles, Ph.D. thesis, University of Colorado, available as NCAR/CT-139 from NCAR, Boulder, CO, 1992.

Davis, K. J., Lenschow, D. H., and Zimmerman, P. R.: Biogenic Nonmethane Hydrocarbon Emissions Estimated from Tethered Balloon Observations, J. Geophys. Res., 99, 25587-25598, 1994.

De Haan, P., and Rotach, M. W.: A novel approach to atmospheric dispersion modelling: The Puff- Particle Model, Q. J. R. Meteorol. Soc., 124, 2771-2792, 1998.

Greenberg, J., Guenther, A., Zimmerman, P., Baugh, W., Geron, C., Davis, K., Helmig, D., and Klinger, L.: Tethered balloon measurements of biogenic VOCs in the atmospheric boundary layer, Atmos. Environ., 33, 855-867, 1999a.

Greenberg, J. P., Guenther, A. B., Madronich, S., Baugh, W., Ginoux, P., Druilhet, A., Delmas, R., and Delon, C.: Biogenic volatile organic compound emissions in central Africa during the Experiment for the Regional Sources and Sinks of Oxidants (EXPRESSO) biomass burning season, J. Geophys. Res., 104, 30659-30671, 1999b.

Greenberg, J. P., Helmig, D., and Zimmerman, P. R.: Seasonal measurements of non-methane hydrocarbons and carbon monoxide at the Mauna Loa Observatory during the Mauna Loa Photochemistry Experiment2, J. Geophys. Res., 101, 14581-14598, 1996.

Griffin, R., Cocker, D., Seinfeld, J., and Dabdub, D.: Estimate of global atmospheric organic aerosol from oxidation of biogenic hydrocarbons, Geophys. Res. Letters, 26, 2721-2724, 1999.

Guenther, A., Zimmerman, P., Harley, P., Monson, R., and Fall, R.: Isoprene and monoterpene emission rate variability: Model evaluation and sensitivity analysis, J. Geophys. Res., 98, 12609-12617, 1993.

Guenther, A., Zimmerman, P., Klinger, L., Greenberg, J., Ennis, C., Davis, K., Pollock, W., Westberg, H., Allwine, E., and Geron, C.: Estimates of regional natural volatile organic compound fluxes from enclosure and ambient measurements, J. Geophys. Res., 101, 1345-1359, 1996.

Hakola, H., Laurila, T., Rinne, J., and Puhto, K.: The ambient concentrations of biogenic hydrocarbons at a northern European, boreal site, Atmos. Environ., 34, 4971-4982, 2000.

Hauglustaine, D. A., Madronich, S., Ridley, B. A., Flocke, S. J., Cantrell, C. A., Eisele, F. L., Shetter, R. E., Tanner, D. J., and Ginoux, P.: Photochemistry and budget of ozone during the Mauna Loa Observatory Photochemistry Experiment (MLOPEX 2), J. Geophys. Res., 104, 30275-30307, 1999.

Hayward, S., Muncey, R. J., James, A. E., Halsall, C. J., and Hewitt, C. N.: Monoterpene emissions from soil in a Sitka spruce forest, Atmos. Environ., 35, 4081-4087, 2001.

Helmig, D.: Ozone removal techniques in the sampling of atmospheric volatile organic trace gases, Atmos. Environ., 31, 3635-3651, 1997.

Helmig, D., Balsley, B., Davis, K., Kuck, L. R., Jensen, M., Bognar, J., Smith, T., Arrieta, R. V., Rodriguez, R., and Birks, J. W.: Vertical profiling and determination of landscape fluxes of biogenic nonmethane hydrocarbons within the planetary boundary layer in the Peruvian Amazon, J. Geophys. Res., 103, 25519-25532, 1998.

Helmig, D., and Greenberg, J.: Artifact Formation from the Use of Potassium-Iodide-Based Ozone Traps During Atmospheric Sampling of Trace Organic Gases, J. High Res. Chromatogr., 18, 15-18, 1995.

Hoffmann, T., Odum, J. R., Bowman, F., Collins, D., Klockow, D., Flagan, R. C., and Seinfeld, J. H.: Formation of organic aerosols from the oxidation of biogenic hydrocarbons, J. Atmos. Chem., 26, 189-222, 1997.

Jang, M., and Kamens, R. M.: Newly characterized products and composition of secondary aerosols from the reaction of □-pinene with ozone, Atmos. Environ., 33, 459 - 474, 1999.

Janson, R., Rosman, K., Karlsson, A., and Hansson, H. C.: Biogenic emissions and gaseous precursors to forest aerosols, Tellus B, 53, 423-440, 2001.

Kainulainen, P., and Holopainen, J. K.: Concentrations of secondary compounds in Scots pine needles at different stages of decomposition, Soil Biol. Biochem., 34, 37-42, 2002.

Kamens, R., Jang, M., Chien, C.-J., and Leach, K.: Aerosol formation from the reaction of a-pinene and ozone using a gas-phase kinetics-aerosol partitioning model, Environ. Sci. Tech., 33, 1430-1438, 1999.

Karl, T. G., Spirig, C., Prévost, P., Stroud, C., Rinne, J., Greenberg, J. P., Fall, R., and Guenther, A. B.: Virtual disjuct eddy covariance measurements of organic compound fluxes from a subalpine forest using proton transfer reaction mass spectrometry, Atmos. Chem. Phys. Discuss.s, 2, 999-1003, 2002.

Kavouras, I., Mihalopoulos, N., and Stephanou, E.: Formation of atmospheric particles from organic acids produced by forests, Nature, 395, 683-686, 1998.

Kavouras, I., Mihalopoulos, N., and Stephanou, E.: Secondary organic aerosol formation vs primary organic aerosol emission: In situ evidence for the chemical coupling between monoterpene acidic photooxidation products and new particle formation over forests, Environ. Sci. Tech., 33, 1028-1037, 1999.

Kavouras, I. G., and Stephanou, E. G.: Direct Evidence of Atmospheric Secondary Organic Aerosol Formation in Forest Atmosphere through Hetermomolecular Nucleation, Environ. Sci. Technol., 36, 5083-5091, 2002.

Kljun, N., Kormann, R., Rotach, M. W., and Meixer, F. X.: Comparison of the Langrangian footprint model LPDM-B with an analytical footprint model, Bound.-Layer Meteor., 106, 349-355, 2003.

Kljun, N., Rotach, M. W., and Schmid, H. P.: A three-dimensional backward lagrangian footprint model for a wide range of boundary-layer stratifications, Bound.-Layer Meteor., 103, 205-226, 2002.

Komenda, M., and Koppmann, R.: Monoterpene emissions from Scots pine (Pinus sylvestris): Field studies of emission rate variabilities, J. Geophys. Res., 107, 10.1029/2001JD000691, 2001.

Kulmala, M., Hameri, K., Aalto, P. P., Makela, J. M., Pirjola, L., Nilsson, E. D., Buzorius, G., Rannik, U., Dal Maso, M., Seidl, W., Hoffman, T., Janson, R., Hansson, H. C., Viisanen, Y., Laaksonen, A., and O'Dowd, C. D.: Overview of the international project on biogenic aerosol formation in the boreal forest (BIOFOR), Tellus B, 53, 324-343, 2001.

Leaitch, W. R., Bottenheim, J. W., Biesenthal, T. A., Li, S. M., Liu, P. S. K., Asalian, K., Dryfhout-Clark, H., Hopper, F., and Brechtel, F.: A case study of gas-to-particle conversion in an eastern Canadian forest, J. Geophys. Res., 104, 8095-8111, 1999.

Lindfors, V., Laurila, T., Hakola, H., Steinbrecher, R., and Rinne, J.: Modeling speciated terpenoid emissions from the European boreal forest, Atmos. Environ., 34, 4983-4996, 2000.

Madronich, S., and Flocke, S.: The role of solar radiation in atmospheric chemistry, in The Handbook of Environmental Chemistry, edited by P. Boule, pp. 1-26, Springer-Verlag Berlin Heidelberg New York, Berlin, 1999.

Mäkelä, J. M., Aalto, P., Jokinen, V., Pohja, T., Nissinen, A., Palmroth, S., Markkanen, T., Seitsonen, K., Lihavainen, H., and Kulmala, M.: Observations of ultrafine aerosol particle formation and growth in boreal forest, Geophys. Res. Letters, 24, 1219-1222, 1997.

Moeng, C. H., and Wyngaard, J. C.: Statistics of Conservative Scalars in the Convective Boundary- Layer, J. Atmos. Sci., 41, 3161-3169, 1984.

Moeng, C. H., and Wyngaard, J. C.: Evaluation of Turbulent Transport and Dissipation Closures in 2nd-Order Modeling, J. Atmos. Sci., 46, 2311-2330, 1989.

Nilsson, E. D., Paatero, J., and Boy, M.: Effects of air masses and synoptic weather on aerosol formation in the continental boundary layer, Tellus B, 53, 462-478, 2001.

Odum, J. R., Hoffmann, T., Bowman, F., Collins, D., Flagan, R. C., and Seinfeld, J. H.: Gas/particle partitioning and secondary organic aerosol yields, Environ. Sci. Technol., 30, 2580-2585, 1996.

Rinne, J., Hakola, H., Laurila, T., and Rannik, Ü. Canopy scale monoterpene emissions of Pinus sylvestris dominated forests, Atmos. Environ., 34, 1099 - 1107, 2000.

Spanke, J., Rannik, Ü., Forkel, R., Nigge, W., and Hoffmann, T.: Emission fluxes and atmospheric degradation of monoterpenes above a boreal forest: field measurements and modelling, Tellus, 53B, 406-422, 2001.

Spirig, C., Neftel, A., Kleinman, L. I., and Hjorth, J.: NOx versus VOC limitation of O-3 production in the Po valley: Local and integrated view based on observations, J. Geophys. Res., 107, art. no.-8191, 2002.

Stull, R. B.: Meteorology for scientists and engineers, 502 pp., Brooks/Cole, Pacific Grove CA, 2000.

Wyngaard, J. C., and Brost, R. A.: Top-Down and Bottom-up Diffusion of a Scalar in the Convective Boundary-Layer, J. Atmos. Sci., 41, 102-112, 1984.

Tables

Table 1: Average concentrations of biogenic VOCs at Hyytiälä and the ratios of their concentrations within (ML) and above the mixed layer (AML).

	isoprene	*α-pinene*	*limonene*	*Δ^3-carene*	*camphene*	*β-pinene*	*Σ terp.*
Average concentrations in mixed layer, μgm^{-3} (40 flights)							
Average	0.041	0.079	0.049	0.041	0.02	0.015	0.26
proportion of total terpenes		38 %	23 %	20 %	9 %	7 %	
Concentration ratios within and above the mixed layer (ML/AML) (7 flights)							
mean	1.75	2.30	2.30	2.10	1.47	3.28	2.01
median	0.93	1.57	1.87	1.98	1.29	1.45	1.77
interquartile range	0.73 - 1.8	1.39 - 2.97	1.67 - 2.25	1.69 - 2.52	0.90 - 1.65	0.93 - 2.67	1.55 - 2.11

Figures

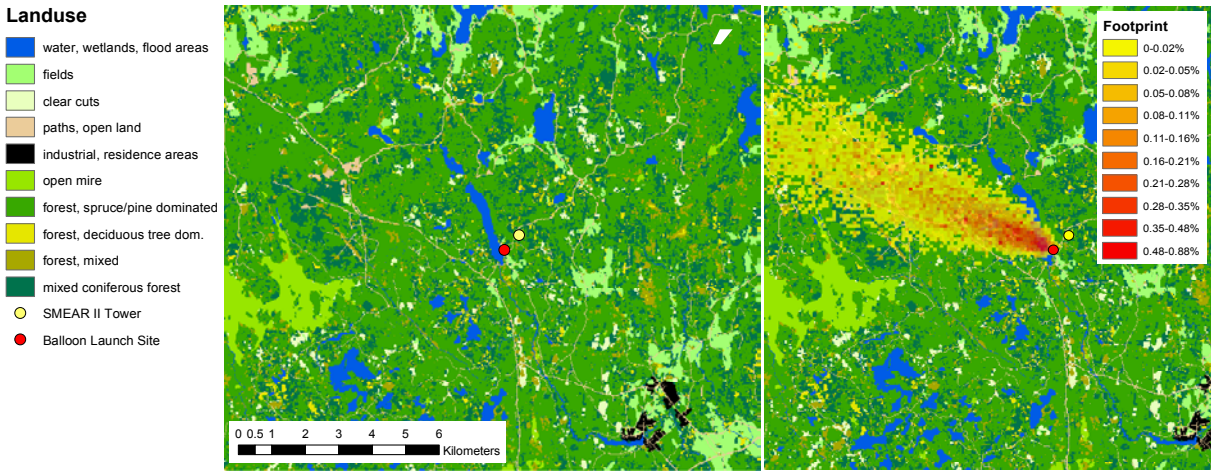

Figure 1: Land cover around the SMEAR II site at Hyytiälä and visualization of a typical footprint for a 30 minute measurement on the tethered balloon (3.8.2001, 13:00, at 150 m above ground level).

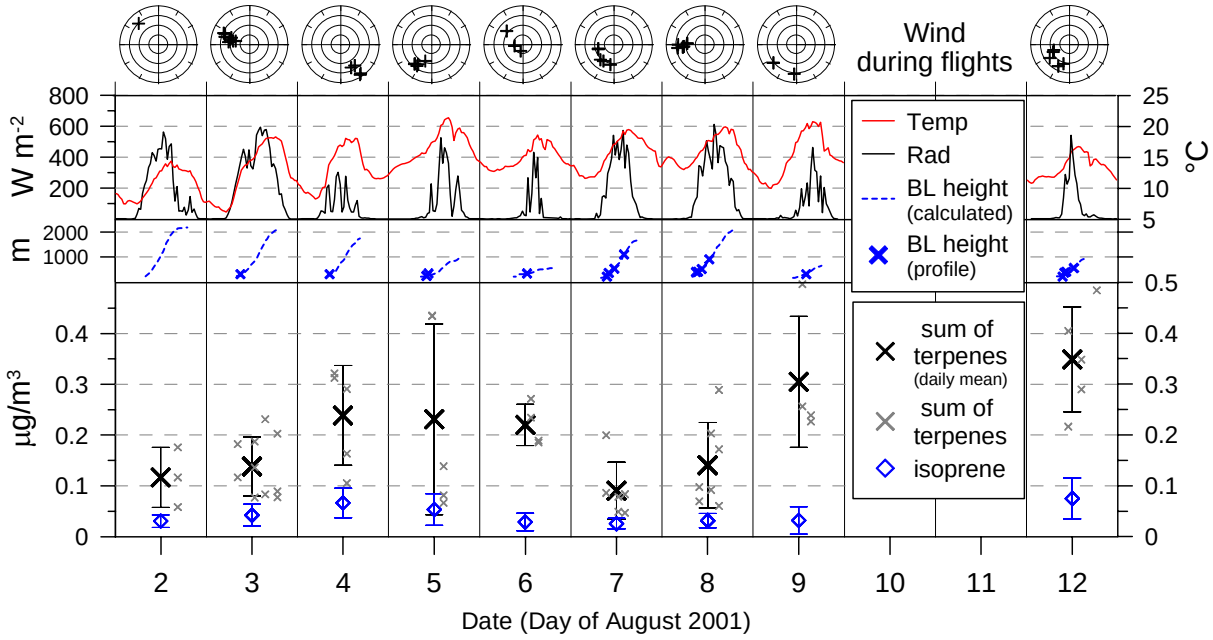

Figure 2: Overview of mean mixed layer concentrations of biogenic VOCs and meteorological conditions during the OSOA campaign at Hyytiälä. The angles of the polar plots correspond to wind directions, the radii to speeds (scale from 0 to 8 ms^{-1}, spacing of concentric circles is 2 ms^{-1}).

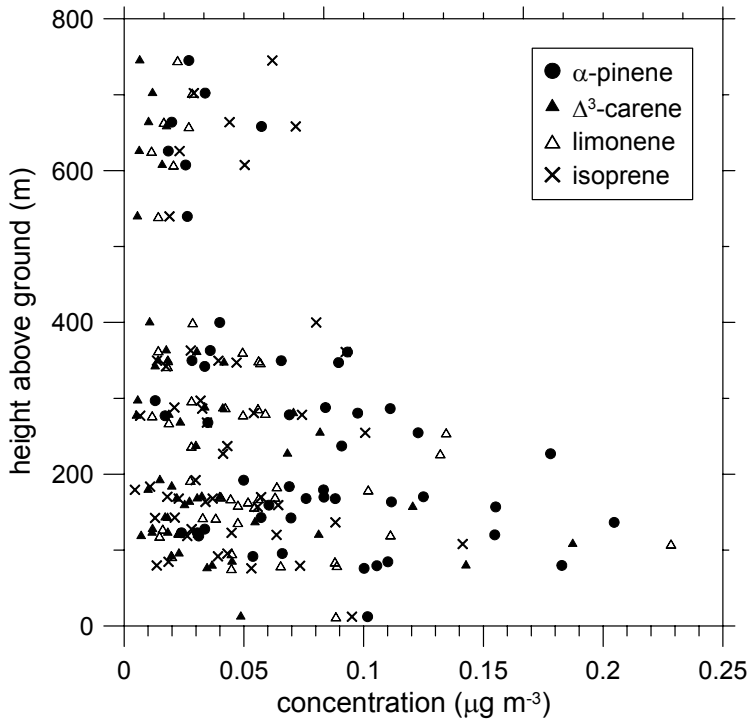

Figure 3: Concentrations of major biogenic VOCs from 20 balloon profile measurements.

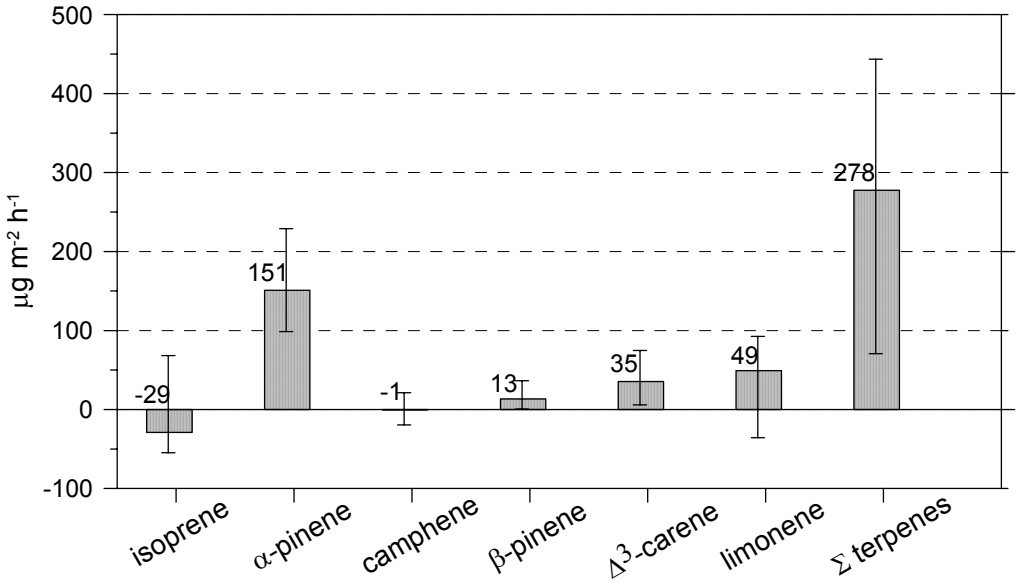

Figure 4: Flux estimates from balloon profiles by the mixed layer gradient technique (medians, error bars are interquartile ranges).

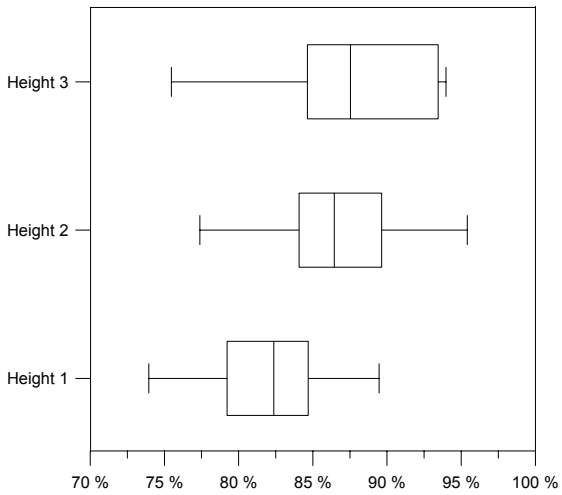

Figure 5: Forest proportions in footprints of the balloon profiles, categorized by sampling levels (Height 1 =100-150 m above ground, Height 2 = 250- 350 m, Height 3 = 450-750 m).

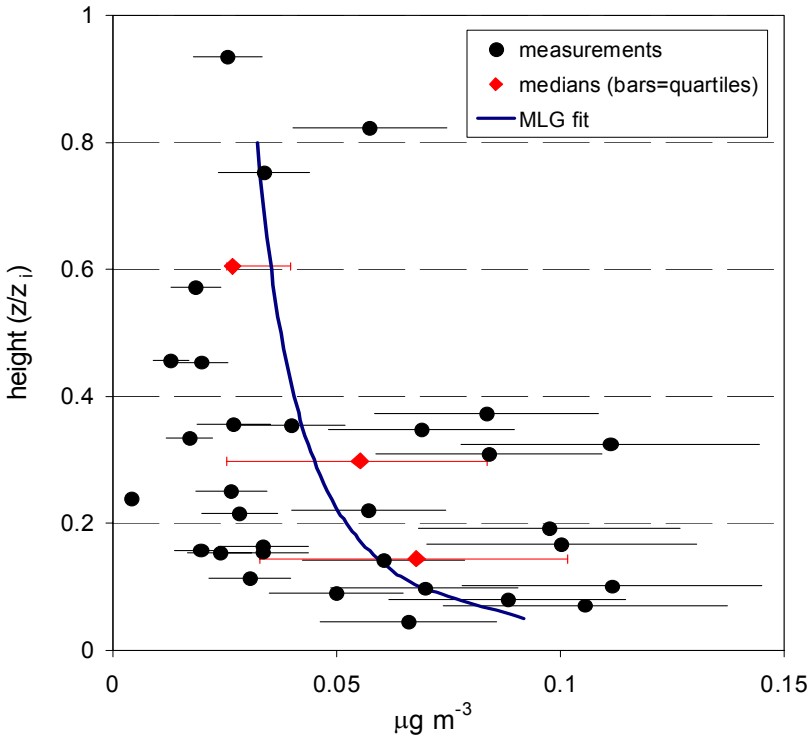

Figure 6: Measurements of α-pinene mixing ratios and predicted profile by the MLG equation for an α-pinene surface emission of 130 µg m^{-2} h^{-1} and the median vertical mixing velocity (1.7 ms^{-1}) of all profiles.

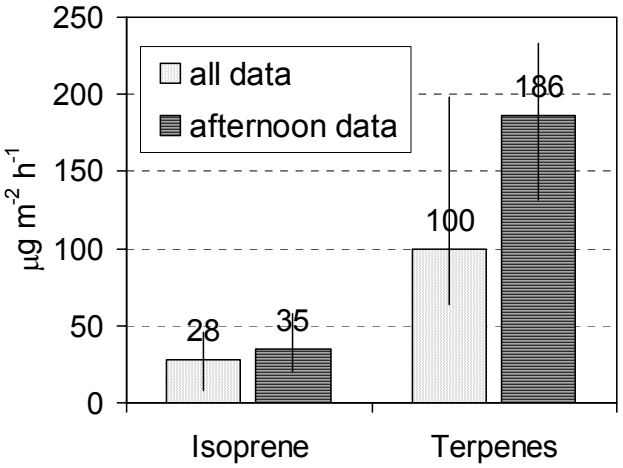

Figure 7: Medians of surface fluxes as calculated by the MB technique during Aug 2- Aug12, 2001, representing 40 individual data points. Error bars denote interquartile ranges.

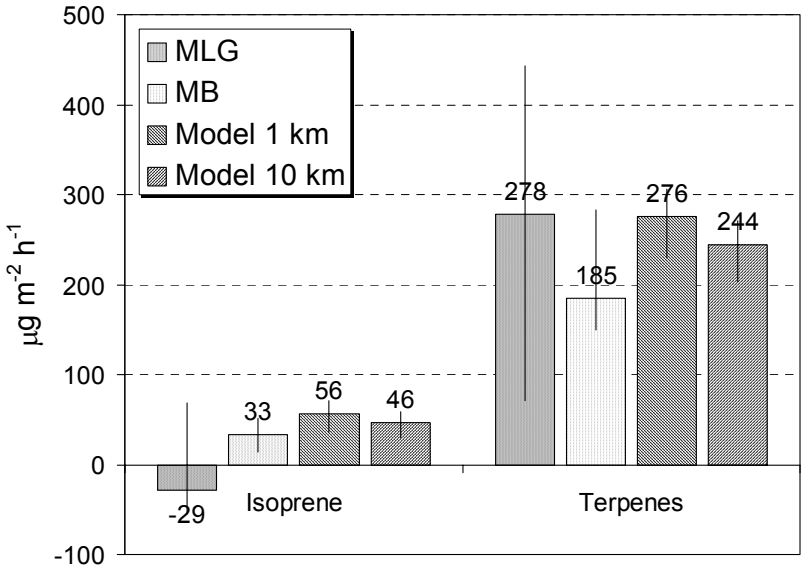

Figure 8: Afternoon surface fluxes (medians) at Hyytiälä as derived from balloon profiles (MLG- and MB-technique) for August 2-12, 2001 and modelled biogenic VOC emissions (Lindfors et al., 2000) for areas of 1×1 km and 10×10 km around the site during the same period. Error bars are interquartile ranges.

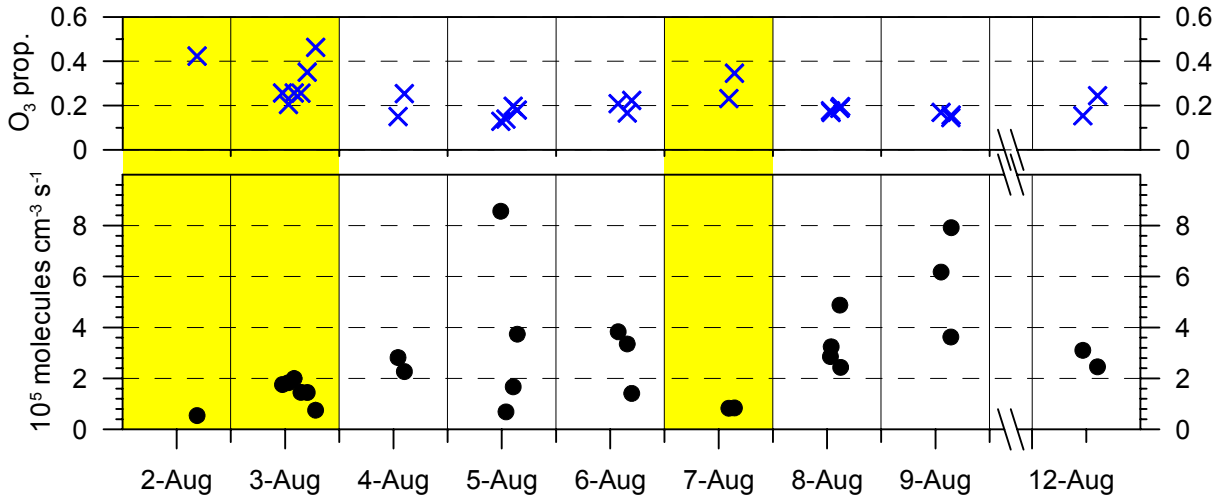

Figure 9: Terpene oxidation rates, total oxidation rate (lower panel) and fraction of O_3-pathway (upper panel) relative to the total rate. Days with observations of new particle formation are highlighted in yellow.

7 Conclusions and outlook

The role of volatile organic compounds (VOCs) in the formation of ozone and secondary organic aerosol was studied within two large field experiments. The PIPAPO campaign investigated the limitation of ozone production in the Po valley (Italy), the OSOA experiment at Hyytiälä (Finland) aimed to improve the understanding of secondary organic aerosol formation.

Within PIPAPO, local ozone productions at two surface stations 5 and 35 km downwind of Milan were characterized based on measurements of various photo-oxidants and their precursors. The analyses with a one-dimensional model revealed the difficulties in relating local ozone productions to the integrated perspective, the sensitivity of ozone concentration. Local ozone productions at the surface tend to be more VOC sensitive than in the mid-boundary layer. Since ozone production at the surface accounts only for a fraction of the ozone concentration, local analyses based on surface observations need careful interpretation. Whether these productions are representative for the conditions throughout the mixed layer, strongly depends on the characteristics of the surface site. If a representative surface site is available, or better, if local analyses can be made based on measurements in mid of the mixed layer, e.g. from aircrafts, useful qualitative information on ozone concentration sensitivity can be derived. However, a quantitative derivation of ozone concentration sensitivity from local sensitivities can not be derived because of the nonlinear relationships between emissions and concentrations of precursors. The qualitative result for the case of the Milan plume is that VOC controls are more effective for reducing ozone during the first 4-5 hours downwind, and NO_x controls are more effective afterwards. The model analysis also revealed that the representation of vertical mixing in the model significantly influences the models' answer on the sensitivity of ozone concentration. Insufficient vertical resolution in the model and too strong vertical mixing pronounce NO_x sensitivity.

A definitive conclusion on the impact of biogenic VOCs on the ozone production in the Po Valley is not possible from the data gathered during PIPAPO, although strong evidence for their significance was found. Total VOC-reactivity at Verzago was dominated by biogenic isoprene (Grüebler, 1999). Isoprene concentrations increased significantly right after the IOPs, indicating that seasonal variations lead to an even stronger influence of biogenic emissions later in the summer. Isoprene emissions around the Verzago site were not homogenously distributed. In such a situation, measurements of concentrations at surface sites allow only limited conclusions on the influence of these compounds on regional chemistry. Flux measurements would be required to assess their impact. Ideally, methods for the determination of emissions over a large area should be applied.

The results of the second field experiment demonstrated that surface fluxes on large spatial scales can be determined from concentration measurements throughout the mixed layer. A gradient technique and a mixed layer budget approach were used to estimate surface fluxes from measurements of biogenic VOCs on tethered balloons. Both techniques proved to be suitable methods for estimating the average fluxes, but were not sensitive enough to also gain a temporal resolution of the low to moderate biogenic emissions at Hyytiälä (FIN). We found a trend of lower emissions close to the Hyytiälä site in comparison to the regional average. These findings agree with the results of an emission model, which calculates biogenic VOC fluxes from landcover information and meteorological observations. The agreement corroborates the approaches used in biogenic emission models, which basically extrapolate experimentally determined emissions of single plant species to landscape emissions based on the composition of vegetation.

The amount of condensable vapours produced by the oxidation of monoterpenes throughout the mixed layer is not sufficient to account for the observed increases in aerosol mass at the surface. On the other hand, chemical analyses of aerosols confirmed that a significant fraction of organic matter arises from secondary organic aerosol formation of locally emitted biogenic VOCs. This might be an indication that aerosol formation primarily occurs close to the surface or within the canopy and does not take place throughout the mixed layer. Therefore, size-resolved particle measurements throughout the mixed layer would be helpful. Our experiment with particle counters on the tethered balloon deomonstrated the possibility of such measurements and induced plans for similar efforts at this site in the future.

The PIPAPO and OSOA experiment revealed the importance of vertically resolved information for the investigation of ozone and aerosol formation. Tethered balloons proved to be a suitable and cost-effective platform for acquiring such type of data. The study in Finland showed that investigations throughout the mixed layer should ideally be combined with detailed vertically resolved measurements within the canopy.

Considering the significance of biogenic VOC in ozone and aerosol formation, research in this field is granted to continue. The role of biogenic VOC in aerosol formation is recognized as important, although their involvement in the nucleation process is still uncertain. Future efforst in this field should also investigate the influence of biogenic VOC that are less abundant, or have not been measured yet because of instrumental limitations. Sesquiterpenes, for example, have certainly the potential to yield low volatile products upon oxidation. There are also indications that a combination of primary and secondary low volatile products from vegetation is responsible for nucleation. Measurements about the chemical composition of freshly nucleated particles would be of particular value for finding a definite answer.

Even in the context of the comparably well understood process of ozone production, more investigations on biogenic VOC emissions are necessary. As the results of PIPAPO demonstrated, policy-relevant decisions heavily rely on analyses with chemical transport models and therefore ultimately depend on accurate emission inventories. The estimates of biogenic VOC emissions are still associated with high uncertainties, especially for compounds other than isoprene or monoterpenes. Longer-term studies on the fluxes of these compounds would be helpful to improve biogenic emission inventories.

The total VOC emissions from vegetation can reach significant fractions of net ecosystem production. Even of more significance than the actual amount of these fluxes is maybe their sensitivity to future changes in climate. In this context, measurements of VOC fluxes relative to CO_2 would be helpful. The actual carbon flux through VOCs depends on the fraction of VOCs that is ultimately oxidized to CO_2. Therefore, an improved knowledge about oxidation pathways will also benefit studies about carbon balance and climate change.

References

Andersson-Sköld, Y., and Simpson, D.: Secondary organic aerosol formation in Northern Europe: a model study, J. Geophys. Res., 106, 7357-7374, 2001.

Andrews, T.: Address on ozone, J. Scott. Meteor. Soc., 4, 122-134, 1874.

Atkinson, R.: Atmospheric chemistry of VOCs and NOx, Atmos. Environ., 34, 2063-2101, 2000.

Baker, B., Guenther, A., Greenberg, J., Goldstein, A., and Fall, R.: Canopy level fluxes of measurements of 2-methyl-3-buten-2-ol by Relaxed eddy accumulation: field data and model comparison, J. Geophys. Res., 104, 26104-26114, 1999.

Bertin, N., Staudt, M., Hansen, U., Seufert, G., Ciccioli, P., Foster, P., Fugit, J.-L., and Torres, L.: Diurnal and seasonal course of monoterpene emissions from Quercus ilex (L.) under natural conditions - Application of light and temperature algorithms, Atmos. Environ., 31, 135-144, 1997.

Bonn, B., and Moortgat, G. K.: New particle formation during α- and β-pinene oxidation by O_3, OH and NO_3, and the influence of water vapour: particle size distribution studies, Atmos. Chem. Phys. Discuss., 2, 469-506, 2002.

Bonn, B., and G.K. Moortgat, Sesquiterpene ozonolysis: Origin of atmospheric new particle formation from biogenic hydrocarbons, Geophys. Res. Letters, 30 (11), art. no.-1585, 2003.

Bowman, F. M., Odum, J. R., Seinfeld, J. H., and Pandis, S. N.: Mathematical model for gas-particle partitioning of secondary organic aerosols, Atmos. Environ., 31, 3921-3931, 1997.

Carter, W. P. L.: Computer Modeling of Environmental Chamber Measurements of Maximum Incremental Reactivities of Volatile Organic-Compounds, Atmos. Environ., 29, 2513-2527, 1995.

Carter, W. P. L.: Documentation of the SAPRC-99 chemical mechanism for VOC reactivity assessment, Report to California Air Resources Board, 2000.

Carter, W. P. L., Pierce, J. A., Luo, D. M., and Malkina, I. L.: Environmental Chamber Study of Maximum Incremental Reactivities of Volatile Organic-Compounds, Atmos. Environ., 29, 2499-2511, 1995.

Chameides, W. L., Lindsay, R. W., Richardson, J., and Kiang, C. S.: The role of biogenic hydrocarbons in urban photochemical smog: Atlanta as a case study, Science, 241, 1-10, 1988.

Ciccioli, P., Fabozzi, C., Brancaleoni, E., Cecinato, A., Frattoni, M., Loreto, F., Kesselmeier, J., Schafer, L., Bode, K., Torres, l., and Fugit, J.: Use of the isoprene algorithm for predicting the monoterpene emission from the Mediterranean holm oak Quercus ilex L.: Performance and limits of this approach., J. Geophys. Res., 102, 23319-23328, 1997.

Croft, K., Juttner, F., and Slusarenko, A.: Volatile products of the lipoxygenase pathway evolved from Phaseolus vulgaris (L.) leaves inoculated with Pseudomonas syringae pv phaseolicola, Plant Physiol., 101, 13-24, 1993.

Derwent, R. G., Jenkin, M. E., Saunders, S. M., and Pilling, M. J.: Photochemical ozone creation potentials for organic compounds in northwest Europe calculated with a master chemical mechanism, Atmos. Environ., 32, 2429-2441, 1998.

Fall, R.: Biogenic emissions of volatile organic compounds from higher plants, in Reactive hydrocarbons in the atmosphere, edited by C. N. Hewitt, pp. 41-96, Academic Press, New York, 1999.

Fall, R., and Benson, A.: Leaf methanol- the simplest natural product from plants, Trends Plant Sci., 1, 296-301, 1996.

Fall, R., Karl, T., Hansel, A., Jordan, A., and Lindinger, W.: Volatile organic compounds emitted after leaf wounding: On-line analysis by proton-transfer-reaction mass spectrometry, J. Geophys. Res., 104, 15963-15974, 1999.

Fehsenfeld, F., Calvert, J., Fall, R., Goldan, P., Guenther, A. B., Hewitt, C. N., Lamb, B., Liu, S., Trainer, M., Westberg, H., and Zimmerman, P.: Emissions of volatile organic compounds from vegetation and the implications for atmospheric chemistry, Global Biochem. Cycles, 6, 389-430, 1992.

Finlayson-Pitts, B. J., and Pitts, J. N.: Chemistry of the Upper and Lower Atmosphere: Theory, Experiments, and Applications, 969 pp., Academic Press, San Diego, 2000.

Forstner, H. J. L., Flagan, R. C., and Seinfeld, J. H.: Secondary organic aerosol from the photooxidation of aromatic: Molecular composition, Environ. Sci. Tech., 31, 1345-1358, 1997.

Fredenslund, A., and Sorensen, J. M.: Group Contribution Estimation Methods, Marcel Dekker Inc., New York, 1994.

Fukui, Y., and Doskey, P. V.: Air-surface exchange of nonmethane organic compounds at a grassland site: Seasonal variations and stressed emissions, J. Geophys. Res., 103, 13153-13168, 1998.

Geron, C., Rasmussen, R., Arnts, R. A., and Guenther, A.: A review and synthesis of monoterpene speciation from forests in the United States, Atmos. Environ., 34, 1761-1781, 2000.

Goldan, P., Kuster, W., Fehsenfeld, F., and Montzka, S.: Hydrocarbon measurements in the southeastern United States: The Rural Oxidants in the Southern Environment (ROSE) Program 1990, J. Geophys. Res., 100, 25945-25963, 1995.

Gray, D. W., Lerdau, M. T., and Goldstein, A. H.: Influences of temperature history, water stress, and needle age on methylbutenol emissions, Ecology, 84, 765-776, 2003.

Griffin, R., Cocker, D., Seinfeld, J., and Dabdub, D.: Estimate of global atmospheric organic aerosol from oxidation of biogenic hydrocarbons, Geophys. Res. Letters, 26, 2721-2724, 1999.

Grosjean, D., and Seinfeld, J. H.: Parametrization of the formation potential of secondary organic aerosols, Atmos. Environ., 23, 1733-1747, 1989.

Grüebler, F. C.: Reactive hydrocarbons in the Milan area: Results from the PIPAPO campaign, PhD thesis, Swiss Federal Institute of Technology (ETH), Zürich, 1999.

Guenther, A.: Seasonal and spatial variations in natural volatile organic compound emissions, Ecol. Appl., 7, 34-45, 1997.

Guenther, A.: The contribution of reactive carbon emissions from vegetation to the carbon balance of terrestrial ecosystems, Chemosphere, 49, 837-844, 2002.

Guenther, A., Baugh, B., Brasseur, G., Greenberg, J., Harley, P., Klinger, L., Serca, D., and Vierling, L.: Isoprene emission estimates and uncertainties for the Central African EXPRESSO study domain, J. Geophys. Res., 104, 30625-30639, 1999.

Guenther, A., Geron, C., Pierce, T., Lamb, B., Harley, P., and Fall, R.: Natural emissions of non-methane volatile organic compounds, carbon monoxide, and oxides of nitrogen from North America, Atmos. Environ., 34, 2205-2230, 2000.

Guenther, A., Hewitt, C., Erickson, D., Fall, R., Geron, C., Graedel, T., Harley, P., Klinger, L., Lerdau, M., McKay, W., Pierce, T., Scholes, B., Steinbrecher, R., Tallamraju, R., Taylor, J., and Zimmerman, P.: A global model of natural volatile organic compound emissions, J. Geophys. Res., 100, 8873-8892, 1995.

Guenther, A., Zimmerman, P., Harley, P., Monson, R., and Fall, R.: Isoprene and monoterpene emission rate variability: Model evaluation and sensitivity analysis, J. Geophys. Res., 98, 12609-12617, 1993.

Haagen-Smit, A. J.: Chemistry and physiology of Los Angeles smog, Ind. Eng. Chem., 44, 1342-1346, 1952.

Hakola, H., Laurila, T., Lindfors, V., Hellen, H., Gaman, A., and Rinne, J.: Variation of the VOC emission rates of birch species during the growing season, Boreal Environ. Res., 6, 237-249, 2001.

Hakola, H., Tarvainen, V., Laurila, T., Hiltunen, V., Hellen, H., and Keronen, P.: Seasonal variation of VOC concentrations above a boreal coniferous forest, Atmos. Environ., 37, 1623-1634, 2003.

Harley, P., Fridd-Stroud, V., Greenberg, J., Guenther, A., and Vasconcellos, P.: Emission of 2-methyl-3-buten-2-ol by pines: A potentially large natural source of reactive carbon to the atmosphere, J. Geophys. Res., 103, 25479-25486, 1998.

Harley, P., Guenther, A., and Zimmerman, P.: Environmental controls over isoprene emission from sun and shade leaves in a mature white oak canopy, Tree Physiology, 17, 705-714, 1997.

Harley, P., Monson, R., and Lerdau, M.: Ecological and evolutionary aspects of isoprene emission from plants, Oecologia, 118, 109-123, 1999.

Hatanaka, A.: The biogeneration of green odour by green leaves, Phytochemistry, 34, 1201-1218, 1993.

Hatanaka, A., Kajuwara, T., and Sekiya, J.: Biosynthetic pathway for C6 aldehyde formation from linolenic acid in green leaves, Chem. Phys. Lipids, 44, 341-361, 1987.

Hering, A. M., Staehelin, J., Baltensperger, U., Prévôt, A. S. H., Kok, G. L., Schillawski, R. D., and Waldvogel, A.: Airborne measurements of atmospheric aerosol particles and trace gases during photosmog episodes over the Swiss plateau and the Southern pre-alpine region, Atmos. Environ., 32, 3381-3392, 1998.

Hoffmann, T., Odum, J. R., Bowman, F., Collins, D., Klockow, D., Flagan, R. C., and Seinfeld, J. H.: Formation of organic aerosols from the oxidation of biogenic hydrocarbons, J. Atmos. Chem., 26, 189-222, 1997.

Holzinger, R., Sandoval-Soto, L., Rottenberger, S., Crutzen, P. J., and Kesselmeier, J.: Emissions of volatile organic compounds from Quercus ilex L. measured by Proton Transfer Reaction Mass Spectrometry under different environmental conditions, J. Geophys. Res., 105, 20573-20579, 2000.

IPCC: Climate Change 2001: The Scientific Basis, Third Assessment Report, 944 pp., World Meteorological Organization, 2001.

Jang, M., Czoschke, N. M., Lee, S., and Kamens, R. M.: Heterogenous Atmospheric Aerosol Production by Acid-Catalyzed Particle Phase Reactions, Science, 298, 814-817, 2002.

Kamens, R. M., Jang, M., Lee, S., Czoschke, N. M., Chandramouli, B., Jaoui, M., and Leungsakul, S.: Secondary Organic Aerosol Formation: Some New and Exciting Insights, Geophys. Res. Abstr., 5, 02915, 2003.

Kamens, R. M., and Jaoui, M.: Modeling Aerosol Formation from a-Pinene + NOx in the Presence of Natural Sunlight Using Gas-Phase Kinetics and Gas-Particle Partitioning Theory, Environ. Sci. Technol., 35, 1394-1405, 2001.

Karl, T., Guenther, A., Lindinger, C., Jordan, A., Fall, R., and Lindinger, W.: Eddy covariance measurements of oxygenated volatile organic compound fluxes from crop harvesting using a redesigned proton-transfer-reaction mass spectrometer, J. Geophys. Res., 106, 24157-24167, 2001.

Karl, T. G., Spirig, C., Rinne, J., Stroud, C., Prevost, P., Greenberg, J., Fall, R., and Guenther, A.: Virtual disjunct eddy covariance measurements of organic compound fluxes from a subalpine forest using proton transfer reaction mass spectrometry, Atmos. Chem. Phys., 2, 279-291, 2002.

Kavouras, I., Mihalopoulos, N., and Stephanou, E.: Formation of atmospheric particles from organic acids produced by forests, Nature, 395, 683-686, 1998.

Kesselmeier, J., Bode, K., Hofmann, U., Muller, H., Schafer, L., Wolf, A., Ciccioli, P., Brancaleoni, E., Cecinato, A., Frattoni, M., Foster, P., Ferrari, C., Jacob, V., Fugit, J. L., Dutaur, L., Simon, V., and Torres, L.: Emission of short chained organic acids, aldehydes and monoterpenes from Quercus ilex L. and Pinus pinea L. in relation to physiological activities, carbon budget and emission algorithms, Atmos. Environ., 31, 119-133, 1997.

Kesselmeier, J., Ciccioli, P., Kuhn, U., Stefani, P., Biesenthal, T., Rottenberger, S., Wolf, A., Vitullo, M., Valentini, R., Nobre, A., Kabat, P., and Andreae, M. O.: Volatile organic compound emissions in relation to plant carbon fixation and the terrestrial carbon budget, Global Biochem. Cycles, 16, art. no.-1126, 2002.

Kleinman, L. I.: Low and high NOx tropospheric photochemistry, J. Geophys. Res., 99, 16,831-16,838, 1994.

Komenda, M. and Koppmann, R.: Monoterpene emissions from Scots pine (Pinus sylvestris): Field studies of emission rate variabilities, J. Geophys. Res., 107, art. no.-4161, 2002.

Kreuzwieser, J., Scheerer, U., and Rennenberg, H.: Metabolic origin of acetaldehyde emitted by poplar (Populus tremula x P-alba) trees, Journal of Experimental Botany, 50, 757-765, 1999.

Kulmala, M., Hämeri, K., Mäkelä, J. M., Aalto, P. P., Pirjola, L., Väkevä, M., Nilsson, E. D., Koponen, I. K., Buzorius, G., Keronen, P., Rannik, Ü., Laakso, L., Vesala, T., Bigg, K., Seidl, W., Forkel, R., Hoffmann, T., Spanke, J., Janson, R., Shimmo, M., Hansson, H.-C., O'Dowd, C., Becker, E., Paatero, J., Teinilä, K., Hillamo, R., Viisanen, Y., Laaksonen, A., Swietlicki, E., Salm, J., Hari, P., Altimir, N., and Weber, R.: Biogenic aerosol formation in the boreal forest, Boreal Environ. Res., 5, 281-297, 2000.

Larsen, B. R., Di Bella, D., Glasius, M., Winterhalter, R., Jensen, N. R., and Hjorth, J.: Gas-phase OH oxidation of monoterpenes: Gaseous and particulate products, J. Atmos. Chem., 38, 231-276, 2001.

Leaitch, W. R., Bottenheim, J. W., Biesenthal, T. A., Li, S.-M., Liu, P. S. K., Asalian, K., Dryfhout-Clark, H., Hopper, F., and Brechtel, F.: A case study of gas-to-particle conversion in an eastern Canadian forest, J. Geophys. Res., 104, 8095 - 8111, 1999.

Leighton, P. A.: Photochemistry of Air Pollution, Academic Press, New York, 1961.

Logan, B. A., and Monson, R. K.: Thermotolerance of leaf discs from four isoprene-emitting species is not enhanced by exposure to exogenous isoprene, Plant Physiol., 120, 821-825, 1999.

MacDonald, R. C., and Fall, R.: Detection of substantial emissions of methanol from plants to the atmosphere, Atmos. Environ., 27A, 1709-1713, 1993.

Marti, J. J., Weber, R. J., McMurry, P. H., Eisele, F., Tanner, D., and Jefferson, A.: New particle formation at a remote continental site: Assessing the contributions of SO2 and organic precursors, J. Geophys. Res., 102, 6331 - 6339, 1997.

Meng, Z., Dabdub, D., and Seinfeld, J. H.: Chemical coupling between atmospheric ozone and particulate matter, Science, 277, 116-119, 1997.

Middleton, J. T., Kendrick Jr., J. B., and Schwalm, H. W.: Injury to herbaceous plants by smog or air pollution, Plant Disease Reporter, 34, 245-252, 1950.

Milford, J. B., Gao, D., and Zafirakou, A.: Ozone precursor levels and responses to emissions reductions: analysis of regional oxidant model results, Atmos. Environ., 28, 2093-2104, 1994.

Nemecek-Marshall, M., MacDonald, R., Franzen, J., Wojciechowski, C., and Fall, R.: Methanol emission from leaves, Plant Physiol., 108, 1359-1368, 1995.

Nozière, B., Barnes, I., and Becker, K. H.: Product study and mechanisms of the reactions of alpha-pinene and of pinonaldehyde with OH radicals, J. Geophys. Res., 104, 23645-23656, 1999.

Nozière, B., Longfellow, C. A., Henry, B. E., Voisin, D., and Hanson, D. R.: Uptake of nopinone by water: Comparison between aqueous-and gas-phase oxidation of organic compounds in the atmosphere, Geophys. Res. Letters, 28, 1965-1968, 2001.

NRC (National Research Council): Rethinking the ozone problem, 489 pp., National Academy Press, Washington DC, 1991.

Odum, J. R., Hoffmann, T., Bowman, F., Collins, D., Flagan, R. C., and Seinfeld, J. H.: Gas/particle partitioning and secondary organic aerosol yields, Environ. Sci. Technol., 30, 2580-2585, 1996.

Odum, J. R., Jungkamp, T. P. W., Griffin, R. J., Flagan, R. C., and Seinfeld, J. H.: The atmospheric aerosol-forming potential of whole gasoline vapor, Science, 276, 96 - 99, 1997a.

Odum, J. R., Jungkamp, T. P. W., Griffin, R. J., Forstner, H. J. L., Flagan, R. C., and Seinfeld, J. H.: Aromatics, reformulated gasoline, and atmospheric organic aerosol formation, Environ. Sci. Tech., 31, 1890-1897, 1997b.

Pandis, S. N., Paulson, S. E., Seinfeld, J. H., and Flagan, R. C.: Aerosol formation in the photooxidation of isoprene and b-Pinene, Atmos. Environ., 25A, 997-1008, 1991.

Pankow, J. F.: An absorption model of gas/aerosol partitioning involved in the formation of secondary organic aerosol, Atmos. Environ., 28, 189-193, 1994a.

Pankow, J. F.: An apsorption model of the gas/aerosol partitioning of organic compounds in the atmosphere, Atmos. Environ., 28, 185-188, 1994b.

Paulson, S. E., and Orlando, J. J.: The reactions of ozone with alkenes: An important source of HOx in the boundary layer, Geophys. Res. Letters, 23, 3727-3730, 1996.

Petron, G., Harley, P., Greenberg, J., and Guenther, A.: Seasonal temperature variations influence isoprene emission, Geophysical Research Letters, 28, 1707-1710, 2001.

Poisson, N., Kanakidou, M., and Crutzen, P. J.: Impact of non-methane hydrocarbons on tropospheric chemistry and the oxidizing power of the global troposphere: 3- dimensional modelling results, J. Atmos. Chem., 36, 157-230, 2000.

Prevot, A. S. H., Staehelin, J., Kok, G. L., Schillawski, R. D., Neininger, B., Staffelbach, T., Neftel, A., Wernli, H., and Dommen, J.: The Milan photooxidant plume, J. Geophys. Res., 102, 23375-23388, 1997.

Raes, F., Van Dingenen, R., Vignati, E., Wilson, J., Putaud, J. P., Seinfeld, J. H., and Adams, P.: Formation and cycling of aerosols in the global troposphere, Atmos. Environ., 34, 4215-4240, 2000.

Rudolph, J.: Biogenic sources of atmospheric alkenes and acetylene, in Biogenic volatile organic carbon compounds in the atmosphere, edited by G. Helas, Slanina, J., and Steinbrecher, R., pp. 53 - 65, SPB Academic Publishing, Amsterdam, 1997.

Sanadze, G.: The nature of gaseous substances emitted by leaves of Robinia pseudoacacia, Soobshch. Akad. Nauk Gruz. SSR, 27, 747-750, 1957.

Schaab, G., Steinbrecher, R., Lacaze, B., and Lenz, R.: Assessment of long-term vegetation changes on potential isoprenoid emission for a Mediterranean-type ecosystem in France, J. Geophys. Res., 105, 28863-28873, 2000.

Schönbein, C. F.: Beobachtungen über den bei der Elodtrolysation des Wassers und dem Ausströmen der gewähnlichen Electricität aus Spitzen sich entwickelnden Geruch, Annalen der Physik und Chemie, 50, 616, 1840a.

Schönbein, C. F.: Recherches sur la nature del'odeur que se manifeste dans certaines réactions chimiques, Comptes Rendus de l'Academie des Sciences II, 15, 706, 1840b.

Schönbein, C. F.: Einige Bemerkungen über die Anwesenheit des Ozons in der atmosphärischen Luft und die Rolle welche dieses bei lansamen Oxydationen spielen dürfte, Annalen der Physik und Chemie, 65, 161-172, 1845.

Schwartz, J., Dockery, D. W., and Neas, L. M.: Is daily mortality associated specifically with fine particles?, J. Air Waste Manage. Assoc., 46, 927-939, 1996.

Schwarzenbach, R., Gschwend, P. M., and Imboden, D. M.: Environmental Organic Chemistry, 681 pp., John Wiley & Sons, Inc., New York, 1993.

Seinfeld, J. H., Erdakos, G. B., Asher, W. E., and Pankow, J. F.: Modeling the formation of secondary organic aerosol (SOA). 2. The predicted effects of relative humidity on aerosol formation in the a-pinene, b-pinene-, sabinene-, D3-carene-, and cyclohexene-ozone systems, Environ. Sci. Tech., 35, 1806-1817, 2001.

Seinfeld, J. H., and Pandis, S. N.: Atmospheric chemistry and physics: From air pollution to climate change, 1326 pp., John Wiley, New York, 1998.

Sharkey, T.: Emission of low molecular mass hydrocarbons from plants, Trends Plant Sci., 1, 78-82, 1996.

Sharkey, T. D., and Singsaas, E. L.: Why plants emit isoprene, Nature, 374, 769, 1995.

Sillman, S.: The use of NOy, H2O2, and HNO3 as indicators for ozone-NOx-hydrocarbon sensitivity in urban locations, J. Geophys. Res., 100, 14,175-14,188, 1995.

Sillman, S., Logan, J. A., and Wolfsy, S. C.: The sensitivity of ozone to nitrogen oxides and hydrocarbons in regional ozone episodes, J. Geophys. Res., 95, 1837 - 1851, 1990.

Simpson, D., Winiwarter, W., Börjesson, G., Cinderby, S., Ferreiro, A., Guenther, A., Hewitt, C. N., Janson, R., Khalil, M. A. K., Owen, S., Pierce, T. E., Puxbaum, H., Shearer, M., Skiba, U., Steinbrecher, R., Tarrason, L., and Öquist, M. G.: Inventorying emissions from nature in Europe, J. Geophys. Res., 104, 8113-8152, 1999.

Singh, H. B., and Zimmerman, P.: Atmospheric distributions and sources of nonmethane hydrocarbons., in Gaseous Pollutants: Characterization and Cycling, edited by J. O. Nriagu, pp. 235f, John Wiley & Sons, Inc., 1992.

Skelly, J. M., Innes, J. L., Snyder, K. R., Savage, J. E., Hug, C., Landolt, W., and Bleuler, P.: Investigations of ozone induced injury in forests of southern Switzerland: Field surveys and open-top chamber experiments, Chemosphere, 36, 995-1000, 1998.

Spirig, C., and Neftel, A.: Biogene VOC und Aerosole, Schriftenreihe der FAL Nr. 42, Swiss Federal Research Station for Agroecology and Agriculture, Zürich, 2002.

Staffelbach, T., and Neftel, A.: Relevance of biogenically emitted trace gases for the ozone production in the planetary boundary layer in Central Europe, Swiss Federal Research Station for Agroecology and Agriculture (FAL) and Institute of Environmental Protection and Agriculture (IUL), Zürich-Reckenholz, 1997.

Staffelbach, T., Neftel, A., Blatter, A., Gut, A., Fahrni, M., Staehelin, J., Prévôt, A., Hering, A., Lehning, M., Neininger, B., Bäumle, M., Kok, G. L., Dommen, J., Hutterli, M., and Anklin, M.: Photochemical oxidant formation over southern Switzerland, 1. Results from summer 1994, J. Geophys. Res., 102, 23345-23363, 1997a.

Staffelbach, T., Neftel, A., and Horrowitz, L. W.: Photochemical oxidant formation over southern Switzerland, 2. Model results, J. Geophys. Res., 102, 23363-23373, 1997b.

Staudt, M., and Seufert, G.: Light-dependent emission of monoterpenes by Holm Oak (Quercus ilex L.), Naturwissenschaften, 82, 89-92, 1995.

Trainer, M., Hsie, E. Y., McKeen, S. A., Tallamraju, R., Parrish, D. D., Fehsenfeld, F. C., and Liu, S. C.: Impact of natural hydrocarbons on hydroxyl and peroxy radicals at a remote site., J. Geophys. Res., 92, 11,879-11,894, 1987a.

Trainer, M., Williams, E. J., Parrish, D. D., Buhr, M. P., Allwine, E. J., Westberg, H. H., Fehsenfeld, F. C., and Liu, S. C.: Models and observations of the impact of natural hydrocarbons on rural ozone., Nature, 329, 705-707, 1987b.

Voisin, D., Smith, J. N., Sakurai, H., McMurry, P. H., and Eisele, F. L.: Thermal desorption chemical ionization mass spectrometer for ultrafine particle chemical composition, Aerosol Sci. Technol., 37, 471-475, 2003a.

Voisin, D., Smith, J., Moore, K., McMurry, P., Eisele, F.: Thermal Desortpion Chemical Ionization Mass Spectrometer for Real Time Chemical Characterization of Fine Aerosol, Geophys. Res. Abstracts, Vol. 5, EGS-AGU-EUG Joint Assembly, 2003b.

Wang, S.-C., Paulson, S. E., Grosjean, D., Flagan, R. C., and Seinfeld, R. C.: Aerosol formation and growth in atmospheric organic/NOx systems - I. Outdoors smog chamber studies of C7 and C8 - hydrocarbons., Atmos. Environ., 26A, 403-420, 1992.

Warneke, C., Karl, T., Judmaier, H., Hansel, A., Jordan, A., Lindinger, W., and Crutzen, P.: Acetone, methanol and other partially oxidized volatile organic emissions from dead plant matter by abiological processes: significance for atmospheric HOx chemistry, Global Biochem. Cycles, 13, 9-17, 1999.

Zhang, J., Ferdinand, J. A., Vanderheyden, D. J., Skelly, J. M., and Innes, J. L.: Variation of gas exchange within native plant species of Switzerland and relationships with ozone injury: an open-top experiment, Environ. Pollut., 113, 177-185, 2001.

Acknowledgements

Most of the work for this thesis was part of the two large field experiments PIPAPO and OSOA. This involved a close collaboration with various research groups that I experienced as extremely enjoyable and fruitful. Besides many thanks to all persons involved in these field campaigns, I would like to express my gratitude to:

Dr. Albrecht Neftel, for guiding me through the ups and downs of PhD work, his always-motivating support and never-ending flow of inspiring ideas.

Prof. Thomas Peter, Institute for Atmospheric and Climate Science (IACETH), for accepting to be my supervisor in awareness of the limited control he could have on me as an "external" PhD student. I never felt external when I needed his support.

Dr. Alex Guenther, for giving me the opportunity to spend two interesting years in his research project at the National Center of Atmospheric Research (NCAR) and for accepting to be my co-examiner.

James Greenberg, NCAR, for introducing me to the secrets of gas chromatography and ensuring to stay on ground when ideas or balloons flew too high.

The whole BAI-group (The Biosphere Atmosphere Interactions Project at NCAR) and technical staff of NCAR for their support in many parts of this thesis and for providing a great working environment. I miss the countless lunch discussions at the Mesa cafeteria!

The TP 11.3 of FAL (The Air Pollution/Climate Group of the Swiss Federal Institute for Agroecology and Agriculture), for welcoming me after two years abroad as if I had always been part of the group.

Prof. Johannes Staehelin, IACETH, for his support in the initial phase of my PhD work. Without him I would not have started my thesis and only thanks to him I managed to meet all regulations during my stay in the US.

Deanne Buck and Dr. Josh Van Buskirk for linguistic corrections of the manuscript.

Curriculum vitae

Christoph Spirig
Born on June 21, 1972 in Altstätten, Switzerland
Citizen of Widnau and Diepoldsau (SG), Switzerland

Education

Dec 1999-2003	PhD studies at the Swiss Federal Research Station for Agroecology and Agriculture, Zürich-Reckenholz and at the Institute for Atmospheric and Climate Research (IACETH), ETH. Visitor at the Biosphere-Atmosphere Interactions Project (BAI) of NCAR, Boulder CO, 2000 – 2002.
1998	Diploma in Environmental Sciences, ETH Zürich
1992-1998	Study of Environmental Sciences: Specialising field: Environmental Chemistry and Atmosphere
1992	Matura Type B, Kantonsschule Heerbrugg (SG).

Professional training

Dec 1998 – Nov 1999	Scientific assistant at the Swiss Federal Research Station for Agroecology and Agriculture (FAL), Bern-Liebefeld.
1996	Internship at the air quality division, canton of Zürich (AWEL).

Scientific projects involved in

COCA (Swiss National Science Foundation), 2001-2003
Characterization of Organic Compounds in the Atmosphere

ECHO, (German Federal Ministry of Education and Research, 2002-2003
Emission and CHemical processing of biogenic volatile Organic compounds

OSOA , (European Commission), 2001
Origin and formation of Secondary Organic Aerosol

PIPAPO/LOOP, (EUROTRAC-2), 1998-2002
Pianura Padana Produzione di Ozono, Limitation of Oxidants Production